TTI: 0-6893

Strengthening of Existing Inverted-T Bent Caps—Volume 1: Preliminary Design

Technical Report 0-6893-R1-Vol1

Cooperative Research Program

TEXAS A&M TRANSPORTATION INSTITUTE
COLLEGE STATION, TEXAS

in cooperation with the
Federal Highway Administration and the
Texas Department of Transportation
http://tti.tamu.edu/documents/0-6893-R1-Vol1.pdf

Technical Report Documentation Page

1. Report No.	2. Government Accession No.	3. Recipient's Catalog No.
FHWA/TX-18/0-6893-R1-Vol1		

4. Title and Subtitle	5. Report Date
STRENGTHENING OF EXISTING INVERTED-T BENT CAPS—VOLUME 1: PRELIMINARY DESIGN	Published: November 2018
	6. Performing Organization Code
7. Author(s) Stefan Hurlebaus, John B. Mander, Anna C. Birely, Tevfik Terzioglu, Jilong Cui, and Sun Hee Park	8. Performing Organization Report No. Report 0-6893-R1-Vol1
9. Performing Organization Name and Address Texas A&M Transportation Institute The Texas A&M University System College Station, Texas 77843-3135	10. Work Unit No. (TRAIS)
	11. Contract or Grant No. Project 0-6893
12. Sponsoring Agency Name and Address Texas Department of Transportation Research and Technology Implementation Office 125 E. 11th Street Austin, Texas 78701-2483	13. Type of Report and Period Covered Technical Report: September 2015–August 2018
	14. Sponsoring Agency Code

15. Supplementary Notes

Project performed in cooperation with the Texas Department of Transportation and the Federal Highway Administration.
Project Title: Strengthening of Existing Inverted-T Bent Caps
URL: http://tti.tamu.edu/documents/0-6893-R1-Vol1.pdf

16. Abstract

Inverted-T bent caps are used extensively throughout Texas to economically satisfy geometric constraints. Since the design approach has changed and the traffic volume has increased over the decades, evaluation of existing inverted-T bent caps is needed. The research objectives were to assess in-service inverted-T bent caps based on field visits and current design methodologies. Based on the 2014 American Association of State Highway and Transportation Official's load and resistance factor design provisions and the Texas Department of Transportation's *Bridge Design Manual*, the demands (girder reaction) and the capacities of the ledge to transfer the applied loads to the web were calculated to evaluate the bent cap for the most critical failure modes: ledge shear friction, ledge flexure, hanger, punching shear, and bearing. Since southbound Bent 13 and northbound Bent 22 had the largest demand, those bents were evaluated and were found to be deficient in ledge flexure, hanger, and punching shear. To address these deficiencies, 18 technical concepts to retrofit inverted-T bent caps were proposed. Retrofit solutions include external post-tensioning, steel brackets to provide supplementary load path, fiber-reinforced polymer wrap with anchors, concrete masonry columns, and increased bearing pad sizes. The proposed retrofit solutions were evaluated using a weighted sum model for the experimental test to validate the satisfactory performance of strengthening existing inverted-T bent caps. Six criteria were considered for the assessment of retrofit solutions: strength increase, total cost, constructability, clearance constraints, durability, and ease of monitoring.

17. Key Words	18. Distribution Statement
Inverted-T Beam, Bent Cap, Bridge, Ledge, Hanger, Punching Shear, Concrete Shear Friction, Ledge Flexure, Retrofit, Strengthening, FRP Wrap, External Post-Tensioning, Bearing pad, WSM, Weighted Sum Model	No restrictions. This document is available to the public through NTIS: National Technical Information Service Alexandria, Virginia http://www.ntis.gov

19. Security Classif. (of this report)	20. Security Classif. (of this page)	21. No. of Pages	22. Price
Unclassified	Unclassified	284	

Form DOT F 1700.7 (8-72) Reproduction of completed page authorized

STRENGTHENING OF EXISTING INVERTED-T BENT CAPS—VOLUME 1: PRELIMINARY DESIGN

by

Stefan Hurlebaus, Ph.D.
Professor
Zachry Department of Civil Engineering
Research Scientist
Texas A&M Transportation Institute

John B. Mander, Ph.D.
Zachry Professor of Design and Construction Integration
Zachry Department of Civil Engineering
Research Scientist
Texas A&M Transportation Institute

Anna C. Birely, Ph.D.
Assistant Professor
Zachry Department of Civil Engineering
Assistant Research Scientist
Texas A&M Transportation Institute

Tevfik Terzioglu, Ph.D.
Postdoctoral Research Associate
Texas A&M Transportation Institute

and

Jilong Cui and Sun Hee Park
Graduate Assistant Researchers
Texas A&M Transportation Institute

Report 0-6893-R1-Vol1
Project 0-6893
Project Title: Strengthening of Existing Inverted-T Bent Caps

Performed in cooperation with the
Texas Department of Transportation
and the
Federal Highway Administration

Published: November 2018

TEXAS A&M TRANSPORTATION INSTITUTE
College Station, Texas 77843-3135

DISCLAIMER

This research was performed in cooperation with the Texas Department of Transportation (TxDOT) and the Federal Highway Administration (FHWA). The contents of this report reflect the views of the authors, who are responsible for the facts and the accuracy of the data presented herein. The contents do not necessarily reflect the official view or policies of FHWA or TxDOT. This report does not constitute a standard, specification, or regulation.

This report is not intended for construction, bidding, or permit purposes. The researcher in charge of the project was Stefan Hurlebaus. The United States Government and the State of Texas do not endorse products or manufacturers. Trade or manufacturers' names appear herein solely because they are considered essential to the object of this report.

ACKNOWLEDGMENTS

This project was conducted in cooperation with TxDOT and FHWA under Project 0-6893, with Chris Glancy serving as project manager. The authors thank Dominique Bechle, Michelle Romage-Chambers, Nicholas Nemac, and Steven Austin.

The project was conducted at Texas A&M University through the Texas A&M Transportation Institute. The authors would like to acknowledge the support of Maria Medrano. The support of postdoctoral researcher Madhu K. Murugesan Reddiar is also greatly appreciated.

TABLE OF CONTENTS

Page

List of Figures ..... **ix**
List of Tables ..... **xii**
Chapter 1 . Introduction **1**
1.1 Overview 1
1.2 Project Objective 2
1.3 Report Outline 2
Chapter 2 . Background **3**
2.1 Behavior and Failure Mechanisms of Inverted-T Bent Caps 3
2.2 Retrofit of Reinforced Concrete Structures 10
2.2.1 Retrofit Methods for Inverted-T Bent Caps and Beams 11
2.2.2 Retrofit Methods for Standard T-Shaped Concrete Structures 11
2.3 Analytical Models 21
2.3.1 Strut-and-Tie Modeling (STM) and Modifications for Analytical Studies 21
2.3.2 Other Analytical Models 24
2.4 Summary 26
Chapter 3 . Analysis and Evaluation of In-Service Inverted-T Bent Caps **29**
3.1 Conditions of In-Service Inverted-T Bent Caps 29
3.1.1 Field Visit for Evaluating IH 35 in Austin 29
3.1.2 Field Visit for Evaluating US 290 in Austin 37
3.2 Bent Characteristics of IH 35 40
3.2.1 Cap and Column Dimensions 40
3.2.2 Girders on Bent Cap 41
3.3 Structural Analysis 45
3.3.1 Demands 45
3.3.2 Bent Cap Capacity Evaluation 48
3.4 Comparison of 1965 AASHO with 2014 AASHTO LRFD Specifications 66
3.5 Closing Remarks 72
Chapter 4 . Design of Potential Retrofit Solutions **73**
4.1 Prestressed High-Strength Threadbar (Solution 1) 73
4.2 Steel Hanger Bracket (Solution 2) 77
4.3 End-Region Stiffener (Solution 3) 81
4.4 Clamped Cross Threadbar (Solution 4) 84
4.5 Grouted Cross Threadbar (Solution 5) 86
4.6 Upper Seat Bracket (Solution 6) 89
4.7 Threadbar Hanger with Steel Bracket (Solution 7) 91
4.8 Clamped Threadbar with Channel (Solution 8) 93
4.9 Grouted Threadbar Anchored with Channel (Solution 9) 96
4.10 Anchored FRP Wrap (Solution 10) 96
4.11 Concrete Infill with Prestressing Threadbar (Solution 11) 101
4.12 Concrete Infill with Hanger Threadbar (Solution 12) 104
4.13 Concrete Masonry Pier (Solution 13) 106

4.14 Load-Balancing Post-Tensioning (Solution 14) 108
4.15 Concrete Infill with FRP Anchored by FRP Anchors (Solution 15) 112
4.16 Concrete Infill with Partial-Depth FRP Anchored by Steel Waling (Solution 16) 114
4.17 Concrete Infill with Full-Depth FRP Anchored by Steel Waling (Solution 17)..... 114
4.18 Large Bearing Pad (Solution 18) 117
4.19 Closing Remarks 118
Chapter 5 . Decision Methodology for Ranking Retrofit Solutions 119
5.1 Retrofit Solutions 119
5.2 Decision Analysis Using Weighted Sum Model 119
5.3 Description of Criteria 121
5.3.1 Strength Increase 121
5.3.2 Cost 125
5.3.3 Constructability 128
5.3.4 Dimensional and Clearance Constraints 130
5.3.5 Durability/Longevity 135
5.3.6 Ease of Monitoring 136
5.4 Unweighted Score 139
5.5 Weight Factors and Ranking 140
5.6 Closing Remarks 149
Chapter 6 . Discussion and Closure 151
6.1 Summary 151
6.2 Discussion and Research Needs 152
Appendix A. CAP 18 Input and Output File 155
Appendix B. Bent Cap Analysis 173
Appendix C. Retrofit Solution 187
References 267

LIST OF FIGURES

Page

Figure 1.1. Inverted-T Bent Cap in Downtown Austin (Image from Google Maps). 1
Figure 2.1. Inverted-T Bent Cap Geometry and Reinforcement. 4
Figure 2.2. Structural Load Actions on Inverted-T Bent Cap (Furlong and Mirza, 1971). 4
Figure 2.3. Failure Mechanisms of Inverted-T Bent Caps (Furlong and Mirza, 1974). 5
Figure 2.4. Ledge Reinforcement Details for Inverted-T Beam (Furlong et al., 1971). 6
Figure 2.5. 2D, 3D, and Whole Bent Test Specimens (Zhu et al., 2001). 8
Figure 2.6. Typical Specimen Geometries (Larson et al., 2013). 9
Figure 2.7. Dimensions and Reinforcement Details of Tested Beams (Deifalla and Ghobarah, 2014). 10
Figure 2.8. Anchored CFRP Rehabilitation Schemes Using Angle Plate (Galal and Sekar, 2008). 12
Figure 2.9. Details of Specimens and Test Setup (Shahawy and Beitelman, 1999). 13
Figure 2.10. Specimen Strengthening (Nanni et al., 2004). 15
Figure 2.11. Repair for Specimens (Higgins et al., 2009). 16
Figure 2.12. Strengthening Schemes (Deifalla and Ghobarah, 2010a). 17
Figure 2.13. Vertically and Diagonally Mounted Near-Surface FRP Rods after Failure (DeLorenzis and Nanni, 2001). 18
Figure 2.14. Specimen Elevation View with Internal Steel Reinforcing (Goebel et al., 2012). 20
Figure 2.15. Various Retrofit Techniques Tested by Chaallal et al. (2011). 21
Figure 3.1. Overview of Field Visit Location: Outer Circle Indicates Referenced Structures and Inner Circle Indicates Location of Field Visit (Image from Google Maps). 30
Figure 3.2. Plan View of Structures Observed during the First Field Visit (Image from Google Earth). 31
Figure 3.3. Southern End of Elevated Main Drop to Grade Level. 31
Figure 3.4. Unequal Overhang Lengths for Bent 16 of Northbound Thruway Lanes. 32
Figure 3.5. Crack at Ledge-Web Interface of End (East) of Northbound Main Lane Bent 13. 33
Figure 3.6. Cracking and Spalling at Ends (East) of Northbound Bents. 33
Figure 3.7. Diaphragms between Girders at Ends of Spans. 34
Figure 3.8. Limited Accessibility to Ends of Bent Caps Due to Adjacent Substructures. 35
Figure 3.9. Edge of Deck Extends Past End of Inverted-T Bent Caps. 36
Figure 3.10. Frontage Road Adjacent to Thruway Lanes. 36
Figure 3.11. Drainage Pipes Attached to Ledge of Multi-Column Bent. 37
Figure 3.12. Location of the Bents Observed during the Second Field Visit (Image from Google Earth). 37
Figure 3.13. Typical Inverted-T Bent Cap. 38
Figure 3.14. Ledge Reinforcement Detail of Typical Double-Column Bent. 39
Figure 3.15. Crack at Ledge-Flange Interface of Exterior of Bent 29. 39
Figure 3.16. Cracks at the Ends of Bents. 39
Figure 3.17. Variable Ledge Depth of Bent Caps in Single-Column Bents. 40

Figure 3.18. Elevation and Cross-Section of Southbound Bent 13. 42
Figure 3.19. Elevation and Cross-Section of Northbound Bent 22. 43
Figure 3.20. Live Load Models on Girder Used for the Computation of Girder Reaction and Torsional Load. 47
Figure 3.21. Notation and Potential Crack Locations for Ledge Beams (AASHTO, 2014). 50
Figure 3.22. Parameters for Calculation of Hanger Capacity. 51
Figure 3.23. Distribution of Hanger Reinforcement. 53
Figure 3.24. AASHTO LRFD (2014) Reinforcement Requirements for the Ledge of Inverted-T Bent Cap. 56
Figure 3.25. Parameters for Calculation of Ledge Shear Friction Capacity. 56
Figure 3.26. Parameters for Calculation of Ledge Flexure with Axial Tension Capacity..... 58
Figure 3.27. Ledge Reinforcement Distribution of Southbound Bent 13. 59
Figure 3.28. Ledge Reinforcement Distribution of Northbound Bent 22. 60
Figure 3.29. Punching Shear Failure Surface. 62
Figure 3.30. Truncated Pyramid for Bearing (TxDOT, 2010). 65
2014 AASHTO LRFD 67
Figure 3.31. Live Load Models (AASHO, 1965). 68
2014 AASHTO LRFD 70
Figure 4.1. Prestress Using High-Strength Threadbars to Supplement Punching Shear and Ledge Flexure Deficiency. 74
Figure 4.2. Solution for Ledge Flexure and Punching Shear Deficiency by Applying Prestress Directly to the Ledges. 76
Figure 4.3. Steel Hanger Bracket to Supplement Punching Shear and Ledge Flexure Deficiency. 78
Figure 4.4. Assumption for Design of Anchor Bolts in Tension Using Whitney Stress Block. 79
Figure 4.5. End-Region Strengthening Using Steel Stiffener to Supplement Hanger, Ledge Flexure, and Punching Shear Capacity in the End Regions. 82
Figure 4.6. Load Path with End-Region Stiffener. 83
Figure 4.7. End-Region Strengthening Method Using Stiffener Plate. 84
Figure 4.8. Clamped Cross Threadbars to Supplement Ledge Flexure and Punching Shear Deficiency. 85
Figure 4.9. Grouted Cross Threadbars to Supplement Ledge Flexure, Punching Shear, and Hanger Deficiency. 88
Figure 4.10. Upper Seat Bracket to Supplement Punching Shear and Ledge Flexure Deficiency. 90
Figure 4.11. Threadbar Hanger with Steel Bracket to Supplement Punching and Ledge Flexure Deficiency. 92
Figure 4.12. Clamped Threadbars to Transfer Loads into Web to Supplement Hanger, Ledge Flexure, and Punching Shear. 94
Figure 4.13. Solution for Hanger, Ledge Flexure, and Punching Shear Deficiency by Clamping from Top of the Web to Bottom of Ledges with Long Threadbar with Channel. 95
Figure 4.14. Grouted Threadbar Anchored at Web to Supplement Hanger, Punching Shear, and Ledge Flexure Deficiency. 97

Figure 4.15. Anchored FRP Wrap to Supplement Hanger, Punching Shear, and Ledge Flexure Deficiency. 98
Figure 4.16. Concrete Infill with Prestressed Threadbars to Supplement Punching Shear, Ledge Flexure, and Hanger Deficiency. 103
Figure 4.17. Concrete Infill with Hanger Threadbars to Supplement Punching Shear, Ledge Flexure, and Hanger Deficiency. 105
Figure 4.18. Concrete Masonry Unit (CMU) Column under Girder. 106
Figure 4.19. Solution for Inverted-T Bent Caps with Hanger, Ledge Flexure, and/or Punching Shear Deficiency. 107
Figure 4.20. PT System Using Load-Balance Techniques to Overcome Predominant Deficiency of Cantilever Portion of the Bent. 110
Figure 4.21. Solution for All Deficiencies by External PT. 111
Figure 4.22. Solution for Punching Shear and Ledge Flexure Failure Using FRP Sheets and FRP Anchors. 113
Figure 4.23. Solution for Punching Shear and Ledge Flexure Failure Using FRP Sheets and Threadbars. 115
Figure 4.24. Solution for Hanger, Punching Shear, and Ledge Flexure Failure Using FRP Sheets and Threadbars. 116
Figure 4.25. Solution for Punching Shear Failure by Increasing Bearing Pad Size. 117
Figure 5.1. Comparison of the Criteria Scores of Retrofit Solutions for Double-Column Bents. 142
Figure 5.2. Comparison of the Criteria Scores of Retrofit Solutions for Single-Column Bents. 143
Figure 5.3. Total Weighted Scores of Retrofit Solutions for Double-Column Bents. 147
Figure 5.4. Total Weighted Scores of Retrofit Solutions for Single-Column Bents. 148

LIST OF TABLES

Page

Table 3.1. Northbound Thruway Bent Summary..... 44
Table 3.2. Southbound Thruway Bent Summary..... 44
Table 3.3. Girder Reactions for Selected Bents..... 46
Table 3.4. Overstrength Factor for Sectional Capacity..... 49
Table 3.5. Hanger Capacity Evaluation..... 54
Table 3.6. Ledge Shear Friction and Ledge Flexure Capacity Evaluation..... 61
Table 3.7. Punching Shear Capacity Evaluation..... 62
Table 3.8. Punching Shear Capacity vs. Demand of Thruway Exterior Girders..... 63
Table 3.9. Punching Shear Capacity vs. Demand of Thruway Interior Girders..... 64
Table 3.10. Bearing Capacity vs. Demand of Typical Bents..... 65
Table 3.11. 1965 AASHO vs. 2014 AASHTO LRFD Specifications..... 67
Table 3.12. Southbound Bent 13—Overstrength Factor..... 70
Table 3.13. Northbound Bent 22—Overstrength Factor..... 71
Table 5.1. Retrofit Solutions..... 120
Table 5.2. Scoring Definitions for Adequate Strength Increase..... 123
Table 5.3. Rating for Strength Increase of Retrofit Solutions for Double-Column Bents..... 124
Table 5.4. Strength Rating of Retrofit Solutions for Single-Column Bents..... 124
Table 5.5. Scoring Definitions for Cost..... 127
Table 5.6. Cost Rating of Retrofit Solutions for Double-Column Bents..... 127
Table 5.7. Cost Rating of Retrofit Solutions for Single-Column Bents..... 128
Table 5.8. Scoring Definitions for Constructability..... 130
Table 5.9. Constructability Rating of Retrofit Solutions for Double-Column Bents..... 132
Table 5.10. Constructability Rating of Single-Column Bents..... 133
Table 5.11. Scoring Definitions for Dimensional and Clearance Constraints..... 133
Table 5.12. Clearance Constraint Score of Retrofit Solutions for Double-Column Bents..... 134
Table 5.13. Clearance Constraint Rating of Retrofit Solutions for Single-Column Bents..... 134
Table 5.14. Scoring Definitions for Durability/Longevity..... 136
Table 5.15. Durability/Longevity Rating of Retrofit Solutions for Double-Column Bents..... 137
Table 5.16. Durability/Longevity Rating of Single-Column Bents..... 138
Table 5.17. Scoring Definitions for Ease of Monitoring..... 138
Table 5.18. Ease of Monitoring Rating of Retrofit Solutions for Double-Column Bents..... 139
Table 5.19. Ease of Monitoring Rating of Single-Column Bents..... 139
Table 5.20. Summary of Unweighted Scores for Rating Retrofit Solutions for Double-Column Bents..... 141
Table 5.21. Summary of Unweighted Scores for Rating Retrofit Solutions for Single-Column Bents..... 143
Table 5.22. Weight Factors for the Considered Criteria..... 144
Table 5.23. Decision Matrix for the Evaluation of Retrofit Solutions..... 145
Table 5.24. Weighted Total Scores of Retrofit Solutions for Double-Column Bents..... 146
Table 5.25. Decision Matrix of Retrofit Solutions for Single-Column Bents..... 148
Table 5.26. Ranking of Proposed Retrofit Solutions for Double-Column Bents..... 149
Table 5.27. Ranking of Proposed Retrofit Solutions for Single-Column Bents..... 149

Table 5.28. Top-Ranking Retrofit Solutions for Double-Column Bents. 150
Table 5.29. Top-Ranking Retrofit Solutions for Single-Column Bents. 150

CHAPTER 1. INTRODUCTION

1.1 Overview

Inverted-T bent caps have been widely used in Texas to reduce the overall elevation of bridges, improve the available clearance beneath beams, and improve aesthetics. The structural behavior of inverted-T bent caps is different than that of conventional top-loaded beams because the loads are introduced into the bottom flange rather than the top of the beam. The flange of the inverted-T serves as a shallow ledge to seat the bridge girders, while the web of the inverted-T, rising above the ledge, have the sufficient depth to deliver the required flexure and shear strength and stiffness.

Diagonal cracks at the reentrant corners between the cantilever ledges and the web in older, existing inverted-T bent caps have been reported throughout the state of Texas. Since bridge design criteria have been improved and modified over the decades, many of the early inverted-T bent caps are deficient when evaluated against the current design approach and/or lack adequate strength to support planned increases to live load demands. One example is the substructure supporting the IH 35 upper deck through downtown Austin (Figure 1.1).

Replacement of deficient bent caps is not always practical due to cost, interruption to traffic, and the acceptable condition of other parts of the structure. Therefore, techniques for strengthening these bent caps are needed. However, despite the need for robust, proven strengthening techniques of inverted-T bent caps in Texas, no formal guidance is available in current standards. As such, there is a need to investigate the effectiveness of retrofit solutions that adequately address the design deficiencies and observed in-service damage of existing inverted-T bent caps.

Figure 1.1. Inverted-T Bent Cap in Downtown Austin (Image from Google Maps).

1.2 Project Objective

This project is focused on the design and validation of satisfactory performance of strengthening existing inverted-T bent cap ledges through experimental testing. A primary objective is to demonstrate and validate, through experimental testing, the satisfactory performance of strengthening existing inverted-T bent caps. The research objectives are to:

1. Evaluate existing inverted-T bent caps based on field visits and current design methodologies.
2. Propose technical concepts to retrofit inverted-T bent caps found to be deficient using current design methodologies.
3. Evaluate the proposed retrofit solutions and make recommendations to test.
4. Conduct experimental tests on half-scaled specimens and analyze the results.
5. Develop design recommendations and provide design examples for the tested retrofit solutions.

The solutions developed by this research are expected to provide increased capacity of existing substructure components on numerous direct connectors and other bridges including the highly congested IH 35 upper deck through downtown Austin.

1.3 Report Outline

The project to design and validate solutions for strengthing existing inverted-T bent caps is documented in three reports. This report documents the background, field evaluations, and preliminary designs. The experimental test program is documented by Hurlebaus et al. (2018a). Design recommendations and a suite of design examples are documented by Hurlebaus et al. (2018b).

In this report, Chapter 2 presents a general background and strengthening methods of inverted-T bent caps. The unique behavior of inverted-T bent caps is also presented, along with the experimental results from the literature. In Chapter 3, an overview of in-service inverted-T bent caps based on the field visits and structural analysis is presented. Potential challenges to strengthening inverted-T bent caps and existing conditions of the bent caps are provided based on the field inspections. In-service inverted-T bent caps are also evaluated under current design specification to determine current status of the bent caps. Based on the evaluation, 18 potential retrofit solutions are proposed in Chapter 4. Proposed retrofit solutions are assessed in Chapter 5 using a weighted sum model (WSM). General information on the WSM, six criteria, and corresponding weighted factors are also introduced in the chapter.

CHAPTER 2. BACKGROUND

In this chapter, previous studies are reviewed to identify relevant technical information on the performance and failure mechanisms of inverted-T bent caps, strengthening methods applicable for inverted-T bent caps, and analytical models for evaluating inverted-T bent caps.

Section 2.1 describes featured behavior and failure modes of inverted-T bent caps. Section 2.2 provides an overview of retrofit solutions and results of previous studies on retrofit of reinforced concrete (RC) structures for which the results can inform the current study. Section 2.3 summarizes analytical models including the strut-and-tie model.

2.1 Behavior and Failure Mechanisms of Inverted-T Bent Caps

Inverted-T bent caps have two components shown in Figure 2.1: (1) stem or web, and (2) ledges or brackets. Loads are applied to the ledges and transferred to the web as shown in Figure 2.2. In an inverted-T bent cap, two types of reinforcement (Figure 2.1[c]) are essential: (1) ledge, which resists flexural and shear friction forces in the cantilevered ledge; and (2) hanger, which are the vertical stirrups that transfer the loads from the ledge to the web.

Flexure, shear, or flexure-shear failure modes in inverted-T beams are more complicated than the conventional. Based on the experimental tests, Furlong and Mirza (1974) identified six failure modes: flexure, flexure-shear, torsion, hanger, punching, and bracket (ledge). Flexural failure, shown in Figure 2.3(a), is characterized by the crushing of the compression face or fracture of the reinforcing steel in tension. Flexural-shear failure, shown in Figure 2.3(b), is characterized by formation of diagonal cracks in the web after the appearance of flexure cracks. This failure typically occurs when the span-to-depth ratio is small enough to have adequate flexural strength to resist the moment through the shear span. Torsional failure, shown in Figure 2.3(c), is characterized by anchorage failure of the reinforcement or crushing along spiral cracks. Hanger failure, shown in Figure 2.3(d), is defined by a vertical separation at the web-ledge interface resulting in yielding of the hanger reinforcement. Punching failure occurs when the applied load exceeds the tensile strength of the concrete along the surface of a truncated pyramid, as depicted in Figure 2.3(e). Ledge failure, shown in Figure 2.3(f), is loss of capacity of the ledge acting as a bracket. Failure can occur as a flexural failure of the ledge or as friction failure at the face of the web, in which the ledge shears off.

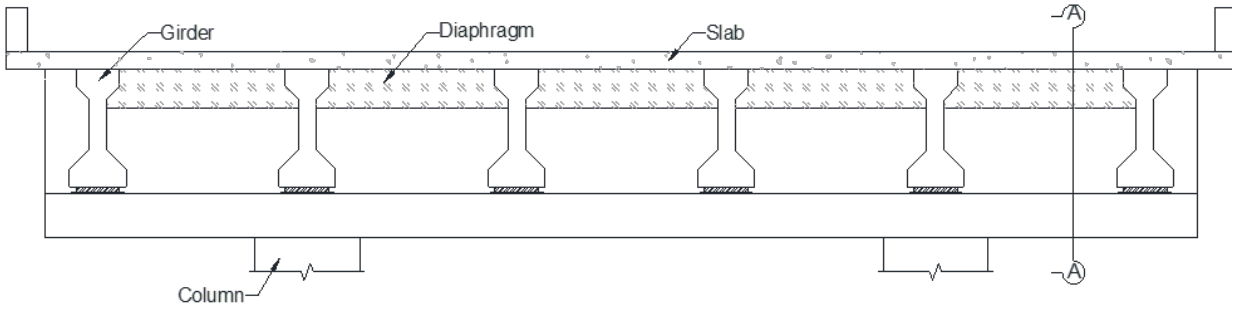

(a) Elevation

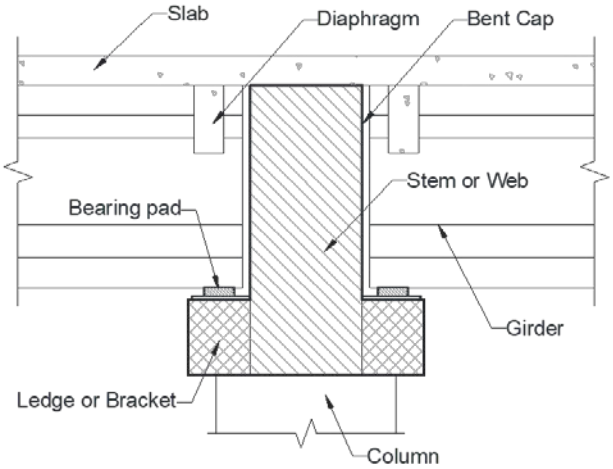

(b) Section A-A

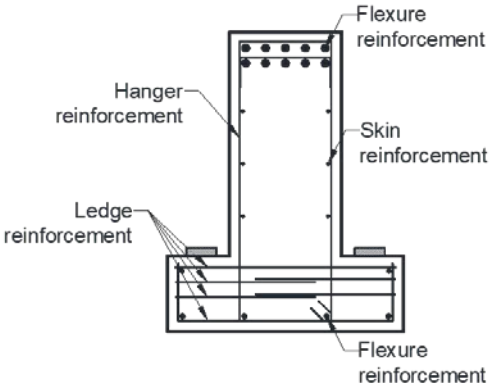

(c) Reinforcement details

Figure 2.1. Inverted-T Bent Cap Geometry and Reinforcement.

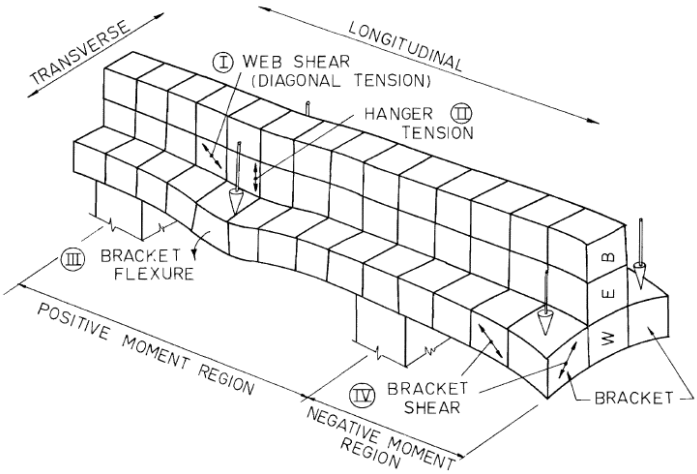

Figure 2.2. Structural Load Actions on Inverted-T Bent Cap (Furlong and Mirza, 1971).

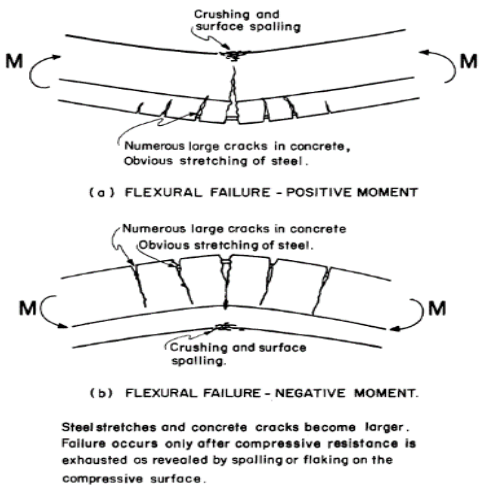

(a) *Flexural failure*

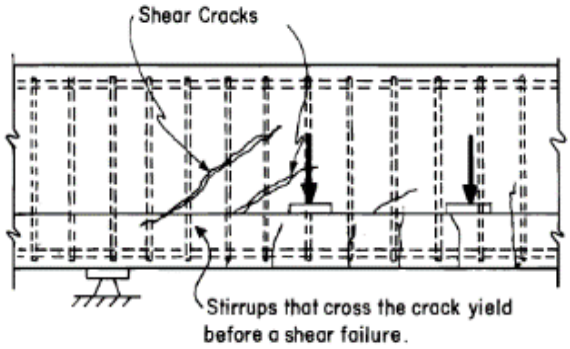

(b) Flexural-shear failure

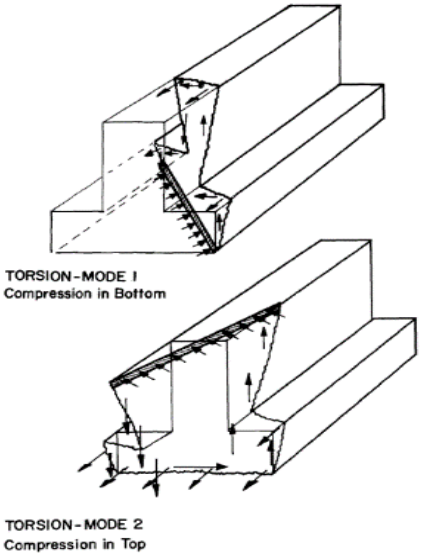

(c) Torsion failure

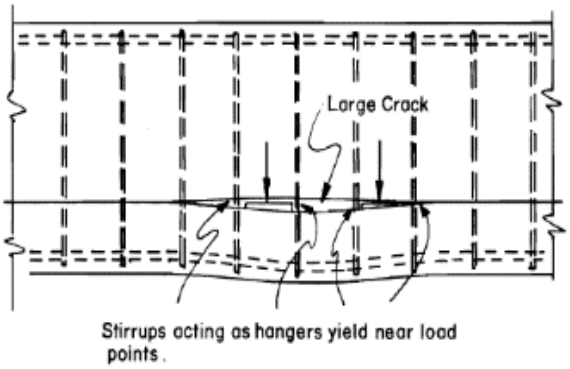

(d) Hanger failure

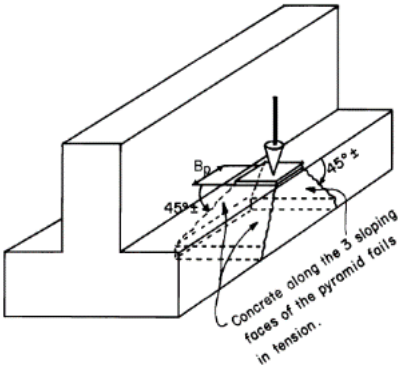

(e) Punching failure

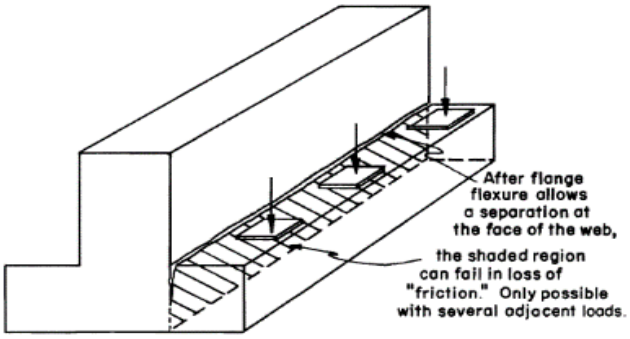

(f) Bracket failure

Figure 2.3. Failure Mechanisms of Inverted-T Bent Caps (Furlong and Mirza, 1974).

Furlong et al. (1971) carried out 24 tests on six inverted-T bent cap specimens (two full-scale and four one-third scale). In addition to testing reinforcement details specified by the Texas Highway Department at the time, the researchers investigated alternative reinforcement designs shown in Figure 2.4. Based on the test results, the authors noted that (a) loads must be supported by stirrups acting as hangers to transmit vertical forces into the body of the web, (b) flange reinforcement perpendicular to the web is necessary to deliver the flange forces to the hangers, and (c) the application of forces to flanges creates greater torsional forces on the web.

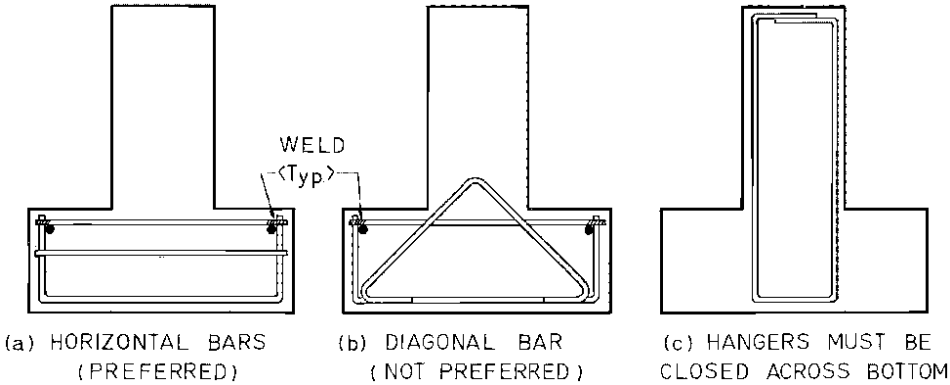

Figure 2.4. Ledge Reinforcement Details for Inverted-T Beam (Furlong et al., 1971).

Furlong and Mirza (1974) studied the strength and serviceability of inverted-T bent caps that were subjected to a combination of flexure, shear, and torsional loads. Load tests were conducted on one-third scale prestressed and non-prestressed inverted-T bent specimens. The tests revealed that the prestressed concrete members exhibited fewer cracks under service load and had lower stresses in the transverse reinforcement. Based on the experimental observations, the authors presented an analysis methodology for the reinforcement details and design of inverted-T beams. The authors recommended that for an inverted-T beam, the ledge must be sufficiently deep to avoid punching shear, the transverse reinforcement strength of the ledge must be sufficient to maintain shear friction resistance at the web face, and there should be sufficient web stirrups to act as hangers to transmit loads from the ledge to the web.

Zhu et al. (2001), Zhu and Hsu (2003), and Zhu et al. (2003), as part of TxDOT Project 0-1854, investigated the causes of diagonal cracking at the reentrant corners between the ledges and the webs of an inverted-T bent cap under service load. The authors attributed the cracks to the ultimate strength design methodology that was adopted in the design of inverted-T bents, which

did not address cracks at service loads. The study was carried out in three phases. In Phase 1 (Zhu et al., 2001), a two-dimensional (2D) compatibility-aided strut-and-tie model (CASTM) was utilized to predict diagonal crack widths in the interior portion of the inverted-T bent caps. The model was compared to the results from seven experimentally tested 2D specimens, as shown in Figure 2.5(a), that represented the dapped ends of a bridge girder. In Phase 2 (Zhu and Hsu, 2003), a three-dimensional (3D) CASTM was utilized to predict diagonal crack widths at the end faces of the exterior portion of the inverted-T bent caps. Experimental results from large-scale 3D tests that represented the end portion of an inverted-T bent cap (Figure 2.5[b]) were used to calibrate the 3D CASTM model. In the final phase (Zhu et al., 2003), two full-scale bent cap specimens were tested, as illustrated in Figure 2.5(c), to investigate impact of hanger spacing and bearing pad size on the service behavior. The following observations were made: (a) the CASTM predictions are well supported by test results; and (b) instead of checking a crack width at service limit state and comparing it to a specified value, the force producing a critical crack width can be calculated and compared to the load designed for service limit state.

Larson et al. (2013) investigated the behavior of reinforced concrete inverted-T straddle bent cap specimens to investigate the causes of diagonal cracking in the ledges. Thirty-three 27 ft 8 in. long (shown in Figure 2.6) specimens were tested to evaluate the impact of ledge depth and length, spacing of web reinforcement, number of point loads, depth of the member, and span and depth ratio. During the tests, it was observed that most of the specimens displayed a web shear failure. However, flexural failure, diagonal strut failure, punching shear, and ledge shear friction failures were also observed. The experimental results showed that increasing the ledge length along the length of the straddle bent increased the shear strength of the inverted-T beams and delayed the appearance of the first diagonal crack, whereas increasing the ledge depth did not have any significant effect on the strength. It was noted that for the diagonal cracking load of inverted-T beams, the primary variables were the shear area and the span-to-depth ratio. For the maximum width of diagonal cracks in inverted-T beams, the primary variable was the quantity of web reinforcement crossing the principal diagonal crack plane. Based on findings from the experimental study, and field inspections of selected field structures, the authors concluded that several existing structures had already been subjected to approximately 70–85 percent of their ultimate capacity.

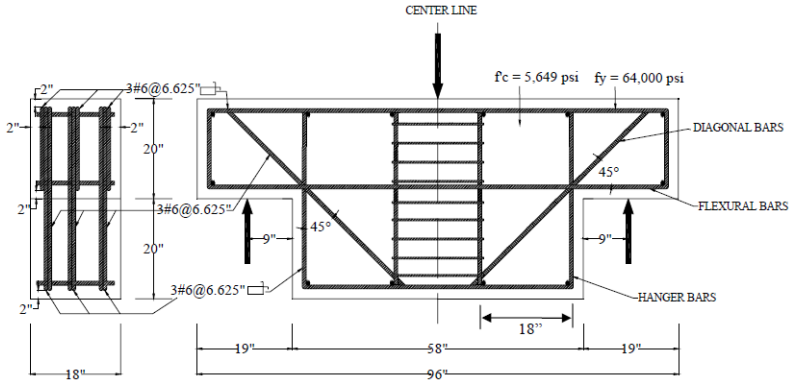

(a) 2D test specimen

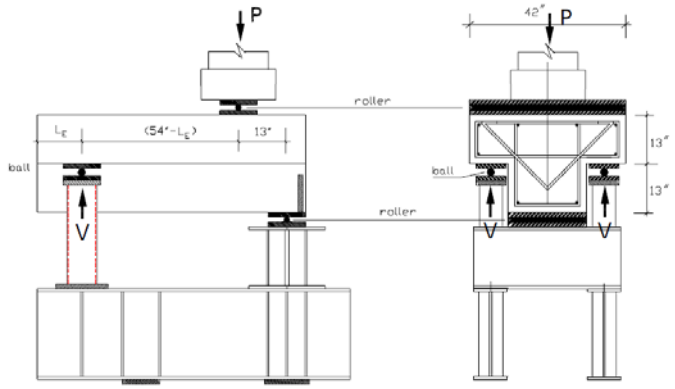

(b) 3D test specimen

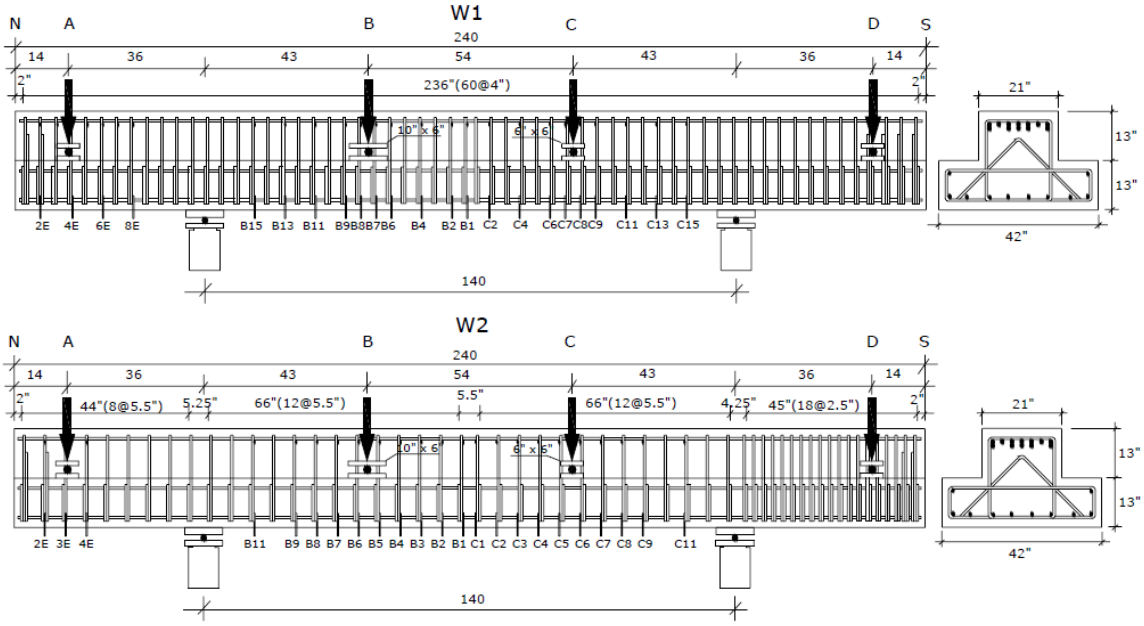

(c) Full bent test specimen

Figure 2.5. 2D, 3D, and Whole Bent Test Specimens (Zhu et al., 2001).

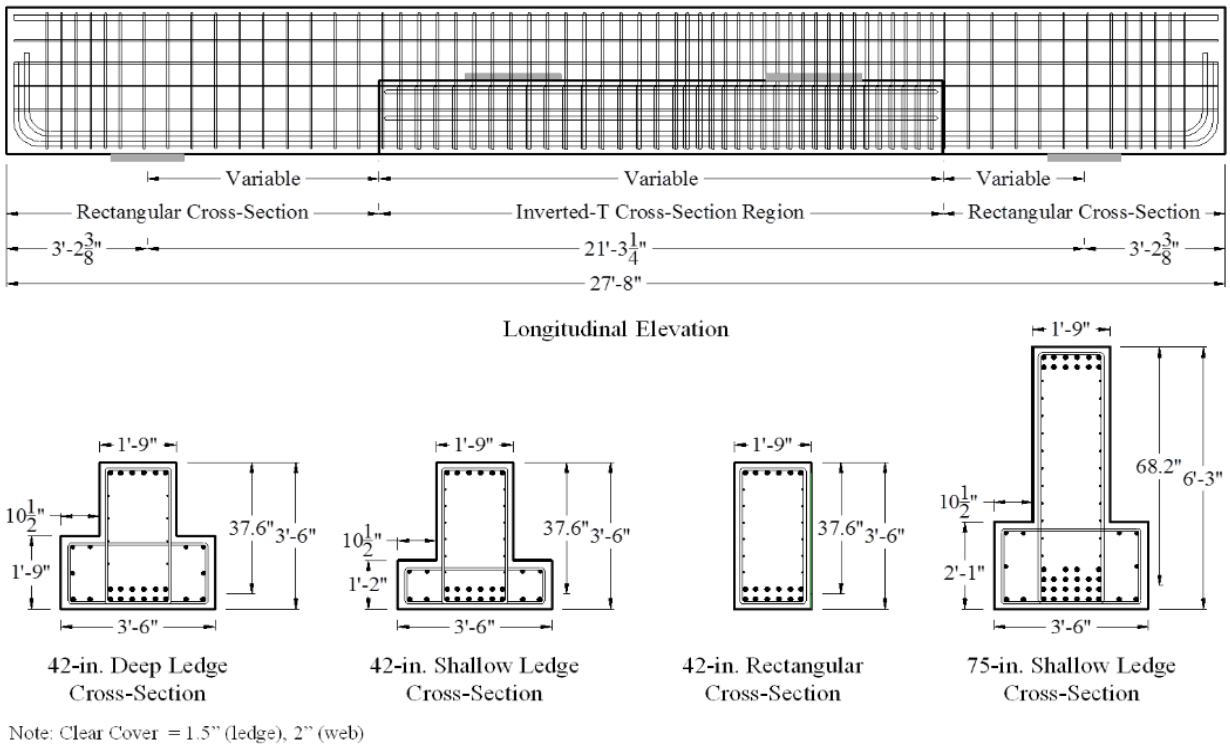

Figure 2.6. Typical Specimen Geometries (Larson et al., 2013).

Deifalla and Ghobarah (2014) investigated the behavior of inverted-T reinforced concrete beams under combined shear and torsion loads. Three inverted-T beams, shown in Figure 2.7, were tested under different ratios of applied torque to applied shear. The test setup was designed to fail the specimens in combined shear and torsion. The behavior was affected by the value of the torque-to-shear ratio. Decreasing the applied torque to the applied shear force ratio resulted in the following: (a) a significant reduction in the spacing between diagonal cracks, strut angle of inclination, cracking and ultimate torque, and flange and web stirrup strain; (b) a significant increase in the failure and cracking load, post-cracking torsional rigidity, and cracking and ultimate shear; and (c) a reduction in the efficiency of the stirrup, causing beam failure due to concrete diagonal failure rather than stirrup yield. The authors also developed an analytical model in which the inverted-T beam was divided into several rectangular subdivisions and each subdivision was analyzed independently for combined applied shear and torsion loads. The proposed analytical model showed remarkable agreement with the experimental results for the behavior of flanged beams under combined actions.

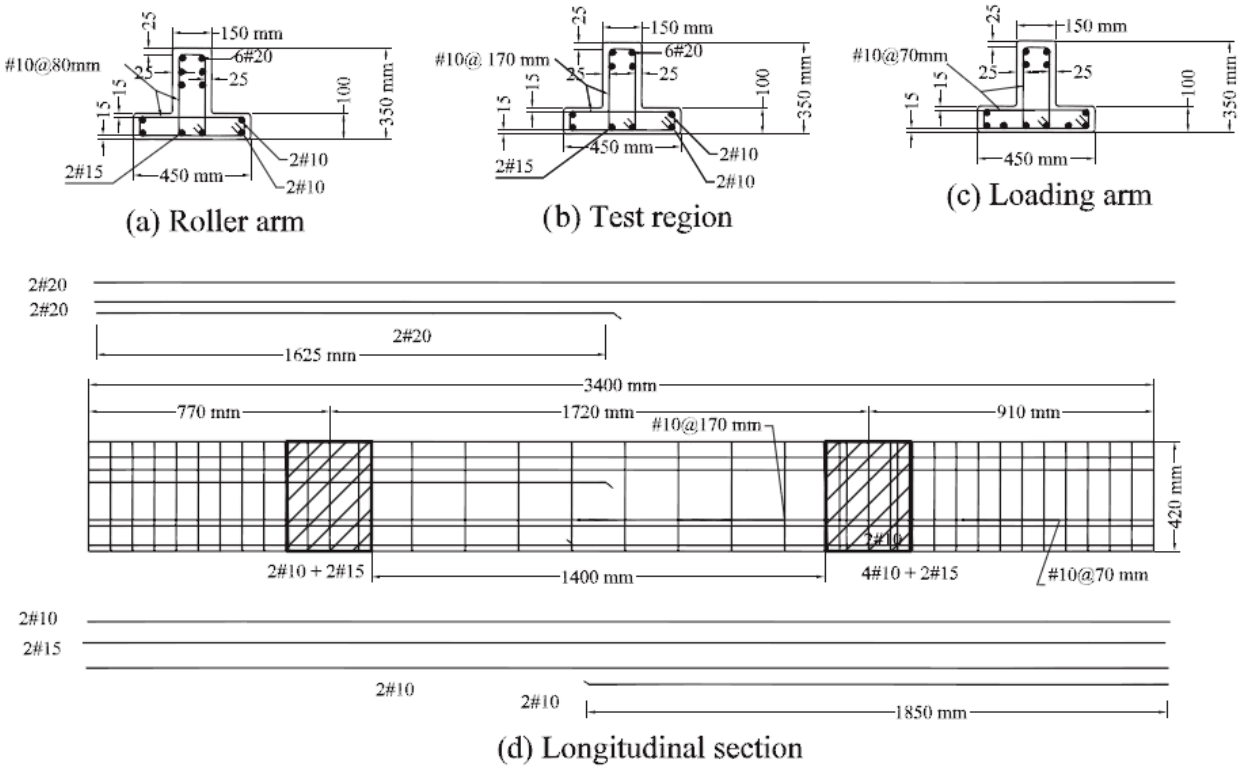

Figure 2.7. Dimensions and Reinforcement Details of Tested Beams (Deifalla and Ghobarah, 2014).

2.2 Retrofit of Reinforced Concrete Structures

ACI 364.2T (ACI Committee 364.2T, 2008) presents methods to increase the shear capacity of existing reinforced concrete structures. Several alternatives are discussed: (a) external reinforcement provided by steel rods, reinforcement bars, post-tensioning, or steel plates; (b) section enlargement using concrete, shotcrete, reinforced concrete, or mortar bonded to the concrete element; (c) internal reinforcement provided by steel or fiber-reinforced polymer (FRP) reinforcement installed by drilling holes, and the dowels being effectively grouted; (d) near-surface-mounted reinforcement provided by steel or FRP rods into grooves; (e) supplemental members; and (f) externally bonded FRP plates and strips. Factors to include in selecting a retrofit method are purpose, magnitude of strength increase required, cost, in-service conditions, dimensional and clearance constraints, aesthetics, material, and equipment availability.

Section 2.2.1 summarizes the literature on retrofit of inverted-T beams. Section 2.2.2 summarizes literature on retrofit of other T-shaped RC beams that are not ledge loaded but have retrofit challenges of value to the present study.

2.2.1 Retrofit Methods for Inverted-T Bent Caps and Beams

Galal and Sekar (2008) experimentally investigated the effectiveness of using anchored carbon fiber-reinforced polymer (CFRP) sheets to eliminate the brittle failure mechanism of the hanger, web, or flange and improve the strength of the inverted-T bent caps. Eight tests were conducted on four one-third scale specimens identical in size. The differences between the specimens were hanger, web shear, and ledge reinforcements. The reinforcement arrangement was selected to simulate three different nonductile failure mechanisms and to avoid having two or more failure modes. As shown in Figure 2.8, the CFRP sheets were wrapped in different configurations to investigate their effectiveness in rehabilitating the hanger, web, and ledge (or flange) zone. Multiple anchoring systems were used: (a) thread rod anchors at the web with the curved angle plate with concave grout to avoid debonding, particularly near reentrant corners; and (b) CFRP fan-type anchor or fiber anchors at the loading plates (Figure 2.8[a]). Experimental results indicated that the anchored CFRP sheets were effective in improving the displacement ductility and the load-carrying capacity of the inverted-T bent cap. CFRP was used to confine the web-compression zone of the inverted-T bent cap to ensure the development of full flexure capacity of the bent cap. The anchored CFRP zone showed better performance compared to not using the fiber anchors.

2.2.2 Retrofit Methods for Standard T-Shaped Concrete Structures

Shahawy and Beitelman (1999) investigated the effectiveness of externally bonded CFRP sheets for flexural strengthening of RC T-beams using experimental tests. The specimens had a flange thickness of 2.32 in., a flange width of 23 in., an overall height of 17.5 in., and a tapered web thickness of 5.91 in. at the flange and 3.58 in. at its bottom. Sixteen specimens, 10 with static loading and six with fatigue loading, were tested in this study. The webs of the specimens were partially or fully wrapped with one, two, three, or four layers of CFRP sheets. The loads were applied at the top of the T-beams as shown in Figure 2.9. Both the partially and fully wrapped specimens were loaded incrementally to failure for the static test. Fatigue testing was performed using fully wrapped specimens. The fatigue loading was sinusoidal and ranged from 25 percent to 50 percent of the capacity of the control specimen at a frequency of 1 Hz. Based on the experimental results, it was evident that the externally bonded CFRP laminates were effective in improving both static and fatigue performance of RC T-beams. The full wrapping technique was found to be more effective than the partial wrapping technique for increasing capacity. However, the limited number of tests failed to support a definitive conclusion.

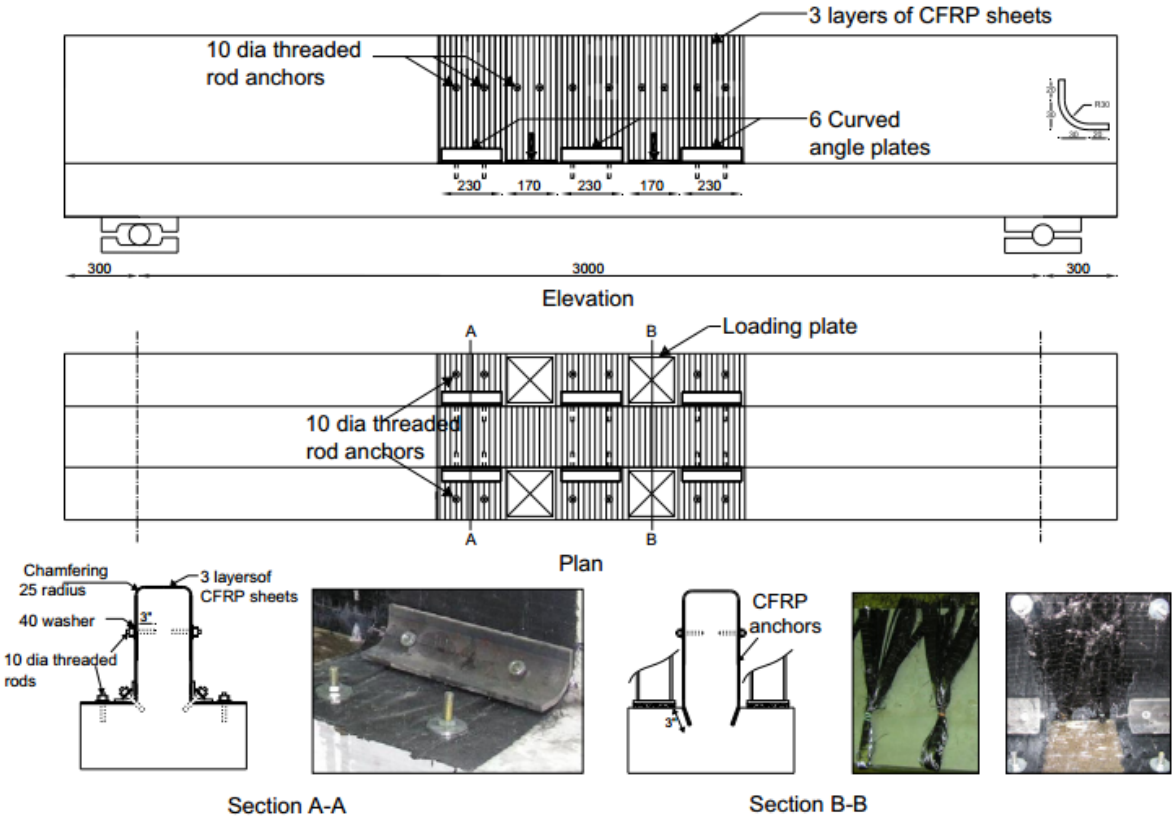

(a) Rehabilitation of hanger zone with fiber anchors

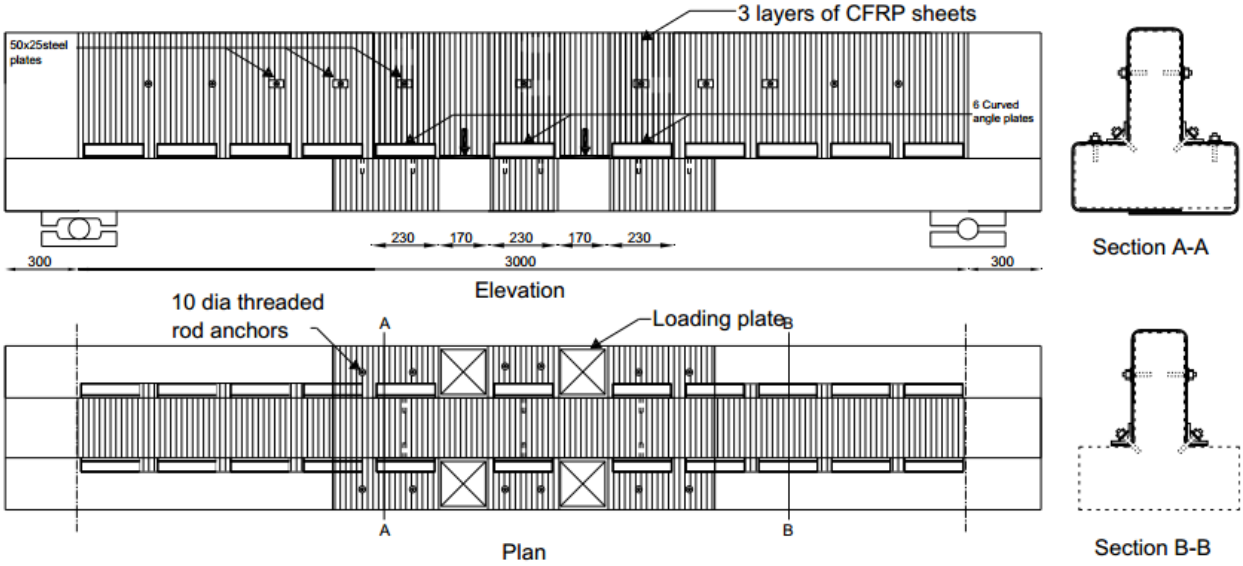

(b) Rehabilitation of hanger zone without fiber anchors

Figure 2.8. Anchored CFRP Rehabilitation Schemes Using Angle Plate (Galal and Sekar, 2008).

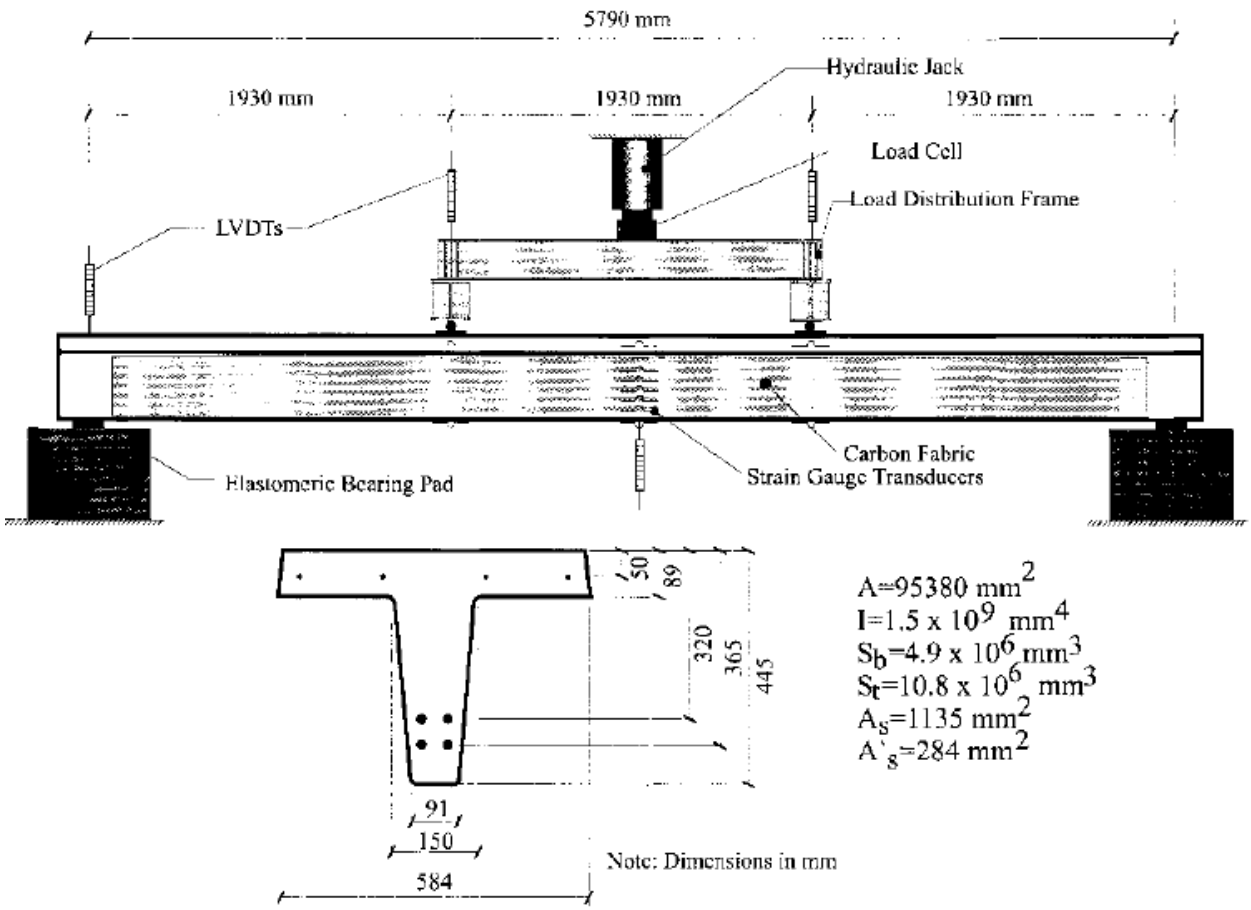

Figure 2.9. Details of Specimens and Test Setup (Shahawy and Beitelman, 1999).

Basler et al. (2003) investigated the use of bonded CFRP L-shaped plates as a method of shear strengthening reinforced concrete beams. The L-shaped brackets had a 90-degree bend with an internal radius of 1 in. and were about 0.055 in. thick. For improved anchorage, the ends of the plate legs to be anchored were coated with a thin layer of adhesive. Advantages of L-shaped CFRP plates include ease of installation, light weight, resistance to corrosion, high strength, predictable mechanical properties, and ability to be produced consistently in a manufacturing unit. Test results indicated that the L-shaped plates were effective in improving the shear capacity of tee beams. In addition, the L-shaped CFRP plates remained undamaged, but local debonding was observed on the sides of the beam.

Nanni et al. (2004) experimentally investigated full-scale prestressed concrete bridge girders strengthened with externally bonded precured CFRP laminate. Two damaged prestressed concrete double-T-shaped girders were taken from an overloaded bridge in Kansas and cut longitudinally to provide four single-T specimens. The specimens had a flange thickness of 5 in.,

a flange width of 36 in., an overall height of 23 in., and a web thickness of 4.5 in. The total length of the specimen was 40 ft. One specimen was left unstrengthened and tested as the benchmark. Two specimens were strengthened with FRP laminates in flexure, while the remaining specimen was strengthened in flexure with FRP laminates and in shear with near-surface mount (NSM) CFRP rectangular strips, as shown in Figure 2.10. The CFRP strips were installed into 0.25 by 0.75 in. grooves with an incline of 60 degrees for shear strengthening. The shear capacity of the specimen increase of shear and flexure strength could not be obtained since the specimen failed due to flexure FRP laminate debonding. However, it was observed that this specimen had a substantially larger ultimate capacity than the specimens strengthened only in flexure.

Higgins et al. (2009) and Howell (2009) experimentally investigated the effect of various shear strengthening techniques on the performance of reinforced T-shape girders. Fifteen full-scale inverted-T beam specimens were tested under four-point bending loads as shown in Figure 2.11. The inverted-T beam specimens, designed to fail in shear, had an overall height of 48 in., a flange width of 36 in., a web width of 14 in., and a flange thickness of 6 in. The specimen length was 26 ft. The specimens were loaded incrementally on the top of the web to produce initial cracking. After the crack initiation, the specimens were strengthened for shear with epoxy injection, external steel stirrups, internal steel stirrups, surface-bonded CFRP stirrups, or NSM FRP, as shown in Figure 2.11. The retrofitted specimens were then loaded to failure. Based on the experimental results, it was evident that the external steel strips, internal steel strips, and surface-bonded CFRP strips were effective in improving the shear capacity of the specimens, while the epoxy injection and FRP NSM retrofit solution was found to be ineffective. To increase shear capacity of the specimens, the authors suggested a reduction of FRP strip spacing. The effect of internal steel strips on the long-term service life performance of the structure were found to be relatively outstanding among these retrofit solutions. No specific recommendation for a single retrofit solution was made.

Galal and Mofidi (2010) experimentally investigated the use of mechanically anchored unbonded dry carbon fiber (CF) sheets for the shear strengthening of T-beams. The method essentially eliminated the debonding of epoxy-bonded CFRP sheets and fully utilized the capacity of dry CF sheets. In this technique, the dry CF sheets were wrapped around and bonded to steel rods, which in turn were anchored to the corners of the web-flange intersection of the T-beam

using bolts. The higher tensile strength and modulus of elasticity of dry CF compared to CFRP helped increase the shear strength of the T-beam.

Deifalla and Ghobarah (2010a) experimentally investigated techniques to strengthen T-beams using CFRP. Six T-beam specimens, two control and four strengthened beams, were tested under combined torsion and shear loading. As shown in Figure 2.12, four CFRP configurations—(a) anchored U-jackets, (b) extended U-jackets, (c) full wrapping, and (d) combination of full wrapping and extended U-jacket—were used to strengthen the damaged tee beams. Techniques (a) and (b) were used when the flange was inaccessible, while techniques (c) and (d) were used where there was unrestricted access to the entire beam. From the experimental results, it was noted that the retrofit techniques significantly improved the shear torsion carrying capacities, post-cracking stiffness, and deformability of the retrofitted tee beam compared to the control specimen. Although the full wrapping techniques were the most effective, the implementation of these techniques is rare because of limited access. The U-jacket, which is the most widely used technique that is applicable to various applications, was the least effective solution. However, the extended CFRP U-jacket solution proved to be a viable and effective alternative and considerably improved the ductility when compared to the U-jacket.

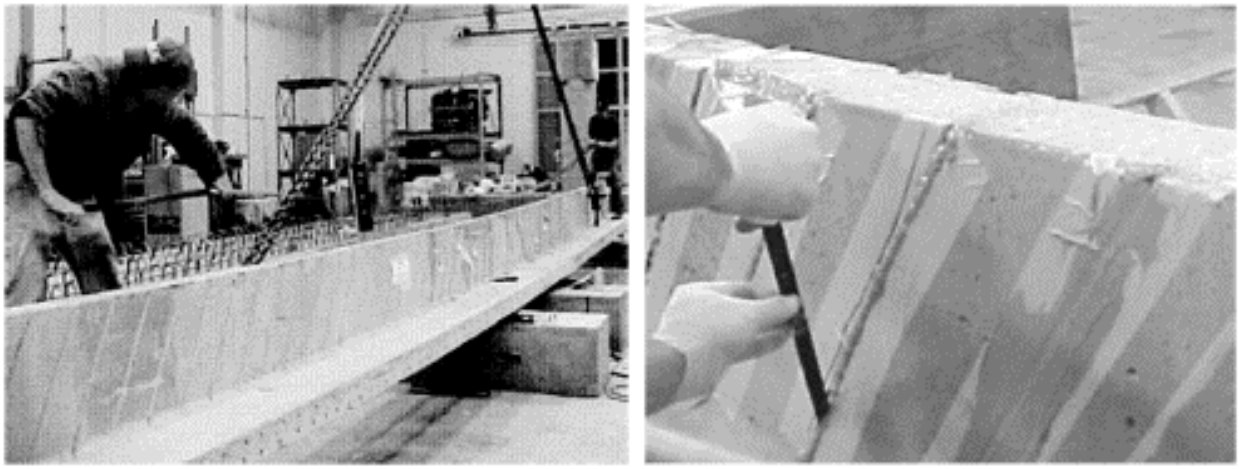

(a) Flexural strengthening installation *(b) Installation of rectangular CFRP bar for shear strengthening*

Figure 2.10. Specimen Strengthening (Nanni et al., 2004).

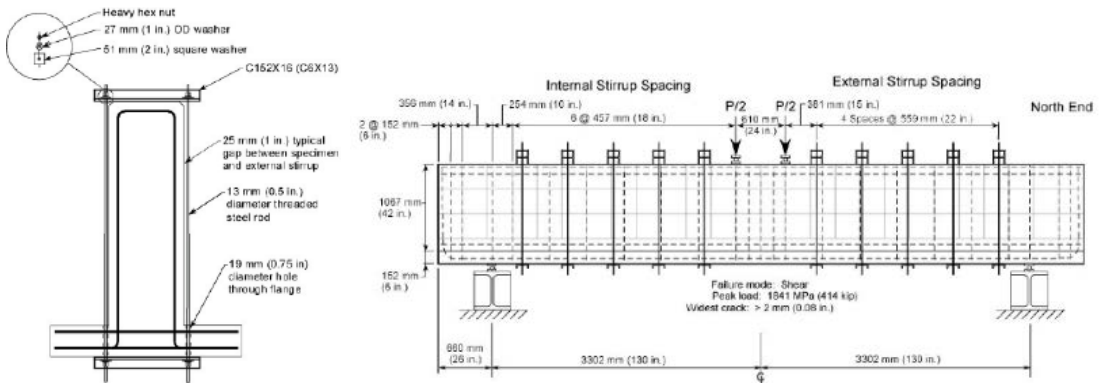

(a) External steel stirrup repair

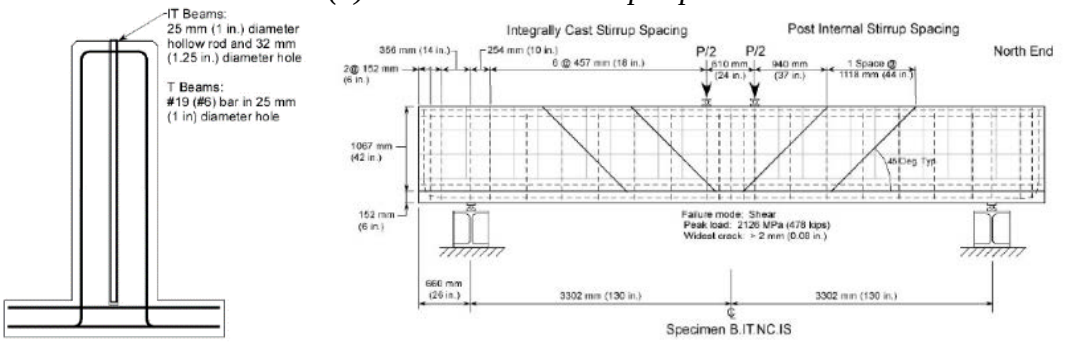

(b) Internal steel stirrup repair

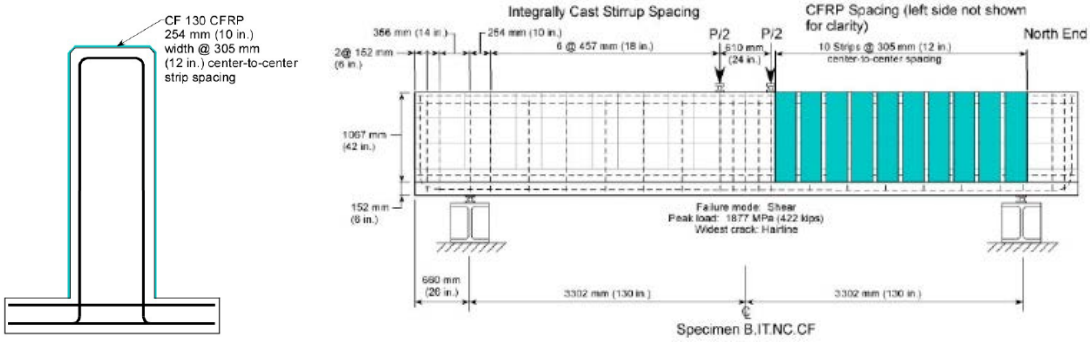

(c) Surface-bonded CFRP strip repair

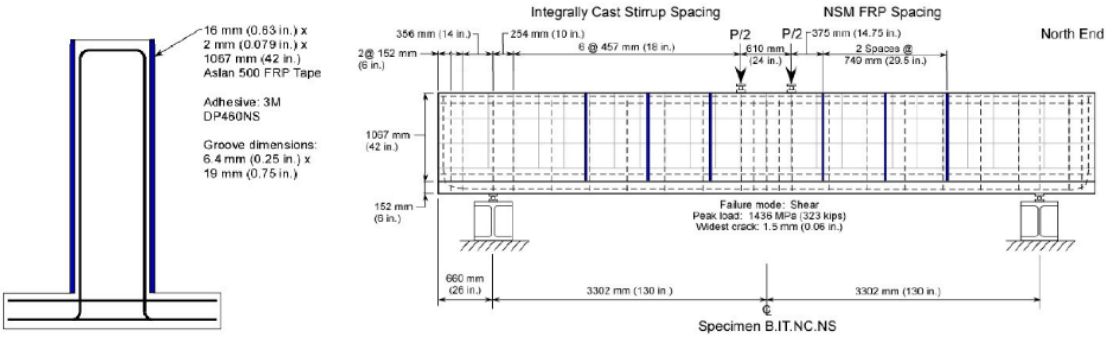

(d) NSM FRP repair

Figure 2.11. Repair for Specimens (Higgins et al., 2009).

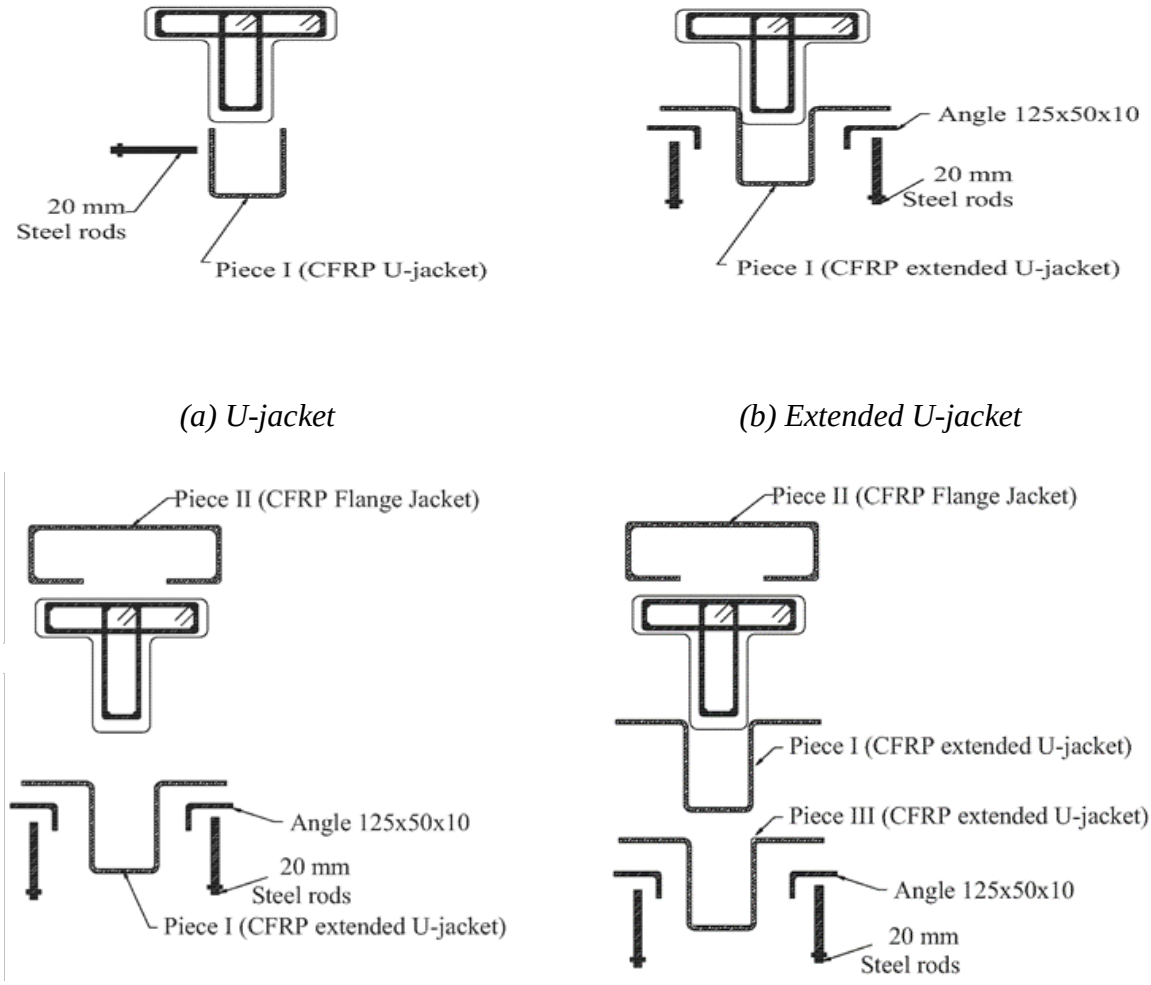

(a) U-jacket *(b) Extended U-jacket*

(c) Full wrapping *(d) Combined gull wrapping and extended U-jacket*

Figure 2.12. Strengthening Schemes (Deifalla and Ghobarah, 2010a).

Deifalla et al. (2013) further investigated the effectiveness of FRP as a method to externally strengthen the flanges of beams subjected to torsion. Unanchored U-jacket strips, anchored U-jacket strips, and extended U-jacket strips were investigated. Various wrapping configurations, like continuous wrapping, vertical strips, and inclined strips were considered. As expected, the anchored solution resulted in greater ultimate strength and ductility compared to the unanchored solutions. The anchored inclined U-jacket strip showed results comparable to the inclined fully wrapped strips. In addition, the extended vertical U-jacket was found to be more effective compared to the vertical U-jacket strip technique.

DeLorenzis and Nanni (2001) investigated shear strengthening of reinforced concrete T-beams by NSM CFRP rods as shown in Figure 2.13. Eight RC beam specimens with a T-shaped cross-section were tested. Specimens were tested under four-point bending. For the strengthened specimens, vertical or 45-degree grooves were saw-cut on the surface of both web sides over the full depth. Deformed CFRP rods were then embedded in epoxy-filled grooves. The examined variables included spacing of the rods, strengthening pattern, end anchorage of the rods, and presence of internal steel shear reinforcement. It was found that the NSM CFRP rods were effective in increasing the shear strength capacity of the reinforced concrete T-beams with and without shear reinforcement. The specimen with CFRP rods at 45 degrees exhibited the largest strength increase. One of the failure modes observed in the strengthened specimen was the debonding of one or more CFRP rods due to splitting of the epoxy cover. This mechanism could be prevented by increasing the bond length by embedding the bars in the flange or using 45-degree rods at a sufficiently close spacing. Splitting of concrete cover of the longitudinal reinforcement was observed as the controlling factor in beams where debonding was prevented.

Figure 2.13. Vertically and Diagonally Mounted Near-Surface FRP Rods after Failure (DeLorenzis and Nanni, 2001).

Dias et al. (2007) carried out an experimental study on low-strength concrete T-beams reinforced in shear with NSM CFRP strips. Three control specimens without CFRP reinforcement and 10 NSM shear-strengthened specimens that had different amounts of CFRP strips at 45 degrees, 60 degrees, and 90 degrees were tested. Specimens had internal steel stirrup spacing of 11.81 in. or 7.09 in. CFRP strips applied at 45 degrees and 60 degrees showed better performance than the one at 90 degrees. The authors noted that increasing the amount of internal

steel stirrups proportionally reduces the contribution of the CFRP strips, and reducing the concrete strength can increase the likeliness of detachment of the cover containing the glued laminates.

Dias and Barros (2008) tested additional T-beams reinforced with NSM CFRP to evaluate the influence of the percentage and inclination of the CFRP laminates on the effectiveness of the NSM shear strengthening. The dimensions, CFRP, and groove size of the test specimens were the same as the specimens reported in Dias et al. (2007). Specimens with no internal shear reinforcement and internal steel stirrups spaced at 5.12 in. and 11.81 in. on the center were tested in this study. Inclination angles of 45 degrees, 60 degrees, and 90 degrees were investigated. Three quantities of NSM CFRP were applied to each inclination angle. Specimens were subjected to service loads based on a deflection of L/400 and maximum loads. Based on the test results, it was determined that the CFRP strips with an inclination angle of 60 degrees were the most effective among the adopted shear strengthening arrangements, and the strips at 45 degrees were more effective than those at 90 degrees. Retrofitted specimens, without and with internal steel stirrups spaced at 5.12 in., were able to achieve nearly the same maximum load. The authors also noted that the NSM-CFRP reinforcing contributed significantly to the stiffness of the specimen after the formation of the shear crack. Similar to previous studies of Dias et al. (2007) and Dias and Barros (2008), Dias and Barros (2010) tested T-shaped RC beams reinforced in shear with NSM CFRP. In addition to NSM reinforcing, the tests also included specimens strengthened in shear with an externally bonded reinforcement (EBR) technique. It was found that the NSM strengthening technique more effectively increased the shear capacity of the specimens than did the EBR strengthening technique.

Goebel et al. (2012) investigated the effectiveness of NSM CFRP as a method to strengthen the shear capacity of girders. Ten full-sized specimens were built. One side of each was over-reinforced in shear to induce failure in the side retrofitted with NSM CFRP, as shown in Figure 2.14. The specimens were tested in four-point bending while loads were applied at the top of the web. After the crack initiation, the load was removed, and the same loading sequence was repeated to obtain baseline behavior of the specimen under the fully cracked condition. Then specimens were loaded to failure after vertical-oriented NSM CFRP strips were installed for shear strengthening. Test results indicated that NSM CFRP transverse reinforcing significantly affected the shear capacity of specimens. The performance of the NSM CFRP retrofit under fatigue loading

and environmental exposure had minimal impact on the shear capacity of the specimen. Recommendations for the design of shear strength with NSM CFRP were provided.

Chaallal et al. (2011) noted that the FRP strengthening methods for shear strengthening may have high potential for debonding and require surface preparation, and there is high uncertainty in the FRP-to-concrete bond. As shown in Figure 2.15, the authors tested the embedded through-section (ETS) FRP method wherein vertical holes were drilled through the middle of the cross-section, after which the holes were cleaned and filled two-thirds with epoxy adhesive. The CFRP rods were also coated with a thin layer of epoxy and installed in the hole. The authors tested externally bounded (EB) CFRP (Figure 2.15) and NSM FRP rods in which grooves were made on both sides of the web, cleaned, and filled two-thirds with epoxy, and then FRP bars coated with a thin layer of epoxy were installed in the grooves. T-beam specimens with and without transverse reinforcement were considered for this experimental study. From the experimental tests, it was evident that the ETS FRP system significantly enhanced the shear capacity of the beam even with limited amounts of transverse reinforcement. Flexure failure occurred in beams with the ETS FRP system, whereas sheet debonding and separation of side concrete were observed in the EB FRP and NSM FRP solutions, respectively. Because the FRP rods in the ETS method were embedded in the core concrete, the contribution of ETS FRP did not decrease in the presence of transverse steel reinforcement, whereas the contributions of EB FRP and NSM FRP were negligible in beams with transverse reinforcement.

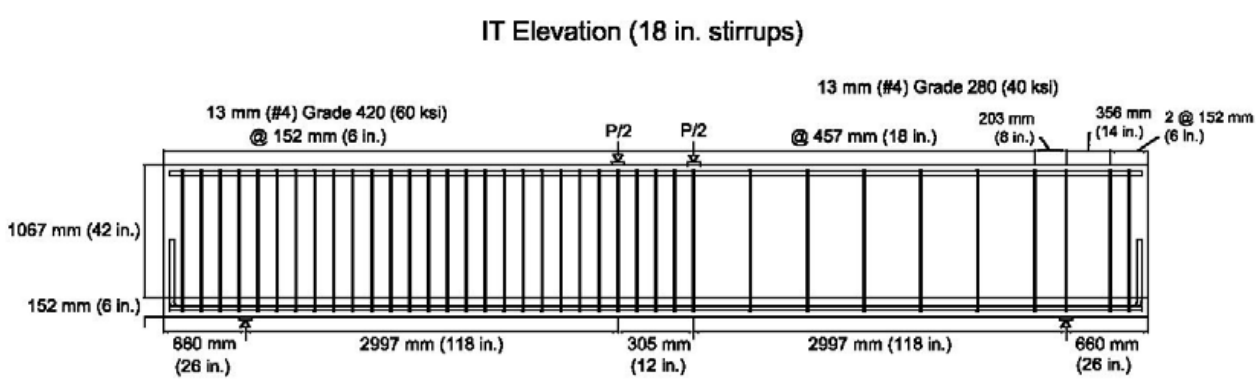

Figure 2.14. Specimen Elevation View with Internal Steel Reinforcing (Goebel et al., 2012).

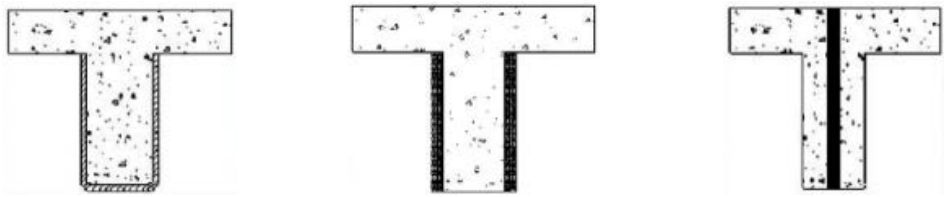

(a) EB CFRP sheets *(b) NSM FRP rods* *(c) ETS FRP rods*

Figure 2.15. Various Retrofit Techniques Tested by Chaallal et al. (2011).

Breveglieri et al. (2015) experimentally investigated the effectiveness of ETS steel bars and CFRP rods on the shear strengthening of RC T-beams. Nineteen specimens were tested under three-point bending with a shear span of 35.4 in. The specimens had an overall height of 14.2 in., a web thickness of 11.8 in., a web width of 7.1 in., a flange thickness of 3.9 in., a flange width of 17.7 in., and a total length of 8 ft 8 in. The examined variables in this study included the inclination angle of the ETS bars and the percentage of internal transverse reinforcement ratio of the specimens. ETS bars at a spacing of either 7.1 in. or 11.8 in. were placed in between existing stirrups to increase the effectiveness of the strengthening technique. From the experimental tests, it was evident that the ETS strengthening technique significantly enhanced the load-carrying capacity of the specimens. The inclined ETS bars were found to be more effective for capacity increase than the vertical ETS bars. It was also noted that the contribution of the ETS strengthening technique decreased with the increase in internal transverse reinforcement ratio.

2.3 Analytical Models

Inverted-T bent caps are typically under complex states of stress along most of their spans. The disturbed stress regions are induced by changes in the cross-section as well as the application of concentrated loads and reactions. Since sectional design is not applicable for disturbed regions, alternative models are needed.

2.3.1 Strut-and-Tie Modeling (STM) and Modifications for Analytical Studies

STM is a lower-bound, force-based, equilibrium analysis approach used for design and analysis of disturbed regions (D-regions) in concrete structures. STM reduces complex states of stress within a D-region into a truss comprised of simple, uniaxial load paths. It offers a rational approach for obtaining conservative solutions for the strength design of deep beams and the connection region. However, the STM may not provide sufficient information on the overall

force-deformation behavior of the structure. To address this shortcoming, a compatibility strut-and-tie model (C-STM) was developed for analyzing the nonlinear force-deformation behavior of disturbed regions and concrete deep beam structures. While STM is unable to easily discriminate between uncracked and cracked performance, such discrimination is a built-in feature of C-STM performance analysis. C-STM can easily be extended to accommodate a cracked versus uncracked torsional analysis provided it gives good insight into the internal behavior and the final cause of failure and failure mode of the structure that can be used to identify the regions that will need strengthening solutions.

Hwang and Lee (1999) used a softened truss model that satisfied equilibrium, compatibility, and material constitutive laws to determine the shear strength of exterior beam-column joints under seismic loading. The statically indeterminate system was comprised of a diagonal mechanism with a single diagonal compression strut; a horizontal mechanism with a horizontal tie and two flat struts; and a vertical mechanism with a vertical tie and two steep struts. The joint shear strengths computed from the model compared well with experimental data. Although this method effectively considers compatibility, constitutive material relations, and softening effects of cracked reinforced concrete, it is unable to provide the global deformational behavior.

Kim and Mander (1999; 2000a) developed a cyclic inelastic STM approach in order to study the structural behavior under a combination of shear and flexure. Both constant angle truss and variable angle truss were investigated, and a numerical integration scheme was adopted to enable the proper selection of element models and their dimensioning. The model captured the combined response of shear and flexure. Kim and Mander (2000b) presented a theoretical framework around the STM approach to predict the inelastic performance of beam-column joints. It was demonstrated that the post-elastic behavior of beam-column joints could be effectively modeled using the SAT technique with a fan-shaped crack pattern. Kim and Mander (2007) studied the influence of transverse reinforcement on the cracked elastic shear stiffness of concrete elements. Various truss models were studied to investigate the viability of using the more convenient continuum truss model instead of the discrete truss model without losing accuracy. From the study, it was concluded that the shear deformation and strength behavior of a cracked reinforced concrete beam column could be represented by any reasonable constant angle or variable angle truss model.

Zhu et al. (2001), Zhu and Hsu (2003), and Zhu et al. (2003) developed 2D and 3D analytical models called the CASTMs to predict the diagonal crack widths in the internal and external portion of bent caps, respectively. The model was calibrated using the results that were obtained from experimental tests on 2D and 3D inverted-T bent cap specimens. Equations were proposed based on CASTM to predict diagonal crack widths at the reentrant corners of inverted-T beams. In the final phase of the project, it was shown that the proposed model was able to predict the diagonal crack widths of the test specimen that represented both 2D and 3D portions of the bent cap. However, no estimation was made on the overall force-deformation behavior or the mode of failure of the specimens.

To et al. (2001) explored if STM is capable of capturing the nonlinear force-displacement response of reinforced concrete structures. All the constituent members of the STM were located at the force centroid of the corresponding force-transfer mechanism. From their STM models, the authors were successful in modeling the force-deformation behavior and predicting the events that caused certain nonlinear behavior in the structure. However, the models were not representative of the reinforcement layout of the actual structure, various factors were used to model the compressive strength of the concrete compressive struts, and separate models were used to model joint opening and joint closing.

To et al. (2009) proposed a hybrid modeling solution that incorporated nonlinear STM into conventional planar frame modeling technique. The hybrid model captured the beneficial aspects of both the STM and planar frame models and proved to be a time-effective modeling solution compared to the STM. However, as in the earlier model by the authors, various arbitrary reduction factors were applied to obtain the effective strength of the concrete struts and elastic stiffness, thus making it difficult to implement in practical areas.

Mander et al. (2012) and Scott et al. (2012a; 2012b) formulated a C-STM for analyzing the nonlinear force-deformation behavior of structural concrete members with significant D-regions. In this formulation, the deformation compatibility and the nonlinear constitutive material properties were considered in addition to the normal STM force equilibrium conditions. The C-STM was presented as a minimalist computational analysis tool. Based on a convergence study, it was determined that the proposed single-point Gauss truss model was sufficient to capture the truss mechanism for a cantilever system. The truss and arch action that contributed toward the shear mechanism were modeled based on the reinforcement layout. It was also noted that post-

analysis strength checks that were not implicitly modeled in the C-STM had to be performed to identify critical failure mechanisms. C-STM was used to model the force-deformation response and the internal nonlinear strain behavior of structures with significant D-regions. The C-STM was validated against three large-scale reinforced concrete bent cap specimens. The overall force-deformation behavior of the bent caps modeled by the C-STM compared well with the experimental results. The C-STM was able to model the internal strains of the structure with good accuracy and gave insight into the progression of the nonlinear mechanisms within the structure. The authors, however, noted that the C-STM was unable to accommodate the second-order effects associated with the compression softening of concrete struts.

The shortcoming was later addressed by Mander et al. (2015), where the softened concrete model was implemented and validated using a nonlinear displacement-control analysis approach. These modifications not only allowed consideration of the loading and unloading curve but also enabled the researchers to determine the displacement corresponding to the failure load with good accuracy. In addition, the authors were able to include the effects of concrete deterioration phenomena into the C-STM model by making appropriate modifications to the material properties and taking into effect the additional forces created by the deterioration mechanisms.

Pan and Li (2013) developed a truss-arch model to predict the shear strength of shear critical reinforced concrete columns subjected to cyclic loading. The proposed model took into account the contributions of concrete and transverse reinforcement to shear in the truss model, and the concrete contribution to shear strength provided by the arch action. The deformation compatibility between the truss model and the arch model were incorporated into the model. The experimental results that were considered in this study indicated that the shear span-to-depth ratio and the axial-load ratio had significant effect on the shear strength of reinforced concrete columns. From the comparison of the measured and predicted shear strengths, a good agreement was found. This indicated that the recommended model represented the effects of the shear span-to-depth ratio and the axial-load ratio well.

2.3.2 Other Analytical Models

Karayannis (1995) proposed an algorithm for the prediction of the torsional behavior of concrete elements with irregular cross-section shapes. The method accounts for the tension softening of concrete and uses a finite difference scheme resulting from a second-order finite element shape

function. Comparisons of predicted behavior of concrete elements with three different cross-section shapes were evaluated using available experimental data. The rectangular-shaped specimen was tested under pure torsion, while L- and T- shaped specimens were tested under pure torsion and combined torsion, bending, and shear. Results indicated that the proposed analytical model accurately predicted torsional behavior of concrete elements, even under combined loading.

Rahal and Collins (1995) developed an analytical model capable of analyzing rectangular reinforced concrete sections subjected to combined biaxial bending, biaxial shear, torsion, and axial load. The model, based on the modified compression field theory (MCFT), provides a check on spalling of the cover of concrete section under combined shear and torsion. This model was adapted by Deifalla and Ghobarah (2010b) and used to analyze RC beams wrapped with FRP. Deifalla and Ghobarah (2014) further adapted the analytical model and applied the model to inverted-T reinforced concrete beams under combined shear and torsion loads. The inverted-T beam was divided into several rectangular subdivisions, and each subdivision was analyzed independently for combined applied shear and torsion loads. The analysis approach was used to model the torsional behavior of the structure up to the ultimate limit state and found to agree well with the experimental results.

Thomsen et al. (2004) analytically investigated the failure mechanisms of RC beams strengthened in flexure with externally bonded FRP. A nonlinear RC beam element model based on a two-node, Euler-Bernoulli RC beam model with bond-slip between the concrete and FRP plate was adopted in this study to investigate the effect of following parameters that may affect the failure modes of composite action: FRP plate length, width, stiffness, and loading type. The element was modeled using the finite element program FEAP. The element is unable to capture a shear failure in a beam since it does not explicitly consider shear deformations.

Hassan et al. (2007) conducted a study on the ability of a finite element model (FEM) to analyze L-shaped, precast, prestressed concrete spandrels constructed with open web reinforcement. The ANATECH Concrete Analysis Program (ANA-CAP) was used in this study to model the behavior of the L-shaped concrete spandrels. The prediction of compressive behavior of modeled concrete material was based on computational plasticity, and the tensile behavior was based on a smeared cracking method. The stress and stiffness of the reinforcing steel were superimposed on the concrete element. The prestressing force was applied gradually to the

spandrel ends in the model to replicate the transfer length of the strands. The proposed FEM also took into account the effects of concrete cracking. The predicted behavior was evaluated against available experimental data and found to be in good agreement with the measured data except the creep effectiveness.

Thiemamn (2009) investigated the behavior of the beam-to-girder connection of an inverted-T bent cap beam bridge using ABAQUS finite element software. A prototype bridge analysis model with an inverted-T bent cap, bearing pads, girders, and a slab with reinforcing bars and prestressing strands was developed. A damage plasticity model, which is suitable to capture the true behavior of concrete under low confining pressures, was assigned to the concrete material. The bearing pads were modeled monolithically to the bent cap ledges. The prediction of the damaged plasticity model performed well in confinement effects but was unable to accurately capture the tensile behavior of concrete under flexure.

Higgins et al. (2009), Howell (2009), and Goebel et al. (2012) used Response 2000 (R2K) and VecTor2 computer programs to predict the structural behavior of normal and strengthened concrete beams. R2K is a sectional analysis program based on the MCFT developed by Bentz (2000). It was noted that R2K is a free program that is effective to predict the behavior of reinforced concrete beams. VecTor2 is a non-commercially available nonlinear finite element program. It was noted that the program predicts the response of concrete elements subjected to in-plane normal and shear stresses only. The cracked concrete can be modeled as an orthotropic material with smeared, rotating cracks. It was also noted that the program can capture the post-cracked load-deflection behavior of repaired concrete beams.

2.4 Summary

In light of the foregoing literature review, the following key research questions related to the strengthening of inverted-T bent cap ledges arose.

Q1: What are the increase in load demands for the vintage of inverted-T bent caps designed and constructed under per 1994 American Association of State Highway and Transportation Officials (AASHTO) load and resistance factor design (LRFD) bridge design specifications?

Comment: Many of the existing inverted-T bent caps would have been designed during the working stress era prior to the 1990s. A greater understanding now exists of the critical shear issues in concrete structures. Moreover, the load demands under HL-93 have increased specifically if the owner chooses to restripe a bridge for three lanes compared to the two lanes assumed at the time of design.

Q2: What is the hierarchy of failure mechanism (weakest-to-strongest links in the chain of resistance) for inverted-T bent caps for (a) cantilever caps and (b) straddle bent caps?

Comment: Bent caps typically possess combined high moment and shear zones together near the connection to the pier columns. The interaction of flexure and shear is difficult to resolve at the ultimate limit state. Neither the MCFT nor flexural theories are particularly well suited to solve this interaction riddle.

Q3: Given the relevant demands versus capacities respectively arising from Q1 and Q2 above, what regions of a typical Texas inverted-T bent are the most pressing to investigate as candidates for strengthening?

Comment: It is likely an inverted-T bent cap can be divided into two regions of concern: (a) the fascia girder seat region that is weak in single shear, and (b) the interior girder seat region that may be weak in other failure modes identified by Furlong and Mirza (1974).

Q4: Given the identified failure hierarchies and critical weaknesses, what are the most favorable retrofit means and methods that should be investigated via large-scale physical testing?

Comment: Ideally, one should attempt at full-scale test, but the large prototype dimensions normally mean that this is physically not possible given laboratory constraints. Therefore, the scale needs to be as large as practical.

CHAPTER 3. ANALYSIS AND EVALUATION OF IN-SERVICE INVERTED-T BENT CAPS

To facilitate practical and impactful results in developing strengthening solutions for inverted-T bent caps, in-service bent caps were studied. Field evaluations were conducted to provide an overview of conditions of the in-service bent cap, and demand and capacity analysis of the bent caps was carried out to evaluate the bent cap capacity with lane increment.

Section 3.1 provides a description of the field inspections for the bent caps, including the location of the structures, and findings during the inspection. Section 3.2 describes the structural characteristics of the individual bents of IH 35 through Austin. Section 3.3 presents the structural analysis, including demands and capacities of the bent caps, based on AASHTO (2014). A comparison of the 2014 AASHTO LRFD specifications and 1965 American Association of State Highway Officials (AASHO) specifications is also provided.

3.1 Conditions of In-Service Inverted-T Bent Caps

Two field investigations were conducted in Austin, Texas. On November 13, 2015, six spans near the north end of elevated sections of IH 35 in Austin, Texas, were evaluated. On February 3, 2017, eight inverted-T bents on US 290 in Austin were investigated. All evaluations were conducted from the ground level.

3.1.1 Field Visit for Evaluating IH 35 in Austin

The first investigated spans of IH 35 were located in a region referred to as “Airport Blvd and Southern Pacific Railroad Overpass” in design drawings. This region and the subsection evaluated by the research team are identified in Figure 3.1. In referring to the structures in the subsequent sections, the bent numbers in the design drawings are referenced. In these, Bent 1 is located at the north end of the freeway system considered; the bent numbers increase progressively southward, with Bent 24 located at the end of the freeway system being investigated in this study. The southbound (SB) thruway lanes are elevated between Bents 9–24, while the northbound (NB) thruway lanes are elevated between Bents 10–24. The bents evaluated in the field visit were Bent 14 through Bent 20, with most observations occurring on the structures for the northbound lanes.

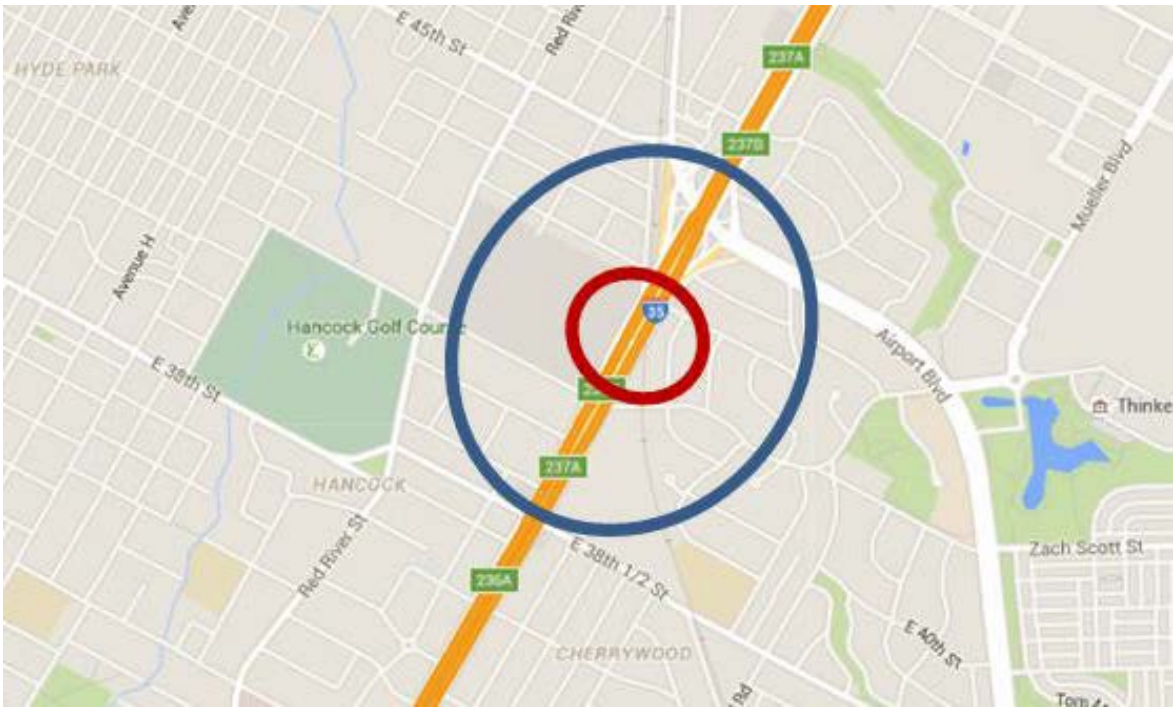

Figure 3.1. Overview of Field Visit Location: Outer Circle Indicates Referenced Structures and Inner Circle Indicates Location of Field Visit (Image from Google Maps).

The elevated roadway can be identified by the four main sets of lanes (excluding on/off ramps) identified in Figure 3.2. The two sets of center lanes are referred to as the main lanes. Each of these sets of lanes consists of two lanes carrying traffic either northbound (right set in the figures) or southbound (left set in the figures). These lanes are elevated between Bents 1 and 18; south of Bent 18, the lanes drop to grade level (see Figure 3.3). On the outside of the main lanes are two sets of two lanes referred to as the thruway lanes (one northbound and one southbound). These lanes are elevated between Bents 9/10 (SB/NB) and 24. North of Bents 9/10, the thruway and main lanes are common to the bents; as such, these main lane bents are longer than the main lane bents south of Bents 9/10.

The main lane bents consist of double-column bents, except Bents 1 through 10, which carry both the main and thruway lanes and have three columns per bent. The thruway bents north of and including Bent 17 are double-column bents, while the bents south of and including Bent 18 are single-column bents.

Figure 3.2. Plan View of Structures Observed during the First Field Visit (Image from Google Earth).

Figure 3.3. Southern End of Elevated Main Drop to Grade Level.

In typical single-column bents and main lane multi-column bents, the bent is symmetric about the center of the bent (same overhang length on both ends with same number and location of girders in the overhang region). In thruway double-column bents, the overhangs on the two ends are not identical. An example of this is shown in Figure 3.4. The interior overhang (adjacent to the main lanes) is shorter than the exterior overhang (adjacent to the frontage road) and supports one girder, while the exterior overhang supports two girders.

Figure 3.4. Unequal Overhang Lengths for Bent 16 of Northbound Thruway Lanes.

Exceptions to the typical configuration occur at Bents 9–13 where railroad tracks and on/off ramps necessitate a change from the typical configuration. Generally, these nontypical bents have nonsymmetric layouts. The most extreme deviation from the typical detailing is northbound Bent 13. Due to railroad tracks, northbound thruway Bent 13 is straddle-like at the interior side, with the interior column also supporting the exterior end of the single-column NB main lane Bent 13.

3.1.1.1 Structural Damage

Discussions with district engineers indicated the expectation that the number of lanes on the thruway structures will be increased from two to three, while the number of lanes on the main

lane structures will be kept at two due to the inability to increase the number of lanes in the sections south of the elevated main lanes.

The research team was interested in damage indicating structural deficiencies of the bent caps that would be amplified by increased demands of restriping the thruway structures to carry additional lanes. From the bents visited, the research team identified one key damage type in the inverted-T bent caps. A crack was observed at the east end of northbound main lane Bent 13. Figure 3.5 shows the crack, which begins at the ledge-web interface. Although the crack extends slightly downward, it is primarily horizontal. The crack extends approximately 1 ft inward toward the centerline of the cap.

A second northbound main bent had cracking and spalling extending along the width of the interface between the web and the ledge. Similar damage is observed in Bent 16 and 17 of the northbound thruway. Figure 3.6 shows the damage in both of these.

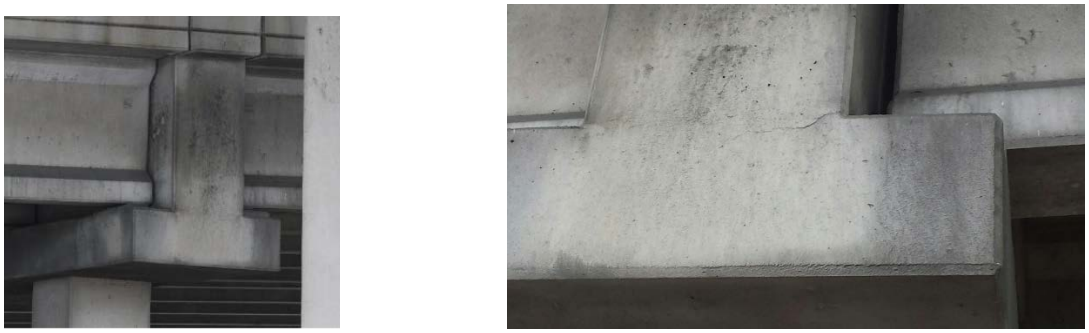

(a) *(b)*

Figure 3.5. Crack at Ledge-Web Interface of End (East) of Northbound Main Lane Bent 13.

(a) Bent 16 *(b) Bent 17*

Figure 3.6. Cracking and Spalling at Ends (East) of Northbound Bents.

3.1.1.2 Nonstructural Challenge

During the field evaluations, the research team was mindful of any nonstructural characteristics of the IH 35 elevated structures that may pose a challenge to implementation of strengthening solutions. These issues are categorized as (a) accessibility challenges, and (b) obstacles.

The most significant nonstructural challenge to implementation of strengthening solutions is the accessibility of the bent caps. The superstructure of the bridge or adjacent substructures can affect accessibility.

A significant accessibility challenge is the presence of diaphragms between the ends of girders. These diaphragms, shown in Figure 3.7, limit accessibility of the tops of the web of the inverted-T bent caps. This limits the applicability of many proposed solutions. The diaphragms extend approximately 2 ft below the bottom of the deck. A gap of approximately 8 in. between the face of the cap and the back of the diaphragm permits limited access for placement of plates or similar material.

(a) Looking at face of bent cap *(b) Looking up toward bottom of deck*

Figure 3.7. Diaphragms between Girders at Ends of Spans.

Another significant accessibility challenge is adjacent structures. For all elevated portions of the main lanes, the north and southbound bents at each bent line are at the same elevation and adjacent to one another, separated by approximately 1 ft 5 in. Figure 3.8(a) shows two adjacent main lane bents. While this significantly limits strengthening solutions implemented at the end of the inverted-T, these bents are expected to not require strengthening. Accessibility to the interior ends of the thruway bents is of a greater concern. Figure 3.8(b) and (c) show, respectively, thruway bents adjacent to the main lane structures at the same and different elevations.

Throughout the IH 35 elevated structures, the deck extends beyond the edge of the bent caps. This overhang, shown in Figure 3.9, restricts access to the top of the bent cap ends and may prove to limit the use of some proposed strengthening solutions.

Obstacles are anything that blocks access to the bent caps but, unlike accessibility issues, can be relocated or temporarily removed. The most significant obstacle to implementation of strengthening solutions is the traffic on, under, and adjacent to the structures. Field evaluation revealed to the research team the large volume of vehicular traffic traveling not just on the IH 35 lanes carried by the structure but also on the frontage road (Figure 3.10) and under the structure.

(a) Adjacent main bent

(b) Thruway bent adjacent to main bent at same elevation

(c) Thruway bent adjacent to main bent at different elevation

Figure 3.8. Limited Accessibility to Ends of Bent Caps Due to Adjacent Substructures.

Figure 3.9. Edge of Deck Extends Past End of Inverted-T Bent Caps.

Figure 3.10. Frontage Road Adjacent to Thruway Lanes.

Other obstacles include drainage pipes attached to the substructures (Figure 3.11) and signs and lighting attached to and/or adjacent to the structures that may prevent access to necessary portions of the bents.

Texas Department of Transportation (TxDOT) engineers that accompanied the research team expressed concerns about the appearance of any strengthening solutions implemented for the elevated IH 35 structure. The need for this is evident in the large volume of traffic near these highly visible structures and the presence of businesses along the frontage roads.

Figure 3.11. Drainage Pipes Attached to Ledge of Multi-Column Bent.

3.1.2 Field Visit for Evaluating US 290 in Austin

Eight inverted-T bents were evaluated during the second field investigation on US 290 in Austin, Texas. The investigated bents are located between Packsaddle Pass and Cactus Ln, which are indicated with the blue arrow in Figure 3.12. In referring to the structures, the bent numbers in the design drawings are referenced. The eastbound lanes of Bent 25 through Bent 32 were evaluated.

Figure 3.12. Location of the Bents Observed during the Second Field Visit (Image from Google Earth).

Figure 3.13(a) shows a side elevation photograph of Bent 32. The evaluated bents consist of double-column bents with symmetric layouts. The height of the bent caps is 79 in., and the bottom width is 76 in. The number of girders on each ledge of the bents is 10, and the longest girder span length is 116 ft, which is l ft longer than that of IH 35.

Inverted-T bent caps of US 290 bridges were designed in accordance with AASHTO Standard Specifications (1989) standard specifications. Figure 3.13(b) shows a typical cross-section of the ledge and hanger reinforcement for US 290. The primary ledge shear reinforcement (#6 S2 bar in Figure 3.14) of the US 290 bents is a single hoop at 9 in. and 10 in. spacing for the exterior and interior spans, respectively. One straight bar (#5 N bar in Figure 3.14) is used as auxiliary reinforcement in the US 290 bents with the same spacing of the primary ledge shear reinforcement.

A major crack type of inverted-T bent caps was identified through field inspection and was observed on the end face of Bent 29 supporting the eastbound lanes. Figure 3.15 shows a close view of the crack, which initiates at the reentrant corner where the ledge meets the web and extends in the diagonal direction but continues in the vertical direction after mid-height of the ledge. Bents under eastbound lanes had cracks extending along the width of the ledge-web interface. Similar damage was observed in Bents 26, 28, and 32. Figure 3.16 shows the cracks observed at the ends of these three bents.

(a) Bent 32 of US 290

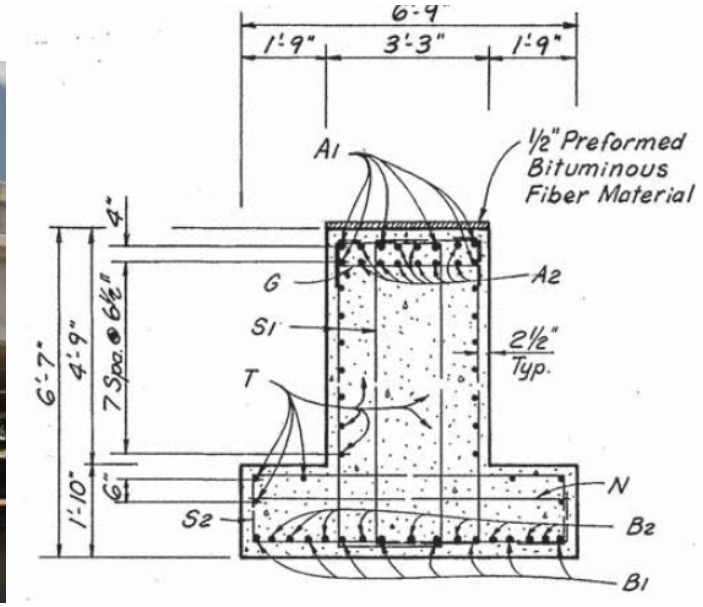

(b) Cross-section of US 290 typical bent cap

Figure 3.13. Typical Inverted-T Bent Cap.

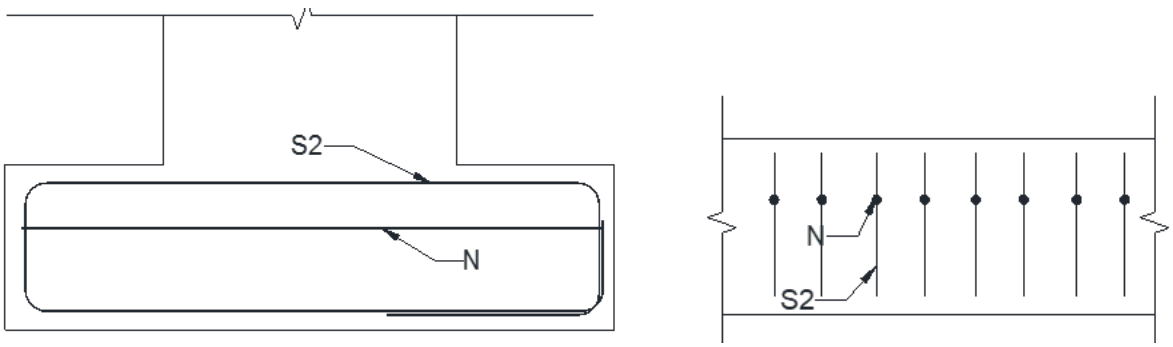

(a) Cross-section of ledge *(b) Side elevation of ledge*

Figure 3.14. Ledge Reinforcement Detail of Typical Double-Column Bent.

(a) *(b)*

Figure 3.15. Crack at Ledge-Flange Interface of Exterior of Bent 29.

(a) Bent 26 *(b) Bent 28* *(c) Bent 32*

Figure 3.16. Cracks at the Ends of Bents.

3.2 Bent Characteristics of IH 35

This section focuses on identifying the structural characteristics of the bent caps of the IH 35 elevated lanes in Austin, and design drawings are used to quantitatively supplement field observations. Bent characteristics considered included (a) cap and column dimensions, and (b) girders. Each of these is detailed in the following sections.

3.2.1 Cap and Column Dimensions

Cross-sectional dimensions are common to all inverted-T bent caps, with the exception of single-column bents of the north and southbound thruway lanes. Single-column bents have a cross-section at the end similar to other bent caps with a ledge that increases gradually until the face of the column (Figure 3.17). The full height of the inverted-Ts is approximately 7 ft, with slight variations due to the slope of the roadway. The minimum ledge depth is 1 ft 8 in. for all bent caps. The full width of the inverted-Ts is 5 ft 3 in., and web width is 2 ft 6 in.

In all bents, the columns are either rectangle or square, and the dimension of the column perpendicular to the cap width is wider than the web. The columns in single-column bents are 6 ft by 4 ft 6 in., providing only 4.5 in. clearance from the edge of the cap on either side (see Figure 3.17). The columns in all multi-column bents are square but vary in size. In most instances, multi-column thruway bents have 3 ft 6 in. square columns and main bents have 3 ft square columns. Exceptions occur in the range of Bents 9 through 13, where on/off ramps and railroad tracks are located. In these bents, columns are larger—4 ft for thruway bents and 3 ft 6 in. or 4 ft for main lane bents.

Figure 3.17. Variable Ledge Depth of Bent Caps in Single-Column Bents.

3.2.2 Girders on Bent Cap

The superstructure of a typical double-column bent consists of seven AASHO-54 standard girders and a 7.5 in. thick concrete deck. The girders are connected transversely using intermediate and end diaphragms. Standard AASHO-54 girders are supported at each of the seven bearing locations. Single-column bents support a total of seven girders, with three girders on either side of the overhang. Typical single-column bents have the same girders and deck thickness as typical double-column bents.

A summary of the northbound and southbound thruway bents is shown in Table 3.1 and Table 3.2, respectively. The girder span lengths of the north and south spans of each bent are also presented in these tables. The number of girders supported by the inverted-T bent caps ranges from 6 to 11, depending on the width of the road on the elevated bridge. The span lengths supported by the inverted-T bent caps range from 75 ft to 115 ft. The longest span supported by the single-column bent is 100 ft (Bent 22 and 23 on northbound thruway), and 115 ft for the double-column bent (Bent 11–13 on southbound thruway). Details of northbound Bent 22 and southbound Bent 13, which have the longest span length among the single- and double-column bents, are shown in Figure 3.18 and Figure 3.19, respectively.

A girder configuration characteristic is the relative placement of girders for the forward and reverse spans. In most locations, the beams are aligned, but in some bent caps (Bents 11–14, Bent 16, and Bent 21 on the northbound thruway, and Bent 10, Bent 11, and Bents 17–19 on the southbound thruway), the girders are offset from one another on either side of the inverted-T bent cap.

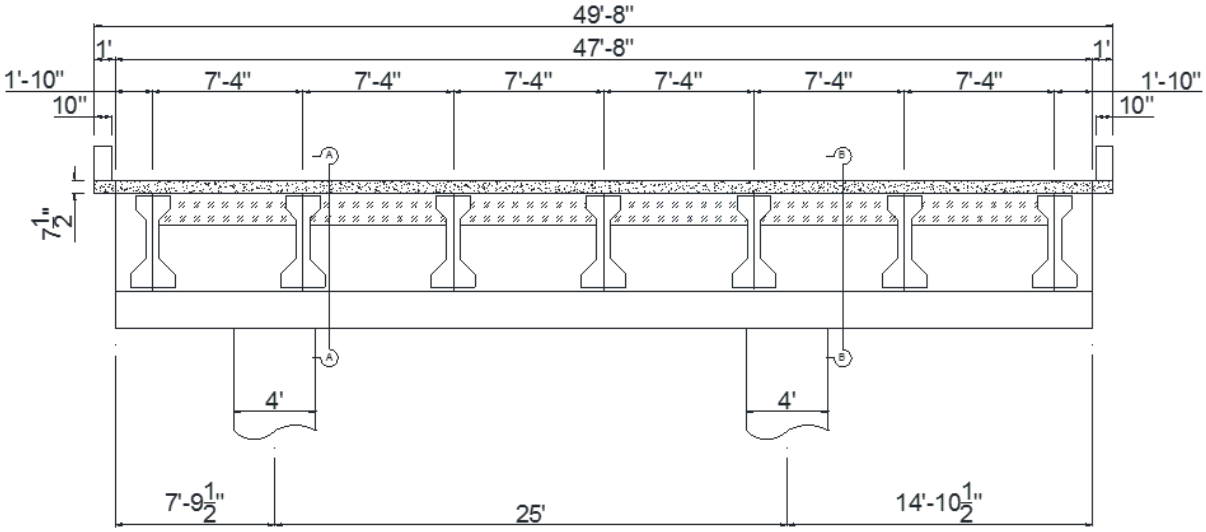

(a) Elevation

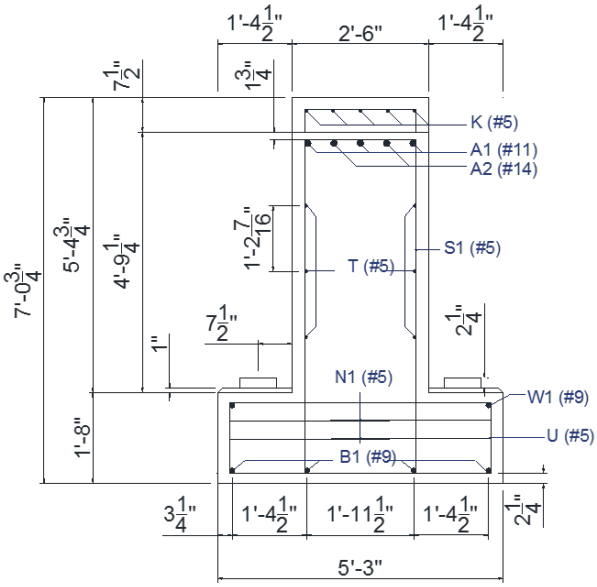

(b) Section A-A

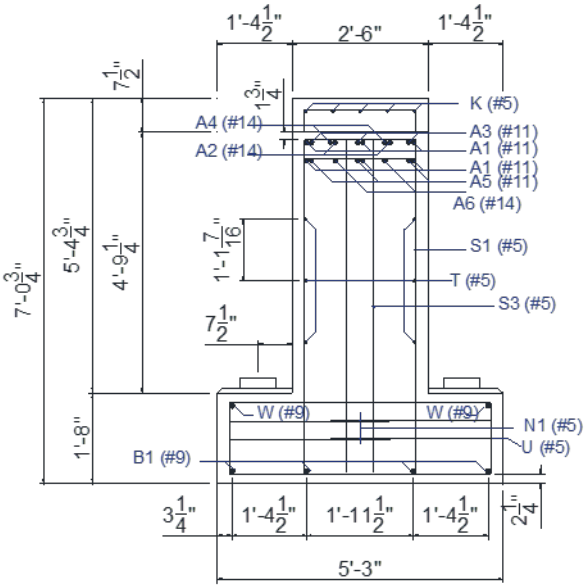

(c) Section B-B

Figure 3.18. Elevation and Cross-Section of Southbound Bent 13.

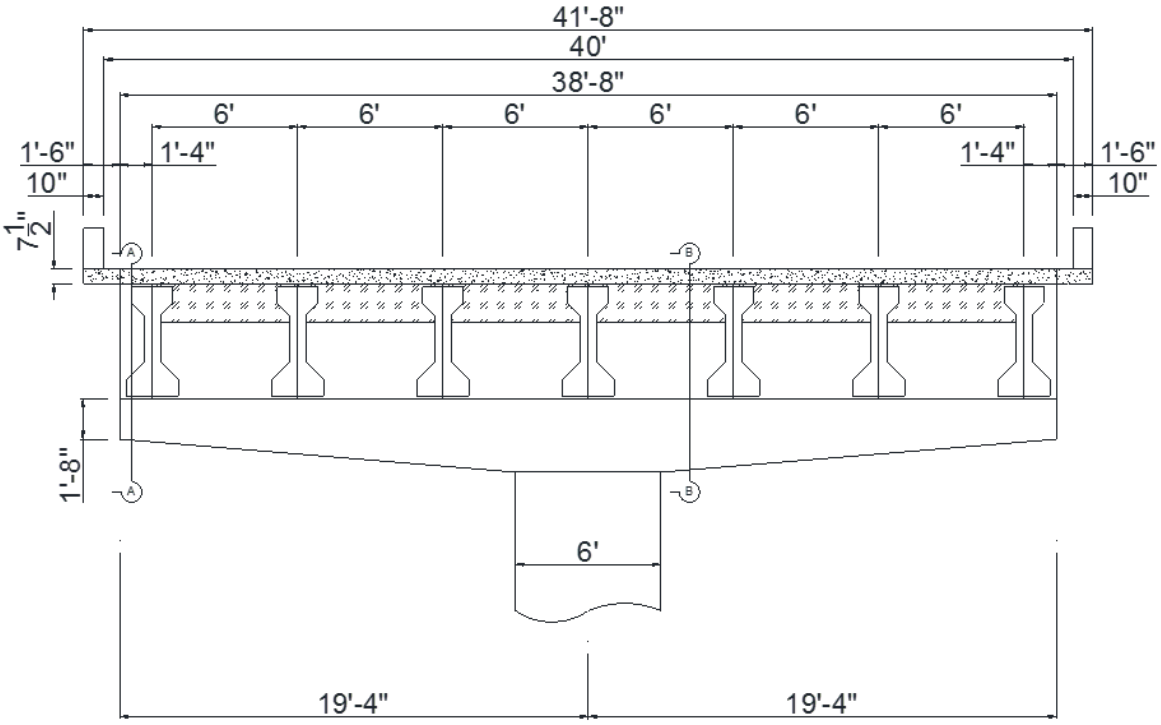

(a) Elevation

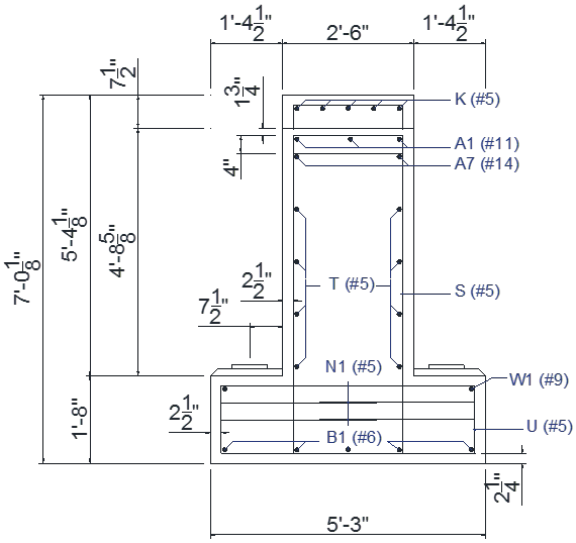

(b) Section A-A

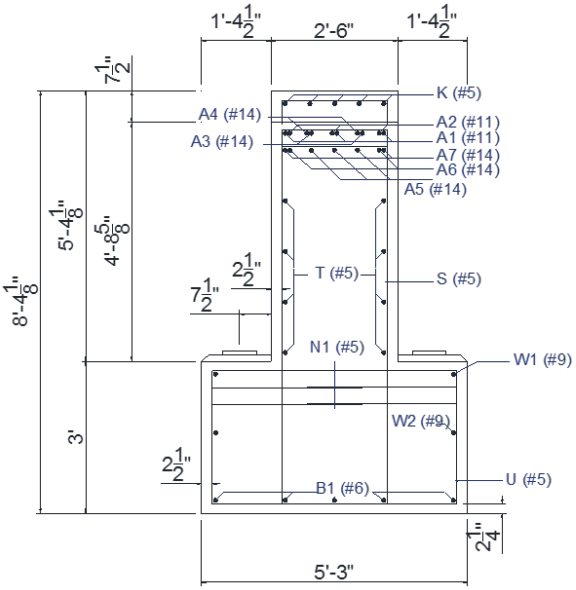

(c) Section B-B

Figure 3.19. Elevation and Cross-Section of Northbound Bent 22.

Table 3.1. Northbound Thruway Bent Summary.

Bent No.	Type of Bent	Span Length (ft)		No. of Girders		Girder Spacing		Road Width (ft)
		North Span	South Span	North Span	South Span	North Span	South Span	
Bent 11	DC	115	115	11	8	4'-8 15/16", 5'-10"	6'-8 1/8"	53
Bent 12	DC	115	115	8	7	6'-1 1/8"	7'-6 3/8", 7'	46.5
Bent 13	DC	115	115	7	7	7'	6'-8 1/8"	44
Bent 14	DC	115	90	7	6	4'-6 7/16", 6.7'	7'-11 7/8", 7'-4"	42
Bent 15	DC	90	90	6	6	7'-4"	7'-4"	40.5
Bent 16	DC	90	90	6	6	6'-8 13/16", 7'-4"	7'-2 3/8"	40
Bent 17	DC	90	90	6	6	7'-2 3/8"	7'-2 3/8"	40
Bent 18	DC	90	90	6	6	7'-2 3/8"	7'-2 3/8"	40
Bent 19	SC	90	75	6	6	7'-2 3/8"	7'-2 3/8"	40
Bent 20	SC	75	75	6	6	7'-2 3/8"	7'-2 3/8"	40
Bent 21	SC	75	100	6	7	7'-2 3/8"	6'	40
Bent 22	SC	100	100	7	7	6'	6'	40
Bent 23	SC	100	100	7	7	6'	6'	40

Note: DC = double column and SC = single column.

Table 3.2. Southbound Thruway Bent Summary.

Bent No.	Type of Bent	Span Length (ft)		Girder No.		Girder Spacing		Road Width (ft)
		North Span	South Span	North Span	South Span	North Span	South Span	
Bent 10	DC	115	115	10	8	5'-1 3/16"	6'-3 3/16", 6'-11 15/16"	50.5
Bent 11	DC	115	115	8	7	6'-3 3/8"	7'-4"	48
Bent 12	DC	115	115	7	7	7'-4"	7'-4"	48
Bent 13	DC	115	115	7	7	7'-4"	7'-4"	48
Bent 14	DC	115	90	7	7	7'-4"	7'-4"	48
Bent 15	DC	90	90	7	7	7'-4"	7'-4"	48
Bent 16	DC	90	90	7	7	7'-4"	7'-4"	48
Bent 17	DC	90	90	7	7	7'-4", 6'-3 7/16"	7'-4", 6'-3 7/16"	47
Bent 18	SC	90	90	7	6	7'-4", 4'-7 1/4", 4'-6 15/16"	7'-4", 8'-2 1/4"	42.5
Bent 19	SC	90	75	6	6	7'-4", 7'- 5/16"	7'-2 3/8"	40
Bent 20	SC	75	75	6	6	7'-2 3/8"	7'-2 3/8"	40
Bent 21	SC	75	75	6	6	7'-2 3/8"	7'-2 3/8"	40
Bent 22	SC	75	115	6	8	7'-2 3/8"	5'-1 3/4"	40

Note: DC = double column and SC = single column.

3.3 Structural Analysis

To establish the strength deficiencies that must be addressed in the design of inverted-T strengthening solutions, the bent caps from the IH 35 field evaluation were analyzed. The potential need to strengthen these particular structures is the result of (a) changes in design provisions since the time of construction in the late 1960s, and (b) interest in increasing the number of lanes on the bridge, thereby increasing the demands. Section 3.3.1 provides an overview of the expected future demands with three lanes on the bent caps. In Section 3.3.2, the capacities of two bent caps are calculated. An evaluation of the demand-capacity ratios is presented to guide the development of strengthening solutions in Chapter 4.

3.3.1 Demands

Bent cap demands are characterized by the internal forces for flexure and shear forces and by girder loads for all other failure mechanisms considered. The TxDOT bent cap analysis program CAP 18 (Version 6.2.2) was used to determine flexural and shear demands. The program utilizes a discrete element model that provides envelopes of internal maximum bending and shear forces of the bridge bent caps (Willis, 1975). The program analyzes dead and live loads that conform to AASHTO standard specifications. CAP 18 has the unique feature of a movable load that runs across the width of the deck. The program determines the largest demands at the bent cap control points (such as column and girder positions) due to the movable load. Bent 13 and Bent 22 are modeled as continuous beams with knife-edge supports. The analysis of the bent caps considered only the Strength 1 limit state specified in Section 3.4.1 of AASHTO (2014).

Dead loads include the self-weight of the girder, deck, and any overlay that may present. The weight of the rails is distributed evenly among the stringers, up to three stringers per rail. To account for the additional dead load from the haunch of the column to the slab ends, the dead load of the slab is increased by 10 percent (TxDOT, 2015).

Live loads are computed in accordance with Sections 3.6.1.2.2 and 3.6.1.2.4 of the AASHTO (2014) LRFD specifications. The vehicular live loading on the roadway consists of a combination of the design truck or the design tandem and the design lane load. The maximum live load is always governed by the design truck over the design tandem for spans greater than 26 ft. Figure 3.20 shows the locations of the HL-93 design truck on the interior girder, which generates the maximum load effect as described in Section 3.6.1.3.1 of AASHTO (2014). When the length

of the spans is different, and the longer span (Span 2) is shorter than twice that of the short span (Span 1) length, the middle axle (32 kips) is placed over the interior support, the front axle (8 kips) is placed on the short span (Span 1), and the rear axle (32 kips) is placed on the long span (Span 2). To account for wheel load impact from moving vehicles, the live load without the design lane load was increased by applying dynamic load allowance factors, as listed in Table 3.6.2.1-1 of AASHTO LRFD (2014). The load effects from the design lane load are subject to multiple presence factors (AASHTO, 2014). The live load applied to the slab is distributed to the beams by assuming the slab is hinged at each beam except the outside beam (TxDOT, 2015).

The girder reaction (V_u in Figure 3.20[d]) is the factored load on each ledge of the inverted-T bent caps. The live load for the girder reaction is maximized by placing the rear axial (32 kips) of the HL-93 truck model over the support as shown in Figure 3.20(c) and multiplied by the shear live load distribution factor. The limit state factors listed in Table 3.4.1-1 of AASHTO (2014) are multiplied to obtain girder reaction. The Service I limit state factors are 1.0 for dead and live load. The Strength I limit state factors are 1.25 and 1.75 for dead and live load, respectively.

Table 3.3 presents the girder reactions for southbound Bent 13 and northbound Bent 22 of IH 35, which have the longest span length that produce the largest load demands among the IH 35 thruway bent caps. These two bents were analyzed for the evaluation in Section 3.4.2.

When a truck is on one span (see Figure 3.20[e]), ledge forces significantly larger than the other side generate torsion in the bent cap. To maximize torsion demand, the live load is positioned in the longer span.

Table 3.3. Girder Reactions for Selected Bents.

Bent ID	Bent Type	Service Limit State		Strength Limit State	
		Ext. (kips)	Int. (kips)	Ext. (kips)	Int. (kips)
Northbound Bent 13	Double Column	167	191	247	287
Southbound Bent 22	Single Column	140	156	207	235

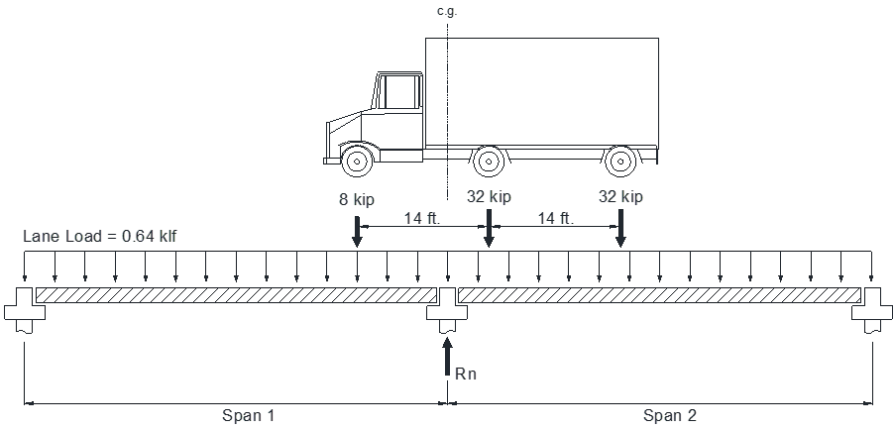

(a) Standard live load model

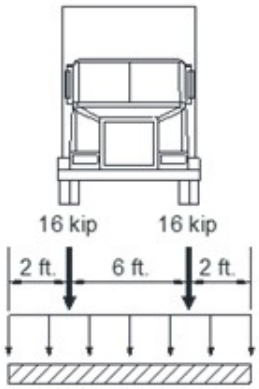

(b) Slab live load model

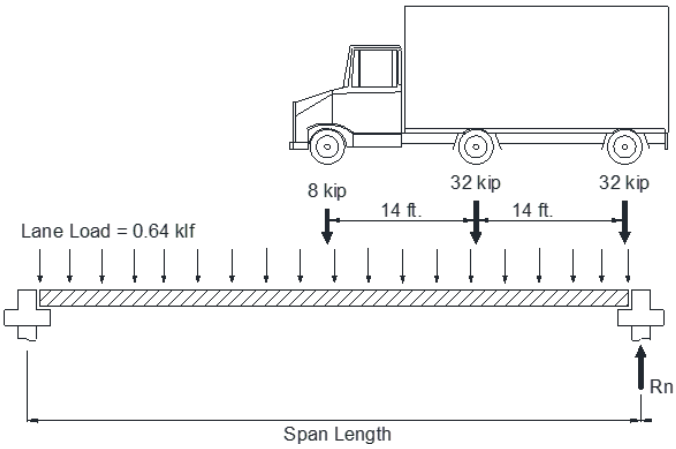

(c) Live load model for girder reaction

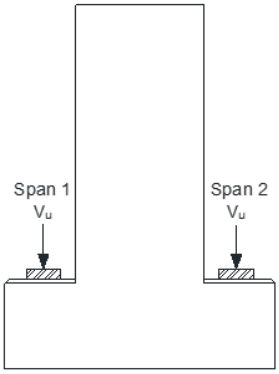

(d) Girder reactions

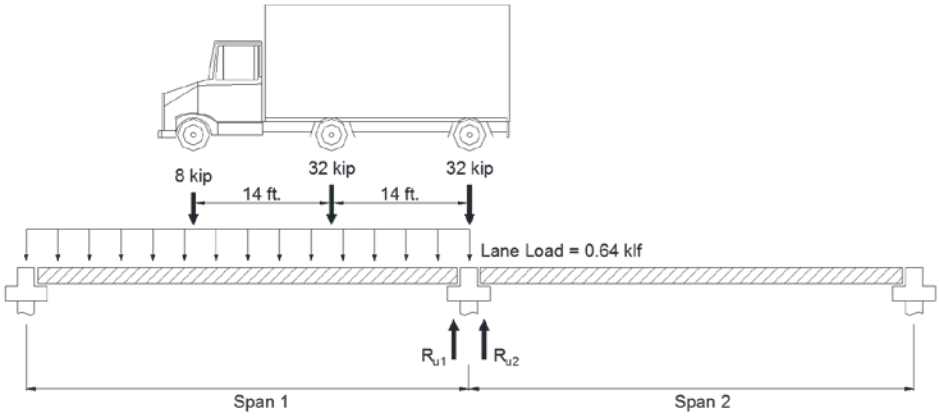

(e) Live load model for torsion

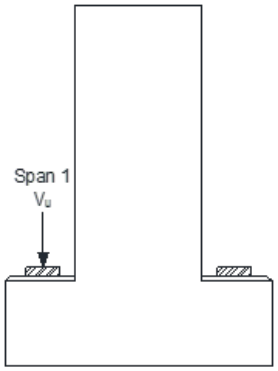

(f) Torsional load

Figure 3.20. Live Load Models on Girder Used for the Computation of Girder Reaction and Torsional Load.

3.3.2 Bent Cap Capacity Evaluation

In this section, the capacity (C) of Bent 13 and 22 is calculated using AASHTO LRFD (2014) sectional methods and is compared to the demands calculated in Section 3.4.1. Flexure, shear, and torsional capacities are considered for the full bent cap and compared to internal demands from the CAP 18 analysis. Ledge, hanger, and punching shear capacities are considered at all load points and compared to the girder loads at those locations.

The adequacy of each mechanism is evaluated by the ratio of the factored capacity (ϕC) to the demand (D), referred to as the overstrength factor, Ω. Overstrength factors greater than 1.0 are considered to have sufficient capacity to resist demands and are colored green in tables summarizing results. Overstrength factors less than 1.0 are considered to have insufficient capacity and are colored yellow ($0.9 \leq \Omega \leq 1.0$) or red ($\Omega \leq 0.9$) in tables summarizing results. When there is insufficient capacity, the amount of additional strength needed, referred to as the deficiency, is calculated as:

$$Deficiency = Demand(D)/\phi - Capacity(C) \tag{3.1}$$

where ϕ = strength reduction factor, 0.9.

3.3.2.1 Sectional Capacity Evaluation

Flexural capacities of the bent caps are calculated in accordance with Article 5.7.3.2 of AASHTO LRFD (2014). The negative moment capacity of the bent caps is evaluated at the most critical section on each column (Section A-A and B-B in Figure 3.18[a] for Bent 13 and Section B-B in Figure 3.19[a] for Bent 22). The positive moment capacity for Bent 13 is evaluated at the center of the mid-span. The calculations for the flexural capacity of the bent cap are presented in Appendix B. Table 3.4 presents the flexural demands, the flexural capacity, and the overstrength factors.

Shear and torsion capacities of the web are calculated following conventional sectional methods in accordance with Article 5.8.3.3 through 5.8.3.6 of AASHTO LRFD (2014). Note that the maximum torsion and maximum shear is assumed to be concurrent in this case. If the maximum shear and maximum torsion do not occur concurrently, then it is necessary to check the location of the maximum torsion with its concurrent shear, and the location of the maximum shear with its concurrent torsion.

The maximum shear and torsion are concurrent with each other for both Bent 13 and Bent 22 at the critical section near the column surface (Section B-B). Double-leg closed stirrups are used near the critical sections. Table 3.4 lists the shear and torsion capacity of Bent 13 and Bent 22 with calculated load demand. Overstrength factors for shear and torsion resistance are higher than 1.00 for both bents. With this value, it was found that the web has sufficient shear and torsional strength to resist the maximum concurrent shear and torsional loading.

Table 3.4. Overstrength Factor for Sectional Capacity.

Bent ID	Section	Flexural Resistance (kip-ft)			
		Capacity	Demand	Deficiency	Ω
Southbound Bent 13	Section A-A	3448	2988	N.A.	1.15
	Section B-B	10089	9021	N.A.	1.12
Northbound Bent 22	Section B-B	12324	11850	N.A.	1.04
		Positive Flexural Resistance (kip-ft)			
Southbound Bent 13		2024	1671	N.A.	1.21
		Shear (kips)			
Southbound Bent 13		1524	953	N.A.	1.60
Northbound Bent 22		1391	1318	N.A.	1.06
		Torsion (kip-ft)			
Southbound Bent 13		1694	628	N.A.	2.70
Northbound Bent 22		3506	732	N.A.	4.79

Legend $\Omega > 1$ $0.9 \leq \Omega \leq 1$ $\Omega < 0.9$

3.3.2.2 Evaluation of Hanger Capacity

AASHTO LRFD (2014) specifies the design methods for the beam ledges in Section 5.13.2.5. Figure 3.21 shows potential cracks and their locations in the ledge of an inverted-T bent cap. AASHTO LRFD (2014) indicates that the beam ledges must resist (a) flexure, shear, and horizontal forces; (b) tension force in the supporting element; (c) punching shear at points of loading; and (d) bearing force.

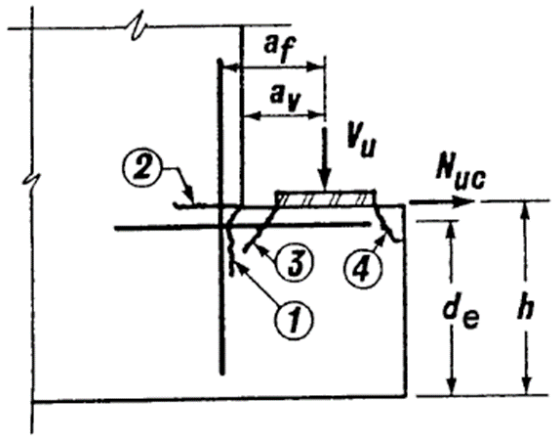

Figure 3.21. Notation and Potential Crack Locations for Ledge Beams (AASHTO, 2014).

The cracks in Figure 3.21 are referred to as ledge shear friction and ledge flexure (1), hanger (2), punching shear (3), and bearing (4). Requirements to address the specific conditions of the inverted-T bent cap ledge component are outlined in Articles 5.13.2.5.2 through 5.13.2.5.5.

Hanger reinforcement must have sufficient capacity to transmit the vertical forces from the ledges to the web. The hangers should resist tension forces at the location of Crack 2 shown in Figure 3.21. Hanger capacity of the inverted-T bent caps is calculated and evaluated for both service limit state and strength limit state.

The distribution width represents the length of ledge considered capable of distributing the concentrated load longitudinally among the hanger reinforcements along the web. The longitudinal distance will be limited either by the longitudinal center-to-center girder spacing, S, which is shown in Figure 3.22(a), or by the capacity of the ledge to distribute the applied force to the hangers, also known as the flexural-shear resistance of the hangers. The latter is limited by the concrete shear capacity combined with the tensile capacity of the hangers within the distribution width of $W+2d_f$, as shown in Figure 3.22(b). For the service limit state, the distribution width is only S, which does not account for flexure-shear of the hanger, while the lesser of the capacity with the distribution width of S or $W+2d_f$ is taken for the strength limit state.

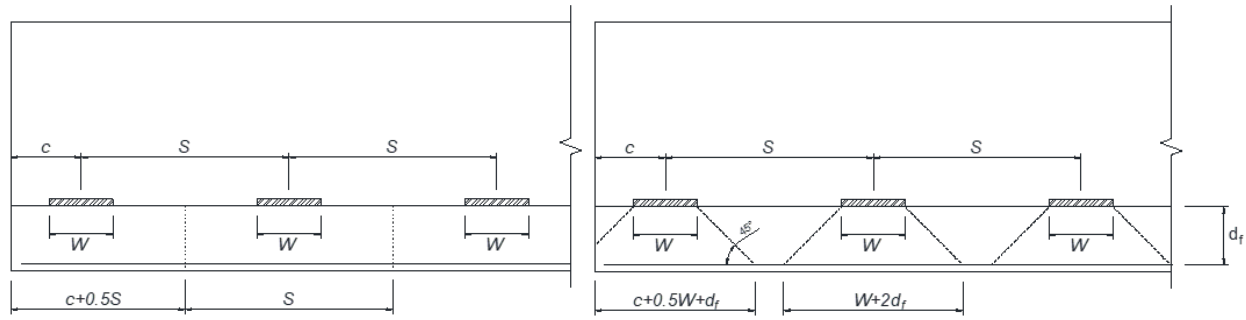

(a) Shear distribution width *(b) Flexural-shear distribution width*

Figure 3.22. Parameters for Calculation of Hanger Capacity.

For the nominal shear resistance of the hanger at the service limit state, TxDOT uses $2/3f_y$ from the study of Furlong and Mirza (1974) instead of $0.5f_y$ from AASHTO LRFD (2014) Equation 5.1.2.5.5-1 (TxDOT, 2015). Thus, for this research, hanger capacity at the service limit state is the lesser of:

$$V_n = \frac{A_{hr}(\frac{2}{3}f_y)}{s}(W + 3a_v) \tag{3.2}$$

$$V_n = \frac{A_{hr}(\frac{2}{3}f_y)}{s}S \tag{3.3}$$

where A_{hr} = area of hanger reinforcement and s = spacing of hanger reinforcements.

For the strength limit state, the hanger capacity is the lesser of the following two AASHTO LRFD (2014) equations:

$$V_n = \frac{A_{hr}f_y}{s}S \tag{3.4}$$

$$V_n = 0.063\sqrt{f_c'}b_f d_f + \frac{A_{hr}f_y}{s}\left(W + 2d_f\right) \tag{3.5}$$

where b_f = width of the bottom flange.

For exterior girders, to consider the limitation of the distribution width to the edge of the cap, TxDOT provides modified equations for the shear resistance of exterior hangers. The exterior girder shear resistance for hanger at the service limit state is the lesser of:

$$V_n = \frac{A_{hr}(\frac{2}{3}f_y)}{s}\left(\frac{W + 3a_v}{2} + c\right) \tag{3.6}$$

$$V_n = \frac{A_{hr}(\frac{2}{3}f_y)}{s}\left(\frac{S}{2} + c\right) \tag{3.7}$$

For the strength limit state, the hanger resistance is taken as the lesser of the following two equations:

$$V_n = \frac{A_{hr}f_y}{s}\left(\frac{S}{2} + c\right) \tag{3.8}$$

$$V_n = 0.063\sqrt{f_c'}b_f d_f + \frac{A_{hr}f_y}{s}\left(\frac{W + 2d_f}{2} + c\right) \tag{3.9}$$

Figure 3.23 shows the shear reinforcement in southbound Bent 13 and northbound Bent 22. Table 3.5 presents the hanger capacities at each girder location for southbound Bent 13 and northbound Bent 22. The hanger capacities and demands at both the service limit state and the strength limit state are presented. Note that as the seats of interior Girder 1 and 4 of Bent 13, and interior Girder 3 of Bent 22 are placed on the ledge above the column, the loads are directly transferred to the column. Therefore, the capacity of the hangers in these portions of the bent are not considered in Table 3.5.

At the service limit state, the hanger capacity for the interior girder locations and the exterior girder locations are controlled by Equations (3.17) and (3.20). Overstrength factors are varied from 0.41 to 0.82 for Bent 13, while overstrength factors for Bent 22 range from 0.54 to 0.80. For both bent caps, the hanger capacity is insufficient at all locations.

At Strength 1 limit state, the exterior hanger capacity for Bent 13 is governed by Equation (3.8), while the interior hanger capacity is controlled by Equation (3.5). The hanger capacity is deficient at most girder locations at the strength limit state. For Bent 13, hanger capacity is deficient at all girders except Girder 5. The overstrength factor for exterior Girders 1 and 2 and interior Girders 2 and 3 is the same. However, the deficiency for interior Girders 2 and 3, with a deficiency of 90 kips, is larger than the deficiency for exterior Girder 1 and 2, with a deficiency of 76 kips. For Bent 22, the hanger capacity is governed by the flexural-shear capacity of the hanger, which can be obtained by Equation (3.4) and (3.8) for the interior and exterior, respectively. The overstrength factor varies from 0.87 to 1.33. Interior Girders 2 and 4 have sufficient shear capacity, while interior Girders 1 and 5 have the largest deficiency of 34 kips. Both exterior girder locations also have a hanger deficiency of 16 kips.

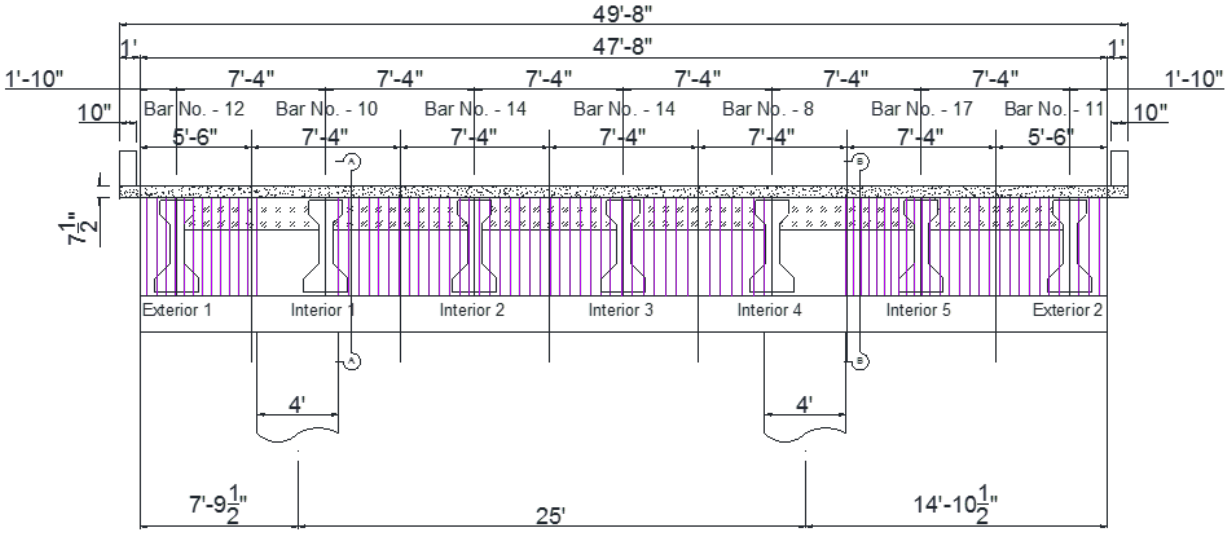

(a) Southbound Bent 13

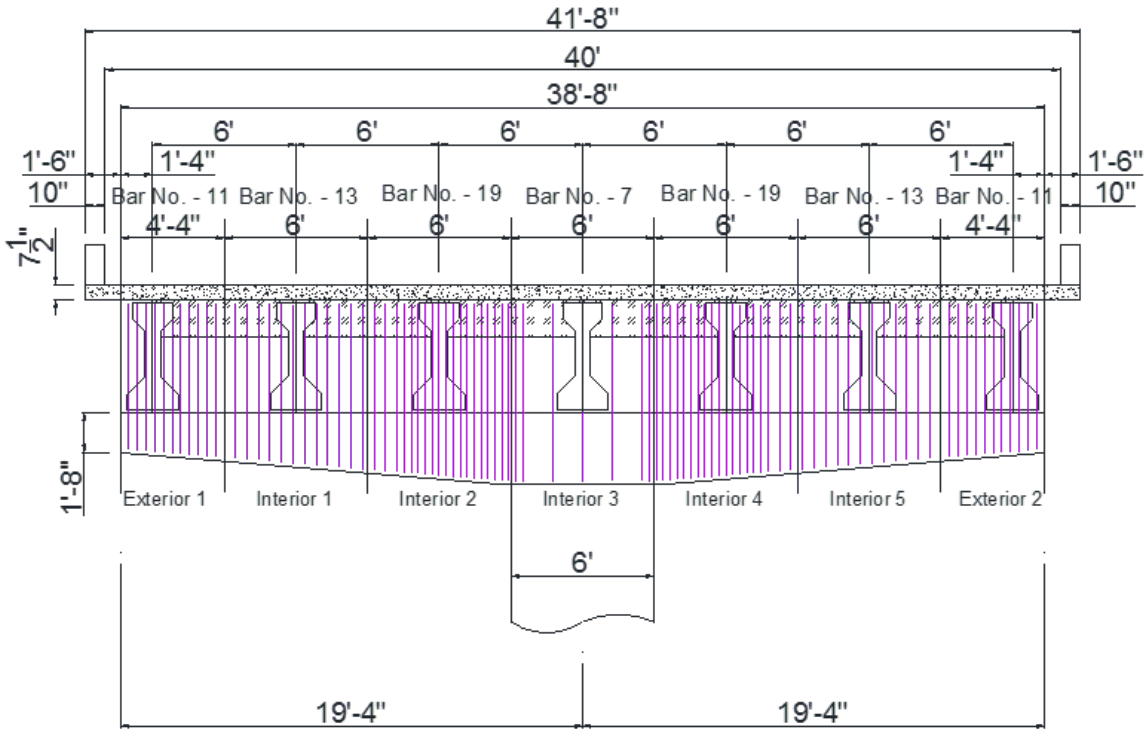

(b) Northbound Bent 22

Figure 3.23. Distribution of Hanger Reinforcement.

Table 3.5. Hanger Capacity Evaluation.

Bent ID	Girder No.	Service Limit State			Strength Limit State			
		Hanger Capacity, C (kips)	Demand, D (kips)	Ω, ϕC/D	Hanger Capacity, C (kips)	Demand, D (kips)	Deficiency, D/ϕ – C (kips)	Ω, ϕC/D
Southbound Bent 13	Ext. 1	88	167	0.47	198	247	76	0.72
	Ext. 2	88	167	0.47	198	247	76	0.72
	Int. 1			*				*
	Int. 2	87	191	0.41	229	287	90	0.72
	Int. 3	87	191	0.41	229	287	90	0.72
	Int. 4			*				*
	Int. 5	174	191	0.82	394	287	N.A.	1.24
Northbound Bent 22	Ext. 1	104	140	0.67	214	207	16	0.93
	Ext. 2	104	140	0.67	214	207	16	0.93
	Int. 1	93	156	0.54	227	235	34	0.87
	Int. 2	139	156	0.80	346	235	N.A.	1.33
	Int. 3			*				*
	Int. 4	139	156	0.80	346	235	N.A.	1.33
	Int. 5	93	156	0.54	227	235	34	0.87

Note: Girder located over column; need for hanger reinforcement is bypassed.*

Legend $\Omega > 1$ $0.9 \leq \Omega \leq 1$ $\Omega < 0.9$

3.3.2.3 Evaluation of Ledge Shear Friction and Flexure Capacity

Figure 3.24 shows the ledge reinforcement details of the inverted-T bent cap specified in AASHTO LRFD (2014). The top layer of the ledge reinforcement (red) is defined as primary tension reinforcement, A_s, to sustain concurrent flexural-tension force at the face of the web. The remainder of the ledge reinforcement (blue) is defined as auxiliary reinforcement, A_h, which only resists shear friction acting normal to the face of the web.

Nominal ledge shear friction (or interface shear) capacity for normal weight concrete is obtained using Equations 5.13.2.4.2-1 and 5.13.2.4.2-2 from AASHTO LRFD (2014). The ledge shear friction capacity is the lesser of:

$$C_s = min \begin{cases} V_n = 0.2 f_c' b_w d_e & (3.10) \\ V_n = 0.8 b_w d_e & (3.11) \\ V_n = c' A_{cv} + \mu\left(A_{vf} f_y + P_c\right) & (3.12) \end{cases}$$

where f_c' = specified concrete strength; b_w = distribution width for the shear friction as specified in Figure 3.25(b); c = distance from the center of bearing pad to the end of the bent cap; W = width of bearing pad; S = girder spacing; a_v = distance from the center of bearing pad to face of the web of the bent cap; d_e = depth of the center of gravity of negative flexural reinforcements as shown in Figure 3.24; A_{cv} = area of concrete considered to be engaged in interface shear transfer; A_{vf} = area of interface shear reinforcement crossing the shear plane within the area A_{cv}; c' = cohesion factor specified in Article 5.8.4.3; μ = friction factor specified in Article 5.8.4.3; and P_c = permanent net compressive force normal to the shear plane. In general, the nominal shear friction resistance is governed by the concrete strength.

Figure 3.25 shows the distribution width, b_w, for shear friction. The AASHTO distribution width of the concrete assumed to participate in the resistance to interface shear friction is the lesser of S and ($W+4a_v$) for interior girders. For exterior girders, the lesser of S, ($W+4a_v$), or $2c$ is used (see Figure 3.25[a]). However, this provides too conservative of results; thus, the rational modification shown in Figure 3.25(b) is proposed: the lesser of S, $c+S/2$, ($W+4a_v$), or $c+(W+4a_v)/2$. This proposed modification will be verified based on the test result. For Bent 13 and 22, since $c+(W+4a_v)/2$ produces the minimum value, $c+(W+4a_v)/2$ is used as a distribution width for exterior girder location.

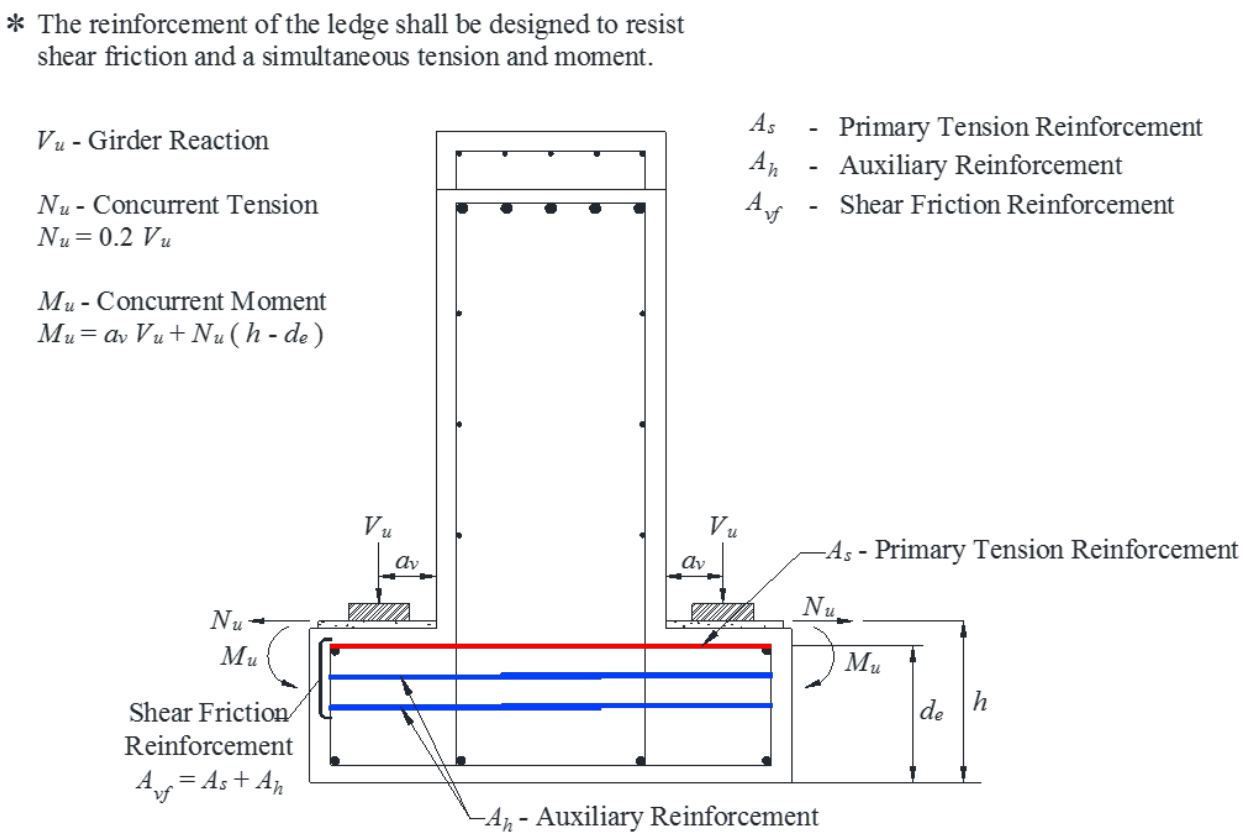

Figure 3.24. AASHTO LRFD (2014) Reinforcement Requirements for the Ledge of Inverted-T Bent Cap.

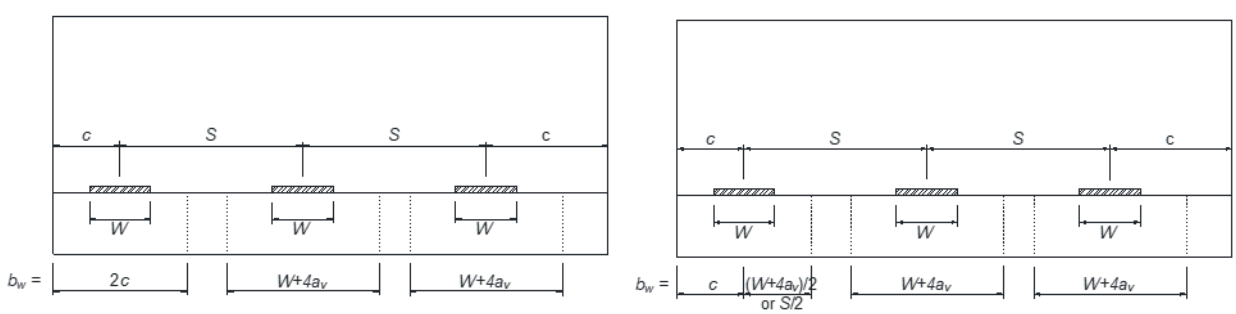

(a) AASHTO distribution widths *(b) Proposed distribution widths*

Figure 3.25. Parameters for Calculation of Ledge Shear Friction Capacity.

The ledge must simultaneously resist a factored girder reaction force, V_u, a factored concurrent horizontal tensile force, N_u, and a factored concurrent moment, M_u. The concurrent horizontal tensile force is regarded as a live load (AASHTO, 2014) and determined by:

$$N_u = 0.2V_u \tag{3.13}$$

The factored concurrent moment M_u is determined using:

$$M_u = V_u a_v + N_u(h - d_e) \tag{3.14}$$

where h = depth of the ledge; and d_e = effective depth of the ledge from extreme compression fiber to the centroid of the tensile force N_u.

Based on Article 3.7.3.2 of AASHTO LRFD (2014), the nominal flexural resistance of the ledge section is taken as:

$$C_f = M_n = A_s f_y \left(d_e - \frac{a}{2}\right) \tag{3.15}$$

where A_s = area of ledge flexure reinforcement specified in Figure 3.24; f_y = yield stress of ledge flexure reinforcement; and a = depth of the equivalent stress block.

The depth of the equivalent stress block, a, should take account of the concurrent horizontal axial tension, N_u, since it already exists. This axial force increases the depth of the equivalent stress block, a, and decreases the ledge flexure capacity based on the equilibrium equation:

$$\frac{N_u}{\phi} + A_s f_y = 0.85 f_c' a b_m \tag{3.16}$$

where b_m = distribution width for ledge flexure and axial tension, as shown in Figure 3.26(a), and a_f = distance from the center of the bearing pad to the center of the nearest stirrup.

Therefore, the depth of the equivalent stress block, a, with axial tension is obtained by:

$$a = \frac{\frac{N_u}{\phi} + A_s f_y}{0.85 f_c' b_m} \tag{3.17}$$

The AASHTO distribution width is taken as the lesser of S and ($W+5a_f$) for interior girders and the lesser of S, ($W+5a_f$), and $2c$ for exterior girders. A rational modification of the distribution width is proposed as the lesser of S, $c+S/2$, ($W+5a_f$), and $c+(W+5a_f)/2$, shown in Figure 3.26(b). In this study, the proposed distribution widths were used to calculate the flexural capacity.

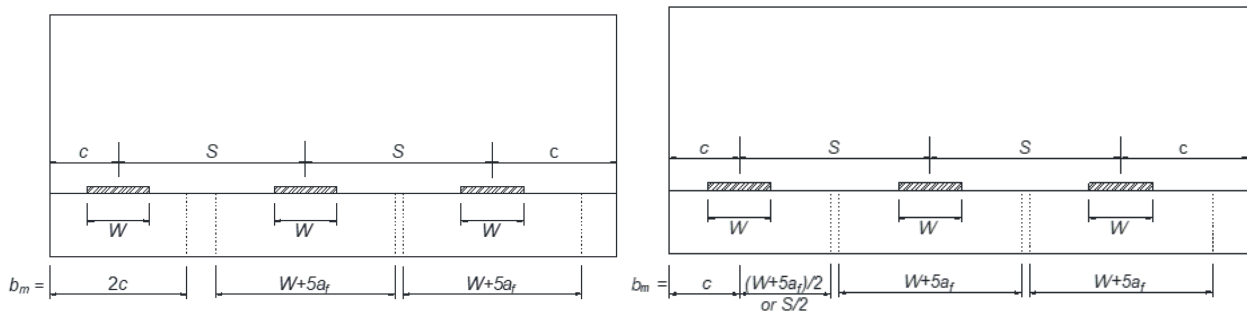

(a) AASHTO distribution widths

(b) Proposed distribution widths

Figure 3.26. Parameters for Calculation of Ledge Flexure with Axial Tension Capacity.

Figure 3.27 and 3.28 show the shear friction, flexural, and axial tension reinforcement layouts in the ledge of southbound Bent 13 and northbound Bent 22. Table 3.6 summaries the ledge shear friction and flexure capacity for each ledge of the bent caps.

For both southbound Bent 13 and northbound Bent 22, ledge shear friction capacity is sufficient with lane increment. However, the overstrength factors for ledge flexure capacity of Bent 13 ranges from 0.94 and 1.08. With an overstrength factor of 0.94, all sections of Bent 13 interior girders have inadequate flexure capacities, with a deficiency of 14 kip-ft. For Bent 22, the overstrength factors range from 1.24 to 2.50.

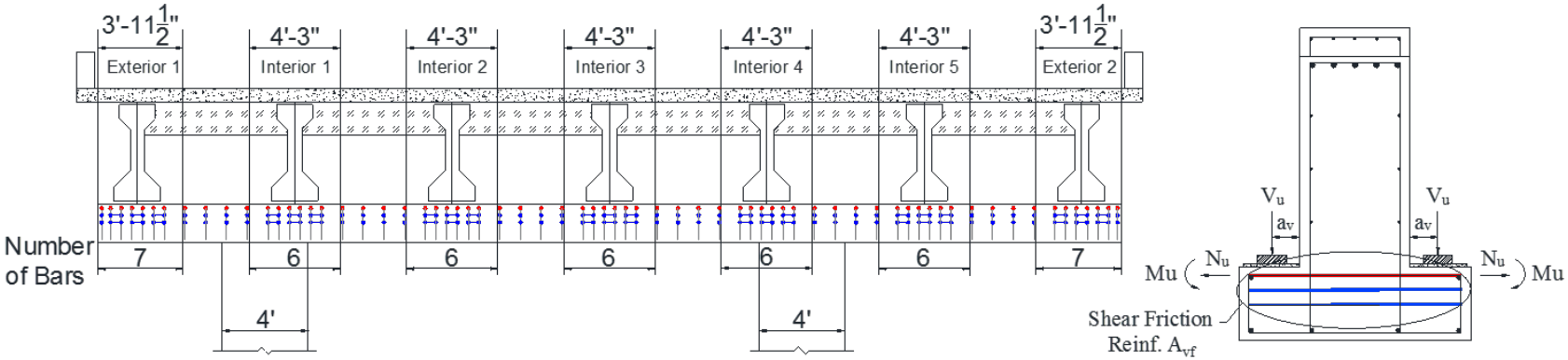

(a) Ledge reinforcement distribution for shear friction

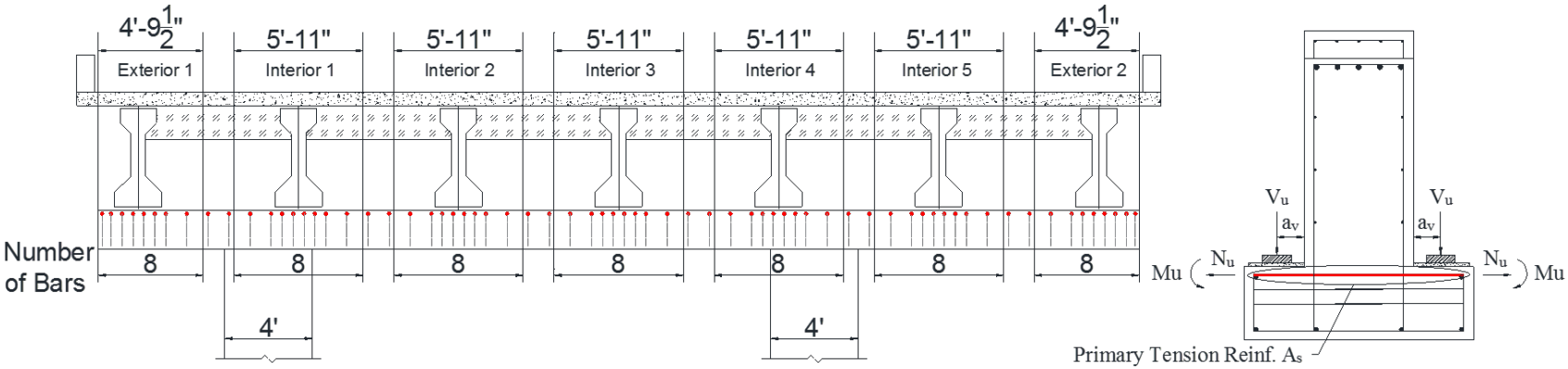

(b) Ledge reinforcement distribution for flexure and axial tension

Figure 3.27. Ledge Reinforcement Distribution of Southbound Bent 13.

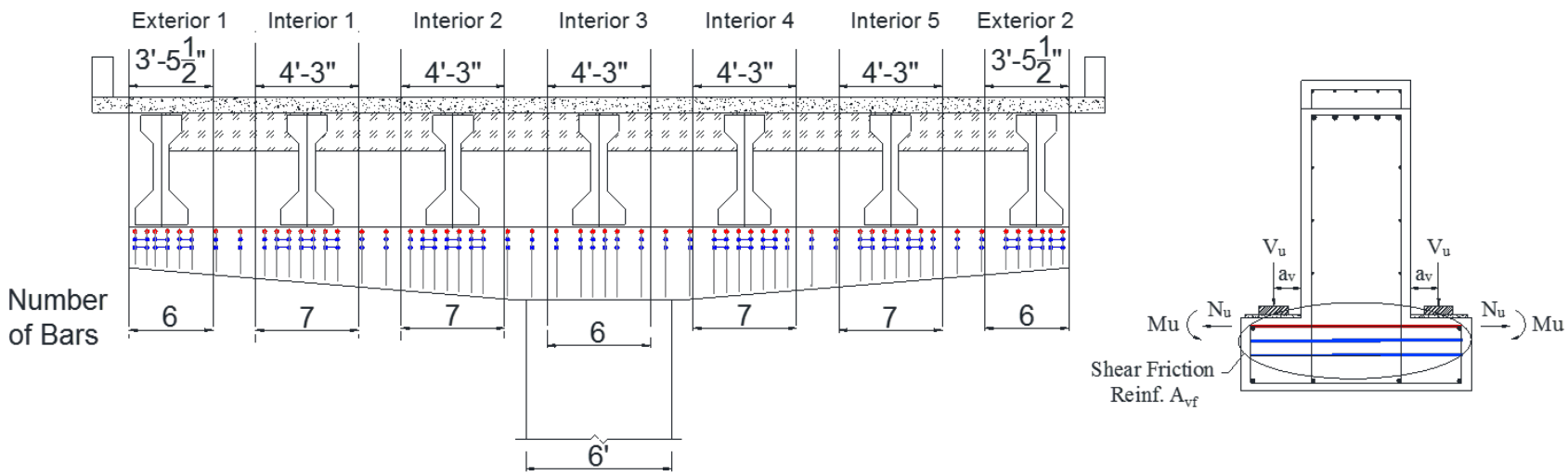

(a) Ledge reinforcement distribution for shear friction

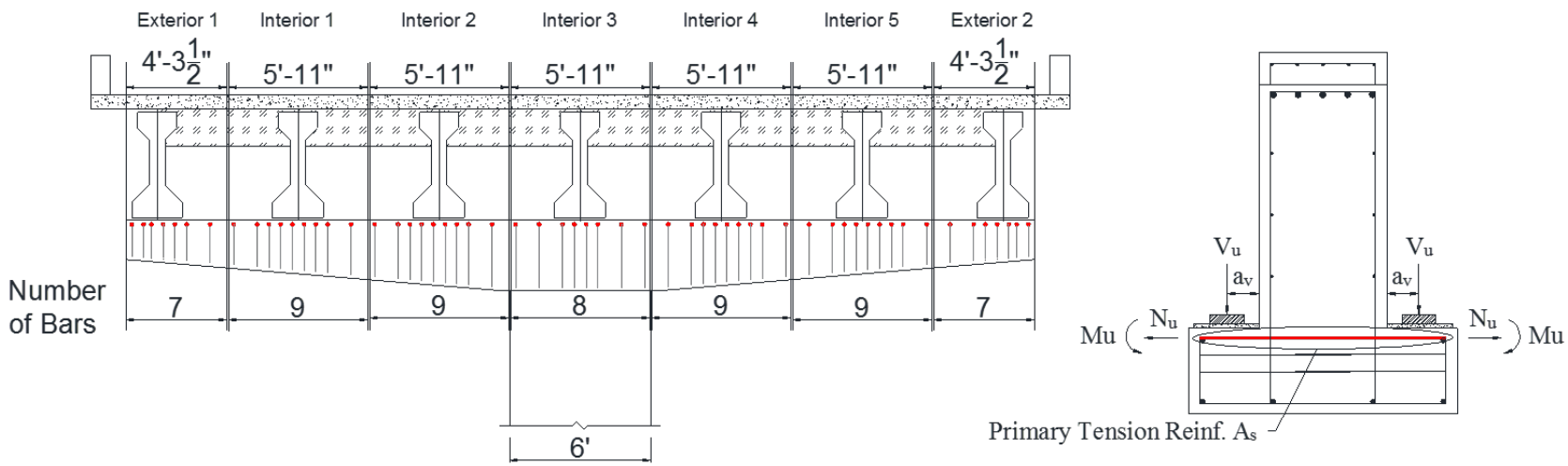

(b) Ledge reinforcement distribution for flexure and axial tension

Figure 3.28. Ledge Reinforcement Distribution of Northbound Bent 22.

Table 3.6. Ledge Shear Friction and Ledge Flexure Capacity Evaluation.

Bent ID	Girder No.	Ledge Shear Friction Capacity C_s (kips)	Demand D (kips)	Ledge Flexure Capacity C_f (kip-ft)	Demand M (kip-ft)	Deficiency $M/\phi - C_f$ (kip-ft)	Ω, $\phi C_f/M$
Southbound Bent 13	Ext. 1	599	247	203	169	N.A.	1.08
	Ext. 2	599	247	203	169	N.A.	1.08
	Int. 1	643	287	204	196	14	0.94
	Int. 2	643	287	204	196	14	0.94
	Int. 3	643	287	204	196	14	0.94
	Int. 4	643	287	204	196	14	0.94
	Int. 5	643	287	204	196	14	0.94
Northbound Bent 22	Ext. 1	444	207	195	141	N.A.	1.24
	Ext. 2	444	207	195	141	N.A.	1.24
	Int. 1	911	235	329	161	N.A.	1.84
	Int. 2	1129	235	409	161	N.A.	2.29
	Int. 3	1230	235	447	161	N.A.	2.50
	Int. 4	1129	235	409	161	N.A.	2.29
	Int. 5	911	235	329	161	N.A.	1.84

Note: ϕ = 0.9 for all capacities.

Legend $\Omega > 1$ $0.9 \leq \Omega \leq 1$ $\Omega < 0.9$

3.3.2.4 Evaluation of Punching Shear and Bearing Capacity

Punching failure can occur if the girder reactions are sufficient enough to punch out a truncated pyramid (shown in Figure 2.3[f]) of concrete beneath the bearing pad. The area of the truncated pyramid shown in Figure 3.29 is approximated as the average of the perimeter of the bearing pad and the perimeter at depth, d_e, assuming 45-degree slopes in AASHTO LRFD (2014). If the adjacent pyramids overlap, an investigation of the combined surface areas is necessary.

When calculating nominal punching shear resistance, TxDOT uses d_f instead of d_e (see Figure 3.29). This is because d_f has traditionally been used for inverted-T bents and was also used in the study of inverted-T beams conducted by Furlong and Mirza (1974). With modifications from the *Bridge Design Manual—LRFD* (BDM-LRFD), Chapter 4, Section 5, design criteria (TxDOT, 2015), the nominal punching shear resistance for interior girders is:

$$V_n = 0.125\sqrt{f_c'}\left(W + 2L + 2d_f\right)d_f \tag{3.18}$$

where L = length of the bearing pad.

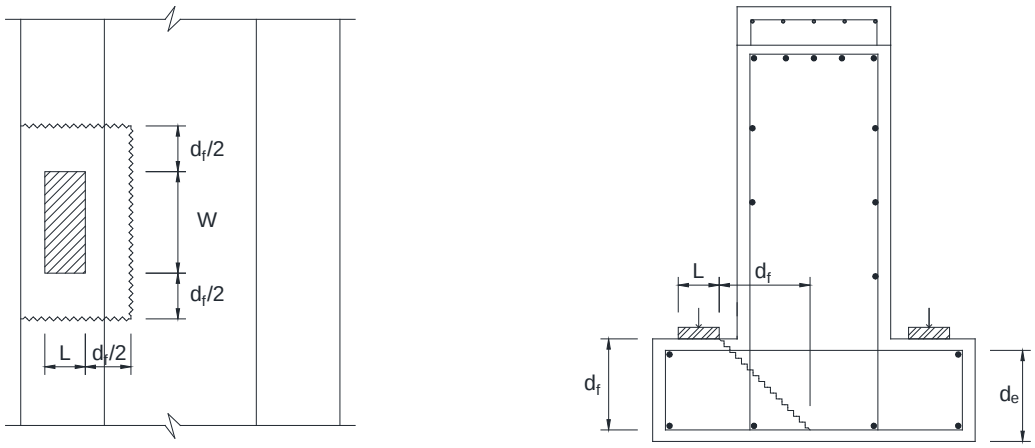

(a) Plan *(b) Cross-section*

Figure 3.29. Punching Shear Failure Surface.

The nominal punching shear capacity for exterior girder locations is the lesser of Equation (3.18) or:

$$V_n = 0.125\sqrt{f_c'}\left(\frac{W}{2} + L + d_f + c\right)d_f \tag{3.19}$$

In general, c is less than $W/2 + L + d_f$, leading to Equation (3.19) controlling the nominal punching shear capacity. Table 3.7 presents the punching shear capacity and demand for southbound Bent 13 and northbound Bent 22. Bent 13 has inadequate punching shear capacity at all girder locations with an overstrength factor of 0.85 and 0.90. Interior girders have deficiencies of 33 kips with an overstrength factor of 0.90, while the exterior girders have a larger deficiency of 42 kips with an overstrength factor of 0.85.

Table 3.7. Punching Shear Capacity Evaluation.

Bent ID	Girder Location	Punching Shear Capacity (kips)	Demand (kips)	Deficiency (kips)	Ω
Southbound Bent 13	Ext. 1 and 2	232	247	42	0.85
	Int. 1 thru 5	286	287	33	0.90
Northbound Bent 22	Ext. 1 and 2	237	207	N.A.	1.03
	Int. 1 and 5	494	235	N.A.	1.89
	Int. 3	806	235	N.A.	3.09
	Int. 2 and 4	700	235	N.A.	2.68

Note: ϕ = 0.9 for all capacities.

Legend $\Omega > 1$ $0.9 \leq \Omega \leq 1$ $\Omega < 0.9$

For northbound Bent 22, all girder portions have sufficient punching shear capacity with an overstrength factor from 1.03 to 3.09. In general, the punching shear capacity of the exterior girders of the single-column bent is larger compared to the double-column bent because of the deeper ledge depth of the single-column bent. Single-column bents have a ledge depth at the end the same as the double-column bent caps, but the ledge depth increases gradually up to the face of the column. Table 3.8 and Table 3.9 present the punching shear resistances at the exterior and interior girders, respectively, on all thruway bent caps. Bent type, span length, and distance from the centerline of the exterior girder to the end face of the bent caps are also listed. For most double-column bents, the centerlines of the exterior girder are 22 in. from the edge except for southbound Bent 10 and northbound Bent 13, which have a larger end face distance of 28 in. and 34 in., respectively.

Table 3.8. Punching Shear Capacity vs. Demand of Thruway Exterior Girders.

Bent No.		Bent Type	Dist. from Ext., Bearing Pad to Cap End (in.)	Capacity (kips)	Demand (kips)	Deficiency (kips)	Ω
Southbound Thruway Bent	10	DC	28	231.5	253	21.5	0.92
	11	DC	22	210	247	37	0.85
	12	DC	22	210	247	37	0.85
	13	DC	22	210	247	37	0.85
	14	DC	22	210	247	37	0.85
	15	DC	22	210	212	2	0.99
	16	DC	22	210	212	2	0.99
	17	DC	22	210	212	2	0.99
	18	DC	22	210	224	14	0.94
	19	SC	16	207	211	4	0.98
	20	SC	16	207	191	N.A.	1.08
	21	SC	16	207	191	N.A.	1.08
	22	SC	16	207	215	8	0.96
Northbound Thruway Bent	11	DC	22	210	260	50	0.81
	12	DC	22	210	251	41	0.84
	13	DC	34	253	266	13	0.95
	14	DC	22	210	237	27	0.89
	15	DC	22	210	212	2	0.99
	16	DC	22	210	212	2	0.99
	17	DC	22	210	210	N.A.	1.00
	8	DC	22	210	210	N.A.	1.00
	19	SC	16	207	214	7	0.97
	20	SC	16	207	191	N.A.	1.08
	21	SC	16	207	207	N.A.	1.00
	22	SC	16	207	207	N.A.	1.00
	23	SC	16	207	207	N.A.	1.00

Legend $\Omega > 1$ $0.9 \leq \Omega \leq 1$ $\Omega < 0.9$

The overstrength factor for the exterior girder of the double-column bent varies from 0.78 to 0.94 depending on the girder span length. For single-column bents, the centerline of the exterior girders is 16 in. from the edge, providing 5 in. past the edge of the bearing pad (Figure 2.3[b]). For single-column bents, the overstrength factors vary from 0.80 to 0.99, which are greater than in the double-column bents. Punching shear deficiencies for interior girders are found only in the double-column bents that have relatively longer span lengths.

Table 3.9. Punching Shear Capacity vs. Demand of Thruway Interior Girders.

Bent ID		Bent Type	Capacity (kips)	Demand (kips)	Deficiency (kips)	Ω
Southbound Thruway Bent	10	DC	259	280	21	0.93
	11	DC	259	289	30	0.90
	12	DC	259	289	30	0.90
	13	DC	259	289	30	0.90
	14	DC	259	289	30	0.90
	15	DC	259	249	N.A.	1.04
	16	DC	259	249	N.A.	1.04
	17	DC	259	249	N.A.	1.04
	18	DC	259	267	8	0.97
	19	SC	446	250	N.A.	1.79
	20	SC	446	226	N.A.	1.97
	21	SC	446	226	N.A.	1.97
	22	SC	446	226	N.A.	1.97
Northbound Thruway Bent	11	DC	259	272	13	0.95
	12	DC	259	279	20	0.93
	13	DC	259	279	20	0.93
	14	DC	259	270	11	0.96
	15	DC	259	247	N.A.	1.05
	16	DC	259	247	N.A.	1.05
	17	DC	259	245	N.A.	1.06
	8	DC	259	245	N.A.	1.06
	19	SC	259	245	N.A.	1.06
	20	SC	446	220	N.A.	2.03
	21	SC	446	235	N.A.	1.90
	22	SC	446	235	N.A.	1.90
	23	SC	446	235	N.A.	1.90

Legend $\Omega > 1$ $0.9 \leq \Omega \leq 1$ $\Omega < 0.9$

The ledge of the inverted-T bent cap should have sufficient bearing capacity to resist the load on the bearing pad at the location of Crack 4 shown in Figure 3.21. The load on the bearing pad distributes along a truncated pyramid as shown in Figure 3.30. The ledge of the bent cap should have bearing resistance as described in Article 5.7.5 of AASHTO LRFD (2014). The bearing capacity of the ledge can be obtained by:

$$V_n = 0.85 f_c' A_1 m \tag{3.20}$$

where A_1 = area under bearing device and m = modification factor, which is the lesser of 2 or:

$$m = \sqrt{\frac{A_2}{A_1}} \tag{3.21}$$

where A_2 = projected bearing area as shown in Figure 3.30, which is described in Article 5.7.5 of AASHTO LRFD (2014).

In general, the bearing capacity is sufficient to resist the girder reaction force, and it is not accounted for as a critical failure mode. However, the bearing capacity should be checked based on the AASHTO LRFD (2014) provisions. Table 3.10 summarizes the evaluation of the bearing capacity of southbound Bent 13 and northbound Bent 22. Overstrength factors for both bents are bigger than 2.00, which indicates that the bearing capacities are sufficient.

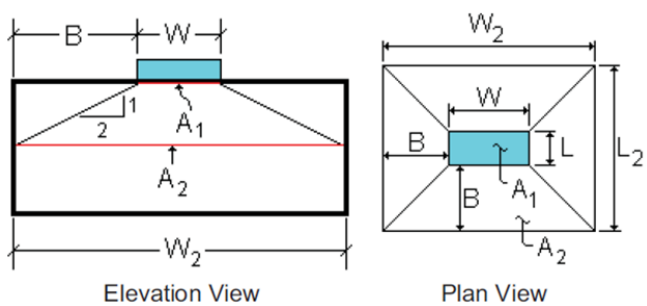

Figure 3.30. Truncated Pyramid for Bearing (TxDOT, 2010).

Table 3.10. Bearing Capacity vs. Demand of Typical Bents.

Bent ID	Girder Location	Bearing Capacity, C (kips)	Demand, D (kips)	Deficiency*, D/ϕ – C (kips)	Ω*, ϕC/D
Southbound Bent 13	Ext.	934	247	N.A.	3.40
	Int.	934	287	N.A.	2.93
Northbound Bent 22	Ext.	937	207	N.A.	4.07
	Int.	937	235	N.A.	3.59

Legend $\Omega > 1$ $0.9 \leq \Omega \leq 1$ $\Omega < 0.9$

3.4 Comparison of 1965 AASHO with 2014 AASHTO LRFD Specifications

The IH 35 bent caps considered in this study were designed following the 1965 edition of the AASHO standard specifications and interim revision for design of highway bridges, which is based on the allowable stress design. The design approach has changed over the past few decades as analysis techniques and quality control for materials have improved. A reliability-based LRFD was adopted by AASHTO in 1994, and since then these specifications have been updated through seven editions, with the latest edition being published in 2014. Some of the major differences between the 1965 AASHO and 2014 AASHTO specifications that can affect the analysis of bent caps are discussed here.

The first major difference is in the live load model. AASHO (1965) specifies that the live load be taken as HS 20-44 lane loadings or HS 20-44 truck or tandem loading, which will produce the maximum stresses at the section considered. As shown in Figure 3.31(a), HS 20-44 lane loading consists of a 0.64 klf uniformly distributed load and a concentrated load with a magnitude of 18 kips for moment and 26 kips for shear traversing the span. As illustrated in Figure 3.31(b), an HS 20-44 truck consists of one front axle weighing 8 kips and two rear axles weighing 32 kips. Tandem loading consists of two 24 kips axles spaced 4 ft apart. For southbound Bent 13 and northbound Bent 22, the HS 20-44 lane loading was used as the live load model. However, the 2014 AASHTO LRFD specifications use a different live load model. That model specifies that the live load be taken as a combination of HS 20-44 truck with a 0.64 klf uniformly distributed lane load (HL-93), or a combination of tandem loading with a 0.64 klf uniformly distributed lane load, which will produce the maximum stresses at the section considered. For Bent 13 and Bent 22, the live loads are larger using AASHTO LRFD (2014) than using the AASHO (1965) used at the time of design.

There is a significant difference in the live load model specified by the 1965 AASHO and 2014 AASHTO LRFD. A single-point load with the magnitude of 26 kips is applied in the 1965 AASHO live load model, whereas multiple point loads with magnitudes of 8, 32, and 32 kips spaced at 14 ft are applied in the 2014 AASHTO LRFD live load model, which yields a 46 kips larger live load shear demand. Also, the 2014 AASHTO LRFD provides a greater impact loading and live load distribution factors than the 1965 AASHO specifications. This can essentially increase the live load shear demand for the designs based on 2014 AASHTO LRFD as compared to the 1965 AASHO. Table 3.11 summarizes the differences between the 1965 AASHO and 2014 AASHTO LRFD for the case of two typical bent caps. The truck loads are placed to yield maximum reaction on the ledge of bent caps.

Table 3.11. 1965 AASHO vs. 2014 AASHTO LRFD Specifications.

	1965 AASHO	2014 AASHTO LRFD
Live Load Model	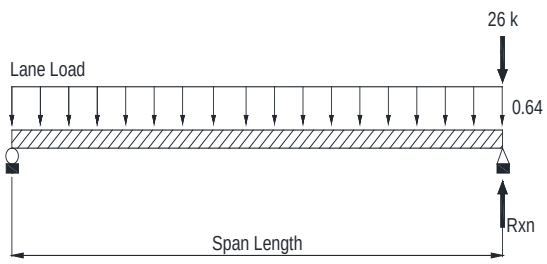 *HS 20-44 Lane Loading*	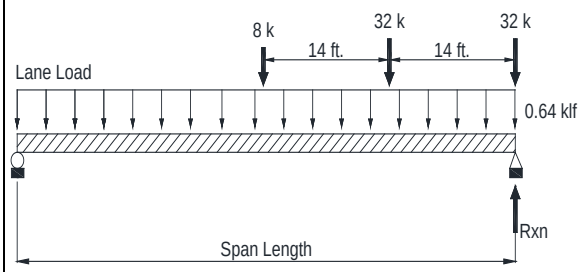 *HL-93 (combined design truck and lane)*
Impact Factor	*IM* = 20.8% for SB Bent 13 *IM* = 22.2% for NB Bent 22	*IM* = 33%
Live Load Distribution Factor	• SB Bent 13 (115 ft – 115 ft): - Exterior – 0.63 - Interior – 0.67 • NB Bent 22 (100 ft – 100 ft): - Exterior – 0.55 - Interior – 0.55	• SB Bent 13 (115 ft – 115 ft): - Exterior – 0.71 - Interior – 0.77 • NB Bent 22 (100 ft – 100 ft): - Exterior – 0.60 - Interior – 0.67

The second difference between the two specifications is the impact factor. The 1965 AASHO expresses the impact factor *IM* as a fraction of live load and a function of span length as:

$$IM = \frac{50}{L + 125} \tag{3.22}$$

where L = span length, ft.

The 2014 AASHTO LRFD gives a constant value for the impact factor depending on the components and limit state under consideration. The impact factor for limit states, other than the fatigue and fracture limit states, turns out to be 0.33. The impact factor for the 1965 AASHO is applicable to truck, lane, and tandem loads; however, the 2014 AASHTO LRFD does not require the lane loading to be increased for dynamic effect.

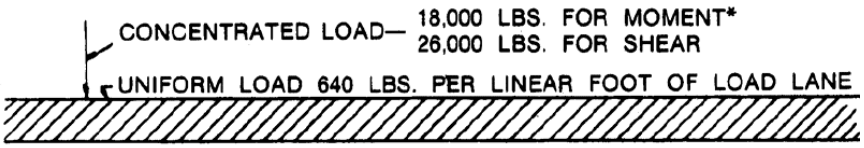

(a) HS 20-44 lane loading

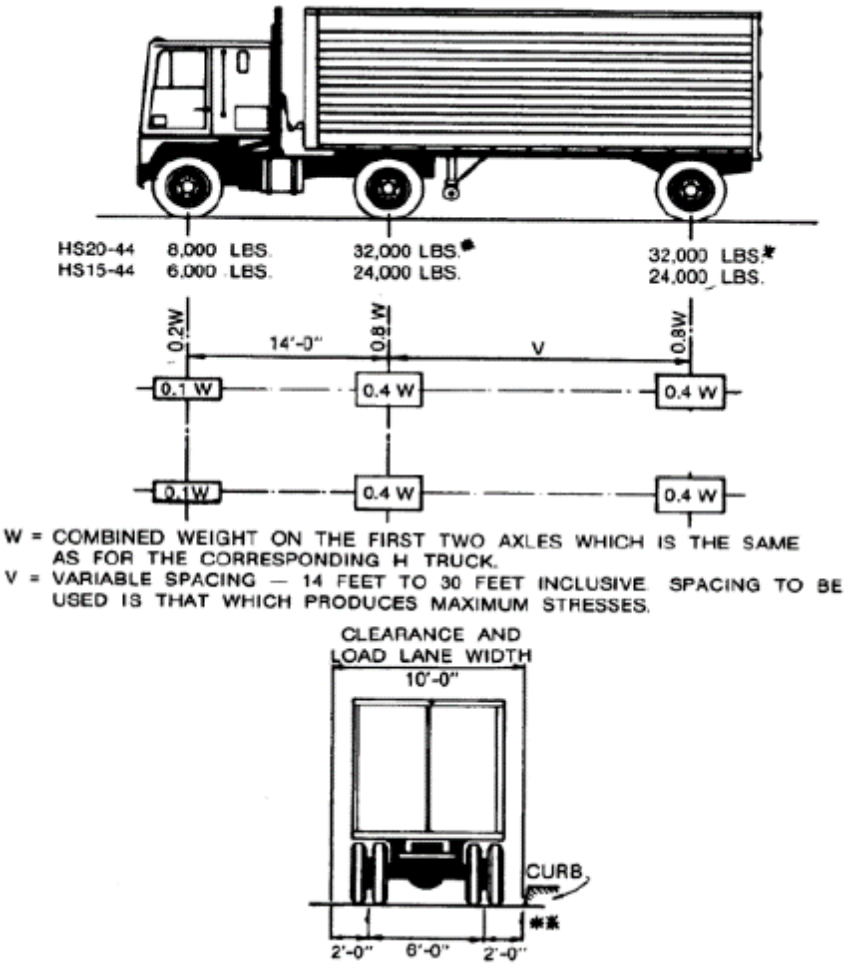

(b) HS 20-44 truck configuration

Figure 3.31. Live Load Models (AASHO, 1965).

Another difference between the two standards is the live load distribution factors (DFs). The live load shear forces, including the effects of impact load, are distributed to the individual girders using the live load distribution factors. The 1965 AASHO specifies a simple formula for live load DF for girder bridges in *S/D* format, where *S* is the girder spacing in feet and *D* is 11 (lanes/girder) for a bridge constructed with a concrete deck on prestressed concrete girders

carrying two or more lanes of traffic. The effects of various parameters such as skew, continuity, and deck stiffness were ignored in this expression, and it was found to be accurate for a few selected bridge geometries and was inaccurate once the geometry was changed (Hueste et al., 2006). For this reason, changes have occurred in the way live load distribution factors are calculated in the LRFD specifications. The 2014 AASHTO LRFD uses a refined analysis for the live load DF. More comprehensive formulas are provided that take into account the span length, girder location, girder depth, transverse and longitudinal stiffness, skew, limit state, and structural type to yield more accurate DF.

For a more in-depth investigation, load demand in accordance with the two standards is calculated and compared below. Strength I limit state of AASHTO LRFD (2014) is selected as follows to evaluate the combined effect of differences between the two standards:

$$V_u = 1.25D + 1.75L_{lane} + 1.75L_{truck}(1 + IM) \tag{3.23}$$

For the 1965 AASHO, the Strength I limit state is:

$$V_u = 1.25D + 1.75L_{lane}(1 + IM) \tag{3.24}$$

Table 3.12 and Table 3.13 provide a summary of demands, all capacities, and overstrength factors of southbound Bent 13 and northbound Bent 22, respectively. The ratio of the design strength ϕV_n (resistance factor ϕ = 0.75) and the factored load demand V_u is defined as the overstrength factor, Ω, which is provided to check the ultimate limit state.

The service demand and factored load demand calculated using AASHTO LRFD (2014) are significantly greater than the load demands calculated using AASHO (1965). The average increase for the factored load demand and service load demand is 43 percent and 35 percent, respectively. The increase in the factored load demand is due to the increased live load demands in AASHTO LRFD (2014).

As evident from Table 3.12, for southbound Bent 13, the Ω computed using the AASHTO LRFD (2014) specifications is less compared to that computed using AASHO (1965). The Ω for the hanger, ledge flexure, and punching shear shows significant changes between the two specifications. It is evident from the Ω of southbound Bent 13 with lane increment that, under ultimate loads, it has considerable hanger, ledge flexure, and punching shear deficiencies when analyzed in accordance with the current AASHTO LRFD specifications.

Table 3.12. Southbound Bent 13—Overstrength Factor.

		1965 AASHO			2014 AASHTO LRFD		
Failure Mode	**Girder No.**	**Capacity (kips)**	**Demand (kips)**	***Ω***	**Capacity (kips)**	**Demand (kips)**	***Ω***
Hanger	Ext. 1	198	190	0.94	198	247	0.72
	Ext. 2	198	190	0.94	198	247	0.72
	Int. 1			*			*
	Int. 2	229	201	1.03	229	287	0.72
	Int. 3	229	201	1.03	229	287	0.72
	Int. 4			*			*
	Int. 5	394	201	1.76	394	287	1.24
Ledge shear friction	Ext. 1	599	190	2.84	599	247	2.18
	Ext. 2	599	190	2.84	599	247	2.18
	Int. 1	643	201	2.88	643	287	2.02
	Int. 2	643	201	2.88	643	287	2.02
	Int. 3	643	201	2.88	643	287	2.02
	Int. 4	643	201	2.88	643	287	2.02
	Int. 5	643	201	2.88	643	287	2.02
Ledge flexure	Ext. 1	297	190	1.41	297	247	1.08
	Ext. 2	297	190	1.41	297	247	1.08
	Int. 1	299	201	1.34	299	287	0.94
	Int. 2	299	201	1.34	299	287	0.94
	Int. 3	299	201	1.34	299	287	0.94
	Int. 4	299	201	1.34	299	287	0.94
	Int. 5	299	201	1.34	299	287	0.94
Punching shear	Ext.	232	190	1.10	232	247	0.85
	Int.	286	201	1.28	286	287	0.90
Bearing	Ext.	934	190	4.42	934	247	3.40
	Int.	934	201	4.18	934	287	2.93

*Note: * Girder located over column; need for hanger reinforcement is bypassed.*

Legend $\Omega > 1$ $0.9 \leq \Omega \leq 1$ $\Omega < 0.9$

Table 3.13 provides a comparison of Ω computed using AASHTO LRFD (2014) and AASHO (1965) specifications for northbound Bent 22. It is evident that Ω computed using the AASHTO LRFD specifications is less compared to AASHO. The Ω for hanger shows considerable changes between the two specifications. It is evident from the Ω of northbound Bent 22 that, under ultimate load, it has hanger deficiencies when analyzed in accordance with the current AASHTO LRFD specifications.

Table 3.13. Northbound Bent 22—Overstrength Factor.

		1965 AASHO			2014 AASHTO LRFD		
Failure Mode	**Girder No.**	**Capacity (kip)**	**Demand (kip)**	***Ω***	**Capacity (kip)**	**Demand (kip)**	***Ω***
Hanger	Ext. 1	214	158	1.22	214	207	0.93
	Ext. 2	214	158	1.22	214	207	0.93
	Int. 1	227	158	1.29	227	235	0.87
	Int. 2	346	158	1.97	370	235	1.33
	Int. 3			*			*
	Int. 4	346	158	1.97	346	235	1.33
	Int. 5	227	158	1.29	227	235	0.87
Ledge shear friction	Ext. 1	575	158	3.28	575	207	2.50
	Ext. 2	575	158	3.28	575	207	2.50
	Int. 1	911	158	5.19	911	235	3.49
	Int. 2	1129	158	6.43	1129	235	4.32
	Int. 3	1230	158	7.01	1230	235	4.71
	Int. 4	1129	158	6.43	1129	235	4.32
	Int. 5	911	158	5.19	911	235	3.49
Ledge flexure	Ext. 1	287	158	1.63	287	207	1.25
	Ext. 2	287	158	1.63	287	207	1.25
	Int. 1	480	158	2.73	480	235	1.84
	Int. 2	598	158	3.41	598	235	2.29
	Int. 3	652	158	3.71	652	235	2.50
	Int. 4	598	158	3.41	598	235	2.29
	Int. 5	480	158	2.73	480	235	1.84
Punching shear	Ext.	237	158	1.35	237	207	1.03
	Int. 1	494	158	2.81	494	235	1.89
	Int. 2	700	158	3.99	700	235	2.68
	Int. 3	806	158	4.59	806	235	3.09
	Int. 4	700	158	3.99	700	235	2.68
	Int. 5	494	158	4.59	494	235	1.89
Bearing	Ext.	937	158	5.34	937	207	4.07
	Int.	937	158	5.34	937	235	3.59

*Note: * Girder located over column; need for hanger reinforcement is bypassed.*

Legend *Ω > 1* *0.9 ≤ Ω ≤ 1* *Ω < 0.9*

3.5 Closing Remarks

Two field visits for evaluating in-service inverted-T bent caps were conducted. During the first visit to the northern end of the elevated lanes of IH 35 through Austin, the structural characteristics, existing condition of the inverted-T bent caps, and nonstructural challenges to implementation of strengthening solutions were investigated. The second field inspection was conducted on US 290 in Austin to mainly evaluate conditions of the inverted-T bent caps. Cracks were observed at the ends of the inverted-T caps of double-column bents in both field inspections. The cracks extended along the ledge-web interface and provided an indication of the mechanisms needed for design of ledge strengthening solutions.

In addition to the field inspections, in-service inverted-T bent caps that are part of the IH 35 thruway system located in downtown Austin were evaluated. Although the bent caps were designed in accordance with the AASHO (1965) specifications, the current performance of the inverted-T bent caps was evaluated according to the current AASHTO LRFD (2014) specifications. Since double-column southbound Bent 13 and single-column northbound Bent 22 were found to have the largest girder reaction force on the ledges, the bent caps were evaluated theoretically. The analysis revealed that the inverted-T bent cap under most internal and external girders of southbound Bent 13 had insufficient overstrength factors for the hanger, ledge flexure, and punching shear. However, in the case of northbound Bent 22, the hanger capacity was insufficient under the exterior girders but sufficient under the interior girders. Ledge flexure capacity was also insufficient at the exterior girder locations, but not beneath the interior girders. There was a sufficient overstrength factor for punching shear for northbound Bent 22.

In the following chapter, potential retrofit solutions to improve the deficiency of the inverted-T bent caps are proposed.

CHAPTER 4. DESIGN OF POTENTIAL RETROFIT SOLUTIONS

Potential retrofit solutions for in-service inverted-T bent caps are proposed in this chapter. Eighteen retrofit solutions were developed to provide enhanced or alternative load paths to augment the existing inverted-T bent caps with deficient capacities. The retrofit solutions are designed to address the largest deficiency of 90 kips found from the bent cap analysis presented in Chapter 3. All solutions are designed to fit the typical double-column bent cap (southbound Bent 13) with the exception of the load-balancing post-tensioning solution (Solution 14) that was developed for both double- and single-column (northbound Bent 22) bent caps. Design concept, general design procedure, and load path of the retrofitted system are presented in the following sections. The details of the final design are discussed briefly. The step-by-step design procedure is provided in **Error! Reference source not found.**.

4.1 Prestressed High-Strength Threadbar (Solution 1)

Figure 4.1 shows a retrofit solution using high-strength prestressed threadbars. Horizontal prestress forces are applied to the ledge of the inverted-T bent cap using externally anchored high-strength threadbars. Busting stresses are avoided by using a continuous angle, as shown in Figure 4.1(a).

This solution is expected to increase the ledge flexure and punching shear capacities. Existing ledge cracks are restrained, and girder loads are distributed by the alternative load paths, as shown in Figure 4.1(b). The induced prestress resists the flexural and shear forces generated by the girders on the ledges as depicted in Figure 4.1(c) and (d).

The size and quantity of threadbars are determined based on the required level of prestress. The design prestressing force is assumed to be 60 percent of the ultimate stress after losses provided by the manufacturer. Negative moment generates tensile stress on the upper chord of the ledges, which causes ledge flexure and punching shear cracks. Therefore, the prestressing force must be larger than the flexural force on the ledges. The applied moment, which is described in Figure 3.24 and Figure 4.1(a), can be obtained by Equation (3.14).

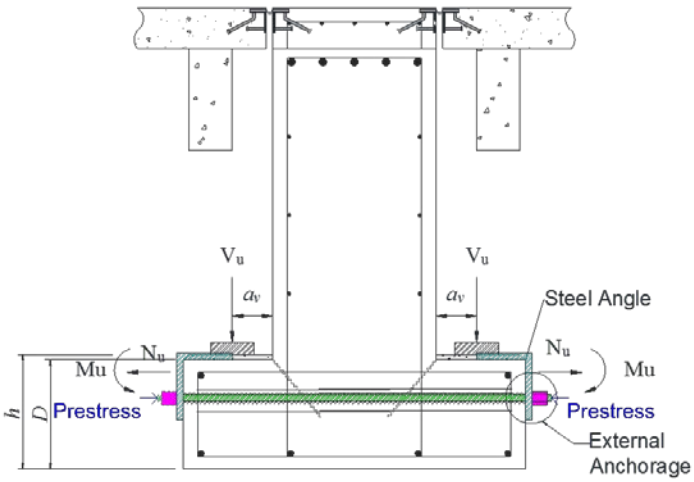

(a) Concept

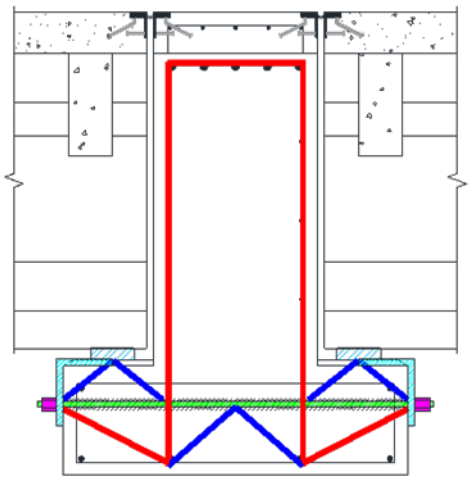

(b) Load paths on cross-section

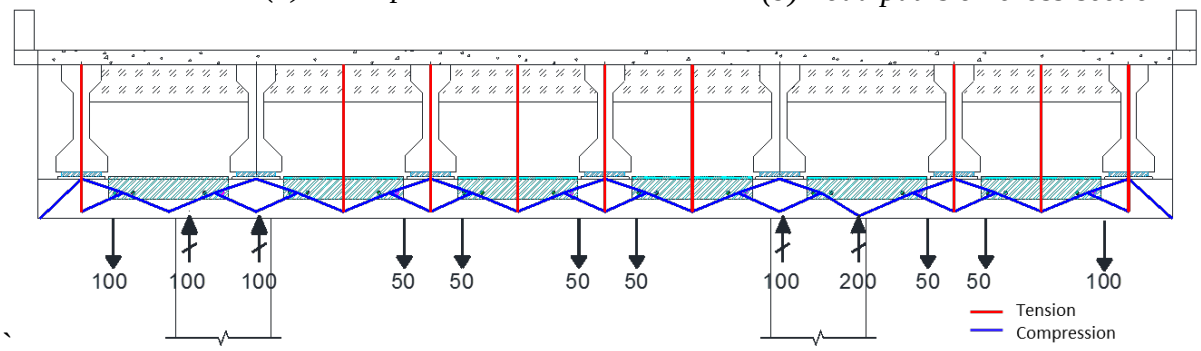

(c) Load paths and forces for additional 100 kip capacity per girder seat (kips)

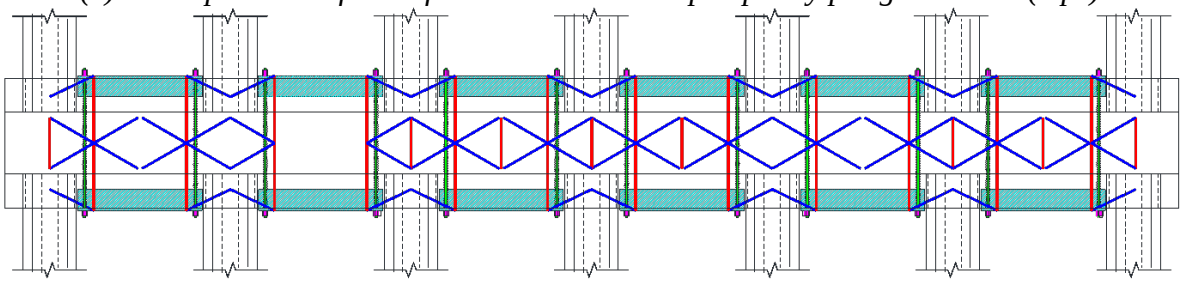

(d) Load paths on plan view

Figure 4.1. Prestress Using High-Strength Threadbars to Supplement Punching Shear and Ledge Flexure Deficiency.

Then, using stress block analysis for a no-tension solution gives the required prestress force:

$$F \geq \left(\frac{0.2 + \frac{6\left(a_v + 0.2(h - d_e)\right)}{D}}{1 + \frac{6e}{D}} \right) V_u \tag{4.1}$$

where V_u = factored load demand; a_v = distance from center of bearing pad to the web surface; D = ledge depth; h = ledge depth plus height of bearing seat; d_e = distance from bottom of ledge to center of the primary axial reinforcement; and e = upward eccentricity from the center line of the ledge. To achieve zero tension on the beam soffit, e should be set at the kern point, specifically $e = D/6$, to ensure enough space for installation.

The required prestress force from Equation (4.1) is converted from the required shear force using the geometry. Based on the geometry, it can be shown that:

$$F \geq 1.33 V_u \tag{4.2}$$

For a 90 kip deficiency, $F = 119.7$ kips. It is assumed that each bar equally resists the shear force in the ledges. The design shear strength of threadbars is 60 percent of ultimate strength and must be greater than the required shear strength, which is the same as V_u. Based on the required prestress and shear capacity of the threadbars, as shown in Figure 4.2, two bars with 1 in. diameter may be used. To avoid the installation of threadbars right beneath the girders, two prestressing bars that are 21 in. away from the center of the girder should be located on either side of the girder, taking into account the stirrups in the ledges and the bearing area. The distance between the two threadbars should be larger than the minimum spacing specified in ACI 318 (ACI Committee 318, 2014):

$$s_{min} = 6 d_b \tag{4.3}$$

where s_{min}= minimum spacing between the threadbars; and d_b = diameter of the threadbars. A spacing of 6.5 in., which satisfies the requirements, was assumed in this study.

The steel angle is designed based on its bearing strength according to the related AISC (2010a; 2010b) manual and specifications. The minimum required thickness is obtained by:

$$t_{min,req} = \max\left(\frac{R_n}{\phi 2.0 d_b f_u}, \frac{V_n}{\phi 2.4 d_b f_u} \right) \tag{4.4}$$

where $t_{min,req}$ = required thickness of the plate for bearing; R_n = nominal bearing strength, which is the maximum prestressing force in this case; ϕ = design factor for LRFD; f_u = ultimate strength of the steel plate; and d_b = diameter of threadbars.

To ensure there is no effect on the original structure, yield strength of the steel angle is used. The required bearing area is calculated by:

$$A_{b,req} = \frac{P_u}{\phi_c 0.85 f_c'} \tag{4.5}$$

where $A_{b,req}$ = required base bearing area; P_u = tensile force, which is the prestressed load in this case; and ϕ_c = 0.65 = design factor for LRFD. Based on the above requirements, the design thickness for the bearing is computed to be 1.25 in. and a customized steel angle with dimensions of 11½ × 10¼ × 1¼, as shown in Figure 4.2(b), is used for each girder.

The dimensions of the nuts and washers used to anchor the threadbars are based on the diameter of the bars, and their dimensions are provided by the manufacturer. The use of hex nuts designed for prestressing threadbars with hardened washers is proposed.

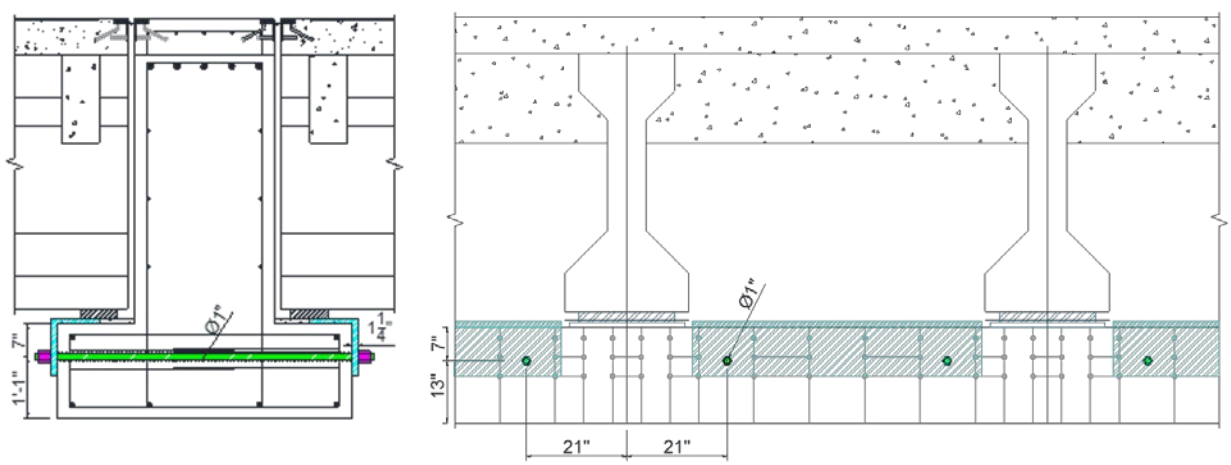

(a) Cross-section *(b) Side elevation*

Figure 4.2. Solution for Ledge Flexure and Punching Shear Deficiency by Applying Prestress Directly to the Ledges.

4.2 Steel Hanger Bracket (Solution 2)

Figure 4.3 shows a retrofit solution in which girders sit on steel brackets anchored to the web. The anchored steel brackets provide a complementary load path that reduces demand on the ledge. Figure 4.3(b) presents an elevation of the expected load path for the design of this retrofit solution. The steel bracket is designed to transfer loads, and the anchors are designed to carry shear and tension loads. Selection of anchors should utilize shear and tension capacity of proprietary anchors to minimize the number used.

The pullout force on the bolts can be estimated from:

$$T_d = \frac{P_u x}{jd} \tag{4.6}$$

where P_u = the demand on a single bracket; x = offset distance to the centroid of the load P_u; and $jd = d - a/2$ = internal lever arm where d = depth (shown in Figure 4.4[a]) and a = stress block depth (shown in Figure 4.4[c]) formed from:

$$a = \frac{T_d}{0.85 f_c' b} \tag{4.7}$$

where b = bracket width as shown in Figure 4.4(a).

The load eccentricity is critical for shear force. The required shear force for each bolt is calculated using:

$$V_{u,i} = \sqrt{\left(\frac{M_{u,v} d_{iy}}{\sum d^2} + R_x\right)^2 + \left(\frac{M_{u,v} d_{ix}}{\sum d^2} + R_y\right)^2} \tag{4.8}$$

where $V_{u,i}$ = required shear strength for i^{th} bolt; $M_{u,v}$ = applied torque due to eccentric load; d_{ix} and d_{iy} = distance from i^{th} bolt to the center of gravity of bolt group in horizontal and vertical direction, respectively; $d = \sqrt{d_{ix}^2 + d_{iy}^2}$ = distance from the center of gravity of bolts group to each bolt; and R_x and R_y = applied eccentric shear force divided by the number of bolts in the horizontal and vertical direction, respectively.

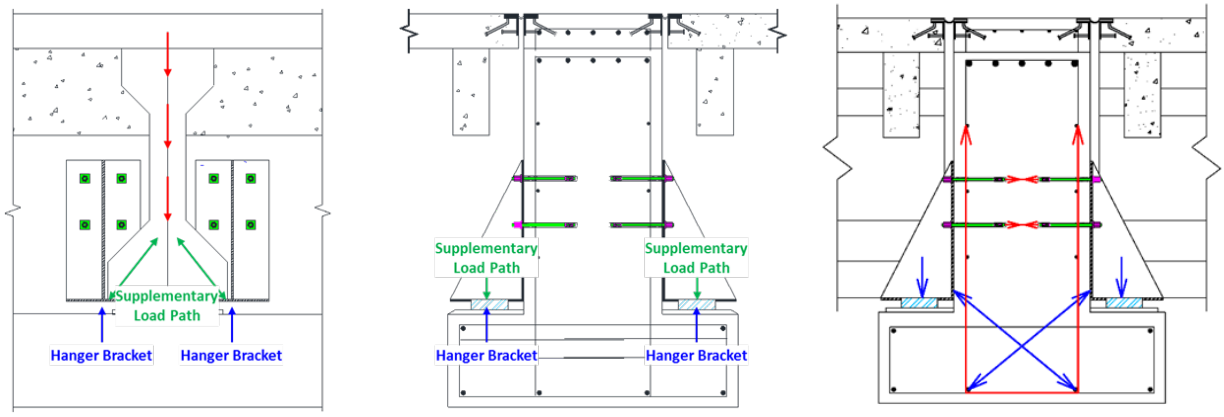

(a) Concept *(b) Load paths on cross-section*

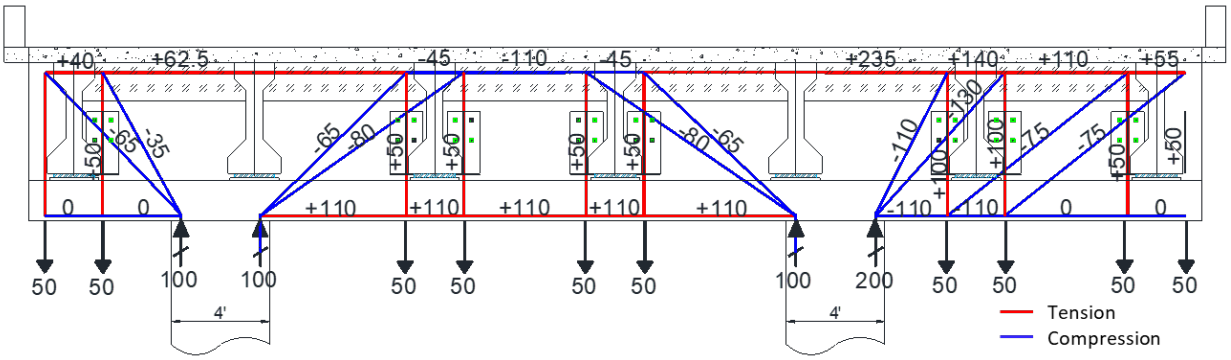

(c) Load paths and forces for additional 100 kip capacity per girder seat (kips)

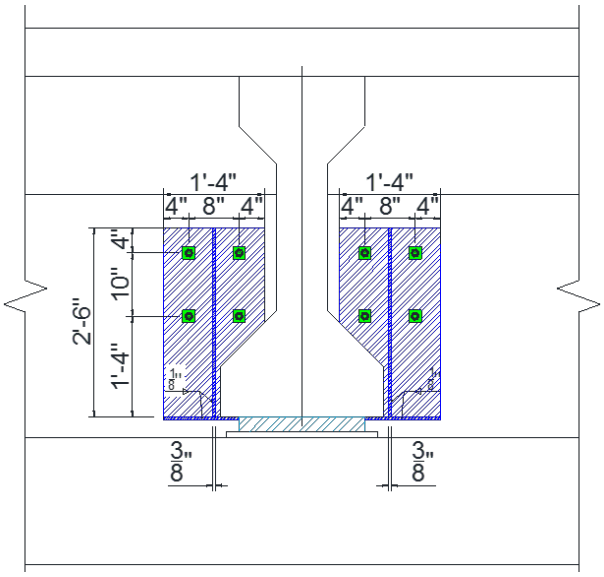

(d) Side elevation

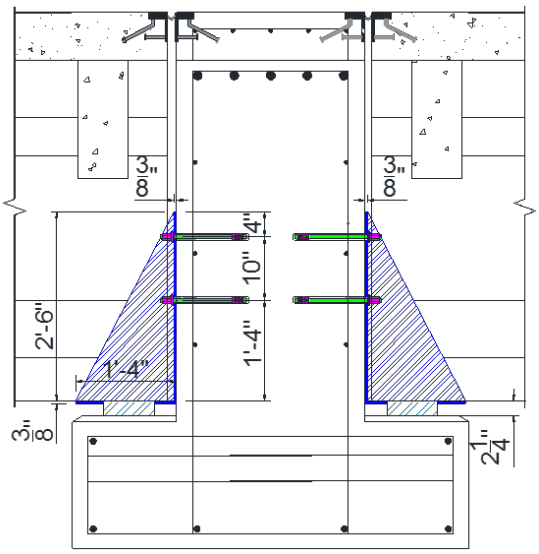

(e) Cross-section

Figure 4.3. Steel Hanger Bracket to Supplement Punching Shear and Ledge Flexure Deficiency.

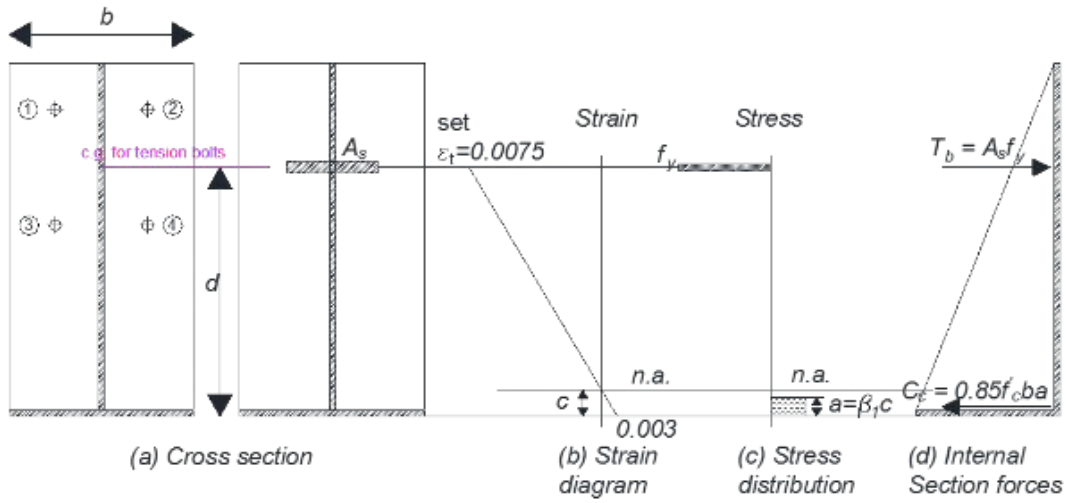

Figure 4.4. Assumption for Design of Anchor Bolts in Tension Using Whitney Stress Block.

The required tension and shear strength should be less than the bolt capacity. Because of their relatively large capacity, adhesive anchors may be used instead of mechanical anchors so that the number of anchors may be minimized. The capacity of an adhesive anchor is given by:

$$N_n = \min(N_{sa}, N_{cb}, N_{ag}) \tag{4.9}$$

$$V_n = \min(V_{sa}, V_{cb}, V_{cpg}) \tag{4.10}$$

where N_n and V_n = tensile and shear capacity of an adhesive anchor, respectively; N_{sa} and V_{sa} = steel strength of anchor for tension and shear, respectively; N_{cb} and V_{cb} = concrete breakout strength of anchor for tension and shear, respectively; N_{ag} = bond strength of adhesive anchor; and V_{cpg} = concrete pryout strength of anchor.

The parameters N_{sa}, V_{sa}, N_{cb}, V_{cb}, N_{ag}, and V_{cpg} are calculated according to ACI 318R (ACI Committee 318, 2014). The combined tensile and shear strengths must satisfy:

$$\left(\frac{N_u}{\phi N_n}\right)^{\varsigma} + \left(\frac{V_u}{\phi V_n}\right)^{\varsigma} \leq 1.0 \tag{4.11}$$

where ς = 5/3, which is a simplified expression given by the code.

Based on the requirements, 1 in. diameter Hilti HIT-HAS-E-B7 rods with HIT-RE 500 V3 epoxy are used for this solution. Four sets of epoxy anchors are used to anchor each bracket to the web of the bent cap with 12 in. embedment depth. The location of the bolts is decided by considering the existing reinforcements within the web of the inverted-T bent cap, as well as the minimum spacing requirement specified by Equation (4.3).

The brackets consist of three steel plates—vertical, triangle, and bottom plates—that are welded together. Geometry is affected by the anchor configuration. Each plate should be designed to meet the thickness requirements based on bearing strength, shear yield strength, tension yield strength, shear rupture strength, tension rupture strength, and weld size as given by AISC (2010a):

$$t_{bearing} \geq \frac{V_u}{\phi 1.8 d_b f_u} \tag{4.12}$$

$$t_{s,y} \geq \frac{\frac{P_u}{n_{bracket}}}{\phi 0.6 h_b f_y} \tag{4.13}$$

$$t_{t,y} \geq \frac{\frac{P_u}{n_{bracket}}}{\phi b_v f_y} \tag{4.14}$$

$$t_{s,r} \geq \frac{\frac{P_u}{n_{bracket}}}{\phi 0.6 h_n f_y} \tag{4.15}$$

$$t_{t,r} \geq \frac{\frac{P_u}{n_{bracket}}}{\phi b_n f_y} \tag{4.16}$$

$$t_{req,w} = \frac{F_{EXX} a}{0.93 f_y} \tag{4.17}$$

where $t_{bearing}$ = minimum thickness for bearing strength; ϕ = strength reduction factor for LRFD; d_b = diameter of the bolt; f_u = ultimate strength of the plate; $t_{s,y}$ = minimum thickness for shear yield strength; $n_{bracket}$ = number of brackets per girder; h_v = height of vertical plate; f_y = yield strength of the plate; $t_{t,y}$ = minimum thickness for tension yield strength; b_v = width of vertical plate; $h_n = h_v - \sum(d_{b,i} + 1/16)$ = nominal height of vertical plate; $t_{s,r}$ = minimum thickness for shear rupture strength; $b_n = b_v - \sum(d_{b,i} + 1/16)$ = nominal width of vertical plate; $t_{t,r}$ = minimum thickness for tension rupture strength; $t_{req,w}$ = required thickness of the plate for weld; F_{EXX} = filler metal classification strength; and a = weld size, which is given by:

$$a_{req} = \frac{F_{wr}}{\phi A_{we} F_{mv}} \tag{4.18}$$

where a_{req} = required weld size; ϕ = design factor from LRFD; A_{we} = effective area of the weld; t = thickness of vertical plate; $F_{mv} = 0.60 F_{EXX}(1.0 + 0.5\sin^{1.5}\theta)$; θ = angle of loading measured from the weld longitudinal axis in degrees ($\theta = 0$); and F_{wr} = fillet weld strength (AISC, 2010a).

The minimum required thickness of the vertical plate is the largest thickness estimated using Equations (4.12) to (4.17). In this case, the bearing strength controls the design.

If the designed thickness meets the required weld thickness, it should be checked by bearing strength considering weld and load eccentricity given by:

$$P_u \leq \frac{\phi 1.8 f_y h_l^2}{6e_p - \frac{h_l}{2}} n_{bracket} \tag{4.19}$$

where h_l = height of base plate.

Plates with the same thickness are welded together to make the bracket. To form a bracket, the strength of the triangular plate should also be checked using:

$$P_u \leq f_y t sin^2\alpha \left(\sqrt{4e^2 + h_l^2} - 2e\right) n_{bracket} \tag{4.20}$$

where t = thickness of the plates for a bracket; α = angle at the bottom of the triangular plate; and e = eccentricity, which is $e = e_p - h_l/2$.

For the prototype example with P_u = 90 kips and based on the above requirements, the designed thickness of the plates is 3/8 in. E70 electrodes may be used to weld the plates together to form the bracket. The size of the weld is determined to be 1/8 in.

4.3 End-Region Stiffener (Solution 3)

Figure 4.5 shows a retrofit in which an anchored steel plate is applied to the end of the bent cap. The anchored end plate is applied to strengthen the end region where distress is typically observed as cracks emanating from the reentrant corner. The solution is only applicable to the end region and may be used in conjunction with other retrofit solutions. Figure 4.6 shows an elevation of the expected load path for the design of the solution. The solution enhances hanger, ledge flexure, and punching shear capacity of the end region of the inverted-T bent cap.

The approach is particularly useful for Bent 22, where only the exterior girders require additional seating capacity, as shown in Figure 4.6(b). The thickness of the plate is primarily controlled by shear and axial bearing force of the anchors. The minimum required thickness of the plate is obtained using Equations (4.12) to (4.16). Because the weight of the stiffener plate is likely to be significant, its weight should be taken into account while calculating the required forces.

The capacity of the anchors is governed by their shear strength, which should be greater than the required strength calculated using Equation (4.8). The anchor capacity is calculated by

multiplying reduction factors to the design strength provided by the manufacturer. The location of the existing reinforcing bars should be taken into account while placing the anchors because the holes for the anchors need to be 1/4 in. larger than the diameter of the anchors. Based on the required strength of each anchor, eight 1-1/4 in. diameter anchors should be used to anchor the stiffener plate. In this case, the anchors at the web and the ledges are calculated on the maximum deficiency of 90 kips. Figure 4.7 shows the location of the anchors and the dimensions of the stiffener plate.

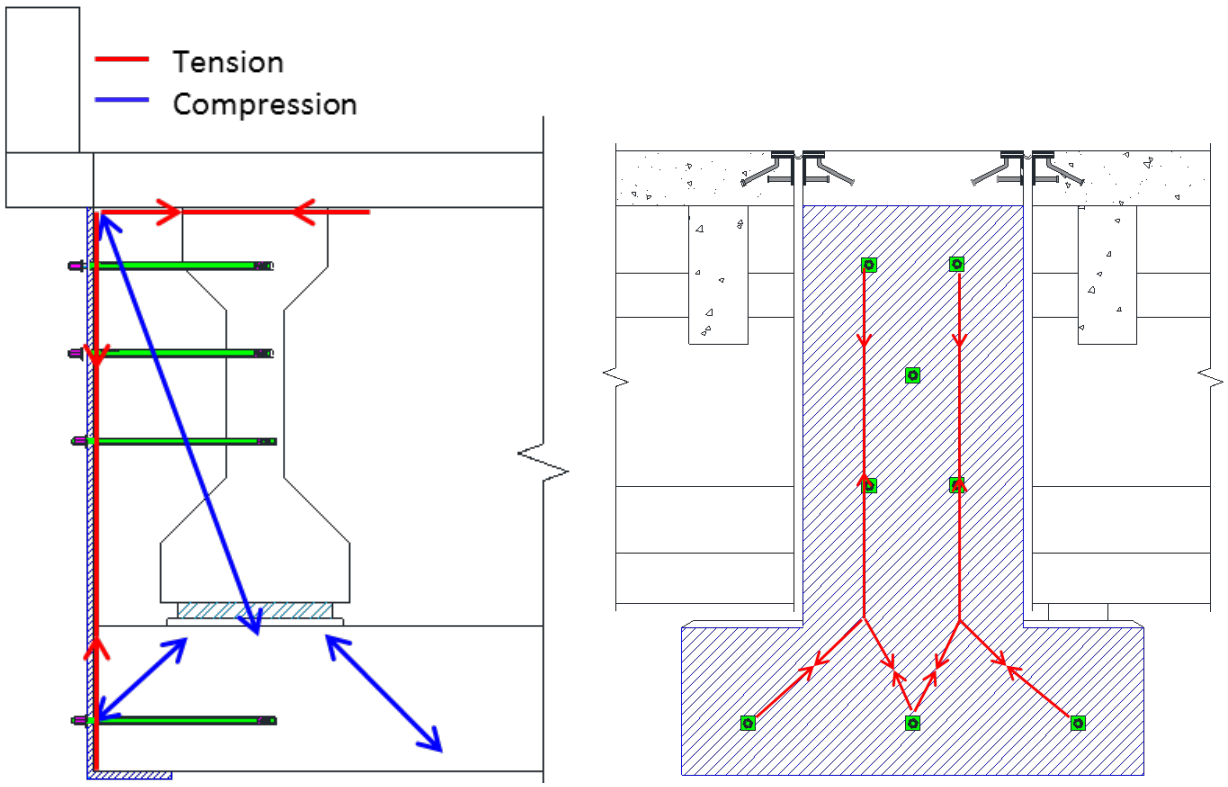

(a) Side elevation *(b) Cross-section*

Figure 4.5. End-Region Strengthening Using Steel Stiffener to Supplement Hanger, Ledge Flexure, and Punching Shear Capacity in the End Regions.

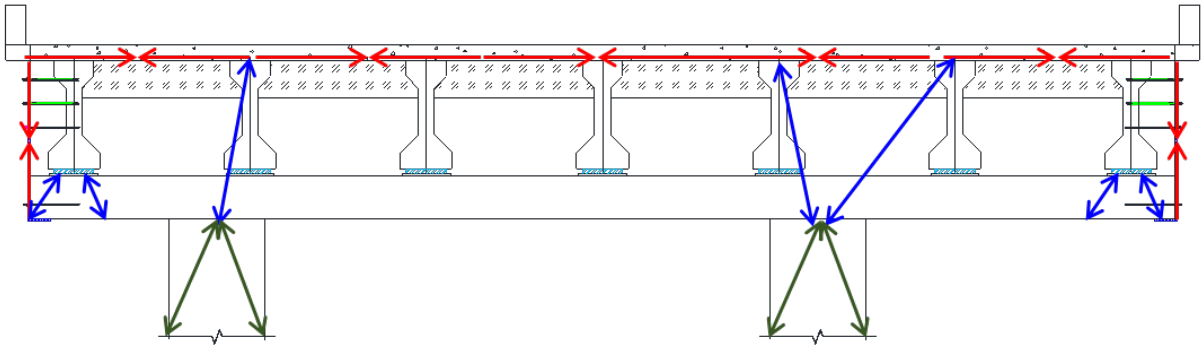

(a) Side elevation of double-column bent

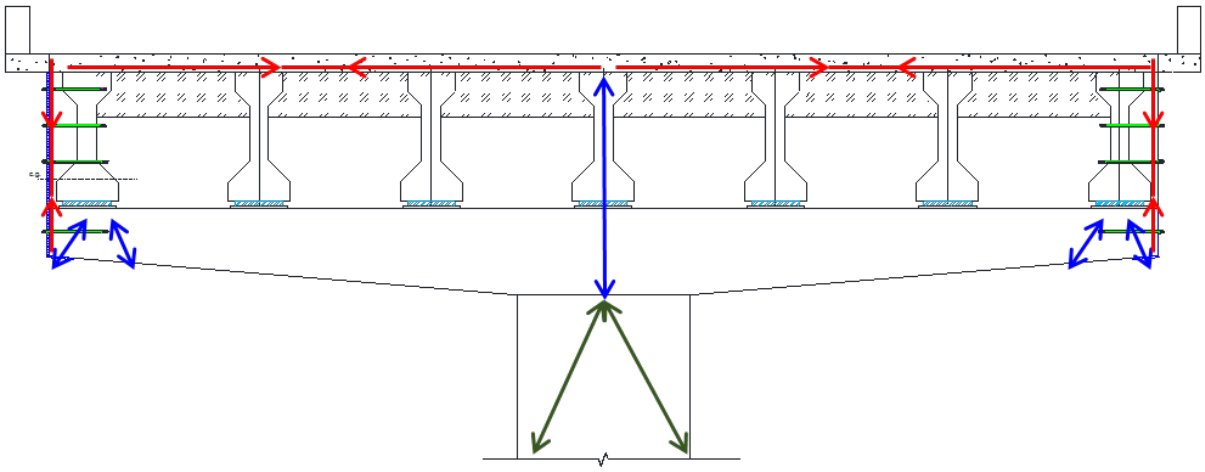

(b) Side elevation of single-column bent

Figure 4.6. Load Path with End-Region Stiffener.

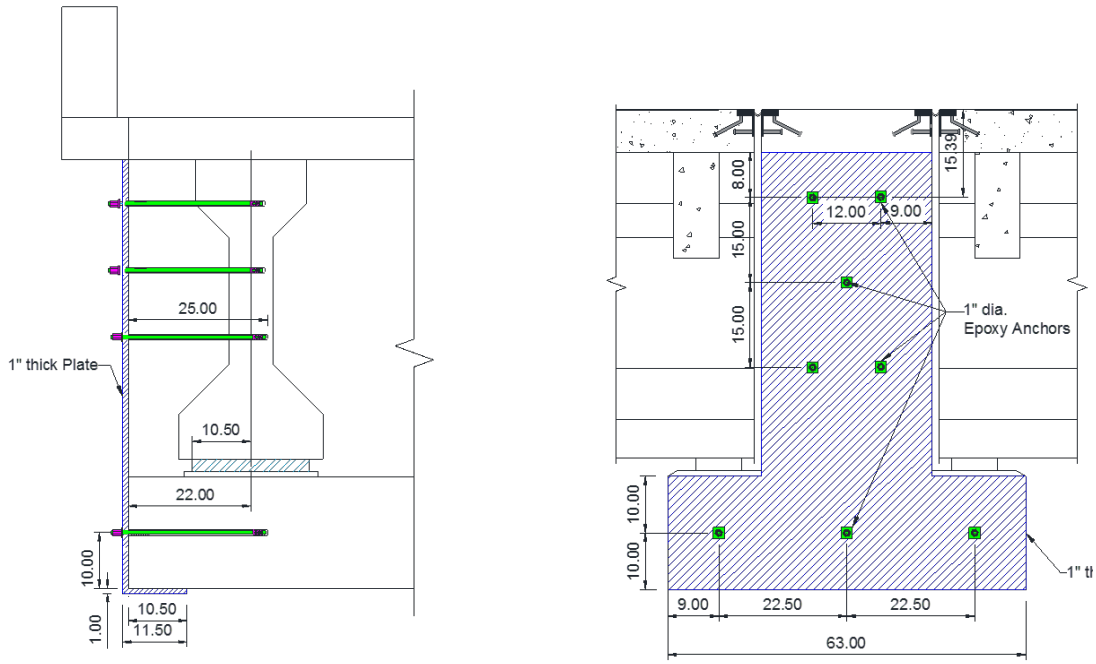

(a) Side elevation *(b) Cross-section*

Figure 4.7. End-Region Strengthening Method Using Stiffener Plate.

4.4 Clamped Cross Threadbar (Solution 4)

Figure 4.8 presents a clamped cross threadbar solution to supplement ledge flexure and punching shear deficiencies. The anchored threadbars provide supplementary load path to transfer the girder loads to the web. Preexisting cracks at the reentrant corners can be restrained by prestressing the threadbars. Beveled washers are required between the nut and bearing plates at each end of the threadbars. An external anchoring system is used to minimize interference with the existing rebar.

Figure 4.8(b) and (c) show the expected load path for the design of the solution. The number of threadbars required for the retrofit is based on the required strength and design strength of the bars. The required strength for each threadbar is obtained by:

$$F_{req} = \frac{P_u}{n_t \sin\theta} \tag{4.21}$$

where F_{req} = required tensile strength; P_u = loads from the girders; n_t = number of bars; and θ = smaller angle between the rod and bottom face of the ledge.

The angle of the threadbars is determined based on the location of the existing reinforcement within the inverted-T bent cap and the maximum adjustable angle of the beveled washers.

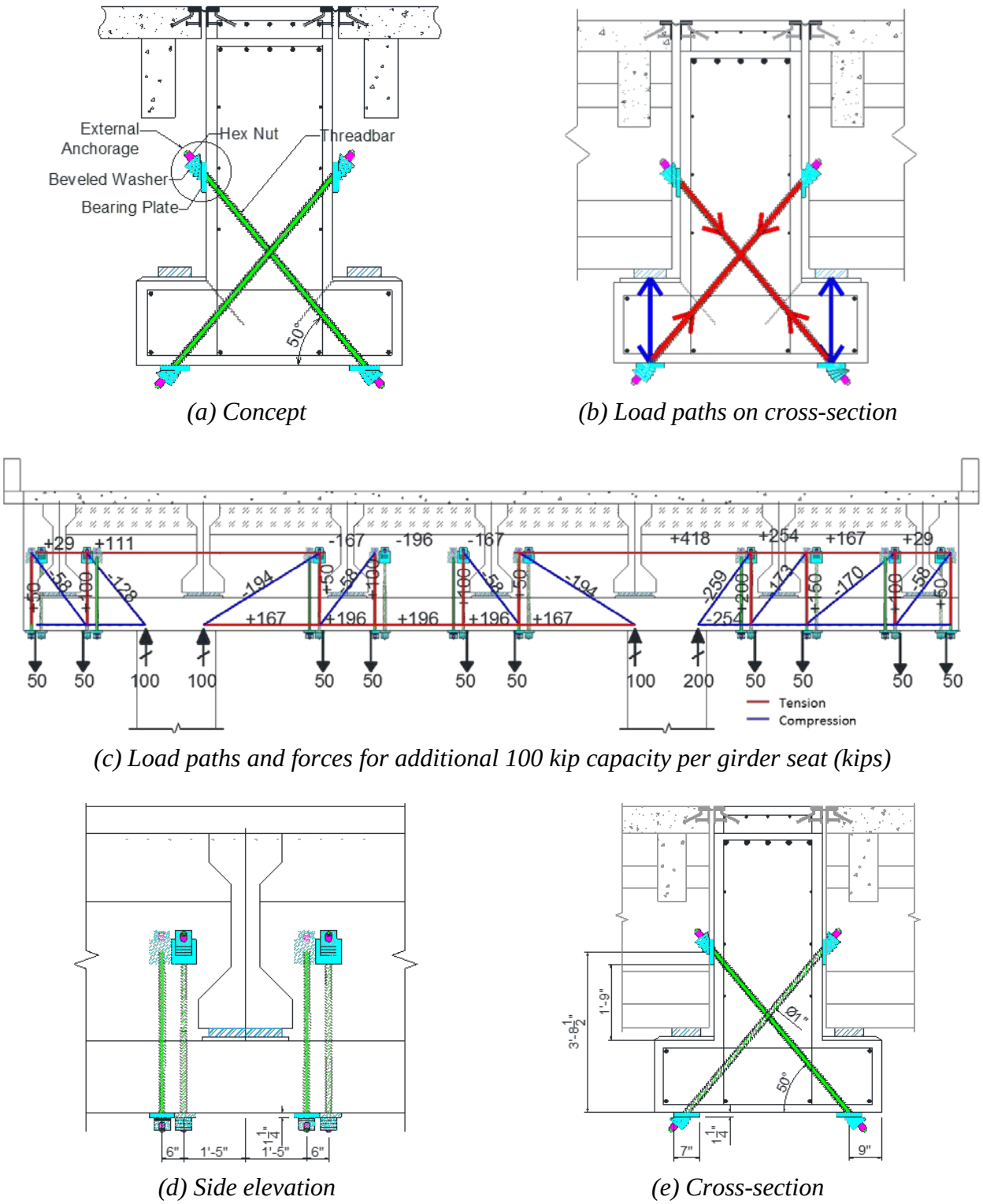

(a) Concept

(b) Load paths on cross-section

(c) Load paths and forces for additional 100 kip capacity per girder seat (kips)

(d) Side elevation

(e) Cross-section

Figure 4.8. Clamped Cross Threadbars to Supplement Ledge Flexure and Punching Shear Deficiency.

The required tensile strength should be less than the design strength of each threadbar. The design strength is the same as the design tensile strength and is given by:

$$T_d = 0.6A_{n,b}f_{pu} \tag{4.22}$$

where T_d = design tensile strength of threadbar; $A_{n,b}$ = minimum net area of the bar; and f_{pu} = ultimate stress of the threadbar.

Based on Equation (4.22), the design tensile strength of the threadbars controls failure. A threadbar with an ultimate strength of 150 ksi and 1 in. diameter sufficient for an optimized angle of 50 degrees should be used for the external anchoring system. The maximum adjustable angle of the beveled two-washer set (manufactured by Dywidag) is 20 degrees for a 150 ksi threadbar. Therefore, a single set of two beveled washers is required for the external anchoring system. At the bottom of the ledges, the threadbars should be anchored at a distance of 9 in. from the edge of the ledges. A total of four bars is required for this retrofit solution.

The size of the bearing plate can be determined using Equations (4.4) and (4.5) since the loads acting on the clamped threadbars are directly induced into the bearing plate. Figure 4.8(d) and (e) show the design details. A square bearing plate with 7 in. sides and a thickness of 1-1/4 in. is used.

The cantilever portion of the bent caps (both single- and double-column bents) may be strengthened by a combination of the end-region stiffener. Post-tensioning of long threadbars should be used in conjunction with the end-region stiffener plates to strength external hanger capacity if needed. To provide sufficient tension forces, 10 ft and 20 ft long post-tensioning bars should be used in the short and long overhang portions, respectively, of the inverted-T bent cap.

The diameter of the long post-tensioning threadbar is decided by the required post-tension force. The required post-tension force can be calculated using:

$$T_{pt} = 0.9T_{SAT} \tag{4.23}$$

where T_{SAT} = top chord tension force obtained from 100 kip increased capacity at each girder seat for STM, as shown in Figure 4.8(b).

4.5 Grouted Cross Threadbar (Solution 5)

Figure 4.9 presents the concept and load path details to be considered in the design of the grouted cross threadbar. The concept, shown in Figure 4.9(a), is similar to that of the clamped cross

threadbar. However, instead of using an external anchoring system in the web, threadbars are grouted to provide anchorage. The grouted threadbars terminate at a location higher than the clamped cross threadbars, as shown in Figure 4.9(b). This concept may be suitable for augmenting an inverted-T bent with a ledge flexure or punching shear deficiency by transferring the loads into the existing hanger reinforcement.

The number of threadbars required for the retrofit is determined based on the required strength and design strength of the bars. The required strength for each threadbar is obtained using Equation (4.21).

The angle is decided by the location of the existing reinforcements in the inverted-T bent cap and the maximum adjustable angle of the beveled washer. The required tensile strength should be less than the design strength of each threadbar.

The design strength of a grouted threadbar is the lesser of its design tensile strength and bond strength. The bond strength is given as:

$$N_{bond} = \tau \pi d h_{ef} \tag{4.24}$$

where N_{bond} = bond strength; τ = bond stress for fully cured grout; d = diameter of drilled hole, which is 1.5 times larger than bar diameter; and h_{ef} = anchor embedment depth.

The effective embedded depth for the grouted threadbar is approximately 43 in., which is measured from the top of the ledge to the end of the bar in the web. US Spec RA Grout, which has a fully cured bond stress of 1.5 ksi, is considered in this design. Based on Equation (4.24), the design tensile strength of the threadbar controls failure for the grouted threadbar.

Figure 4.9(d) and (e) show the design details. A threadbar with an ultimate strength of 150 ksi and 1-1/4 in. diameter is adapted with an optimized angle of 70 degrees for the grouted system. The maximum adjustable angle of the beveled two-washer set (manufactured by Dywidag) is 20 degrees for a 150 ksi threadbar. A single set of beveled washers is used. At the bottom of the ledges, the threadbars are anchored at a distance of 16 in. from the edge of the ledges. A total of two bars, spaced 22 in. from each other, are used for the grouted threadbar retrofit solution.

The size of the bearing plate can be determined using Equations (4.4) and (4.5) since the load from the girder to the threadbars is directly induced into the bearing plate. A square bearing plate with 7 in. sides and 1.125 in. thickness is used.

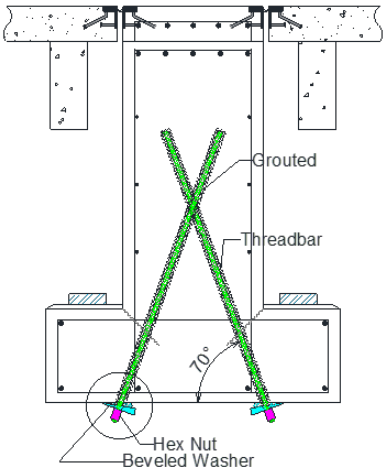

(a) Concept

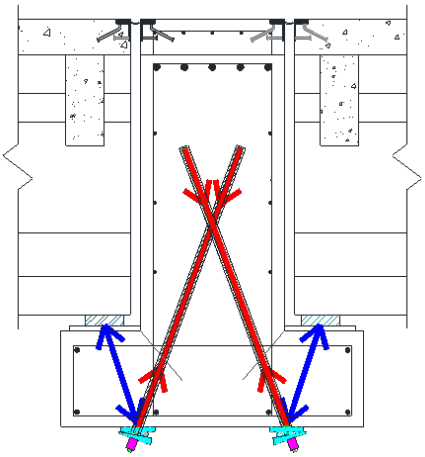

(b) Load paths on cross-section

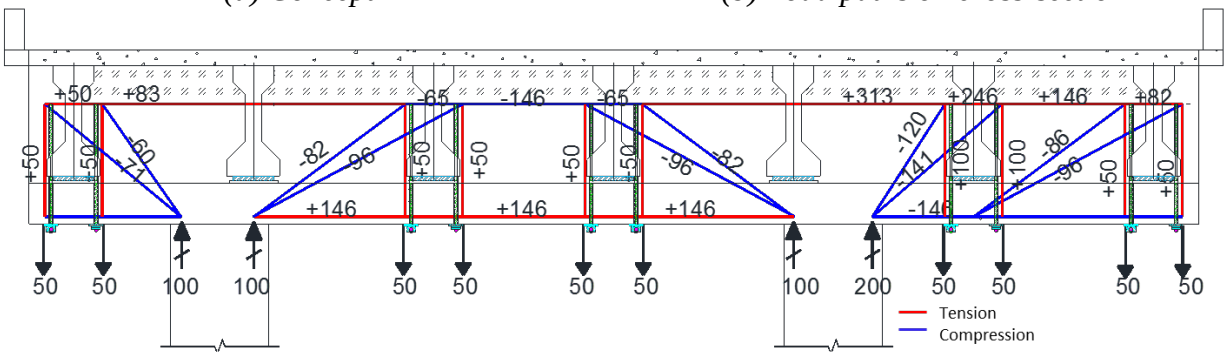

(c) Load paths and forces for additional 100 kip capacity per girder seat (kips)

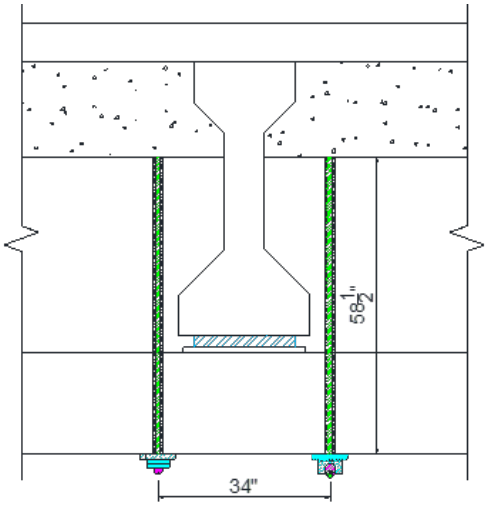

(d) Side elevation

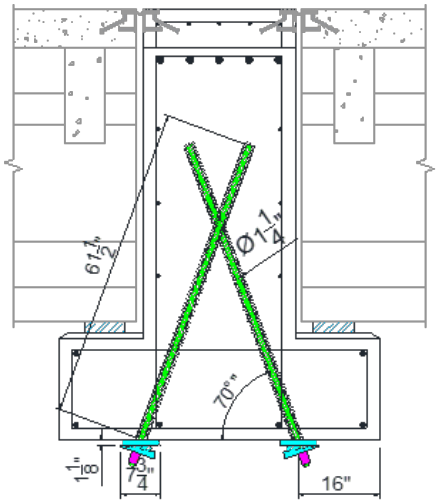

(e) Cross-section

Figure 4.9. Grouted Cross Threadbars to Supplement Ledge Flexure, Punching Shear, and Hanger Deficiency.

4.6 Upper Seat Bracket (Solution 6)

Figure 4.10 shows the retrofit solution using upper seat brackets. The basic concept of this solution is to provide supporting elements below the diaphragm to provide a complementary load path directly form the bridge deck slab. Because an additional load path, as shown in Figure 4.10(a), is provided to reduce the loads from the slab to the girder, the loads on the ledge of the inverted-T bent cap are reduced. This solution will indirectly account for the insufficient shear resistance of the ledge. However, the load from the brackets must be transferred into the web of the inverted-T bent cap beam, and in turn, the shear carried by the hangers as before. To help bypass the existing hangers, some of the load can be transferred into the end plate system.

The seat bracket consists of lateral, vertical, and triangle steel plates and is designed to support the diaphragms so that the loads from the slabs directly transfer into the web of the inverted-T bent cap. Adhesive anchors are used to anchor the steel brackets to the web of the bent cap. As illustrated in Figure 4.10, the loads are transferred to the web through the steel brackets and the anchor bolts.

Anchor bolts are designed in accordance with ACI Committee 318 (2014). Anchors are chosen based on their combined pullout and shear capacity. The required strength of the bolts is obtained from Equations (4.7) and (4.8) and checked using Equation (4.11). This is the same procedure as that used for the steel hanger bracket solution (Solution 2). For the example solution design calculations, Hilti HAS-E-B7 bolts with HIT-RE-500 V3 epoxy are adapted as the anchor bolts for this application. Six sets of 7/8 in. diameter anchors are required to anchor the steel brackets to the web of the bent cap with 10.5 in. embedded depth.

The height and width of the steel plates for the bracket are chosen based on the location of the anchor. Based on Equations (4.12) to (4.16), it is established that the vertical plate for the bracket is controlled by shear rupture, with the thickness of the plate determined using Equation (4.15). For welding purposes, each steel plate ideally should have the same thickness. Based on the thickness of the vertical plate, the weld size can be determined from Equation (4.18).

The required thickness of the vertical plates should also be checked for bearing strength using Equation (4.17).

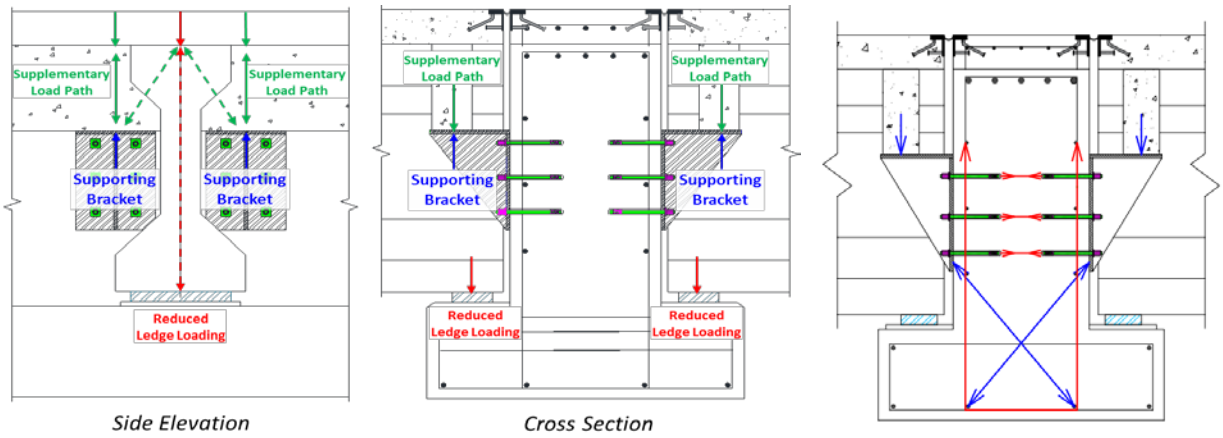

(a) Concept *(b) Load paths on cross-section*

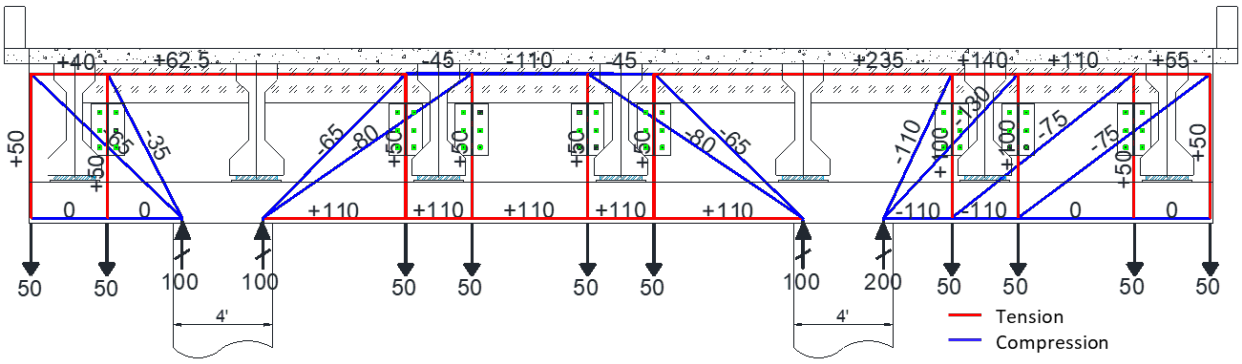

(c) Load paths and forces for additional 100 kip capacity per girder seat (kips)

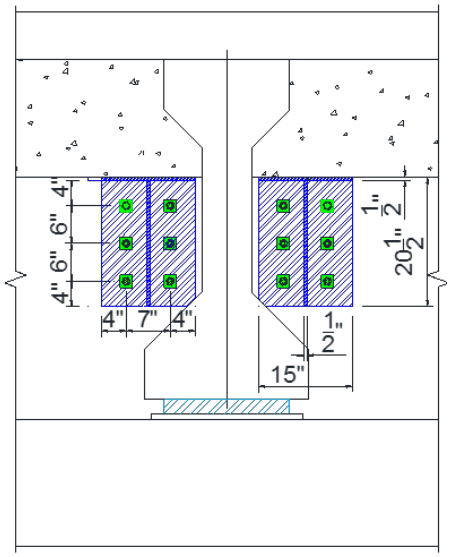

(d) Side elevation

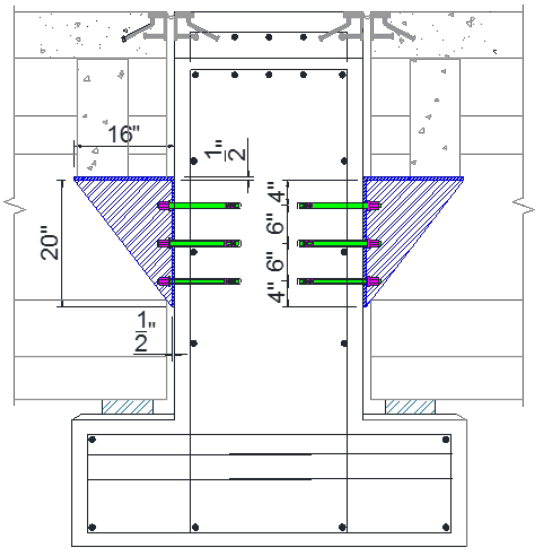

(e) Load paths on cross-section

Figure 4.10. Upper Seat Bracket to Supplement Punching Shear and Ledge Flexure Deficiency.

Buckling of the triangular plate should be checked using the following:

for $0.5 \leq \frac{h_l}{h_v} \leq 1.0$ $$\frac{h_l}{t} \leq 1.47\sqrt{\frac{E}{f_y}} = \frac{250}{\sqrt{f_{y(ksi)}}} \tag{4.25}$$

for $1.0 \leq \frac{h_l}{h_v} \leq 2.0$ $$\frac{h_l}{t} \leq 1.47\left(\frac{h_l}{h_v}\right)\sqrt{\frac{E}{f_y}} = \frac{250(\,h_l/h_v)}{\sqrt{f_{y(ksi)}}} \tag{4.26}$$

where E = Young's modulus of steel.

Based on the thickness of the vertical plate, the size of the other plates for the bracket is determined, and the strength of the triangular plate is checked using Equation (4.20). Based on the design calculations, 0.5 in. thickness plates should be used for the brackets. Figure 4.10(d) and (e) show the dimensions of the bracket.

4.7 Threadbar Hanger with Steel Bracket (Solution 7)

Figure 4.11 shows a retrofit in which partial-depth hanger threadbars are supported by anchored steel brackets at mid-depth of the web. The retrofit system provides supplementary load paths to transfer the girder loads to the web at mid-depth; therefore, the system is expected to enhance only the punching shear and ledge flexure capacity. The expected load paths for the strengthened system are shown in Figure 4.11(b) and (c). The threadbars are designed to transfer the girder loads, and the steel brackets are designed to provide support to the threadbars. The bolts used to anchor the steel brackets are designed to carry shear and tension loads.

The design tensile strength of threadbars should be larger than the girder loads:

$$N_u \leq \phi N_n = \phi A_s f_u \tag{4.27}$$

where N_u = loads from the girders; ϕ = 0.75 tension factor for LRFD; N_n = nominal tensile strength; A_s = minimum net area through treads; and f_u = ultimate stress of the threadbar.

Once the threadbars are chosen, anchor bolts for the brackets are selected. The required strength of the bolts to anchor the bracket can be calculated using Equations (4.7) and (4.8) by adopting the same procedure used for the anchor bolts for the hanger bracket solution. Since there is no shear eccentricity for the bracket anchors, $M_{u,v} = 0$ and $R_x = 0$.

For design strength of the proprietary anchor bolt system, the reduction factors provided by the manufacturer should be adopted. Interaction between tension and shear for each bolt should also be checked using Equation (4.11).

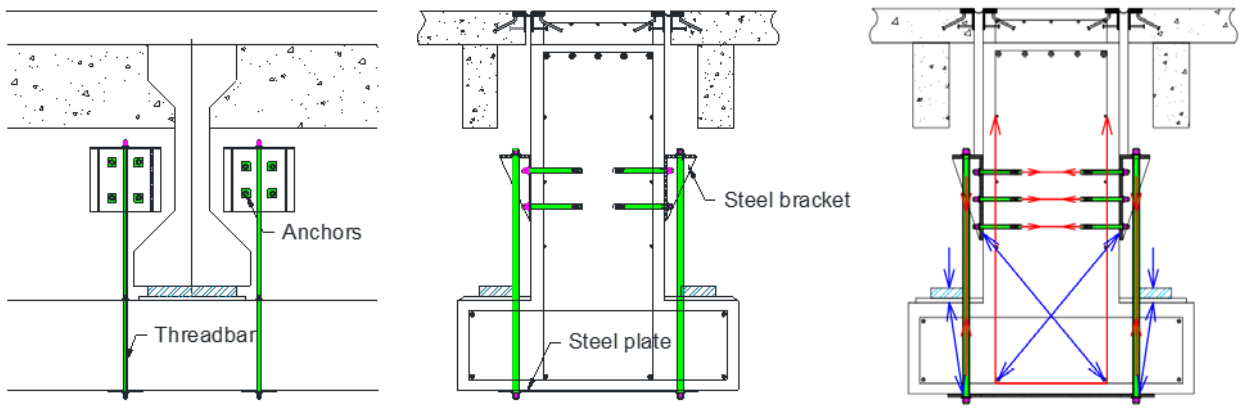

(a) Concept *(b) Load paths on cross-section*

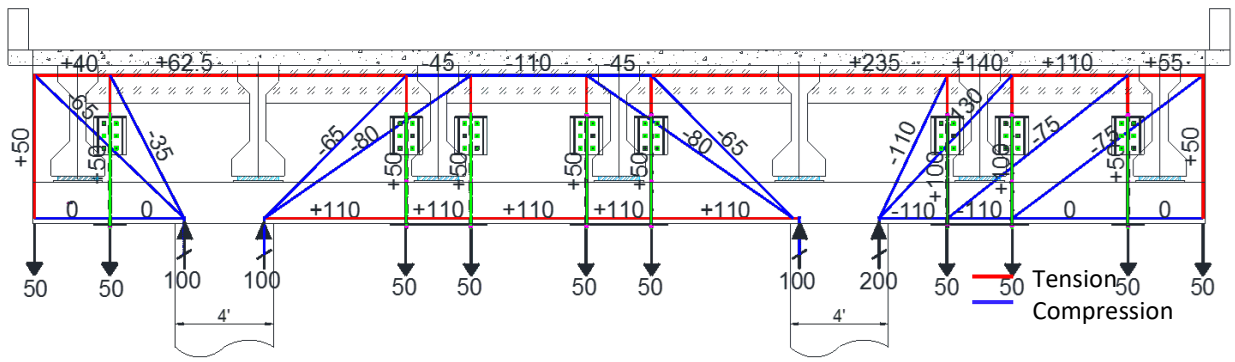

(c) Load paths and forces for additional 100 kip capacity per girder seat (kips)

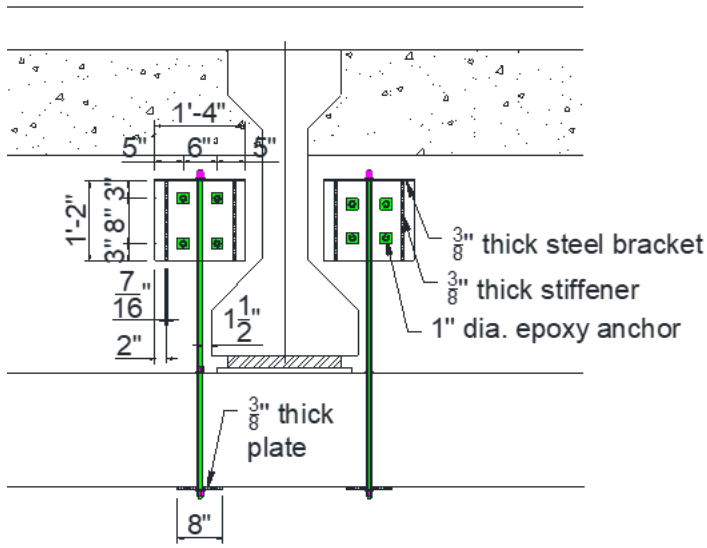

(d) Side elevation

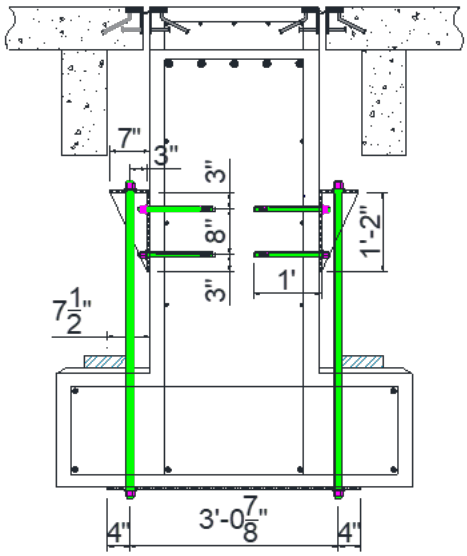

(e) Cross-section

Figure 4.11. Threadbar Hanger with Steel Bracket to Supplement Punching and Ledge Flexure Deficiency.

Design details for the example bent cap are presented in Figure 4.11(d) and (e). According to the design calculations, 150 ksi threadbars of 1 in. diameter should be adequate for the design example. Hilti HAS-E-B7 anchor rods with HIT-RE-500 V3 epoxy can be used for anchoring the brackets to the web. For each bracket, four 1 in. diameter rods should be used. Height and width of the steel plates for the hanger brackets should be based on the anchor location. Using Equations (4.12) to (4.16), it is determined that the thickness of the vertical plate for the brackets is controlled by shear rupture; thus, the thickness of the vertical plate should be determined using Equation (4.15). Based on the thickness of the vertical plate, the weld size can be calculated using Equation (4.18). The thickness of the plate should be checked for weld using Equation (4.17) and for buckling using Equation (4.20). Plates with a thickness of 0.5 in. are sufficient for the brackets.

4.8 Clamped Threadbar with Channel (Solution 8)

Figure 4.12 shows the retrofit solution using long threadbars embedded in the web of the inverted-T bent cap that may be deficient in hanger capacity as well as ledge flexure and/or punching shear capacity. This solution results in transferring the loads from the ledge into the web via a series of threadbars with the load paths depicted in Figure 4.12(b) and (c).

A key feature of this solution is the hanger threadbars. The bar is placed, and the upper anchorage is essentially a nut and thick plate washer. It should be noted that the alignment of the hangers is staggered to avoid the top level of reinforcing bars in the bent cap. The threadbars may be torqued to induce prestress. The prestressing force should inhibit cracking in the web and ledges.

The threadbars anchored at the web should have sufficient strength to transfer the loads from the girders into the web. Figure 4.13 presents the solution for the example bent cap. The size of the bearing plate was determined using Equations (4.4) and (4.5) since the load from the girder to the threadbar is directly induced by the bearing plate. A 0.75 in. thick plate with an outer diameter of 7 in. is sufficient.

To avoid damage on the existing horizontal reinforcement bars at the top of the web, as shown in Figure 4.13, the clamped threadbars are arranged in a zigzag pattern with bearing plates at the top.

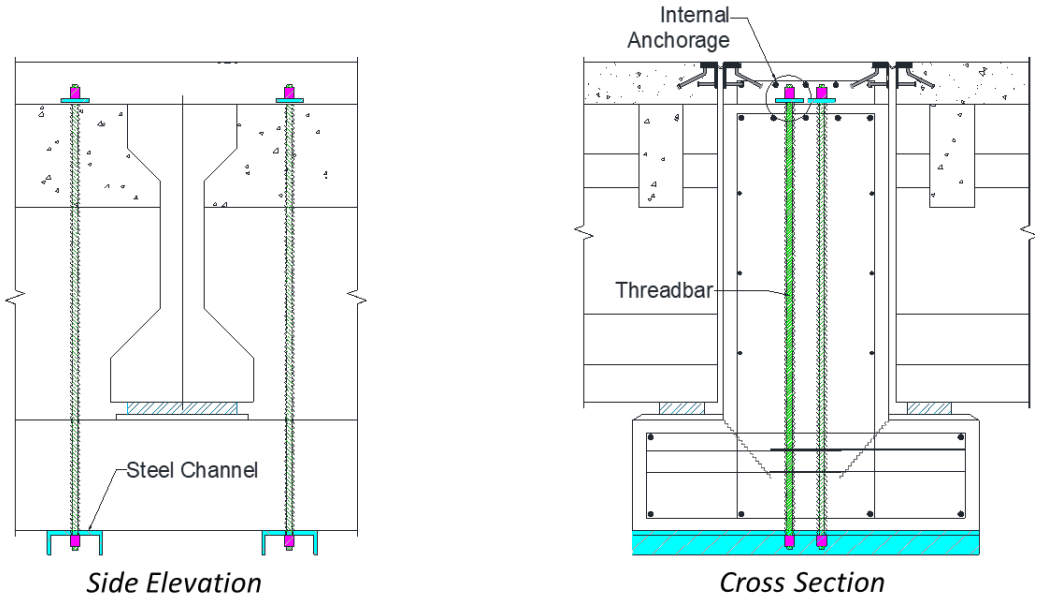

(a) Concept

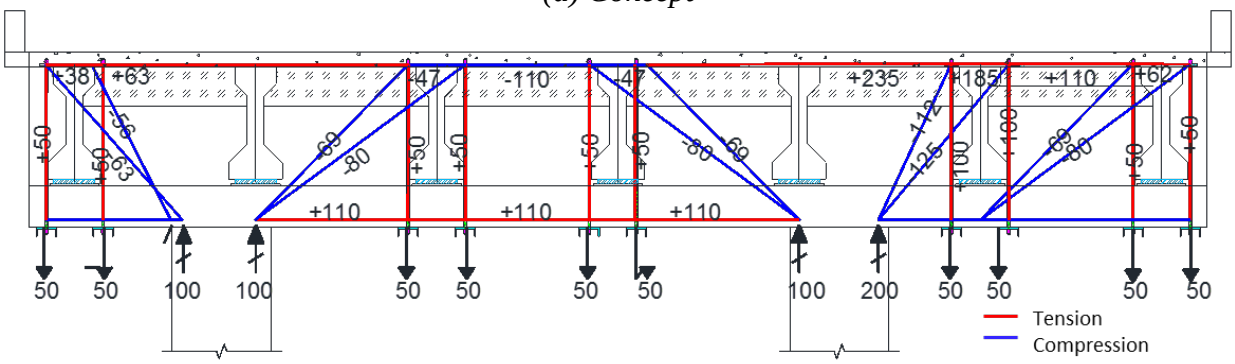

(b) Load paths and forces for additional 100 kip capacity per girder seat (kips)

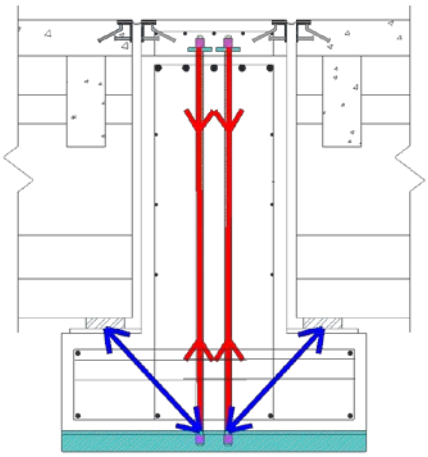

(c) Load paths on straddle bent cross-section

Figure 4.12. Clamped Threadbars to Transfer Loads into Web to Supplement Hanger, Ledge Flexure, and Punching Shear.

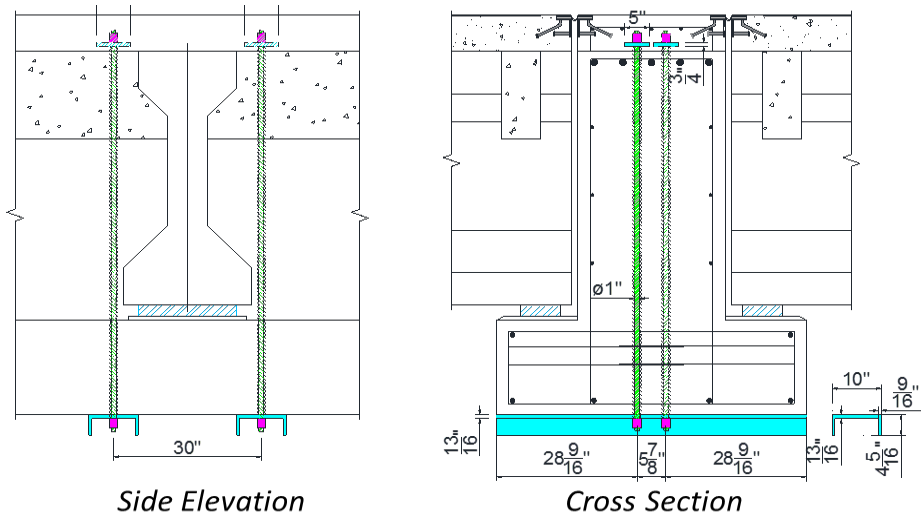

(a) General cross-section and elevation view

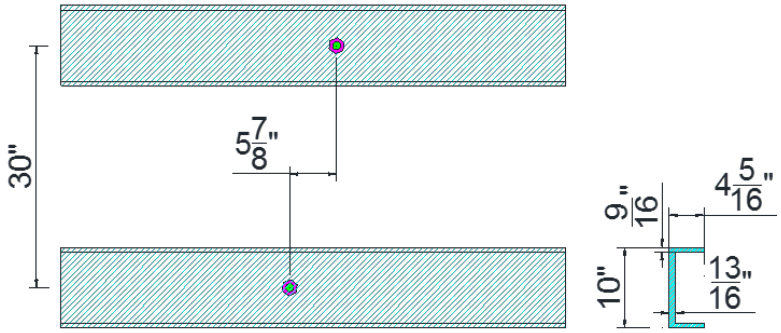

(b) View from the bottom

Figure 4.13. Solution for Hanger, Ledge Flexure, and Punching Shear Deficiency by Clamping from Top of the Web to Bottom of Ledges with Long Threadbar with Channel.

Since the threadbars anchored at the web are only designed for tension, steel channels are provided to resist ledge shear friction and flexural forces that are generated by the girders. The channels are placed to bend about the minor axis; compactness is checked according to AISC Specification Table B4.1b (2010a). As the width-to-thickness ratio of MC-type channels is less than the limit state of compact/noncompact channels, MC channels are determined as compact sections. Yielding does not control the capacity of the channel because no flange local buckling or web local buckling is expected. However, the web thickness of the channel should meet the thickness requirements, which is determined using Equation (4.5). With known web thickness of the steel channel, the other dimension of the channel can be obtained by checking the flexural capacity as given by:

$$M_n \leq min\left(F_y Z_y, 1.6 F_y S_y\right) \tag{4.28}$$

where M_n = nominal flexural force, which is the bending force due to loads from the girder; F_y = yield strength of the steel channel in ksi; Z_y = plastic modulus of the channel section; and S_y = elastic modulus of the section. For this retrofit solution, MC 10×41 was selected, as shown in Figure 4.13.

4.9 Grouted Threadbar Anchored with Channel (Solution 9)

Figure 4.14 presents a similar concept as the previous solution but with partial-depth grouted threadbars. The bonded threadbars should be used as internally anchored bars within the web when there is not sufficient gap or access for top-down hole boring. This solution transfers the loads on the ledge into the web, thereby strengthening the hanger, ledge flexure, and punching shear capacity of the inverted-T bent cap.

As in the case of clamped threadbars, the grouted anchor threadbars within the web are a tension-only solution; both aim to supplement existing hanger deficiency. The design for this solution proceeds in a similar fashion to the previous case. In particular, Equation (4.21) and (4.22) are used, along with Equation (4.23) and (4.24).

The design details are shown in Figure 4.14(d) and (e). With known web thickness of the steel channel, the other dimension of the channel can be obtained by checking the flexural force using Equation (4.28). For this retrofit solution, MC 12×50 is adopted.

4.10 Anchored FRP Wrap (Solution 10)

Figure 4.15 shows a retrofit utilizing anchored FRP that wraps around the side of the web and the ledges of the inverted-T section in critical regions. This solution strengthens the bent cap for ledge, punching, and hanger by providing additional multiple load paths to the girder loads. The FRP sheets are anchored at the termination region by FRP anchors, and a steel angle is mechanically anchored at the corner between the web and ledge to reduce the potential for FRP debonding.

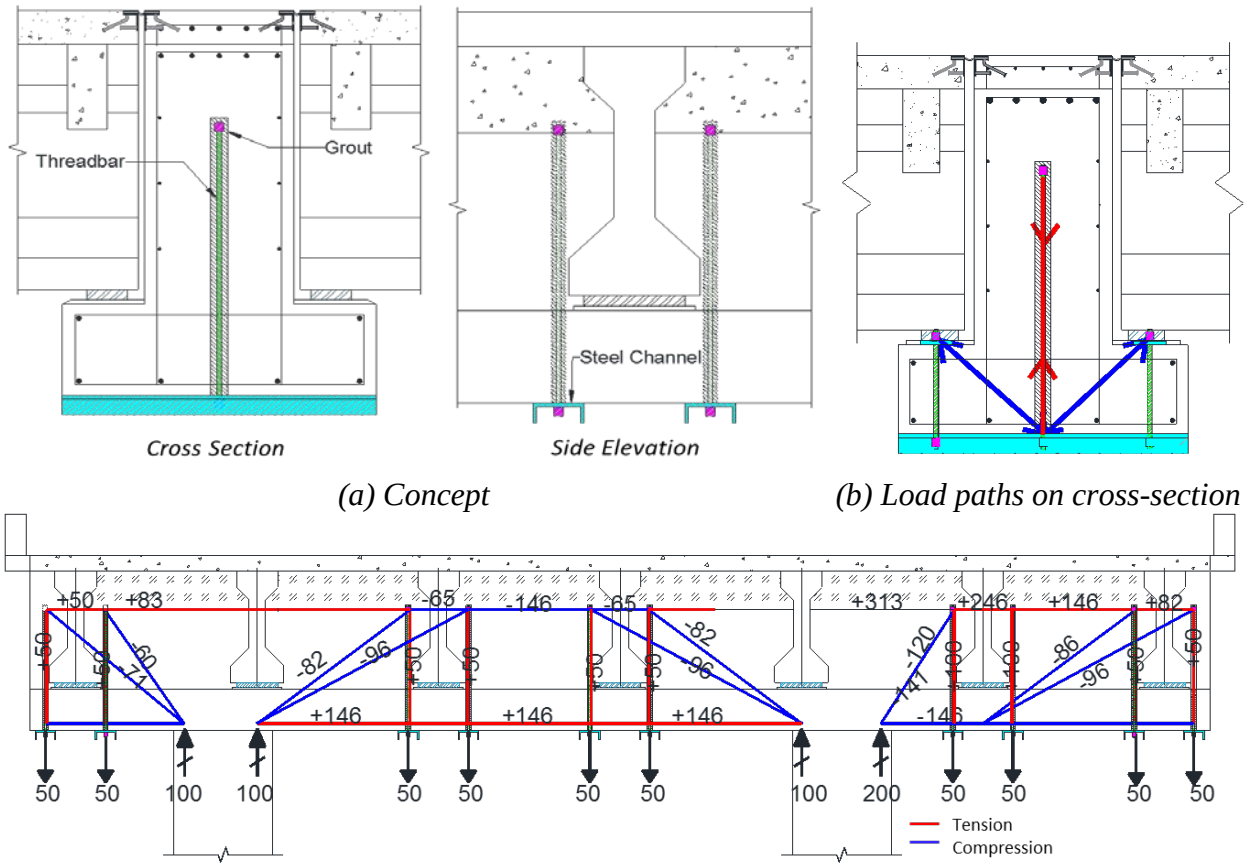

(a) Concept *(b) Load paths on cross-section*

(c) Load paths and forces for additional 100 kip capacity per girder seat (kips)

(d) Side elevation *(e) Cross-section*

Figure 4.14. Grouted Threadbar Anchored at Web to Supplement Hanger, Punching Shear, and Ledge Flexure Deficiency.

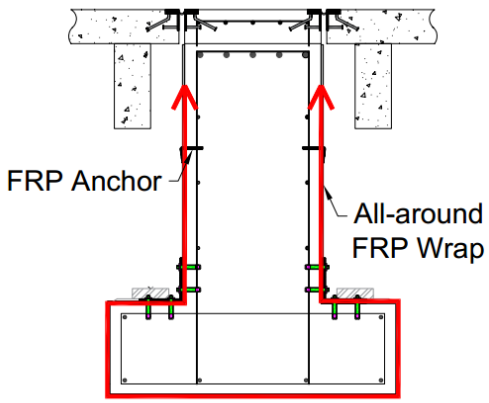

(a) Concept

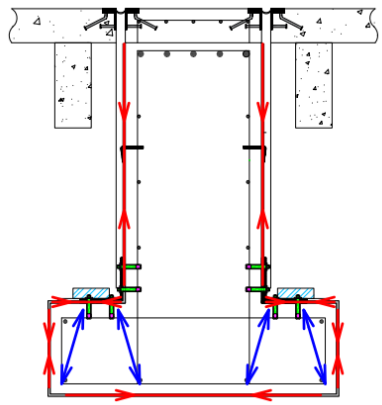

(b) Load paths on cross-section

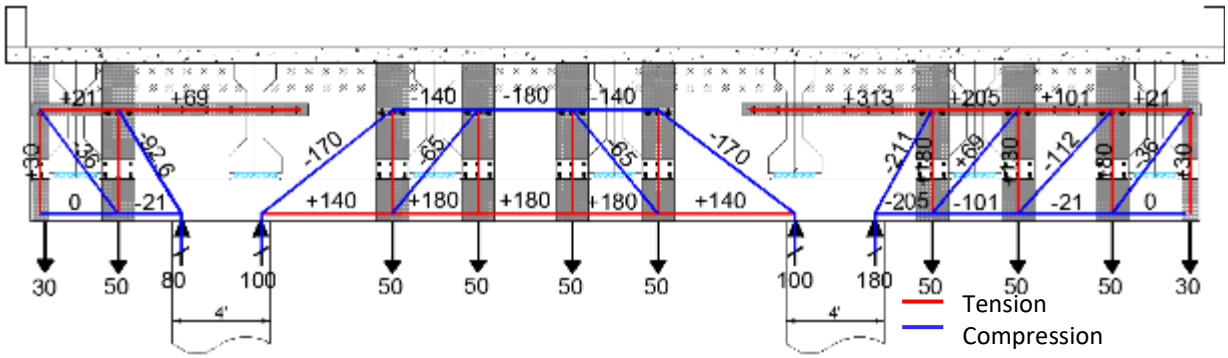

(c) Load paths and forces for additional 100 kip capacity per girder seat (kips)

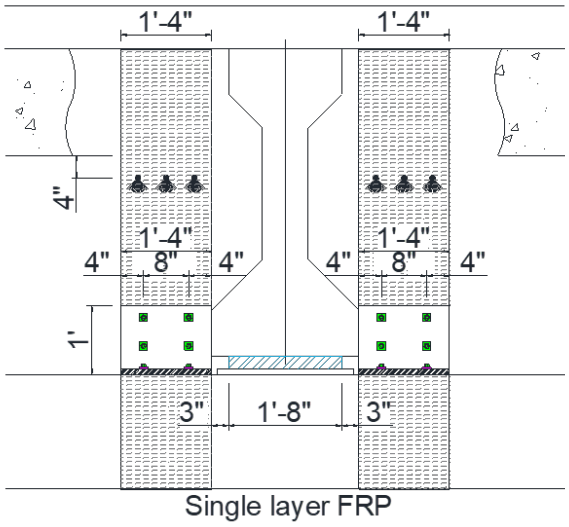

(d) Side elevation

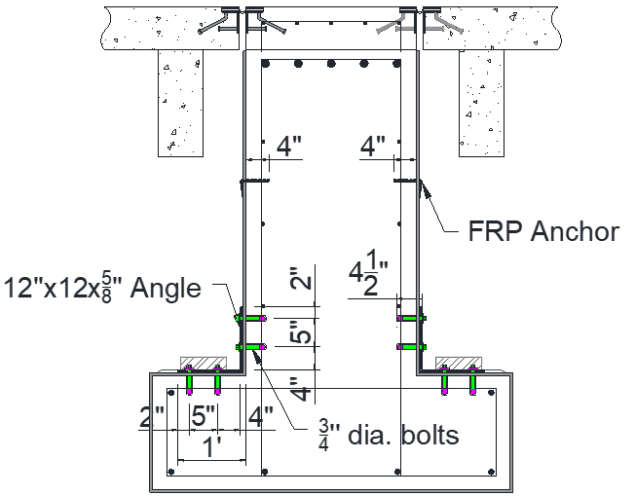

(e) Cross-section

Figure 4.15. Anchored FRP Wrap to Supplement Hanger, Punching Shear, and Ledge Flexure Deficiency.

The design shear strength of a concrete member strengthened with FRP composites can be calculated by multiplying the nominal shear strength by the strength reduction factor ϕ as specified by ACI 440.2R (ACI Committee 440, 2008). The code recommends an additional reduction factor ψ_f for FRP composites based on the shape around which they are wrapped.

The shear capacity of the retrofitted inverted-T cap beam is given by:

$$V_n = V_c + V_s + V_f \tag{4.29}$$

in which V_c = the contribution of the concrete; V_s = the contribution of the transverse steel; and V_f = the contribution of the FRP wrap, where according to ACI 440.2R (ACI Committee 440, 2008):

$$V_f = \frac{A_{fv} + f_{fe}(\sin\alpha + \cos\alpha)d_{fv}}{s_f} \tag{4.30}$$

where, f_{fe} = tensile stress of FRP strip; d_{fv} = effective depth of FRP strip; α = inclination angle; s_f = spacing of FRP strip; and A_{fv} = area of FRP shear reinforcement within the spacing s_f. The area of FRP shear reinforcement, A_{fv}, is given by:

$$A_{fv} = 2nt_f w_f \tag{4.31}$$

where n = number of FRP layers per strip; t_f = thickness of FRP layer; and w_f = width of FRP strip.

The tensile stress f_{fe} (in Equation (4.30)) of the FRP composites at nominal strength is obtained by multiplying the elastic modulus of the FRP by the effective strain as follows:

$$f_{fe} = \varepsilon_{fe} E_f \tag{4.32}$$

where E_f = elastic modulus of FRP in ksi; and ε_{fe} = effective strain of FRP. The effective strain ε_{fe} in Equation (4.32) is the maximum strain that can be achieved in the FRP system at nominal strength. Determination of effective strain depends on the configurations of FRP composites used for shear strengthening. For partially wrapped FRP composites, the effective strain should be taken as follows:

$$\varepsilon_{fe} = k_v \varepsilon_{fu} \leq 0.004 \tag{4.33}$$

where ε_{fu} = ultimate strain of FRP and k_v = bond-reduction coefficient.

The bond-reduction coefficient k_v in Equation (4.33) is a function of the concrete strength, the type of wrapping scheme used, and the stiffness of the FRP composites, which is modified from ACI 440.2R (ACI Committee 440, 2008) as follows:

$$k_v = \frac{k_1 k_2 L_e}{468\varepsilon_{fu}} \leq 0.75 \tag{4.34}$$

with,

$$L_e = \frac{45.5}{\left(nt_f E_f\right)^{0.58}} \tag{4.35}$$

$$k_1 = \left(\frac{f_c'}{4}\right)^{2/3} \tag{4.36}$$

$$k_2 = \frac{d_{fv} - L_e}{d_{fv}} \tag{4.37}$$

where k_1 and k_2 = modification factors; L_e = active bond length; and f_c' is in ksi units.

The total shear strength provided by the reinforcement should be taken as the sum of the contribution of the FRP shear reinforcement and the steel shear reinforcement. The sum of the shear strengths provided by the shear reinforcement should be limited based on the criteria given for steel alone in ACI 318R (ACI Committee 318, 2014). This limit is stated as:

$$V_s + V_f \leq 8\sqrt{\frac{f_c'}{1000}}\, b_w d \tag{4.38}$$

where b_w = width of web; d = effective depth of the section; and f_c' is in ksi units.

Figure 4.15(d) and (e) present the solution for the hanger, punching shear, and ledge flexure failure using FRP sheets and anchor bolts applied to the prototype structure. In the anchored FRP wrap retrofit solution, a single layer of high-strength CF fabric Tyfo SCH-41-2X is used. Power bolt+ with a diameter of 0.75 in., manufactured by Power Fasteners, is used for anchoring the steel angle to prevent detachment of the FRP at the edges. Eight bolts should be used for each steel angle.

4.11 Concrete Infill with Prestressing Threadbar (Solution 11)

In the construction of structural concrete parking garages, flange-hung double-T precast prestressed concrete beams are commonly used for the floor system. In this way, the overall depth of the support beam plus floor system can be kept shallow. The intent of such building designs is not unlike bridge designs where inverted-T bent caps are used. The principal difference with buildings is that the floor reaction is from the flange, whereas for bridges, it is from the girder.

Solution 11 applies the attribute of providing extra support capacity to a bridge deck system by providing a measure of the total girder reaction being taken by the deck slab (the flange) of the overall deck slab flange-girder system. In this way, the ledge of the inverted-T beam can release some of the total support reaction of the bridge deck.

Figure 4.16 presents the solution for bridge decks that place end diaphragms between girders. By placing infill concrete between the diaphragms, the diaphragms are clamped to the web of the inverted-T bent cap member to provide a reaction support to the deck slab, as shown in Figure 4.16(a) and (b).

A high-strength prestressing threadbar, as depicted in Figure 4.16(b), is used to clamp the newly formed flange to form a composite I-beam-shaped bent cap. It should be noted that for this solution, several holes need to be drilled from the top of the deck slab to pour concrete between the diaphragms and the girders. For the successful implementation of this method, some traffic control may be required until the concrete has hardened.

Figure 4.16(c) shows the load paths of the retrofitted system. As depicted in Figure 4.16(d), prestressing threadbars directly transfer the loads from the infilled concrete and the diaphragms by integrating them to form an upper flange to the web of the inverted-T bent cap. The mid-span of the structure will work as an arch system to bypass partial loadings directly to the column support through compression struts, and thus reduce the loads from the girders and eventually reduce the load demands on the ledge as well as hanger capacity of the bent cap.

However, as shown in Figure 4.16(c), the cantilever parts have a slightly different mechanism. The cantilever system relies on the top tension chord to transfer the loads to the column support. For the retrofit system to work independently, as shown in Figure 4.16(e), a supplemental post-tensioned threadbar needs to be installed at the top of the section.

Furthermore, as shown in Figure 4.16(c), the cantilever part on the right needs an additional vertical tension chord for hanging the loads to the top tension chord because it cannot transfer the

loads directly to the column support due to the long overhang. Therefore, an additional hanger solution (such as a clamped cross threadbar) can be used in combination with this retrofit solution for the cantilever portion of the inverted-T bent cap.

Design of the prestressed threadbars is similar to the prestressed all-threaded rod retrofit solution. The negative moment caused by the eccentric prestress is ignored since the concrete deck is expected to have sufficient strength and stiffness to resist the negative moment. The prestressed threadbars are designed to resist shear force induced from the deck live load, and the weight of the newly formed flange. It is assumed that each bar equally resists the shear force. The design shear strength of threadbars is 60 percent of ultimate strength and must be greater than the required shear strength. Based on the required shear capacity, four threadbars with 1 in. diameter are used per girder. The first threadbar is placed 14 in. from the centerline of the girder, and the rest of the threadbars are spaced equally at 20 in., based on the consideration of minimum spacing defined by Equation (4.3) and the size of the steel bearing plate.

The minimum required thickness of the steel bearing plate is obtained using Equation (4.4), and the required area of the bearing steel plate is computed using Equation (4.5). Based on the design calculations, a square 6 in. diameter and 1 in. thick plate is required.

Additionally, to prevent shear failure of the newly formed flange, stirrups are placed in the gap of the diaphragm and stem of the bent cap using the usual code-based design method. As a result, No. 5 double-leg stirrups are evenly distributed with an 8 in. spacing.

Figure 4.16(e) and (f) show the detailed dimensions of the concrete infill with the prestressed threadbar retrofit solution. The dimensions of the nuts and washers used to anchor the threadbars are based on the diameter, and their dimensions are provided by the manufacturer. Use of hex nuts designed for prestressing threadbars and hardened washers is proposed.

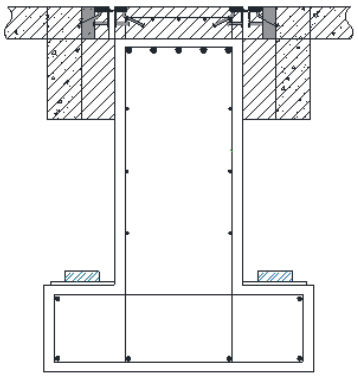

(a) Newly formed flange

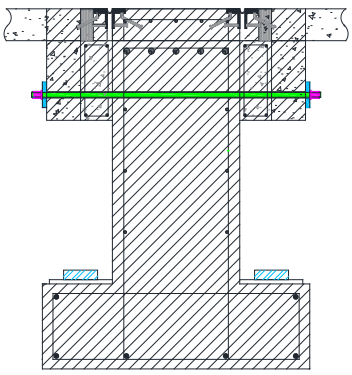

(b) Transformed section

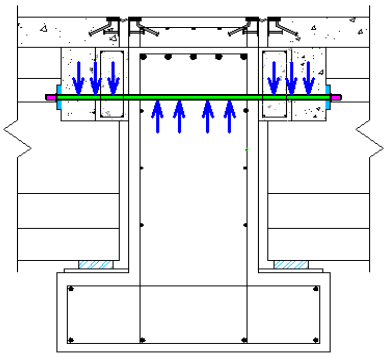

(c) Cross-section load path

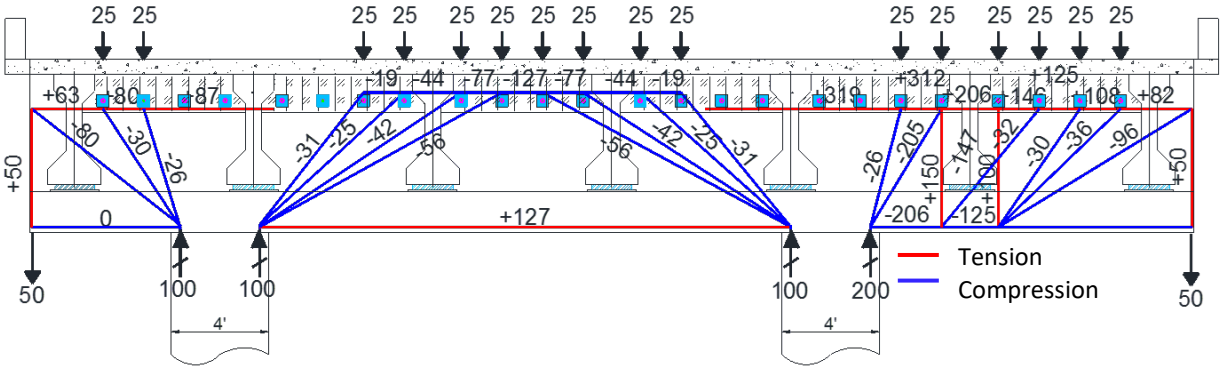

(d) Load paths and forces for additional 100 kip capacity per girder seat (kips)

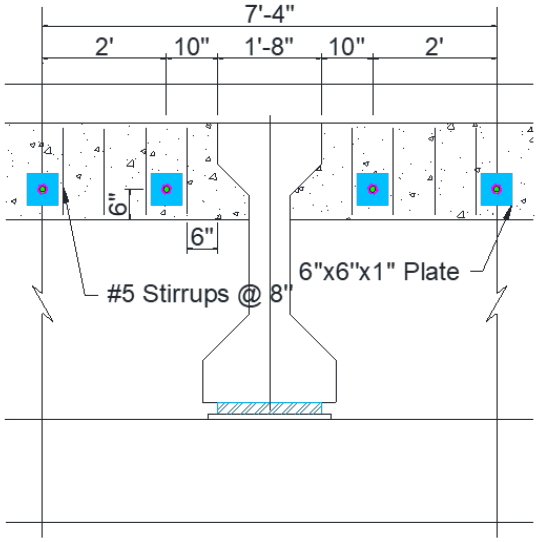

(e) Side elevation

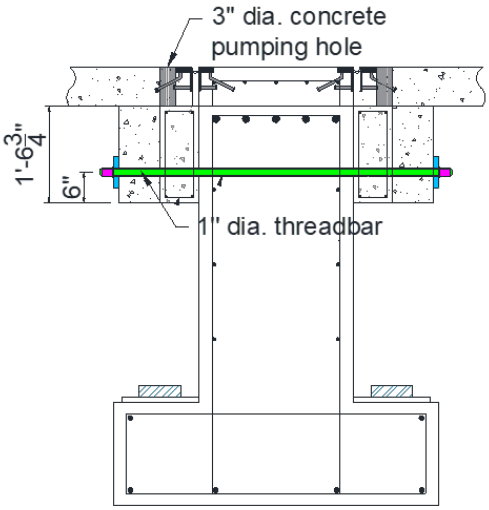

(f) Cross-section

Figure 4.16. Concrete Infill with Prestressed Threadbars to Supplement Punching Shear, Ledge Flexure, and Hanger Deficiency.

4.12 Concrete Infill with Hanger Threadbar (Solution 12)

Figure 4.17 presents the proposed concrete infill with hanger threadbar retrofit solution. The web is locally thickened with concrete infill. The hanger threadbars are embedded within the concrete infill to effectively transfer the girder loads to the top of the web. Figure 4.17(b) and (c) show the load paths of the retrofitted system. The girder loads can then be effectively transferred by struts (arch action) directly to the column. This solution is expected to address ledge flexure and hanger deficiencies.

The threadbar designs are similar to the clamped threadbar with channel solution (Solution 8). Figure 4.17(d) and (e) show the design details. High-strength threadbars with 1 in. diameter are used.

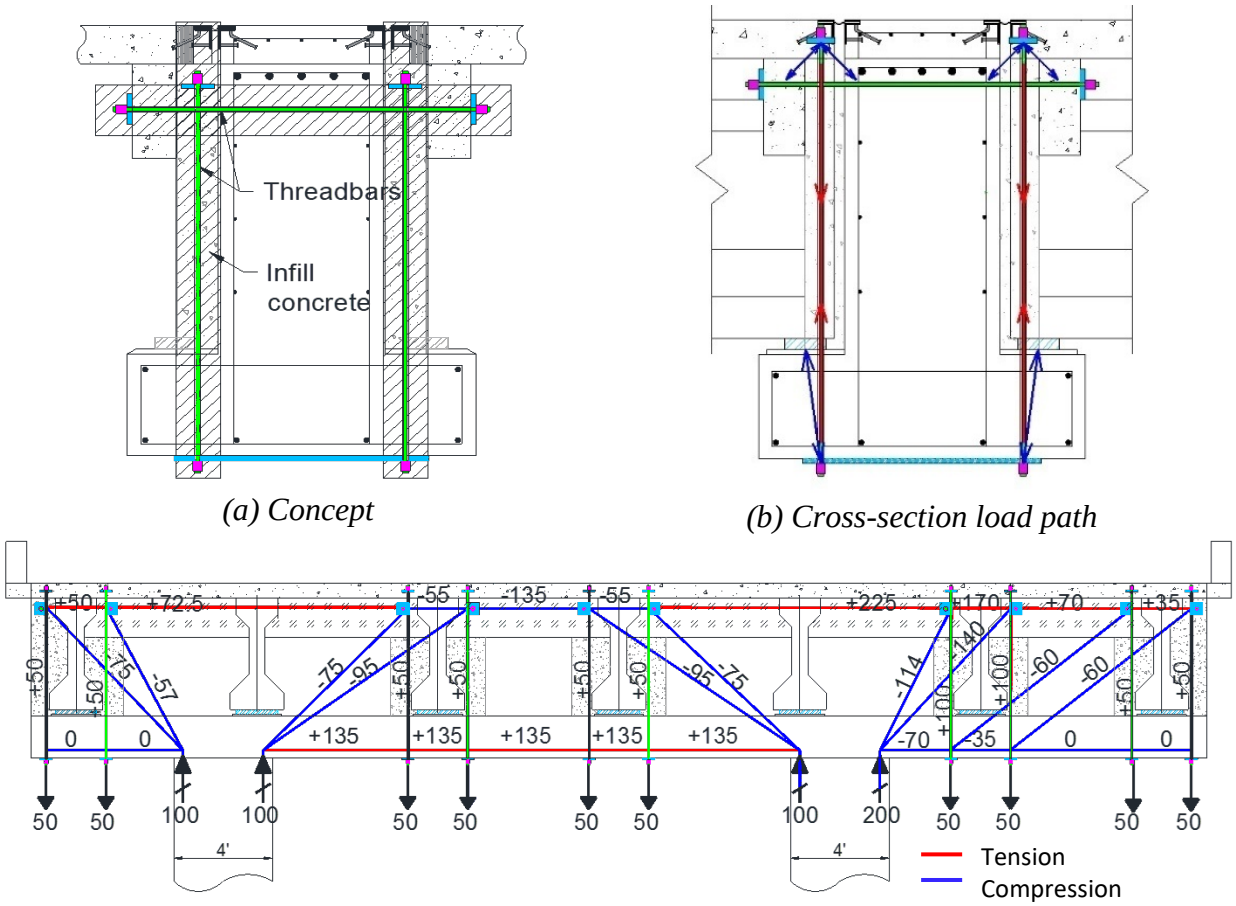

(a) Concept

(b) Cross-section load path

(c) Load paths and forces for additional 100 kip capacity per girder seat (kips)

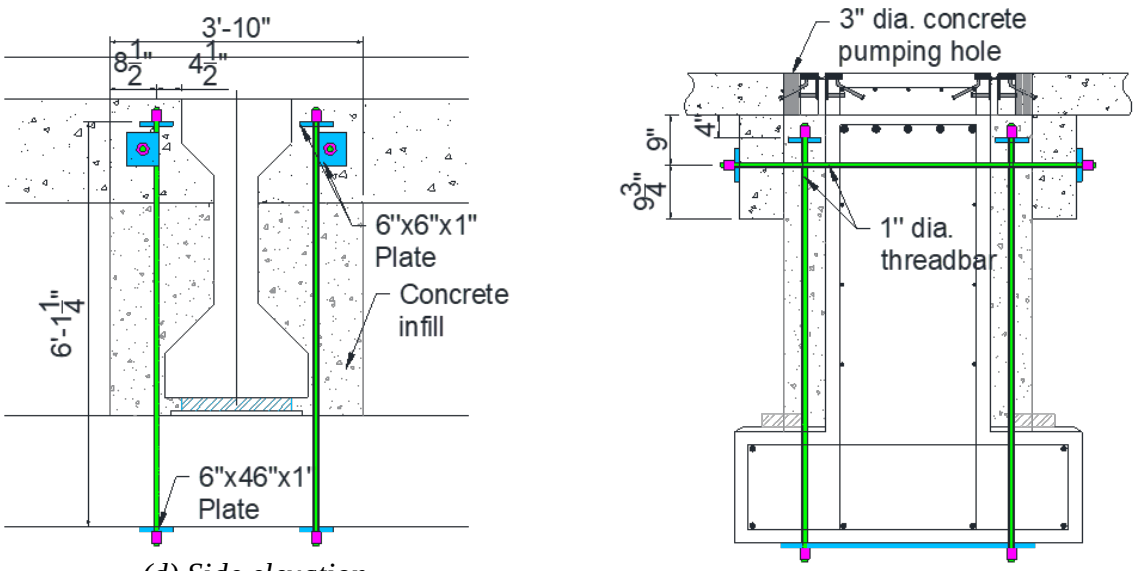

(d) Side elevation

(e) Cross-section

Figure 4.17. Concrete Infill with Hanger Threadbars to Supplement Punching Shear, Ledge Flexure, and Hanger Deficiency.

4.13 Concrete Masonry Pier (Solution 13)

Figure 4.18 shows a retrofit that provides additional support to the inverted-T bent cap by concrete masonry piers beneath each interior girder. The masonry piers are seated on a reinforced concrete foundation cast between the existing drilled shafts. This solution strengthens the interior of the bent cap ledge, punching, and hanger by providing additional multiple load paths to the girder loads.

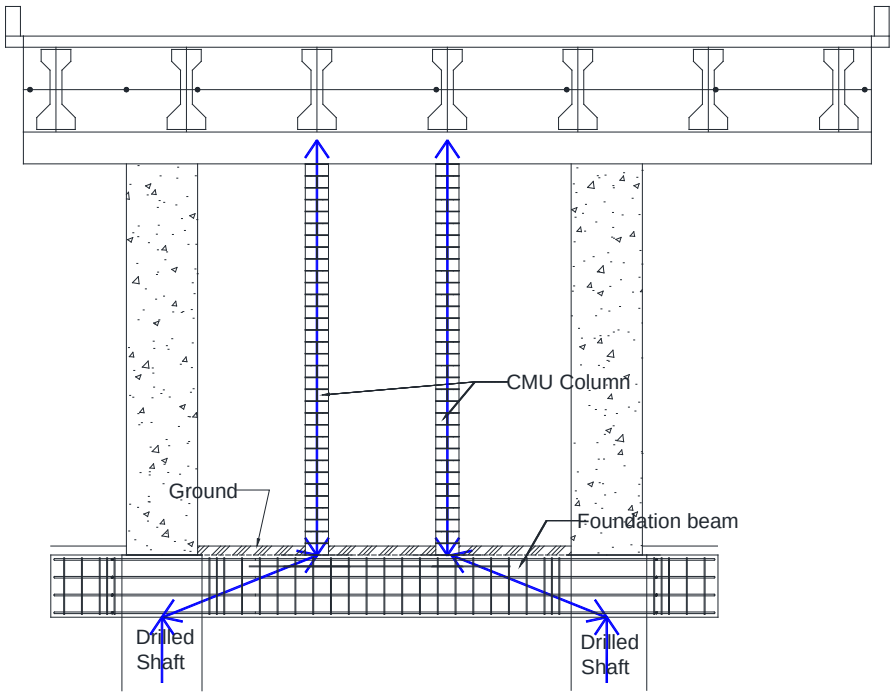

Figure 4.18. Concrete Masonry Unit (CMU) Column under Girder.

The design assumes that there are only axial compression forces acting on concrete masonry piers. Using the strength design method (MSJC, 2011), the nominal axial strength reinforced masonry is given by:

$$P_n = 0.8\left[0.8f'_m(A_n - A_{st}) + f_y A_{st}\right]\left[1 - \left(\frac{h}{140r}\right)^2\right] \tag{4.39}$$

where A_n = net area of the masonry unit; f'_m = specified compressive strength of masonry in ksi; f_y = specified yield strength of steel for reinforcement and anchors in ksi; A_{st} = total area of laterally tied longitudinal reinforcing steel in in^2; h = height of the column; and r = radius of gyration.

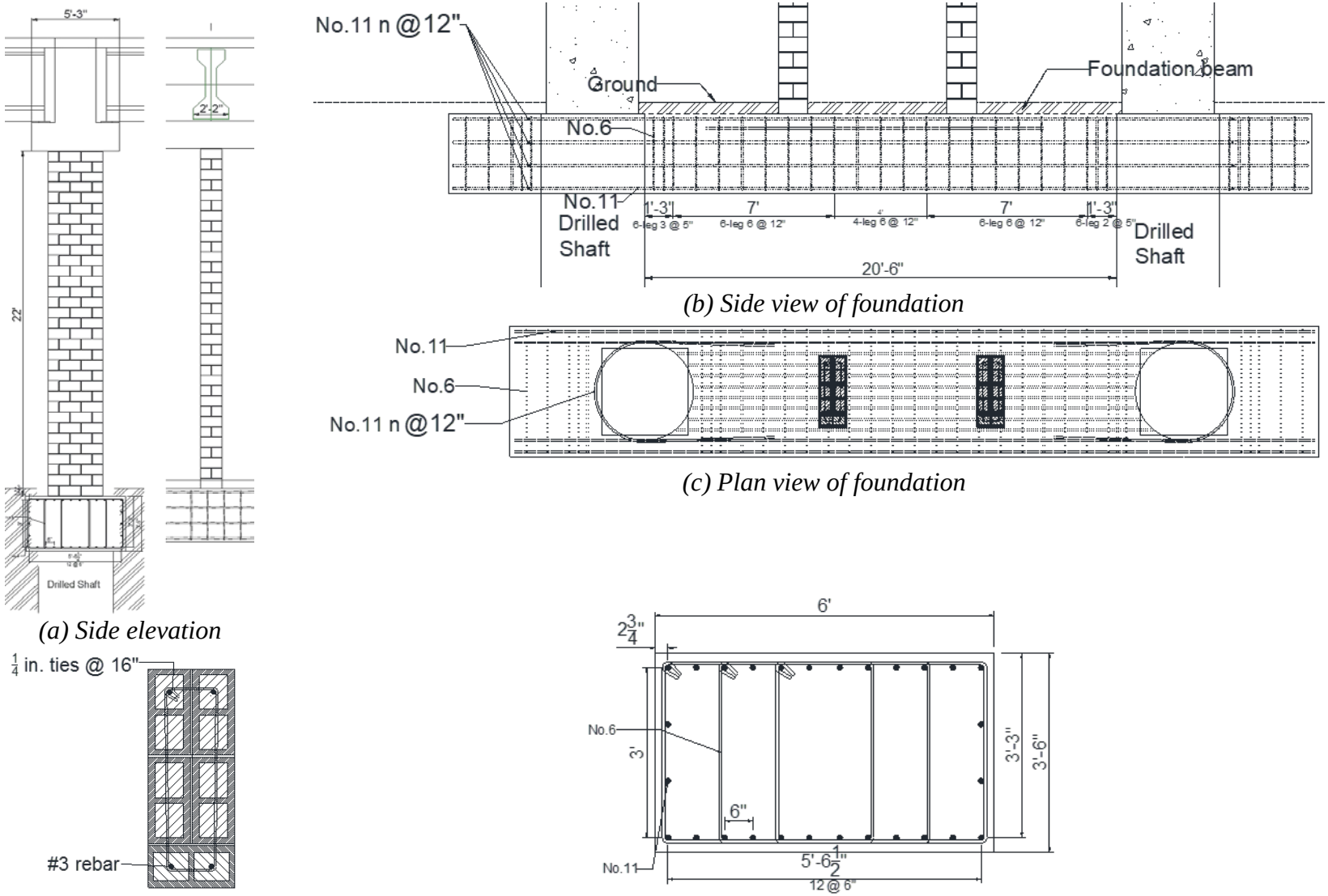

(a) Side elevation

(b) Side view of foundation

(c) Plan view of foundation

(b) Cross-section of CMU Pier

(d) Cross-section of reinforced concrete beam of foundation

Figure 4.19. Solution for Inverted-T Bent Caps with Hanger, Ledge Flexure, and/or Punching Shear Deficiency.

Vertical reinforcement is required in masonry piers to prevent brittle failure. Four bars are required so that ties can be used to provide a confined core for the masonry. The amount of vertical reinforcement is determined based on the nominal strength of unreinforced masonry piers as well as minimum requirements. A beam connecting the existing drilled shafts is used as a foundation for the masonry piers. The foundation beam is designed as a fixed-fixed beam with point loads from the masonry pier reactions. The width of the beam should be larger than the diameter of the drilled shaft and the width of the masonry piers. Figure 4.19 presents the example solution for the prototype bridge structure and shows section details and reinforcement layout for the foundation beam. Twelve No. 11 rebars should be used as the longitudinal reinforcement for the compression and tension region. Six-leg No. 6 stirrups with 12 in. spacing are used for the shear reinforcement. Four No. 11 U-shape rebars are used to connect the beam to the drilled shafts at both ends of the beam. Figure 4.19(b) and (c) show the side view and plan view of the foundation.

4.14 Load-Balancing Post-Tensioning (Solution 14)

All solutions discussed previously provide local sections of the inverted-T bent cap with increased seating capacity for individual girders. However, the proposed load-balancing system presented in this subsection uses a post-tensioning (PT) solution that retrofits the entire inverted-T bent at once. As shown in Figure 4.20(a), a reinforced concrete saddle is newly formed over each column. PT strands are installed over the bent cap and anchored at the end of the bent cap with an end-region stiffener. The PT strands strengthen the hanger capacity of the bent cap by providing upward forces, by lifting the cantilever parts with the end-region stiffener. As shown in Figure 4.20(a) and (b), the reaction forces to the PT are directly transferred to the columns. However, the post-tension strands need to be installed in the gap between the web of the bent and the girders, as shown in Figure 4.20(c). The use of unbonded sheathed strands permits the PT to be applied within the confines of the restricted space.

As shown in Figure 4.20(a), the application of this retrofit solution to single-column bent caps such as northbound Bent 22 is straightforward. However, a different approach is required for the double-column bent cap. Due to the relatively long mid-span of the double-column bent, it is difficult to obtain an effective inclination angle. For an effective implementation of this technique in the double-column bents, the PT strands require installation as shown in Figure 4.20(b). The

solution in the cantilever part of the bent is similar to the single-column bent. In the region between the two columns, the PT strands are placed beneath the girders as shown in Figure 4.20(c). For the two prototype structures considered herein, the retrofit solution to enhance overall hanger and seat capacity using external PT is presented in Figure 4.21.

The required tension strength of the PT forces, after losses, is simply obtained from geometry:

$$F = \frac{P}{\sin(\alpha)} \tag{4.40}$$

where F = required tension force; P = required supplemental load capacity; and $\alpha = \tan^{-1}(h/L)$, which is the angle of the post-tension bars, where h and L are described in Figure 4.20.

It should be noted that one of the key advantages of this system is that essentially no holes need to be bored within the existing bent cap. Most of the construction activities can be executed from snooper trucks by reaching from below; the upper deck need not be closed to existing traffic.

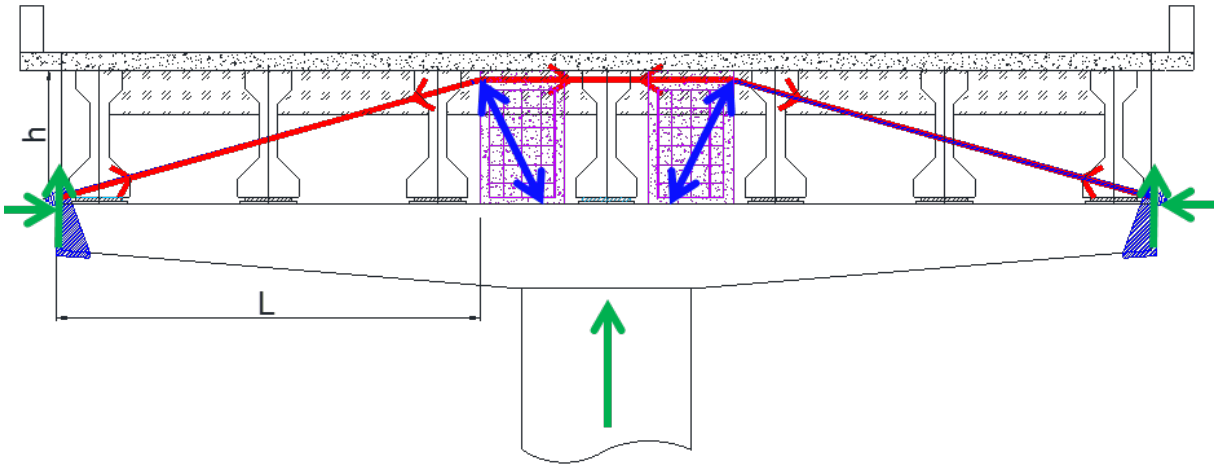

(a) Elevation of single-column bent

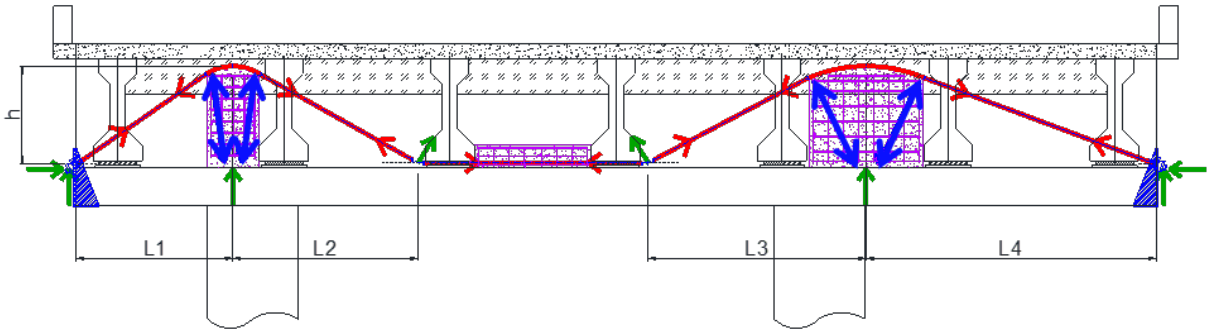

(b) Elevation of double-column bent

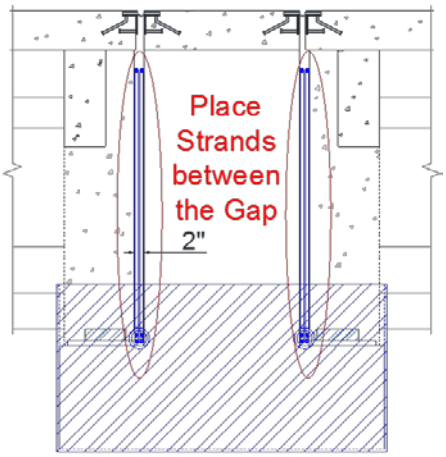

(c) Cross-section at the end of the bent

Figure 4.20. PT System Using Load-Balance Techniques to Overcome Predominant Deficiency of Cantilever Portion of the Bent.

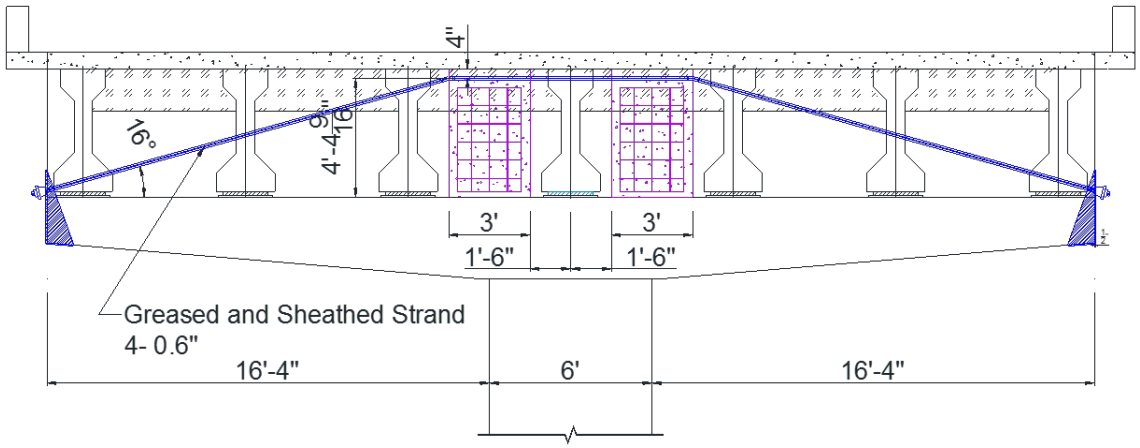

(a) Elevation of single-column bent

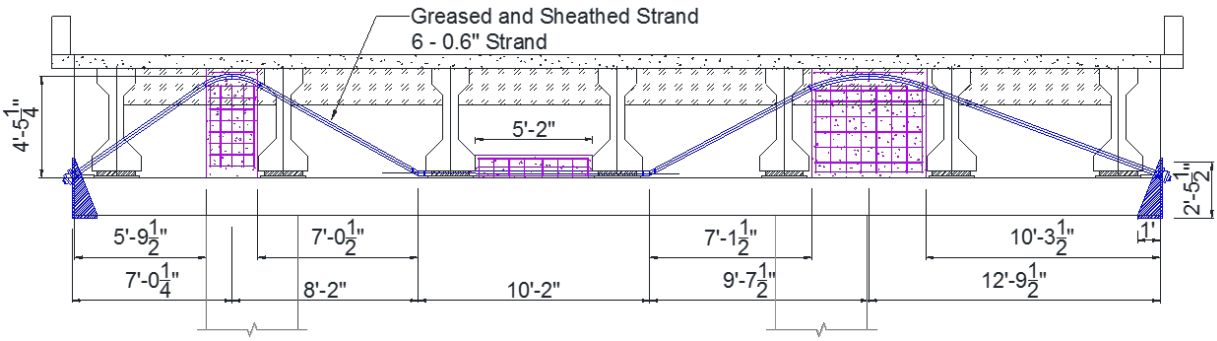

(b) Elevation of double-column bent

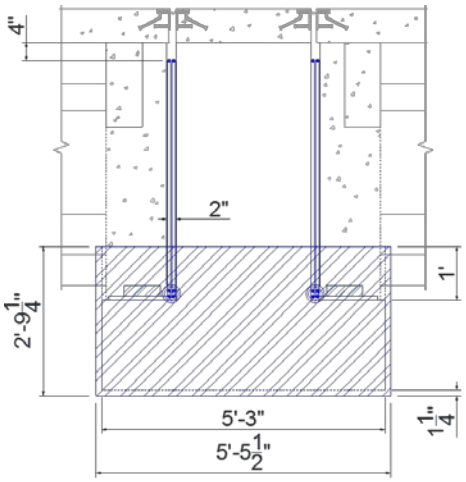

(c) Section of single-column bent

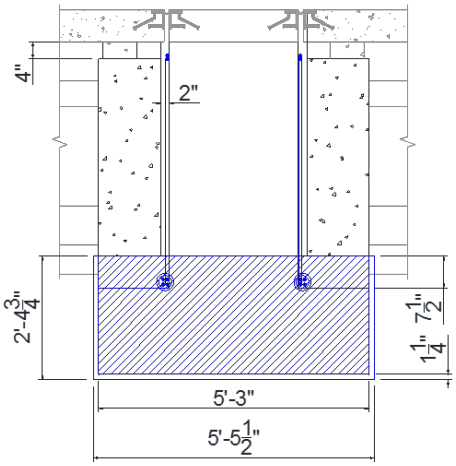

(d) Section of double-column bent

Figure 4.21. Solution for All Deficiencies by External PT.

4.15 Concrete Infill with FRP Anchored by FRP Anchors (Solution 15)

Figure 4.22 shows an FRP with infill concrete retrofit solution. Infill concrete transforms the inverted-T cross-section to a rectangular cross-section, and the FRP provides an alternative load path for the girder load by wrapping the overall section. The FRP sheet cannot be applied beyond the diaphragm since the depth of the infill concrete is limited by the presence of the diaphragm. Therefore, the solution only works for punching shear and ledge flexure deficiencies.

By placing infill concrete with minimum reinforcement on the ledge, FRP sheets may be installed without concern for debonding at the edge of the ledge. The embedded threadbars are used to connect the web and infill concrete. The FRP sheets are anchored at the termination regions by FRP anchors.

The shear strength contribution of the FRP composites is calculated according to ACI 440.2R (ACI Committee 440, 2008). The strengthened shear capacity of the inverted-T bent cap is then obtained using Equation (4.29) to (4.38).

Figure 4.22 presents the solution for punching shear and ledge flexure failure using FRP sheets and threadbars applied to the prototype structure. A single layer of high-strength carbon fiber fabric Mbrace CF160 is used with Mbrace CF160 carbon fiber anchors. In addition, six high-strength (150 ksi) threadbars with 1 in. diameter are provided. Figure 4.22 shows the detailed sizes of the FRP layers and threadbars.

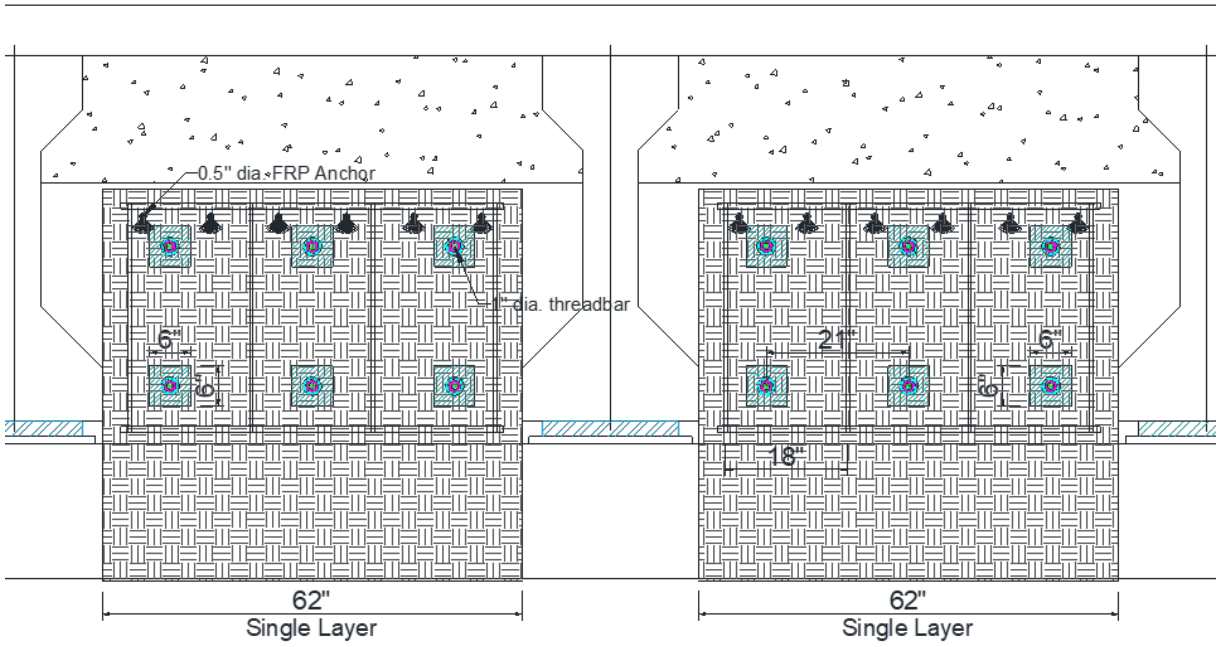

(a) Side elevation

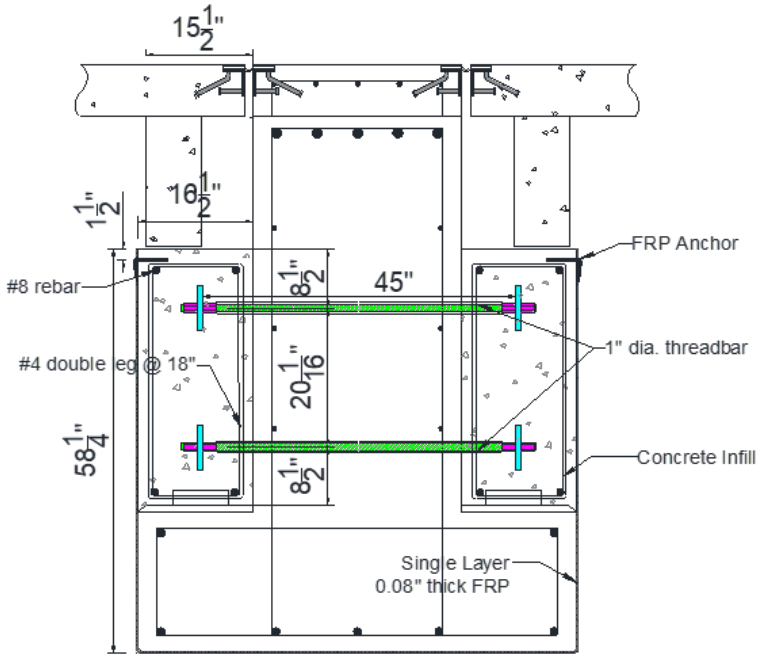

(b) Cross-section

Figure 4.22. Solution for Punching Shear and Ledge Flexure Failure Using FRP Sheets and FRP Anchors.

4.16 Concrete Infill with Partial-Depth FRP Anchored by Steel Waling (Solution 16)

Figure 4.23 shows an FRP retrofit similar to Solution 15 but with shallower infill concrete and a different FRP anchoring scheme. A shallower infill concrete is used, and the FRP sheet is anchored at the termination region by steel waling. The solution is intended for inverted-T bent caps with a diaphragm and provides an increase in the ledge flexure and punching shear capacity.

Threadbars are used to connect the web and infill concrete and to provide a location for attachment of the waling. Steel walings are used on each side of the beam to provide an end anchorage to the FRP sheets.

The FRP wrap is primarily designed for shear as specified by ACI 440.2R (ACI Committee 440, 2008). The effective strain of FRP in Equation (4.32) is taken as 0.0014, which is elongation at the breakout, to obtain the shear contribution of FRP composites to the concrete member using Equation (4.29). Single layers of high-strength carbon fiber fabric Mbrace CF160 anchored by 0.75 in. thick steel waling with five 1 in. diameter high-strength (150 ksi) threadbars are used.

4.17 Concrete Infill with Full-Depth FRP Anchored by Steel Waling (Solution 17)

Figure 4.24 shows an FRP retrofit that is intended for inverted-T bent caps without a diaphragm. Full-depth infill concrete and the FRP sheet is achieved. Therefore, the solution provides an increase in the hanger, ledge flexure, and punching shear capacities. Threadbars are placed in two layers with the steel waling at the top layer. The FRP sheet is anchored at the end by steel waling.

The effective strain of FRP is taken as 0.014, which is elongation at the breakout, to obtain the contribution of FRP composites to the concrete member using Equation (4.29). Minimum reinforcement is provided for the infill concrete. Single layers of high-strength carbon fiber fabric Mbrace CF160 anchored by 0.75 in. thick steel waling with three 1 in. diameter high-strength (150 ksi) threadbars are used.

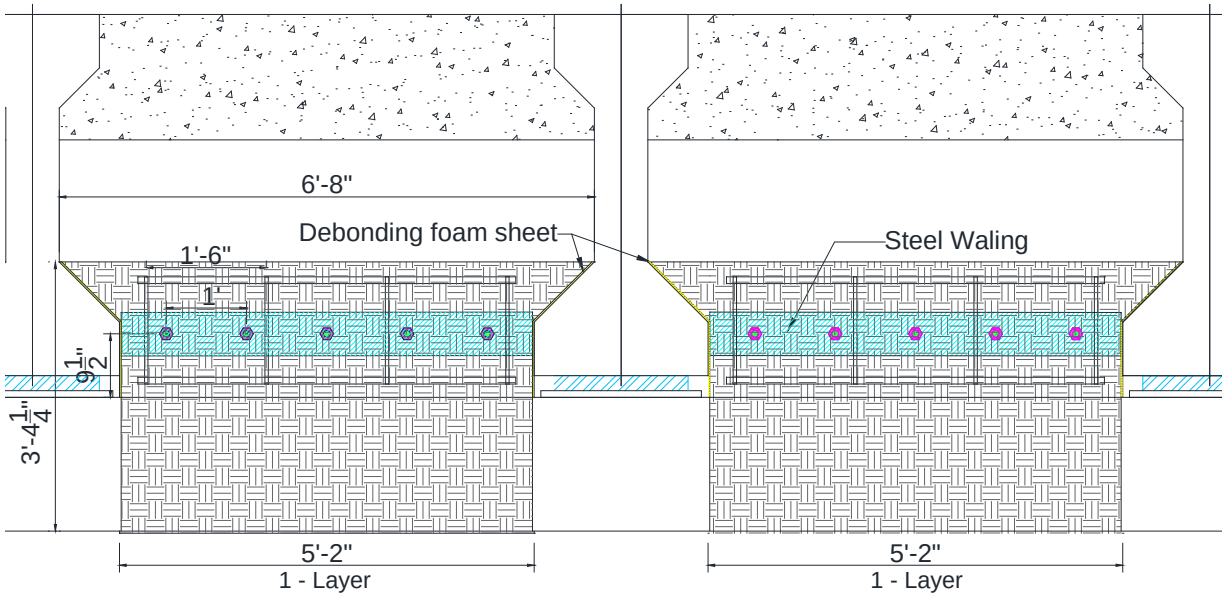

(a) Side elevation

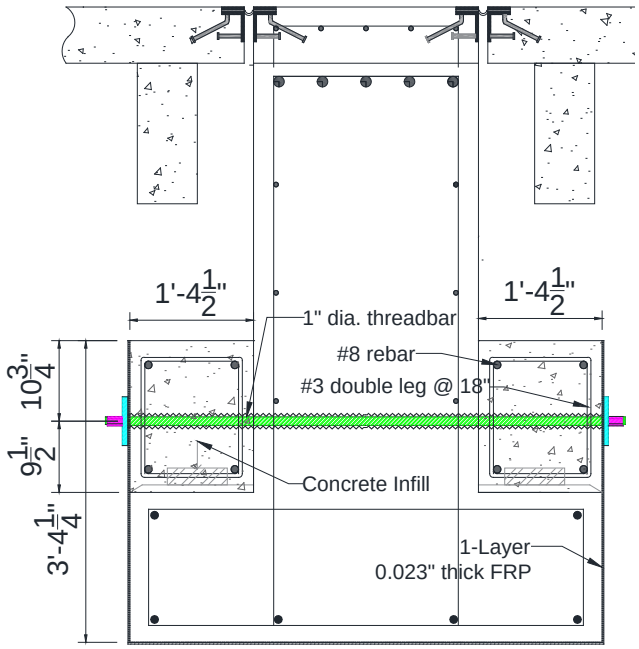

(b) Cross-section

Figure 4.23. Solution for Punching Shear and Ledge Flexure Failure Using FRP Sheets and Threadbars.

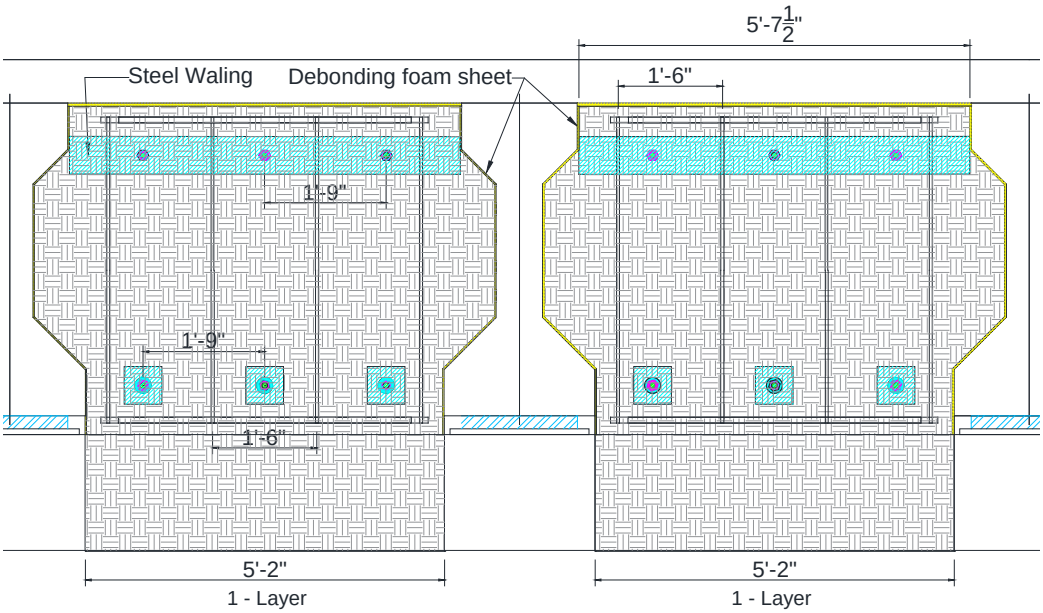

(a) Side elevation

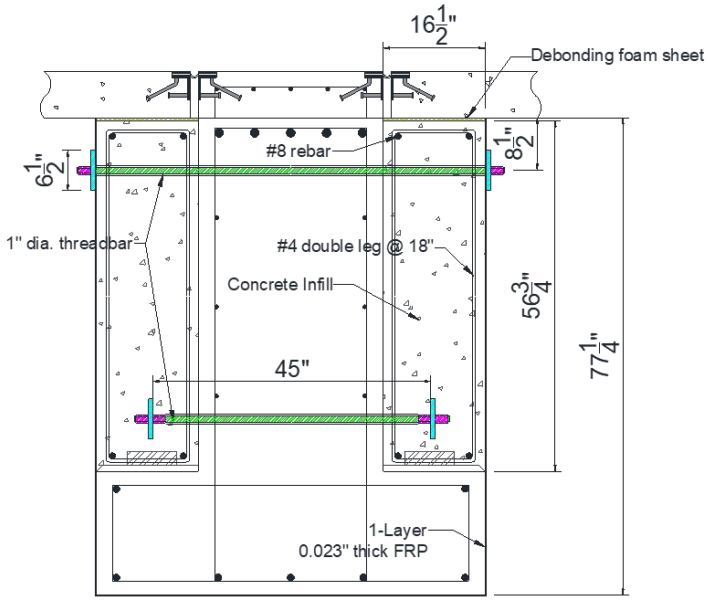

(b) Cross-section

Figure 4.24. Solution for Hanger, Punching Shear, and Ledge Flexure Failure Using FRP Sheets and Threadbars.

4.18 Large Bearing Pad (Solution 18)

Figure 4.25 shows the concept of the retrofit solution to improving punching shear capacity using different sizes of the bearing pads. Punching shear capacity is dependent on edge distance, spacing between the girders, depth of the ledge, and width of the bearing pad. The spacing between the girders, distance from the edge, or depth of the ledge cannot be changed for the real structure, but the size of bearing pads can be replaced. In this proposed solution, larger bearing pads replace the original bearing pads using a hydraulic jack to lift girders.

With the TxDOT (2015) BDM-LRFD, the nominal punching shear resistance for interior and exterior girders should be taken as described in Equation (3.18) and Equation (3.19), respectively. By increasing the size of the bearing pads, W in the equations will be increased, therefore increasing the punching shear capacity. Figure 4.25 shows how the size of bearing pads will affect the punching shear capacity of the inverted-T bent cap.

To address the 90 kip deficiency, an increment of $\Delta(w/2 + L)$ = 22.5 in. is required. However, the required increment cannot be achieved since the bearing pad size is limited by the geometry of the girder and ledge. The maximum viable bearing pad size that can be used is 25 in. x 14 in., which can enhance the punching shear capacity by 32 kips out of 90 kips deficiency.

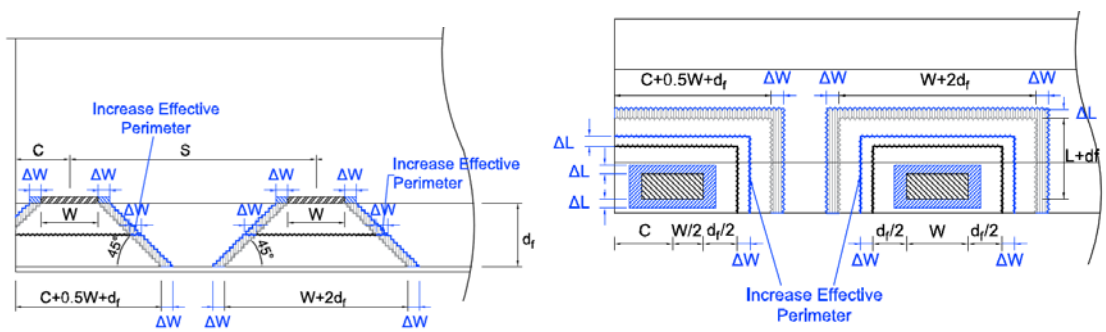

(a) Side elevation *(b) Plan view*

Figure 4.25. Solution for Punching Shear Failure by Increasing Bearing Pad Size.

4.19 Closing Remarks

The concept and design of each retrofit solution were discussed in detail based on the preliminary analysis of the inverted-T bent caps presented in Chapter 3. Each solution is designed to improve either the hanger capacity, ledge flexure capacity, punching shear capacity, or a combination of these by providing enhanced or alternative load paths. The retrofit solutions considered:

- Prestressed High-Strength Threadbar.
- Steel Hanger Bracket.
- End-Region Stiffener.
- Clamped Cross Threadbar.
- Grouted Cross Threadbar.
- Upper Seat Bracket.
- Threadbar Hanger with Steel Bracket.
- Clamped Threadbar with Channel.
- Grouted Threadbar Anchored with Channel.
- Anchored FRP Wrap.
- Concrete Infill with Prestressing Threadbar.
- Concrete Infill with Hanger Threadbar.
- Concrete Masonry Pier.
- Load-Balancing Post-Tensioning.
- Concrete Infill with FRP Anchored by FRP Anchors.
- Concrete Infill with Partial-Depth FRP Anchored by Steel Waling.
- Concrete Infill with Full-Depth FRP Anchored by Steel Waling.
- Large Bearing Pad.

Analysis of these potential solutions is a critical step prior to experimental validation. The analysis for the solutions has been conducted using the classical strut-and-tie method to estimate the load-carrying capacity of the structure.

CHAPTER 5. DECISION METHODOLOGY FOR RANKING RETROFIT SOLUTIONS

Eighteen retrofit solutions were developed for inverted-T bent caps deficient per current design codes and specifications. This chapter presents the systematic procedure used to evaluate these retrofit options in terms of specific criteria, and to rate each retrofit solution using specified weight factors. The purpose of rating the retrofit solutions was to create a decision matrix to identify the most viable solutions.

Section 5.1 provides a summary of the proposed retrofit solutions that were evaluated with a weighted sum model (WSM). In Section 5.2, use of a WSM as the decision analysis tool is presented. Section 5.3 presents a summary of the proposed retrofit solutions, description of the six criteria, and scoring definitions for each criterion. Unweighted overall scores for each solution are presented in Section 5.4. Section 5.5 presents weight factors for each criterion and the decision matrix for double- and single-column bents, including an explanation of how each solution was rated and ranked to provide guidance in selecting the most viable retrofit solutions.

5.1 Retrofit Solutions

Table 5.1 summarizes the 18 retrofit solutions, including an indication of the retrofit intent: ledge flexure, punching shear, and hanger capacities. A few retrofit solutions (Solutions 2, 6, 7, and 11) have variations “a” and “b,” where “a” is the original design and “b” is the original design plus an end-region stiffener (Solution 3).

All retrofit solutions except Solution 18 (large bearing pad) strengthen both ledge flexure and punching shear deficiencies. Solutions 2, 6, 7, and 11 lack sufficient hanger capacity for the external girder locations, leading to the “b” alternative solutions that strengthen all deficiencies concerned.

5.2 Decision Analysis Using Weighted Sum Model

There are many decision analysis tools available to rate the alternatives in multi-criteria systems. The method used should be simple yet robust enough to take into account different considerations of the problem at hand. It is important to understand the requirements and different considerations of the problem before choosing the decision analysis method.

Table 5.1. Retrofit Solutions.

Solution No.	Description of Retrofit Solution	Purpose of Retrofit			Applied Bent Type	
		Ledge Flexure	Punching Shear	Hanger	Single Column	Double Column
1	Prestressed high-strength threadbar	X	X			X
2a	Steel hanger bracket	X	X			X
2b	Steel hanger bracket + End-region stiffener	X	X	X		X
3	End-region stiffener	X	X	X	X	X
4	Clamped cross threadbar	X	X	X		X
5	Grouted cross threadbar	X	X	X		X
6a	Upper seat brackets	X	X			X
6b	Upper seat brackets + End-region stiffener	X	X	X		X
7a	Threadbar hanger with steel bracket	X	X			X
7b	Threadbar hanger with steel bracket + End-region stiffener	X	X	X		X
8	Clamped threadbar with channel	X	X	X	X	X
9	Grouted threadbar anchored with channel	X	X			X
10	Anchored FRP wrap	X	X	X	X	X
11a	Concrete infill with prestressing threadbar	X	X			X
11b	Concrete infill with prestressing threadbar + End-region stiffener	X	X	X		X
12	Concrete infill with hanger threadbar	X	X	X		X
13	Concrete masonry piers	X	X	X		X
14	Load-balancing PT	X	X	X	X	X
15	Concrete infill with FRP anchored by FRP anchors	X	X		X	X
16	Concrete infill with partial-depth FRP anchored by steel waling	X	X		X	X
17	Concrete infill with full-depth FRP anchored by steel waling	X	X	X	X	X
18	Large bearing pad		X		X	X

The current problem is to rate and rank the retrofit methods in terms of strength increase, cost, constructability, dimensional and clearance constraints, durability, and ease of monitoring. The objective is to assess retrofit methods that provide sufficient strength increase at a lower cost and at the same time are easy to implement, durable, easy to monitor, and create minimal dimensional and clearance constraints. Although these criteria are considered, some are more important than others. Therefore, the decision analysis tool must provide enough flexibility to consider different weight factors for each criterion.

A simple and popular multi-criteria decision analysis method, the WSM, can be used to evaluate several alternatives in terms of various criteria and allows assigning different weight factors for different criteria. The WSM is the most widely used model for normalized multi-

dimensional problems. While other models may incorporate more parameters for effective decision-making, the additional information required made their use in this research undesirable.

The WSM can be formulated as:

$$A_i = \sum_{j=1}^{N} w_j a_{ij}, \text{ for } i = 1,2,3, \dots M \tag{5.1}$$

where A_i is the total score for alternative i, w_j is the relative weight factor for criteria j, and a_{ij} is the individual score for alternative i when evaluated in terms of criteria j. The above general formula considers a total of M alternative retrofit solutions in terms of N criteria.

The individual scores for each criterion must be normalized in order to not lose meaning when summed to calculate the total score. In this research, the score range changes from 0 to 10, where 0 represents the *lowest undesirable score* possible, and 10 represents the *highest desirable score*. Thus, large strength increase, low cost, easy constructability, less dimensional and clearance constraints, high durability/longevity, and easy monitoring are assigned high scores.

The importance of each criterion is addressed by assigning weight factors. Each criterion must be weighted to emphasize its desired influence among the remaining criteria, and the sum of all the individual weights must be equal to unity.

5.3 Description of Criteria

Six criteria were considered for the assessment of retrofit solutions: strength increase, total cost, constructability, clearance constraints, durability, and ease of monitoring. These criteria were selected according to their specific importance in the decision-making process for selecting the potential retrofit solution and based on the needs prescribed by TxDOT.

These six criteria and scoring of the retrofit alternatives based on the criteria considered are discussed in the following subsections.

5.3.1 Strength Increase

Ability to provide sufficient increase in strength is the most important criteria to evaluate the retrofit solutions. As addressed in Chapter 3, the proposed solutions strengthen ledge flexure deficiency, punching shear deficiency, hanger deficiency, or any combination of the three.

All 18 retrofit solutions are designed to provide sufficient strength increase. Therefore, the strength increase criteria focus on two subcategories: (a) the location and deficiency addressed, and (b) the effectiveness and robustness.

Retrofit solutions were first evaluated based on the location (internal or external) strengthened and the primary purpose of the proposed solution. For example, the retrofit solution is assigned a higher score if the proposed solution strengthens the inverted-T bent at all girder locations and for all deficiencies. The retrofit solution (e.g., prestressed high-strength thread rods) is assigned a lower score if it strengthens only ledge flexure and punching shear deficiencies for the internal girder locations. Six subcategories are defined for strength increase in terms of location and deficiency: (a) interior ledge flexure deficiency, (b) interior punching shear deficiency, (c) interior hanger deficiency, (d) exterior ledge flexure deficiency, (e) exterior punching shear deficiency, and (f) exterior hanger deficiency. For single-column bents, the score is based on the strengthening location for the exterior girder and the retrofit system only because single-column bents are mostly deficient at the exterior girder locations. Table 5.2 presents the details of these definitions and their associated score values. Scores for each subcategory are scaled such that a retrofit is assigned 3 points for strengthening each deficiency for all three interior girder locations. Similarly, retrofit solutions are assigned 2 points for strengthening each deficiency at both exterior girder locations. Full scores for these six subcategories sum to 15. The total score for the location and deficiency addressed is normalized to 10 to combine with the score for another subcategory of the retrofit system that has a full score of 10.

The effectiveness and robustness of the proposed retrofit solution is another important strength consideration. Retrofit solutions are categorized as one of four retrofit systems: (a) active support system, (b) passive support system, (c) alternate load path system, and (d) strengthening system. Table 5.2 presents the details of these definitions and their associated score values.

An *active support system* actively supports a share of the total load prior to any potential overload being applied. For example, a PT system that uses inclined angles or draped tendons is an active support system since the vertical component of the PT force is actively resisting a portion of the preexisting gravity loads.

A *passive support system* is supplementary to the original structure and its associated load paths. For a passive system to work under overload, the primary structure will need to start failing by incurring greater-than-normal structural deformations. As the deformations markedly increase, the passive system commences engaging by providing a supplementary load path. For example, the FRP system that consists of a polymer fabric glued to the concrete will remain unstressed and passive until the concrete in the ledge or web of the bent cracks. The FRP is then activated and

provides a supplementary load path, and if correctly designed, will passively support the additional load that the original primary structure system is not capable of supporting.

An *alternate load path system* relieves some of the girder reaction on the bearing pad and directs it elsewhere by providing an alternative path. The standard design of an existing inverted-T bent system applies the reaction of the girder onto the bearing seat on the ledges of the inverted-T beam. Any system that provides a new load path relieving the load from the ledge and providing an alternative path to the web of the inverted-T bent cap can be considered an alternative load path system. For example, several retrofit solutions (e.g., upper seat bracket) provide a direct load path from the deck slab of the bridge into the bent cap via the web of the inverted-T beam. Such a load path is common place for the flange-hung support of precast double-T beams used in parking garages.

A strengthening system enhances the capacity of the existing resisting mechanism to provide greater overall capacity. In contrast, active and passive support systems are augmentation systems that are new to the structure. For example, the prestressed high-strength threadbar solution applied to the ledge raises the existing (deficient) shear capacity to a high level of shear resistance. The existing shear mechanism is thereby strengthened.

Table 5.3 and Table 5.4 summarize the ratings of each retrofit option for double- and single-column bents, respectively.

Table 5.2. Scoring Definitions for Adequate Strength Increase.

Scoring for Location and Deficiency		
Shear/Hanger for Interior Girders	**Score**	
No strengthening	0	
Strengthening one interior girder	1	
Strengthening two interior girders	2	
Strengthening three interior girders	3	
Shear/Hanger for Exterior Girders	**Score for Double-Column Bent**	**Score for Single-Column Bent**
No strengthening	0	0
Partial strengthening of exterior girder	1	2.5
Full strengthening of exterior girders	2	5
Scoring for Retrofit System		
Retrofit System	**Score**	
Passive support system	4	
Strengthening system	6	
Alternative load path	8	
Active support system	10	

Table 5.3. Rating for Strength Increase of Retrofit Solutions for Double-Column Bents.

		Location and Deficiency							Retrofit System		Avg. Score
		Interior			Exterior			Score	System	Score	
No.	Retrofit Solution	LF	P	H	LF	P	H				
1	Prestressed high-strength threadbar	3	3	0	0	0	0	4.0	Strengthening	6	5.0
2a	Steel hanger bracket	3	3	0	1	1	0	5.3	Alt. load path	8	6.7
2b	Steel hanger bracket + End-region stiffener	3	3	0	2	2	2	8.0	Alt. load path	8	8.0
3	End-region stiffener	0	0	0	2	2	2	4.0	Passive	4	4.0
4	Clamped cross threadbar	3	3	0	2	2	0	6.7	Passive	4	5.3
5	Grouted cross threadbar	3	3	0	2	2	0	6.7	Passive	4	5.3
6a	Upper seat brackets	3	3	0	1	1	0	5.3	Alt. load path	8	6.7
6b	Upper seat brackets + End-region stiffener	3	3	0	2	2	2	8.0	Alt. load path	8	8.0
7a	Threadbar hanger with steel bracket	3	3	0	1	1	0	5.3	Passive	4	4.7
7b	Threadbar hanger with steel bracket + End-region stiffener	3	3	0	2	2	2	8.0	Passive	4	6.0
8	Clamped threadbar with channel	3	3	3	2	2	2	10.0	Alt. load path	8	9.0
9	Grouted threadbar anchored with channel	3	3	0	2	2	0	6.7	Passive	4	5.3
10	Anchored FRP wrap	3	3	3	2	2	2	10.0	Passive	4	7.0
11a	Concrete infill with prestressing threadbar	3	3	1	1	1	1	6.7	Alt. load path	8	7.3
11b	Concrete infill with prestressing threadbar + End-region stiffener	3	3	1	2	2	2	8.7	Alt. load path	8	8.3
12	Concrete infill with hanger threadbar	3	3	3	2	2	2	10.0	Alt. load path	8	9.0
13	Concrete masonry piers	3	3	3	2	2	2	10.0	Alt. load path	8	9.0
14	Load-balancing PT	3	3	3	2	2	2	10.0	Active	10	10.0
15	Concrete infill with FRP anchored by FRP anchors	3	3	0	2	2	2	8.0	Passive	4	6.0
16	Concrete infill with partial-depth FRP anchored by steel waling	3	3	0	2	2	2	8.0	Alt. load path	8	8.0
17	Concrete infill with full-depth FRP anchored by steel waling	3	3	3	2	2	2	10.0	Alt. load path	8	9.0
18	Large bearing pad	3	0	0	2	0	0	3.3	Active	10	6.7

Note: LF = ledge flexure, P = punching shear, and H = hanger.

Table 5.4. Strength Rating of Retrofit Solutions for Single-Column Bents.

		Deficiency				Retrofit System		Avg. Score
		Exterior			Score	System	Score	
No.	Retrofit Solution	LF	P	H				
3	End-region stiffener	5	5	5	10.0	Passive	4	7.0
8	Clamped threadbar with channel	5	5	5	10.0	Alt. load path	8	9.0
10	Anchored FRP wrap	5	5	5	10.0	Passive	4	7.0
14	Load-balancing PT	5	5	5	10.0	Active	10	10.0
15	Concrete infill with FRP anchored by FRP anchors	5	5	0	6.7	Passive	4	5.3
16	Concrete infill with partial-depth FRP anchored by steel waling	5	5	0	6.7	Alt. load path	8	7.3
17	Concrete infill with full-depth FRP anchored by steel waling	5	5	5	10.0	Alt. load path	8	9.0
18	Large bearing pad	0	5	0	3.3	Active	10	6.7

Note: LF = ledge flexure, P = punching shear, and H = hanger.

5.3.2 Cost

This section presents information on the estimation and evaluation of the total construction cost of each retrofit solution. The required work items and bill of quantities for each retrofit solution are determined based on the designs presented in Chapter 4. The required work items are decomposed as primary activities (drilling holes, welding steel plates, etc.), major items (steel angle, steel bracket, threadbar, anchor bolts, etc.), and their ancillary items that support the primary activities such as equipment rental and operator costs. The costs of required items are categorized as material, labor, and equipment costs, and calculated using the unit cost method. The unit prices of each work item are estimated mainly based on the contractor's prices for materials, labor, and equipment. The cost data are established based on E-base and historical data from previous TxDOT projects. Adjustments are made to unit prices to reflect specific conditions such as quantity (unit prices for larger quantities of a material are less than smaller quantities), availability (if the complete unit is available), and commonality of the items.

Among the work items, a boom lift is considered as a general requirement item since the bent caps are elevated around 26 ft from the ground. The labor cost of construction workers is also common to all cases. It is assumed that three construction workers will engage in the whole construction process. A telehandler with an operator is considered if the weight of a component exceeds 500 lb.

Drilling of concrete may also be considered as a common operation since most of the proposed retrofit solutions require drilling and anchoring into the concrete. There are several drilling methods that can be used to drill the concrete depending on the depth and diameter of the hole. Hammer drills may be used for drilling shallow and small diameter holes at a fairly low cost. Concrete core drills or rock-bolt drills may be used for drilling relatively deep holes and various diameters that can go up to 5 ft for the core drill. The drilling depth was considered as the critical factor in this study, and the concrete drilling method was selected based on the required drilling depth.

Hammer drills can be selected to drill a hole that has a drilling depth smaller than 2 ft; otherwise, core drills can be considered for estimating the relative cost. Rock-bolt drills can also be used for deep concrete drilling operations and can be more cost effective if there are a large number of holes to be drilled. For the hammer drills, the cost of hammer drill bits is considered as an ancillary item. For the core drills, which require relatively higher expertise, labor cost for a core

drill specialist, rental cost for a core drill rig, and material cost for a diamond core drill bit are taken into account. The same drilling speed rate is assumed for all solutions for estimating the work hours required for concrete drilling.

Steel components (steel angle, steel bracket, etc.) are another major item that may significantly contribute to the total cost. The unit price of A36 steel is estimated based on the provided contractor's price, and a markup of 30 percent is applied to take into account the wastage cost. Plasma cutting of the steel plate, welding, and corresponding labor costs, if any, are considered as ancillary items of steel components.

In the case of grouted and epoxy anchored bolts and rods, the cost of grout and epoxy resin is considered as the material cost, and equipment cost includes specific epoxy guns, grouting mixer, and pump. The cost of the grouted threadbars that are longer than 5 ft considers the use of hollow bars with grout inlet holes. For the FRP application, the costs of grinding and epoxy resin are considered as ancillary items. For PT bars, extra costs of a post-tension jack and post-tension specialist are also included in the total cost.

After the costs of work items have been determined, the mobilization cost is estimated as a lump sum bid item and added to the total cost. Considering the bent caps are located in Austin, the mobilization cost is conservatively taken at around 20 percent of the total cost of work items. Then, an additional markup of 20 percent of the total construction cost is allocated as a contingency cost and added to the total cost to account for uncertainties in quantities of work items, unit prices, and potential risk events during the construction of retrofits. The detailed lists of costs for each work item for each proposed retrofit solution are presented in **Error! Reference source not found.**.

Table 5.5 presents the defined scoring ranges for a total cost of the retrofit solutions. The scores range from 0 to 10, where 0 represents an undesirable score and 10 represents the highest desirable score.

Table 5.6 presents the rating of each retrofit solution in terms of the total cost. As evident from Table 5.6, Solution 3 has the highest score of 10 with a total cost of $10,000. However, this end-region stiffener improves the capacity of the bent only at the location of the exterior girders. The end stiffener retrofit solution was mainly proposed to be used in combination with other retrofit solutions that cannot be applied at the exterior region due to limited space or for the bents

where the deficiency is only for the exterior girders. Therefore, this solution is a special case and should be distinguished from the other solutions.

Table 5.5. Scoring Definitions for Cost.

Score	Cost (K)
0	>$100
1	$91–$100
2	$81–$90
3	$71–$80
4	$61–$70
5	$51–$60
6	$41–$50
7	$31–$40
8	$21–$30
9	$11–$20
10	$0–$10

Table 5.6. Cost Rating of Retrofit Solutions for Double-Column Bents.

No.	Retrofit Solution	Total Cost	Score
1	Prestressed high-strength threadbar	$34K	7
2a	Steel hanger bracket	$17K	9
2b	Steel hanger bracket + End-region stiffener	$24K	8
3	End-region stiffener	$10K	10
4	Clamped cross threadbar	$39K	7
5	Grouted cross threadbar	$31K	7
6a	Upper seat brackets	$25K	8
6b	Upper seat brackets + End-region stiffener	$31K	7
7a	Threadbar hanger with steel bracket	$21K	8
7b	Threadbar hanger with steel bracket + End-region stiffener	$28K	8
8	Clamped threadbar with channel	$19K	9
9	Grouted threadbar anchored with channel	$22K	8
10	Anchored FRP wrap	$35K	7
11a	Concrete infill with prestressing threadbar	$28K	8
11b	Concrete infill with prestressing threadbar + End-region stiffener	$38K	7
12	Concrete infill with hanger threadbar	$63K	4
13	Concrete masonry piers	$83K	2
14	Load-balancing PT	$24K	8
15	Concrete infill with FRP anchored by FRP anchors	$62K	4
16	Concrete infill with partial-depth FRP anchored by steel waling	$35K	7
17	Concrete infill with full-depth FRP anchored by steel waling	$39K	7
18	Large bearing pad	$6K	10

Among the remaining retrofits, Solution 18 (increasing bearing pad) and Solution 2a (steel hanger bracket) have a minimum cost of $6,000 and $17,000, resulting in the highest rating score of 10 and 9, respectively. Solutions 2b, 6a, 7a, 7b, 9, 11b, and 14 are the next most cost-effective

solutions with a score of 8. Out of these, Solutions 6a and 7a provide only partial strengthening, while other solutions strengthen the whole bent. Solutions 1, 4, 5, 6b, 10, 11b, 16, and 17 that have a rating score of 7 may also be considered cost-effective retrofit solutions that, with the exception of Solution 1, can strengthen the whole bent cap. Solution 13 (concrete masonry piers) is the costliest solution, with a cost of $83,000 and the lowest rating score of 2.

Table 5.7 presents information about the total construction cost of each retrofit solution for external support regions of the single-column bents. Solutions 3, 8, and 18 have the highest score of 10. Although Solution 18 has the smallest total cost of $4,000, this solution is able to strengthen only punching shear capacity, while other solutions strengthen ledge flexure and hanger capacities as well. Solutions 10 and 14 are the next most cost-effective solutions, with a score of 9. Solution 15 is the costliest solution, with a cost of $49,000 and the lowest rating score of 6. The detailed lists of costs for each work item for each proposed retrofit solution are presented in **Error! Reference source not found.** with the designs that are used to determine the required work items and bill of quantities for each retrofit solution.

Table 5.7. Cost Rating of Retrofit Solutions for Single-Column Bents.

No.	Retrofit Solution	Total Cost	Score
3	End-region stiffener	$7K	10
8	Clamped threadbar with channel	$7K	10
10	Anchored FRP wrap	$14K	9
14	Load-balancing PT	$20K	9
15	Concrete infill with FRP anchored by FRP anchors	$49K	6
16	Concrete infill with partial-depth FRP anchored by steel waling	$33K	7
17	Concrete infill with full-depth FRP anchored by steel waling	$35K	7
18	Large bearing pad	$4K	10

5.3.3 Constructability

Constructability is considered as the successful implementation of all operations. Identification of possible difficulties and issues that could be encountered during the application of a specific retrofit solution is necessary to assess constructability. Thus, constructability involves thoroughly thinking about how to build and implement the retrofit solution. The constructability of each retrofit solution is evaluated based on the difficulty of required operations and certain risk factors involved during the application of these operations. The constructability considerations include (a) risk of damaging reinforcement, (b) accessibility requirements, (c) possible lane closures, and (d) the weight that must be lifted. Table 5.8 lists the scoring for constructability of the solutions. Since there is a possible lane closure above and below the bridge, five categories are defined for

constructability with the considerations as shown in Table 5.8. Each category has a highest score of 10 and lowest score of 0. Total score is 50 and averaged to 10 to have a final score of 10.

Most retrofit solutions require some drilling and anchoring into the concrete, which may create a risk of damaging the existing mild steel reinforcement in the bent. This risk is greater as the drilling depth and diameter increase. Although it is possible to identify the location of reinforcement accurately, there may still be some level of risk associated with drilling holes at an angle. For example, the clamped cross threadbar solution requires drilling a long diagonal hole from the bottom of the ledge through the web, which has a high risk of damaging hanger stirrups. On the other hand, the steel hanger brackets having several anchor bolts have a low risk of damaging existing reinforcement since the short-distance horizontal drilling operation has to avoid just one layer of stirrups. The retrofit options are rated relative to each other in terms of the risk involved in damaging the existing reinforcement.

Another difficulty is the accessibility requirement for the installation of various steel and bar components on the inverted-T bents. Each retrofit solution has different steel plates, threaded bars, steel brackets, etc., and the size of these components necessitates different accessibility requirements. Each retrofit solution is rated such that solutions that use smaller components and requires less accessibility are assigned a higher score. One of the major operations is lifting and installing heavy steel components on the bent. Most of these operations require a telehandler, which increases the time and cost of operations. The retrofit solution can be considered less attractive as the number of heavyweight components increases.

Lane closure is an important consideration for evaluating the viability of retrofit solutions. Lane closures cause some level of disturbance to the public, creating direct and indirect costs. Direct costs include workers, additional traffic signs to reroute traffic, and the like. Indirect costs incurred by the public include extra gasoline consumption and delay due to congestion. The solution that creates the minimum disturbance to the public and requires minimum lane closures gets the highest score (Solution 8). The total lane closure times for the lanes above and below the bridge are estimated to provide quantifiable information, which provides objective guidance for rating the retrofit solutions. The solutions that require less lane closure time are assigned a higher score.

Total weight of the components that need to be lifted up is an important factor to assess the constructability of each solution since the bent caps are located approximately 26 ft from the ground, and the heavier components are more difficult to lift up. Therefore, the highest score of

10 is assigned for the solution with a component under 1,000 lb, and the lowest score of 0 is assigned for solution components over 10,000 lb.

Table 5.8. Scoring Definitions for Constructability.

Score	Risk of Damaging Reinforcement	Accessibility Requirement	Total Weight of Components to Be Lifted Up (lb)	Lane Closure below the Bridge (days)	Lane Closure above the Bridge (days)
0	Very high risk	Diaphragm and web	>10,000	>30	>30
1	—	—	9,001–10,000	27–29	27–29
2	High risk	Behind the girders	8,001–9,000	24–26	24–26
3	—	—	7,001–8,000	21–23	21–23
4	Medium risk	Deck and/or bottom	6,001–7,000	18–20	18–20
5	—	—	5,001–6,000	15–17	15–17
6	Low risk	Web and/or ledges	4,001–5,000	12–14	12–14
7	—	—	3,001–4,000	9–11	9–11
8	Very low risk	Bottom	2,001–3,000	6–8	6–8
9	—	—	1,001–2,000	3–5	3–5
10	No risk	Sides and/or ends	0–1,000	0–2	0–2

Table 5.9 and Table 5.10 summarize the constructability rating of each retrofit solution for double- and single-column bents, respectively. Although the scoring definitions and rating considerations for single-column bents are the same as those for double-column bents, the scores for retrofit solutions are updated based on the specific construction procedures required for the implementation of the retrofits for single-column bents.

5.3.4 Dimensional and Clearance Constraints

Inverted-T bent caps are generally used to reduce the overall elevation of bridges, to improve the available clearance beneath the beams, and to improve the aesthetics. Most of the proposed retrofit solutions suggest using components such as steel plates extruding from the surface of the bent cap, which decreases the clearance either underneath or on the sides of the inverted-T bent. Therefore, dimensional and clearance constraints are one of the essential criteria to evaluate the retrofit solutions. In most practical applications, the clearance constraints beneath the bridge are more critical than horizontal clearances at the sides of the bents. Therefore, only the dimensional and clearance constraints beneath the bridge are considered.

Table 5.11 shows scoring definitions for different ranges of dimensional and clearance constraint criteria, which can easily be quantified based on the amount of protrusion beneath the

bent. The highest score of 10 indicates that there are no changes in vertical clearance due to the retrofitting.

Table 5.9. Constructability Rating of Retrofit Solutions for Double-Column Bents.

No.	Retrofit Solution	Risk of Damaging Reinforcement		Accessibility Requirements		Below Lane Closure		Above Lane Closure		Total Weight		Avg. Score
		Risk	Score	Accessibility	Score	Days	Score	Days	Score	lbs.	Score	
1	Prestressed high-strength threadbar	Low	6	Sides and/or Ends	10	12	6	0	10	18000	0	6.4
2a	Steel hanger bracket	Very low	8	Behind the Girders	2	5	9	0	10	2250	8	7.4
2b	Steel hanger bracket + End-region stiffener	Very low	8	Behind the Girders	2	10	7	0	10	4450	6	6.6
3	End-region stiffener	High	2	Sides and/or Ends	10	2	10	0	10	1005	9	8.2
4	Clamped cross threadbar	Very High	0	Web and/or Ledges	6	17	5	0	10	1060	9	6.0
5	Grouted cross threadbar	High	2	Bottom	8	16	5	0	10	550	10	7.0
6a	Upper seat brackets	Very Low	8	Web and/or Ledges	6	7	8	0	10	3165	7	7.8
6b	Upper seat brackets + End-region stiffener	Very Low	8	Web and/or Ledges	6	11	7	0	10	5295	5	7.2
7a	Threadbar hanger with steel bracket	Medium	4	Web and/or Ledges	6	7	8	0	10	2010	8	7.2
7b	Threadbar hanger with steel bracket + End-region stiffener	Medium	4	Web and/or Ledges	6	12	6	0	10	4140	6	6.4
8	Clamped threadbar with channel	Very High	0	Deck and/or Bottom	4	7	8	7	8	5370	5	5.0
9	Grouted threadbar anchored with channel	Medium	4	Bottom	8	15	5	0	10	5130	5	6.4
10	Anchored FRP wrap	Medium	4	Diaphragm and Web	0	13	6	0	10	1900	9	5.8
11a	Concrete infill with prestressing threadbar	Low	6	Deck and/or Bottom	4	12	6	6	9	1280	9	6.8
11b	Concrete infill with prestressing threadbar + End-region stiffener	Low	6	Deck and/or Bottom	4	13	6	6	9	3120	7	6.4
12	Concrete infill with hanger threadbar	Medium	4	Deck and/or Bottom	4	23	3	7	8	1830	9	5.6
13	Concrete masonry piers	No Risk	10	Bottom	8	>30	0	0	10	4500	6	6.8
14	Load-balancing PT	Medium	6	Behind the Girders	2	3	9	4	9	5750	5	6.2
15	Concrete infill with FRP anchored by FRP anchors	Medium	4	Web and/or Ledges	6	10	7	6	9	1900	9	7.0
16	Concrete infill with partial-depth FRP anchored by steel waling	Medium	4	Web and/or Ledges	6	16	5	0	10	1500	9	6.8
17	Concrete infill with full-depth FRP anchored by steel waling	Medium	4	Web and/or Ledges	6	10	7	6	9	1900	9	7.0
18	Large bearing pad	Very Low	10	Under the Girders	0	2	10	2	10	900	10	8.0

Table 5.10. Constructability Rating of Single-Column Bents.

No.	Retrofit Solution	Risk of Damaging Reinforcement		Accessibility Requirements		Below Lane Closure		Above Lane Closure		Total Weight to Be Lifted		Avg. Score
		Risk	Score	Accessibility	Score	Days	Score	Days	Score	lbs.	Score	
3	End-region stiffener	Medium	4	Sides and/or Ends	10	2	10	0	10	1005	9	8.6
8	Clamped threadbar with channel	High	2	Deck and/or Bottom	4	3	8	1	10	1200	9	6.6
10	Anchored FRP wrap	Medium	4	Diaphragm and Web	0	5	9	0	10	360	10	6.6
14	Load-balancing PT	Low	6	Behind the Girders	2	3	9	4	9	4420	6	6.4
15	Concrete infill with FRP anchored by FRP anchors	Medium	4	Web and/or Ledges	6	10	7	6	9	1900	9	7.0
16	Concrete infill with partial-depth FRP anchored by steel waling	Medium	4	Web and/or Ledges	6	16	5	0	10	1500	9	6.8
17	Concrete infill with full-depth FRP anchored by steel waling	Medium	4	Web and/or Ledges	6	10	7	6	9	1900	9	7.0
18	Large bearing pad	Very Low	10	Under the Girders	0	2	10	2	10	900	10	8.0

Table 5.11. Scoring Definitions for Dimensional and Clearance Constraints.

Score	Dimensional and Clearance Constraints (in.)
0	>9
1	8–9
2	7–8
3	6–7
4	5–6
5	4–5
6	3–4
7	2–3
8	1–2
9	0–1
10	0 (No changes)

As shown in Table 5.12 and Table 5.13, the solutions with components primarily above the ledge of the bent cap have high scores, while the retrofit solutions with components beneath the bent cap have relatively lower scores. The concrete masonry pier solution is assigned a score of zero because the piers cannot be installed where there is a road underneath the bridge.

Table 5.12. Clearance Constraint Score of Retrofit Solutions for Double-Column Bents.

No.	Retrofit Solution	Dimensional and Clearance Constraint (in.)	Score
1	Prestressed high-strength threadbar	0.0	10
2a	Steel hanger bracket	0.0	10
2b	Steel hanger bracket + End-region stiffener	0.5	9
3	End-region stiffener	0.5	9
4	Clamped cross threadbar	5.5	3
5	Grouted cross threadbar	5.5	3
6a	Upper seat brackets	0.0	10
6b	Upper seat brackets + End-region stiffener	0.5	9
7a	Threadbar hanger with steel bracket	2.8	7
7b	Threadbar hanger with steel bracket + End-region stiffener	2.8	7
8	Clamped threadbar with channel	4.5	5
9	Grouted threadbar anchored with channel	4.5	5
10	Anchored FRP wrap	0.0	10
11a	Concrete infill with prestressing threadbar	0.0	10
11b	Concrete infill with prestressing threadbar + End-region stiffener	0.5	9
12	Concrete infill with hanger threadbar	3.8	6
13	Concrete masonry piers	>9	0
14	Load-balancing PT	0.5	9
15	Concrete infill with FRP anchored by FRP anchors	0.0	10
16	Concrete infill with partial-depth FRP anchored by steel waling	0.0	10
17	Concrete infill with full-depth FRP anchored by steel waling	0.0	10
18	Large bearing pad	0.0	10

Table 5.13. Clearance Constraint Rating of Retrofit Solutions for Single-Column Bents.

No.	Retrofit Solution	Dimensional and Clearance Constraint (in.)	Score
3	End-region stiffener	0.5	9
8	Clamped threadbar with channel	4.5	5
10	Anchored FRP wrap	0.0	10
14	Load-balancing PT	0.5	9
15	Concrete infill with FRP anchored by FRP anchors	0.0	10
16	Concrete infill with partial-depth FRP anchored by steel waling	0.0	10
17	Concrete infill with full-depth FRP anchored by steel waling	0.0	10
18	Large bearing pad	0.0	10

5.3.5 Durability/Longevity

Durability is the ability of the material/retrofit to resist any kind of damage such as corrosion, wear, fatigue, and/or disintegration due to cyclic moisture and temperature changes that may compromise the life expectancy of the retrofitted structure. Longevity of a structure can be defined as the ability of the structure to have a longer life span under continuous service. It is imperative to select appropriate construction material for durable construction, which simply provides longevity by increasing the life cycle of the structure. Therefore, the durability of the proposed solutions is also considered while rating the viability and effectiveness of the retrofit method. The durability of the retrofit solution can increase the overall long-term economic efficiency while assuring sufficient capacity throughout the intended lifetime of the structure.

One of the most common durability concerns is corrosion of the steel components used for the retrofit. Corrosion causes degradation of the metallic area by chemical reaction with the environment, especially when the moisture content is high. Substructure components are particularly susceptible to corrosion due to runoff through expansion joints, leading to faster and more severe corrosion around that region. The proposed retrofit solutions on the inverted-T bents are probably in such critical high-risk regions where they can be exposed to moisture more often. Although there are methods to provide additional corrosion protection, such as galvanizing or epoxy coating, these methods are not considered in scoring the retrofit solutions because they can be applied to all steel components and do not affect the relative score. Instead, the retrofit solutions are evaluated based on the materials used, the concrete or grout cover provided for the steel components, and whether they are directly exposed to the environment or enclosed within a drilled hole.

Another parameter that affects the durability and longevity of the retrofit solution is the effectiveness of the bond between concrete and epoxy. The mechanical properties and short-term behavior of such systems have been well studied, but the long-term performance is largely uncertain. The concrete-epoxy interface may experience debonding due to moisture ingress, freeze-thaw cycles, or thermal loading coupled with mechanical loading. Although epoxy anchored bolts may experience debonding, moisture-affected debonding failures in FRP retrofitted systems can be a more critical issue in terms of durability of the retrofit system. These differences and risk levels are taken into account while scoring the retrofit solutions. Table 5.14 lists the scores for durability/longevity of the retrofit solutions.

Table 5.14. Scoring Definitions for Durability/Longevity.

Score	Corrosion	Debonding	Risk of Fatigue and Fracture
0	Directly exposed to the environment on the web/ledges	FRP installation without anchors	Very high
2	Directly exposed to environment below the bent	Anchored FRP installation using epoxy	High
4	Partially enclosed	Grouted threadbars under concentric loading	Medium
6	Fully enclosed	Large-diameter epoxy anchor bolts	Low
8	Enclosed and grouted	Small-diameter epoxy anchor bolts	Very low
10	Noncorrosive material	No risk of debonding	None

Table 5.15 and Table 5.16 provide the rating of retrofit solutions in terms of durability/longevity for double- and single-column bents, respectively. The scores assigned to all the retrofit solutions for single-column bents are the same as the scores assigned for the double-column bents because the considerations remain the same for both cases. Since Solution 13 (concrete masonry piers) and Solution 18 (large bearing pad) are designed to last for the life cycle of the bridge and not to replace any parts of the solutions, these two solutions have the highest score of 10. On the other hand, the solutions using steel brackets (Solutions 2a, 2b, 6a, 6b, 7a, and 7b) have the lowest scores of 2.0 and/or 3.3. This is because the steel bracket and anchors have a high risk of corrosion. Because of the same issue, Solution 3 (end-region stiffener) has a relatively low score of 5.3. Solutions using FRPs have low scores because of the high risk of debonding.

5.3.6 Ease of Monitoring

Monitoring and condition assessment of critical components, and of the entire retrofit solution, is also an important consideration. Condition assessment allows bridge owners or departments of transportation (DOTs) to take timely, proactive actions to mitigate or prevent further deterioration and unanticipated failure of structural components.

Although corrosion protection methods and construction practices have improved over the past decades, there is always the possibility of some degree of corrosion, which may be significant over many years and might affect the longevity of the proposed retrofit solution. There may be significant consequences if inspection, maintenance, and repairs are not performed in a timely manner.

Table 5.15. Durability/Longevity Rating of Retrofit Solutions for Double-Column Bents.

No.	Retrofit Solution	Corrosion		Debonding		Risk of Fatigue and Fracture		Avg. Score
1	Prestressed high-strength threadbar	Directly exposed to environment below the bent	2	No risk of debonding	10	None	10	7.3
2a	Steel hanger bracket	Directly exposed to environment on the web/ledges	0	Large-diameter epoxy anchor bolts	6	Very high	0	2.0
2b	Steel hanger bracket + End-region stiffener	Directly exposed to environment on the web/ledges	0	Large-diameter epoxy anchor bolts	6	Very high	0	2.0
3	End-region stiffener	Directly exposed to environment on the web/ledges	0	Small-diameter epoxy anchor bolts	8	Very low	8	5.3
4	Clamped cross threadbar	Fully enclosed	6	No risk of debonding	10	None	10	8.7
5	Grouted cross threadbar	Enclosed and grouted	8	Grouted threadbars under concentric loading	4	None	10	7.3
6a	Upper seat brackets	Directly exposed to environment on the web/ledges	0	Small-diameter epoxy anchor bolts	8	High	2	3.3
6b	Upper seat brackets + End-region stiffener	Directly exposed to environment on the web/ledges	0	Small-diameter epoxy anchor bolts	8	High	2	3.3
7a	Threadbar hanger with steel bracket	Directly exposed to environment on the web/ledges	0	Small-diameter epoxy anchor bolts	8	High	2	3.3
7b	Threadbar hanger with steel bracket + End-region stiffener	Directly exposed to environment on the web/ledges	0	Small-diameter epoxy anchor bolts	8	High	2	3.3
8	Clamped threadbar with channel	Fully enclosed	6	No risk of debonding	10	Very low	8	8.0
9	Grouted threadbar anchored with channel	Enclosed and grouted	8	Grouted threadbars under concentric loading	4	Very low	8	6.7
10	Anchored FRP wrap	Noncorrosive material	10	Anchored FRP installation using epoxy	2	None	10	7.3
11a	Concrete infill with prestressing threadbar	Enclosed and grouted	8	No risk of debonding	10	None	10	9.3
11b	Concrete infill with prestressing threadbar + End-region stiffener	Partially enclosed	4	No risk of debonding	10	Very low	8	7.3
12	Concrete infill with hanger threadbar	Enclosed and grouted	8	No risk of debonding	10	None	10	9.3
13	Concrete masonry piers	Noncorrosive material	10	No risk of debonding	10	None	10	10.0
14	Load-balancing PT	Enclosed and grouted	8	No risk of debonding	10	Medium	4	7.3
15	Concrete infill with FRP anchored by FRP anchors	Enclosed and grouted	8	Anchored FRP installation using epoxy	2	None	10	6.7
16	Concrete infill with partial-depth FRP anchored by steel waling	Directly exposed to environment on the web/ledges	0	Anchored FRP installation using epoxy	2	None	10	4.0
17	Concrete infill with full-depth FRP anchored by steel waling	Directly exposed to environment on the web/ledges	0	Anchored FRP installation using epoxy	2	None	10	4.0
18	Large bearing pad	Noncorrosive material	10	No risk of debonding	10	None	10	10.0

Table 5.16. Durability/Longevity Rating of Single-Column Bents.

No.	Retrofit Solution	Corrosion	Debonding	Risk of Fatigue and Fracture	Avg. Score
3	End-region stiffener	0	8	8	5.3
8	Clamped threadbar with channel	6	10	8	8.0
10	Anchored FRP wrap	10	2	10	7.3
14	Load-balancing PT	8	10	4	7.3
15	Concrete infill with FRP anchored by FRP anchors	8	2	10	6.7
16	Concrete infill with partial-depth FRP anchored by steel waling	0	2	10	4.0
17	Concrete infill with full-depth FRP anchored by steel waling	0	2	10	4.0
18	Large bearing pad	10	10	10	10.0

It is possible to use a relatively cheaper visual testing method for external retrofit solutions where corrosion distress can be identified by visual staining, cracking, or spalling of the concrete cover. However, these distress indicators are typically not visible when the threaded bars are enclosed or embedded in concrete. In that case, inspectors may have to use relatively time-consuming and expensive nondestructive testing (NDT) methods such as a borescope. It is desirable to have a retrofit solution that can be easily inspected, and retrofit solutions are rated based on the difficulty of inspection. Table 5.17 defines the scores for ease of monitoring of the retrofit solutions. Table 5.18 and Table 5.19 summarize the scores of retrofit solutions in terms of ease of monitoring for double- and single-column bents, respectively.

Table 5.17. Scoring Definitions for Ease of Monitoring.

Score	Ease of Monitoring
0	Not possible to monitor
2	Inspection using NDT
4	Borescope testing
6	Detailed hands-on inspection
8	Visual inspection using lift
10	Visual inspection from ground

Table 5.18. Ease of Monitoring Rating of Retrofit Solutions for Double-Column Bents.

No.	Retrofit Solution	Ease of Monitoring	Score
1	Prestressed high-strength threadbar	Borescope testing	4
2a	Steel hanger bracket	Visual inspection using a lift	8
2b	Steel hanger bracket + End-region stiffener	Borescope testing	4
3	End-region stiffener	Visual inspection using a lift	8
4	Clamped cross threadbar	Borescope testing	4
5	Grouted cross threadbar	Inspection using NDT	2
6a	Upper seat brackets	Visual inspection using a lift	8
6b	Upper seat brackets + End-region stiffener	Borescope testing	4
7a	Threadbar hanger with steel bracket	Borescope testing	4
7b	Threadbar hanger with steel bracket + End-region stiffener	Borescope testing	4
8	Clamped threadbar with channel	Borescope testing	4
9	Grouted threadbar anchored with channel	Inspection using NDT	2
10	Anchored FRP wrap	Detailed hands-on inspection	6
11a	Concrete infill with prestressing threadbar	Inspection using NDT	2
11b	Concrete infill with prestressing threadbar + End-region stiffener	Inspection using NDT	2
12	Concrete infill with hanger threadbar	Inspection using NDT	2
13	Concrete masonry piers	Visual inspection from ground	10
14	Load-balancing PT	Visual inspection using a lift	8
15	Concrete infill with FRP anchored by FRP anchors	Inspection using NDT	2
16	Concrete infill with partial-depth FRP anchored by steel waling	Borescope testing	4
17	Concrete infill with full-depth FRP anchored by steel waling	Inspection using NDT	2
18	Large bearing pad	Visual inspection using a lift	8

Table 5.19. Ease of Monitoring Rating of Single-Column Bents.

No.	Retrofit Solution	Ease of Monitoring	Score
3	End-region stiffener	Visual inspection using a lift	8
8	Clamped threadbar with channel	Borescope testing	4
10	Anchored FRP wrap	Detailed hands-on inspection	6
14	Load-balancing PT	Visual inspection using a lift	8
15	Concrete infill with FRP anchored by FRP anchors	Inspection using NDT	2
16	Concrete infill with partial-depth FRP anchored by steel waling	Borescope testing	4
17	Concrete infill with full-depth FRP anchored by steel waling	Inspection using NDT	2
18	Large bearing pad	Visual inspection using a lift	8

5.4 Unweighted Score

In order to provide guidance on computing the individual scores (value of parameter a in the matrix), the scores for the different criteria are discussed in detail in the earlier sections. Each criterion has descriptions of how the retrofit method should be ranked (between 0 and 10). If a criterion has subcategories (e.g., corrosion and debonding under durability/longevity criterion), then the scores are scaled to get the maximum overall category score of 10. It is important to scale

the scores of each criterion to a fixed value in order not to create inconsistencies while applying the WSM. Scores for double-columns are presented in Table 5.20 and Figure 5.1. Scores for single-columns are presented in Table 5.21 and Figure 5.2.

Tables summarize the total scores from each criterion gathered from previous sections for double-column bents and single-column bents, respectively. The scores are a direct implementation of scoring definitions without any consideration of desired influence of each criterion relative to others.

Figures show comparative bar charts of each retrofit solution for each criterion for visual investigation of their relative scores for double-column bents and single-column bents, respectively. Using unweighted scores, the top three solutions are large bearing pad size (18), load-balancing PT (14), and end-region stiffener (3) for both double- and single-column bents.

5.5 Weight Factors and Ranking

The WSM provides an overall score for the considered alternatives (retrofit solutions) by summing individual scores under each criterion multiplied by the weight factor of the associated criterion. The weight factors must be selected such that the desired influence of each criterion is reflected relative to the others. The WSM provides flexibility for the bridge owners and DOTs for future modification of the decision analysis process by changing weight factors or adding new criteria to the list. The current weights considered for this project, listed in Table 5.22, were established based on the recommendations and priorities of TxDOT bridge engineers. This scenario uses a strength-driven approach by emphasizing the strength category with a 50 percent weight.

The scoring system using weights is straightforward for engineers to apply as well as easy to modify. If the bridge engineer wants to add a new retrofit solution or modify existing solutions, he or she can do so by simply inserting a new row to the individual scoring tables as defined in the previous sections. Similarly, a new criterion (such as aesthetics) can be added by preparing the scoring definitions and rating table for this new criterion. Then the weight factor table should be modified to incorporate the new criterion, with the sum of all factors equal to unity.

Table 5.20. Summary of Unweighted Scores for Rating Retrofit Solutions for Double-Column Bents.

No.	Retrofit Solution	Strength Increase	Total Cost	Constructability	Clearance	Durability/ Longevity	Ease of Monitoring	Total Score[1]
1	Prestressed high-strength threadbar	5.0	7.0	6.4	10.0	7.3	4.0	39.7
2a	Steel hanger bracket	6.7	9.0	7.4	10.0	2.0	8.0	43.1
2b	Steel hanger bracket + End-region stiffener	8.0	8.0	6.6	9.0	2.0	4.0	37.6
3	End-region stiffener	4.0	10.0	8.2	9.0	5.3	8.0	44.5
4	Clamped cross threadbar	5.3	7.0	6.0	3.0	8.7	4.0	34.0
5	Grouted cross threadbar	5.3	7.0	7.0	3.0	7.3	2.0	31.7
6a	Upper seat brackets	6.7	8.0	7.8	10.0	3.3	8.0	43.8
6b	Upper seat brackets + End-region stiffener	8.0	7.0	7.2	9.0	3.3	4.0	38.5
7a	Threadbar hanger with steel bracket	4.7	8.0	7.2	7.0	3.3	4.0	34.2
7b	Threadbar hanger with steel bracket + End-region stiffener	6.0	8.0	6.4	7.0	3.3	4.0	34.7
8	Clamped threadbar with channel	9.0	9.0	5.0	5.0	8.0	4.0	40.0
9	Grouted threadbar anchored with channel	5.3	8.0	6.4	5.0	6.7	2.0	33.4
10	Anchored FRP wrap	7.0	7.0	5.8	10.0	7.3	6.0	43.1
11a	Concrete infill with prestressing threadbar	7.3	8.0	6.8	10.0	9.3	2.0	43.5
11b	Concrete infill with prestressing threadbar + End-region stiffener	8.3	7.0	6.4	9.0	7.3	2.0	40.1
12	Concrete infill with hanger threadbar	9.0	4.0	5.6	6.0	9.3	2.0	35.9
13	Concrete masonry piers	9.0	2.0	6.8	0.0	10.0	10.0	37.8
14	Load-balancing PT	10.0	8.0	6.2	9.0	7.3	8.0	48.5
15	Concrete infill with FRP anchored by FRP anchors	6.0	4.0	7.0	10.0	6.7	2.0	35.7
16	Concrete infill with partial-depth FRP anchored by steel waling	8.0	7.0	6.8	10.0	4.0	4.0	39.8
17	Concrete infill with full-depth FRP anchored by steel waling	9.0	7.0	7.0	10.0	4.0	2.0	39.0
18	Large bearing pad	6.7	10.0	8.0	10.0	10.0	8.0	52.7

[1] Red indicates the top three scores

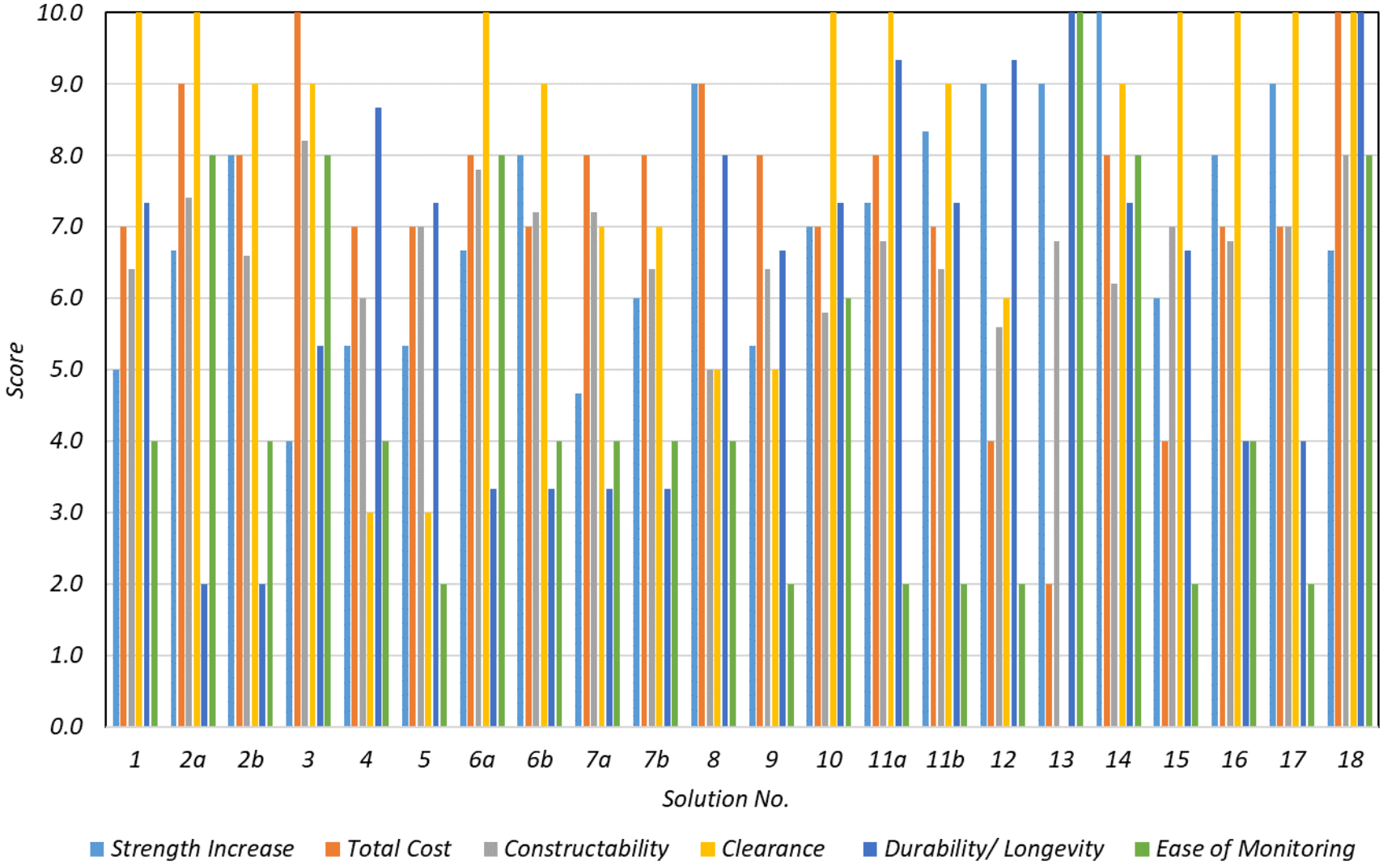

Figure 5.1. Comparison of the Criteria Scores of Retrofit Solutions for Double-Column Bents.

Table 5.21. Summary of Unweighted Scores for Rating Retrofit Solutions for Single-Column Bents.

No.	Retrofit Solution	Strength Increase	Total Cost	Constructability	Clearance	Durability/ Longevity	Ease of Monitoring	Total Score[1]
3	End-region stiffener	7.0	10.0	8.6	9.0	5.3	8.0	47.9
8	Clamped threadbar with channel	9.0	10.0	6.6	5.0	8.0	4.0	42.6
10	Anchored FRP wrap	7.0	9.0	6.6	10.0	7.3	6.0	45.9
14	Load-balancing PT	10.0	9.0	6.4	9.0	7.3	8.0	49.7
15	Concrete infill with FRP anchored by FRP anchors	4.5	6.0	7.0	10.0	6.7	2.0	36.2
16	Concrete infill with partial-depth FRP anchored by steel waling	6.5	7.0	6.8	10.0	4.0	4.0	38.3
17	Concrete infill with full-depth FRP anchored by steel waling	9.0	7.0	7.0	10.0	4.0	2.0	39.0
18	Large bearing pad	6.3	10.0	6.0	10.0	10.0	8.0	52.7

[1] Red indicates top three scores

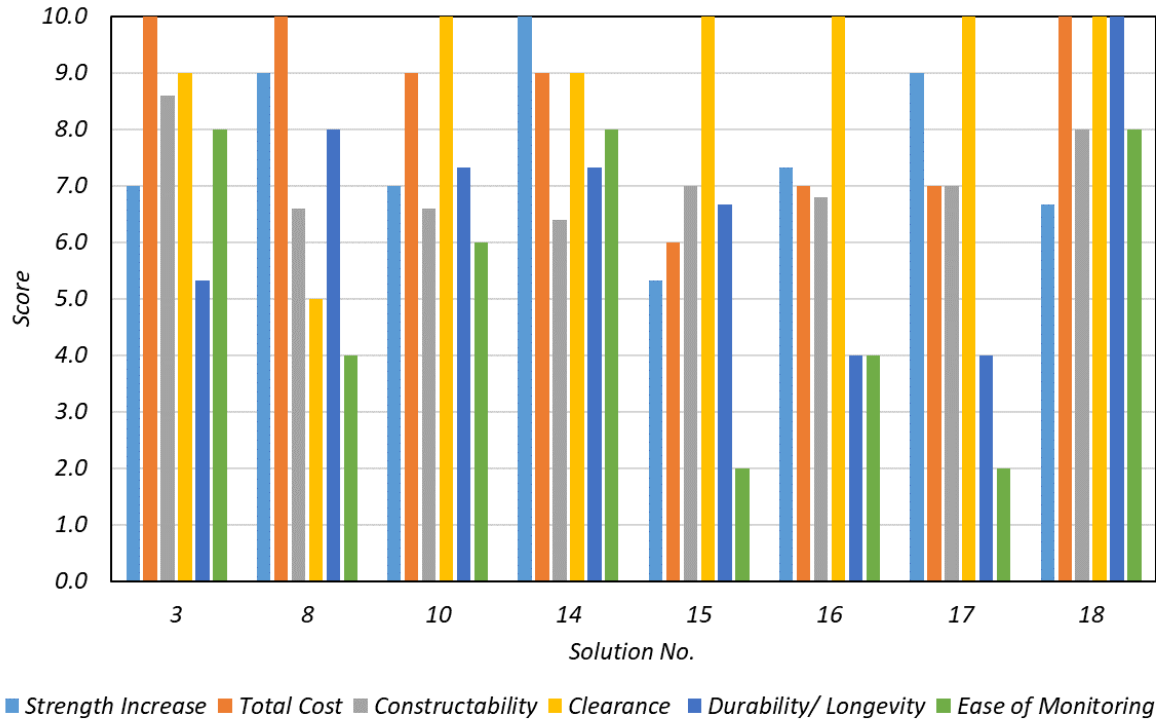

Figure 5.2. Comparison of the Criteria Scores of Retrofit Solutions for Single-Column Bents.

Table 5.22. Weight Factors for the Considered Criteria.

Criteria		Weight Factors	
C_1	Strength increase	w_1	50%
C_2	Total cost	w_2	15%
C_3	Constructability	w_3	10%
C_4	Clearance constraints	w_4	15%
C_5	Durability/longevity	w_5	5%
C_6	Ease of monitoring	w_6	5%

The decision matrix is a representation of ratings and rankings for all retrofit solutions, in which the overall scores for each retrofit solution are collected and summarized in a more concise and practical format. The decision matrix must rely on quantitative metrics that relate the rehabilitation needs of the structure and the performance of the proposed retrofit solution. Having quantifiable metrics enables the decision matrix to be repeated and general enough for the inclusion of new retrofit alternatives.

Systematic evaluation of retrofit options requires rating and ranking based on their ability to provide sufficient strength at a lower cost while creating minimum clearance and constructability issues. In order to create a systematic procedure for developing the decision matrix, scoring definitions are provided for each criterion in the previous section. Most of the definitions provide measurable benchmarks for the assigned scores such as in the case of strength and cost criteria. Although for most of the considered criteria it is possible to identify some measurable outcomes, it may not always be possible to establish a quantifiable benchmark such as in the case of durability criterion. In that case, relatively subjective evaluation categories are created based on engineering judgment.

Table 5.23 describes the implementation of the WSM for evaluating the retrofit alternatives in terms of the criteria considered, along with the weight factors. Weighted scores were calculated using weight factors specified in Table 5.22, and Table 5.24 and Table 5.25 present the weighted scores for each criterion and the total weighted score of each retrofit solution for double- and single-column bents, respectively. Figure 5.3 and Figure 5.4 illustrate a comparative bar chart for the total weighted scores of each criterion for double- and single-column bents, respectively.

Table 5.23. Decision Matrix for the Evaluation of Retrofit Solutions.

			Criteria						Score
			C_1, Strength Increase	**C_2, Total Cost**	**C_3, Constructability**	**C_4, Clearance**	**C_5, Durability/ Longevity**	**C_6, Ease of Monitoring**	
Weight Factor:			w_1	w_2	w_3	w_4	w_5	w_6	
Retrofit Alternatives	1	Prestressed high-strength threadbar	$a_{1,1}$	$a_{1,2}$	$a_{1,3}$	$a_{1,4}$	$a_{1,5}$	$a_{1,6}$	A_1
	2	Steel hanger bracket	$a_{2,1}$	$a_{2,2}$	$a_{2,3}$	$a_{2,4}$	$a_{2,5}$	$a_{2,6}$	A_2
	3	End-region stiffener	$a_{3,1}$	$a_{3,2}$	$a_{3,3}$	$a_{3,4}$	$a_{3,5}$	$a_{3,6}$	A_3
	4	Clamped cross threadbar	$a_{4,1}$	$a_{4,2}$	$a_{4,3}$	$a_{4,4}$	$a_{4,5}$	$a_{4,6}$	A_4
	5	Grouted cross threadbar	$a_{5,1}$	$a_{5,2}$	$a_{5,3}$	$a_{5,4}$	$a_{5,5}$	$a_{5,6}$	A_5
	6	Upper seat brackets	$a_{6,1}$	$a_{6,2}$	$a_{6,3}$	$a_{6,4}$	$a_{6,5}$	$a_{6,6}$	A_6
	7	Threadbar hanger with steel bracket	$a_{7,1}$	$a_{7,2}$	$a_{7,3}$	$a_{7,4}$	$a_{7,5}$	$a_{7,6}$	A_7
	8	Clamped threadbar with channel	$a_{8,1}$	$a_{8,2}$	$a_{8,3}$	$a_{8,4}$	$a_{8,5}$	$a_{8,6}$	A_8
	9	Grouted threadbar anchored with channel	$a_{9,1}$	$a_{9,2}$	$a_{9,3}$	$a_{9,4}$	$a_{9,5}$	$a_{9,6}$	A_9
	10	Anchored FRP wrap	$a_{10,1}$	$a_{10,2}$	$a_{10,3}$	$a_{10,4}$	$a_{10,5}$	$a_{10,6}$	A_{10}
	11	Concrete infill with prestressing threadbar	$a_{11,1}$	$a_{11,2}$	$a_{11,3}$	$a_{11,4}$	$a_{11,5}$	$a_{11,6}$	A_{11}
	12	Concrete infill with hanger threadbar	$a_{12,1}$	$a_{12,2}$	$a_{12,3}$	$a_{12,4}$	$a_{12,5}$	$a_{12,6}$	A_{12}
	13	Concrete masonry piers	$a_{13,1}$	$a_{13,2}$	$a_{13,3}$	$a_{13,4}$	$a_{13,5}$	$a_{13,6}$	A_{13}
	14	Load-balancing PT	$a_{14,1}$	$a_{14,2}$	$a_{14,3}$	$a_{14,4}$	$a_{14,5}$	$a_{14,6}$	A_{14}
	15	Concrete infill with FRP anchored by FRP anchors	$a_{15,1}$	$a_{15,2}$	$a_{15,3}$	$a_{15,4}$	$a_{15,5}$	$a_{15,6}$	A_{15}
	16	Concrete infill with partial-depth FRP anchored by steel waling	$a_{16,1}$	$a_{16,2}$	$a_{16,3}$	$a_{16,4}$	$a_{16,5}$	$a_{16,6}$	A_{16}
	17	Concrete infill with full-depth FRP anchored by steel waling	$a_{17,1}$	$a_{17,2}$	$a_{17,3}$	$a_{17,4}$	$a_{17,5}$	$a_{17,6}$	A_{17}
	18	Large bearing pad	$a_{18,1}$	$a_{18,2}$	$a_{18,3}$	$a_{18,4}$	$a_{18,5}$	$a_{18,6}$	A_{18}

Table 5.24. Weighted Total Scores of Retrofit Solutions for Double-Column Bents.

No	Retrofit Solution	Strength Increase	Total Cost	Constructability	Clearance	Durability/ Longevity	Ease of Monitoring	Total Score
	Weight Factors:	50%	15%	10%	15%	5%	5%	
1	Prestressed high-strength threadbar	2.5	1.1	0.6	1.5	0.4	0.2	6.3
2a	Steel hanger bracket	3.3	1.4	0.7	1.5	0.1	0.4	7.4
2b	Steel hanger bracket + End-region stiffener	4.0	1.2	0.7	1.4	0.1	0.2	7.5
3	End-region stiffener	2.0	1.5	0.8	1.4	0.3	0.4	6.3
4	Clamped cross threadbar	2.7	1.1	0.6	0.5	0.4	0.2	5.4
5	Grouted cross threadbar	2.7	1.1	0.7	0.5	0.4	0.1	5.3
6a	Upper seat brackets	3.3	1.2	0.8	1.5	0.2	0.4	7.4
6b	Upper seat brackets + End-region stiffener	4.0	1.1	0.7	1.4	0.2	0.2	7.5
7a	Threadbar hanger with steel bracket	2.3	1.2	0.7	1.1	0.2	0.2	5.7
7b	Threadbar hanger with steel bracket + End-region stiffener	3.0	1.2	0.6	1.1	0.2	0.2	6.3
8	Clamped threadbar with channel	4.5	1.4	0.5	0.8	0.4	0.2	7.7
9	Grouted threadbar anchored with channel	2.7	1.2	0.6	0.8	0.3	0.1	5.7
10	Anchored FRP wrap	3.5	1.1	0.6	1.5	0.4	0.3	7.3
11a	Concrete infill with prestressing threadbar	3.7	1.2	0.7	1.5	0.5	0.1	7.6
11b	Concrete infill with prestressing threadbar + End-region stiffener	4.2	1.1	0.6	1.4	0.4	0.1	7.7
12	Concrete infill with hanger threadbar	4.5	0.6	0.6	0.9	0.5	0.1	7.1
13	Concrete masonry piers	4.5	0.3	0.7	0.0	0.5	0.5	6.5
14	Load-balancing PT	5.0	1.2	0.6	1.4	0.4	0.4	8.9
15	Concrete infill with FRP anchored by FRP anchors	3.0	0.6	0.7	1.5	0.3	0.1	6.2
16	Concrete infill with partial-depth FRP anchored by steel waling	4.0	1.1	0.7	1.5	0.2	0.2	7.6
17	Concrete infill with full-depth FRP anchored by steel waling	4.5	1.1	0.7	1.5	0.2	0.1	8.1
18	Large bearing pad	3.3	1.5	0.8	1.5	0.5	0.4	8.0

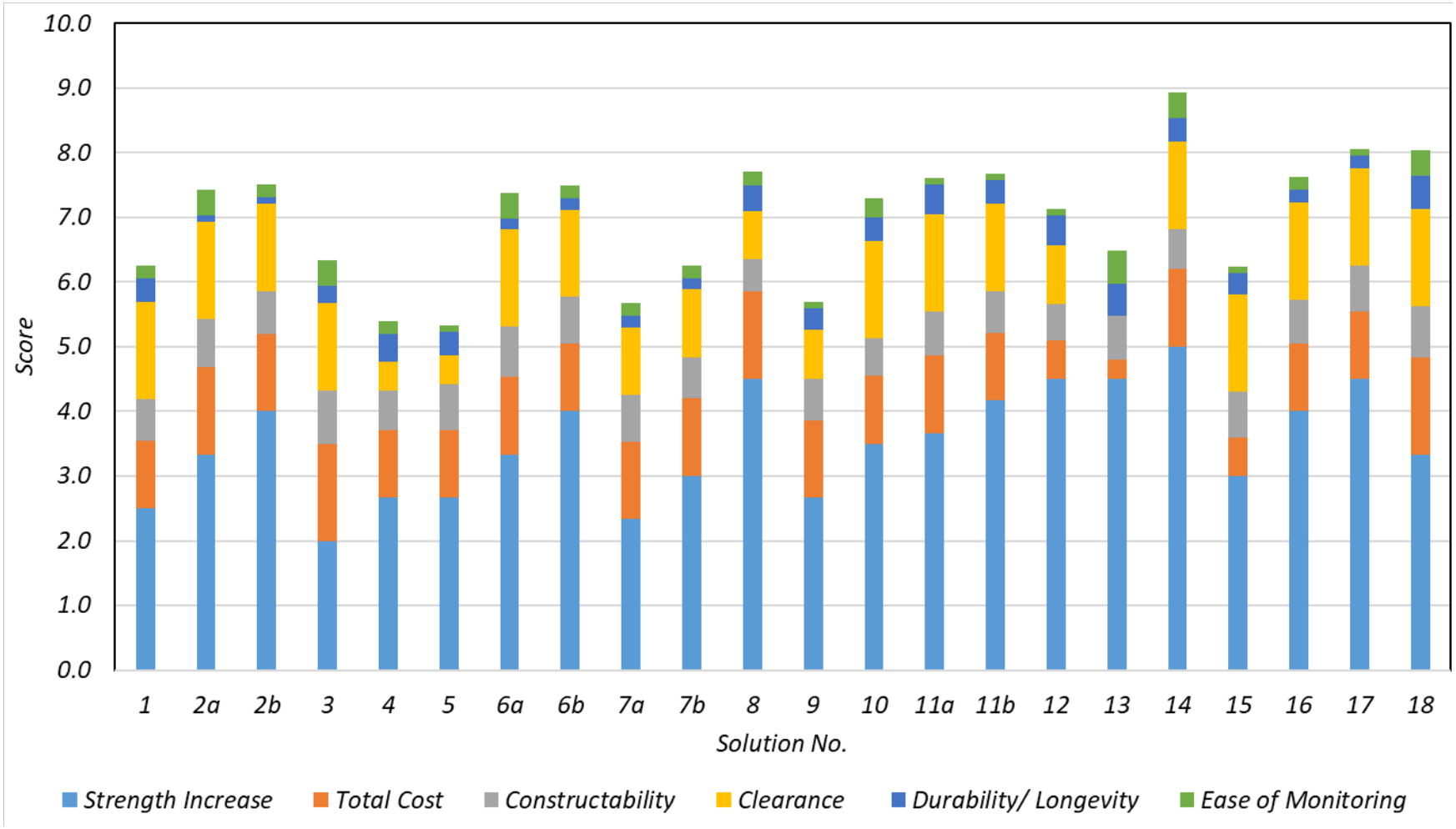

Figure 5.3. Total Weighted Scores of Retrofit Solutions for Double-Column Bents.

Table 5.25. Decision Matrix of Retrofit Solutions for Single-Column Bents.

No	Retrofit Solution	Strength Increase	Total Cost	Construct-ability	Clearance	Durability/ Longevity	Ease of Monitoring	Total Score
	Weight Factors:	50%	15%	10%	15%	5%	5%	
3	End-region stiffener	3.5	1.5	0.9	1.4	0.3	0.4	7.9
8	Clamped threadbar with channel	4.5	1.5	0.7	0.8	0.4	0.2	8.0
10	Anchored FRP wrap	3.5	1.4	0.7	1.5	0.4	0.3	7.7
14	Load-balancing PT	5.0	1.4	0.6	1.4	0.4	0.4	9.1
15	Concrete infill with FRP anchored by FRP anchors	2.7	0.9	0.7	1.5	0.3	0.1	6.2
16	Concrete infill with partial-depth FRP anchored by steel waling	3.7	1.1	0.7	1.5	0.2	0.2	7.3
17	Concrete infill with full-depth FRP anchored by steel waling	4.5	1.1	0.7	1.5	0.2	0.1	8.1
18	Large bearing pad	3.3	1.5	0.8	1.5	0.5	0.4	8.0

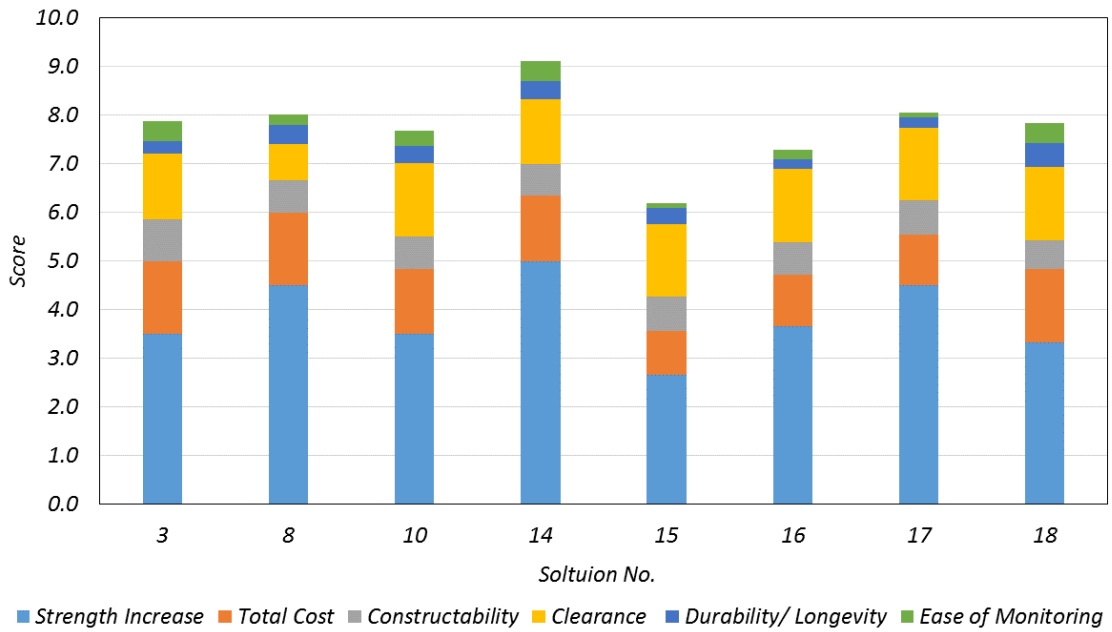

Figure 5.4. Total Weighted Scores of Retrofit Solutions for Single-Column Bents.

Table 5.26 and Table 5.27 list the final ranking of the solutions based on the weighted scores. The top three solutions for double-column bents are load-balancing PT (14), concrete infill with full-depth FRP anchored by steel waling (17), and large bearing pad (18). For single-column bents, the top two solutions are the same as for double-column bents, while the third solution is clamped threadbar with channel (8), which is ranked fourth for double-column bents. The fifth-ranked solution for single-column bent is end region stiffener (3) which is included in Solution 11b (concrete infill with prestressing threadbar +end region stiffener) which is ranked at fifth for double-column bents.

Table 5.26. Ranking of Proposed Retrofit Solutions for Double-Column Bents

No.	Retrofit Solution	Total Score
14	Load-balancing PT	8.9
17	Concrete infill with full-depth FRP anchored by steel waling	8.1
18	Large bearing pad	8.0
8	Clamped threadbar with channel	7.7
11b	Concrete infill with prestressing threadbar + End-region stiffener	7.7
16	Concrete infill with partial-depth FRP anchored by steel waling	7.6
11a	Concrete infill with prestressing threadbar	7.6
2b	Steel hanger bracket + End-region stiffener	7.5
6b	Upper seat brackets + End-region stiffener	7.5
2a	Steel hanger bracket	7.4
6a	Upper seat brackets	7.4
10	Anchored FRP wrap	7.3
12	Concrete infill with hanger threadbar	7.1
13	Concrete masonry piers	6.5
3	End-region stiffener	6.3
1	Prestressed high-strength threadbar	6.3
7b	Threadbar hanger with steel bracket + End-region stiffener	6.3
15	Concrete infill with FRP anchored by FRP anchors	6.2
9	Grouted threadbar anchored with channel	5.7
7a	Threadbar hanger with steel bracket	5.7
4	Clamped cross threadbar	5.4
5	Grouted cross threadbar	5.3

Table 5.27. Ranking of Proposed Retrofit Solutions for Single-Column Bents.

No.	Retrofit Solution	Total Score
14	Load-balancing PT	9.1
17	Concrete infill with FRP anchored by steel waling (w/o diaphragm)	8.1
8	Clamped threadbar with channel	8.0
18	Large bearing pad	8.0
3	End-region stiffener	7.9
10	Anchored FRP wrap	7.7
16	Concrete infill with FRP anchored by steel waling (w/ diaphragm)	7.3
15	Concrete infill with FRP anchored by FRP anchors	6.2

5.6 Closing Remarks

Chapter 4 described 18 retrofit solutions designed for the inverted-T bents. Each proposed solution either improved capacity by directly strengthening the ledges and hanger capacity or by providing alternate load paths.

For deciding the most viable retrofit solution, the objective of the task described in this chapter was to further assess the proposed retrofit solutions in terms of strength increase, cost, constructability, clearance constraints, durability/longevity, and ease of monitoring. A simple and popular multi-criteria decision analysis tool, the WSM, was used to evaluate and rank the retrofit solutions based on the above listed criteria by including their relative weights. The weights provide engineers the ability to control and represent the desired influence of each criterion. All 18 retrofit solutions were rated based on the six considered criteria, and the total scores were calculated by summing the weighted scores under each criterion. Finally, the total scores were ranked from most viable to least viable for both double-column and single-column bents. Table 5.28 summarizes the seven top-ranking retrofit solutions for strengthening double-column bents, and Table 5.29 lists the ranking of retrofit solutions for single-column bents.

Based on the ranking for both double- and single-column bents, Solutions 14, 17, 18, 8, 3, and 16 have been selected for experimental testing to investigate their ability to strengthen the capacity of the inverted-T bent cap. Since it is hard to mimic diaphragms in the lab specimens for the experimental test, Solution 11 was not chosen, but Solution 3 was selected since it is highly ranked for single-column bents. In addition, Solution 3 is also included in Solution 11b, which is highly ranked for double-column bents.

Table 5.28. Top-Ranking Retrofit Solutions for Double-Column Bents.

No.	Retrofit Solution	Total Score
14	Load-balancing PT	8.9
17	Concrete infill with full-depth FRP anchored by steel waling	8.1
18	Large bearing pad	8.0
8	Clamped threadbar with channel	7.7
11b	Concrete infill with prestressing threadbar + End-region stiffener	7.7
16	Concrete infill with partial-depth FRP anchored by steel waling	7.6
11a	Concrete infill with prestressing threadbar	7.6

Table 5.29. Top-Ranking Retrofit Solutions for Single-Column Bents.

No.	Retrofit Solution	Total Score
14	Load-balancing PT	9.1
17	Concrete infill with FRP anchored by steel waling (w/o diaphragm)	8.1
8	Clamped threadbar with channel	8.0
18	Large bearing pad	8.0
3	End-region stiffener	7.9

CHAPTER 6. DISCUSSION AND CLOSURE

6.1 Summary

Inverted-T bent caps are widely used throughout Texas to overcome geometric constraints and to improve aesthetical appearance. Traffic volume increases and design provisions have changed over the decades, and many in-service inverted-T bent caps are deficient for future needs. Replacing a deficient bent cap is not always practical due to cost, interruption to traffic, and the acceptable condition of other parts of the structure. Therefore, strengthening solutions for in-service bent caps are needed.

To facilitate practical and impactful results in developing strengthening solutions for inverted-T bent caps, two field evaluations were conducted on in-service inverted-T bent caps of IH 35 and US 290. From the field evaluations, conditions of in-service bent caps were provided, and the major crack types of in-service inverted-T bent caps were observed, including the following:

- Crack initiates at the ledge-web interface and extends in the diagonal direction but continues in the vertical direction after mid-height of the ledge. The crack extends along the width of ledge-web interface.
- Crack begins at the ledge-web interface and extends slightly downward, but it is primarily horizontal. The crack extends approximately 1 ft inward toward the centerline of the cap.

To address the strength deficiencies and the observed in-service damage for the design of inverted-T strengthening solutions, the IH 35 bent caps in Austin, Texas, were evaluated in this research. Structural analysis for the typical double- and single-column bents of the IH 35 bent caps was conducted based on AASHTO LRFD (2014) and TxDOT Bridge Design Manual (2015), which specify five critical failure modes of the ledge beam section: ledge shear friction, ledge flexure, hanger, punching shear, and bearing. The double-column bent was found to be deficient in ledge flexure, hanger, and punching shear with lane increment, while the single-column bent was found to have only hanger deficiency. Thus, 18 potential retrofit solutions were proposed to strengthen the inverted-T bent caps:

- Prestressed High-Strength Threadbar.
- Steel Hanger Bracket.
- End-Region Stiffener.

- Clamped Cross Threadbar.
- Grouted Cross Threadbar.
- Upper Seat Bracket.
- Threadbar Hanger with Steel Bracket.
- Clamped Threadbar with Channel.
- Grouted Threadbar Anchored with Channel.
- Anchored FRP Wrap.
- Concrete Infill with Prestressing Threadbar.
- Concrete Infill with Hanger Threadbar.
- Concrete Masonry Pier.
- Load-Balancing Post-Tensioning.
- Concrete Infill with FRP Anchored by FRP Anchors.
- Concrete Infill with Partial-Depth FRP Anchored by Steel Waling.
- Concrete Infill with Full-Depth FRP Anchored by Steel Waling.
- Large Bearing Pad.

Each solution was designed to address the deficiencies of double-column bents since double-column bents have larger deficiencies than single-column bents.

Proposed solutions were evaluated in terms of six criteria: strength increase, total cost, constructability, clearance constraints, durability, and ease of monitoring. Using a weighted sum model with specified weight factors, the retrofit solutions were rated and ranked to create a decision matrix to choose the most viable solutions. The top-ranked solutions for both double- and single-column bents are end-region stiffener (Solution 3), clamped threadbar with channel (Solution 8), load-balancing PT (Solution 14), concrete infill with partial- and full-depth FRP anchored by steel waling (Solutions 16 and 17), and large bearing pad (Solution 18).

6.2 Discussion and Research Needs

The solutions must be evaluated and further investigated based on an experimental program. Based on the analysis and evaluation of each retrofit solution, the following items are identified for the experimental test:

- The experimental test program should investigate serviceability and strength requirements.

- The experimental test should be able to assess the bent caps based on the regions (exterior or interior) and the critical failure modes (ledge flexure, punching shear, and hanger).
- The control specimens need to emphasize hanger, ledge flexure, and punching shear deficiencies to address the deficiencies of in-service bent caps.
- The specimens retrofitted by solutions should be tested without interrupting each solution to assess each solution under the same condition.

APPENDIX A. CAP 18 INPUT AND OUTPUT FILE

A.1 CAP 18 INPUT FILE

```
00001 ___County____   Highwy  Pro#  XXXX-XX-XXX  BRG                Comment
CAP18 Version 6.10 Inverted Tee Cap, Southbound Bent 13 Skew = 0.00
    1 E   (Spans 115'-115', Type AASHO 54 Girder @ 7.33', 7.5" Slab)
Table 1                                        18                        0.0
Table 2          100 5.000E-01        20    2   78    1    3    1.25     1.75
     1.50          3  1.2       1.0       0.85      0.65      0.65
Table 3(No.In)     3    7    2    9    4
  (Lane Left)      2   34   65
  (Lane Right)    34   65   98
  (Stringers)    5.7 20.4 35.1 49.8 64.5 79.2 93.9
  (Supports)      18   68
  (Mom CP)         6   18   20   35   50   64   68   79   94
  (Shear CP)      16   20   66   70
Table 4  (CAP)     2  100      3.786E+07             -1.55
(DL Span1, Bm1)    6    6                           -98.67              -9.83
(DL Span1, Bm2)   20   20                           -98.67              -9.83
(DL Span1, Bm3)   35   35                           -98.67              -9.83
(DL Span1, Bm4)   50   50                           -98.67              -9.83
(DL Span1, Bm5)   64   64                           -98.67              -9.83
(DL Span1, Bm6)   79   79                           -98.67              -9.83
(DL Span1, Bm7)   94   94                           -98.67              -9.83
(DL Span2, Bm1)    6    6                           -98.67              -9.83
(DL Span2, Bm2)   20   20                           -98.67              -9.83
(DL Span2, Bm3)   35   35                           -98.67              -9.83
(DL Span2, Bm4)   50   50                           -98.67              -9.83
(DL Span2, Bm5)   64   64                           -98.67              -9.83
(DL Span2, Bm6)   79   79                           -98.67              -9.83
(DL Span2, Bm7)   94   94                           -98.67              -9.83
(Dist. Lane Ld)    0   20                                      -6
(Conc. Lane Ld)    4    4                                  -21.3
(Conc. Lane Ld)   16   16                                  -21.3
```

A.2 CAP 18 OUTPUT FILE

```
JAN 12, 2016      TEXAS DEPARTMENT OF TRANSPORTATION (TxDOT)           PAGE
1
 CAP18                          BENT CAP ANALYSIS        Ver. 6.2   (Jul,
2011)


 00001 ___County____   Highwy  Pro#  XXXX-XX-XXX  BRG               Comment
 CAP18 Version 6.10 Inverted Tee Cap Design Example, Skew = 0.00

 PROB      1   (Spans 115'-115', Type TX54 Girder @ 7.33', 7.5" Slab, 2"
O'lay)


 ENGLISH SYSTEM UNITS

 TABLE 1. CONTROL DATA

      OPTION TO PRINT TABLE SRS (1=YES)                                    0

                                                  ENVELOPES    TABLE NUMBER
                                                  OF MAXIMUMS   2    3    4
      KEEP FROM PRECEDING PROBLEM (1=YES)               0       0    0    0
      CARDS INPUT THIS PROBLEM                                          18

      OPTION TO CLEAR ENVELOPES BEFORE LANE LOADINGS (1=YES)               0

      OPTION TO OMIT PRINT FOR TABLES (TABLE DESIGNATIONS IN PARENTHESES)
         -1(4A), -2(5) -3(4A,5), -4(4A,5,6), -5(4A,5,6,7):                 0

      SKEW ANGLE, DEGREES                                             0.000


 TABLE 2. CONSTANTS

      NUMBER OF INCREMENTS FOR SLAB AND CAP                             100
      INCREMENT LENGTH, FT                                            0.500
      NUMBER OF INCREMENTS FOR MOVABLE LOAD                              20
      START POSITION OF MOVABLE-LOAD STA ZERO                             2
      STOP POSITION OF MOVABLE-LOAD STA ZERO                             78
      NUMBER OF INCREMENTS BETWEEN EACH POSITION OF MOVABLE LOAD          1

      ANALYSIS OPTION (1=WORKING STRESS, 2=LOAD FACTOR, 3=BOTH)           3

      LOAD FACTOR FOR DEAD LOAD                                        1.25
      LOAD FACTOR FOR OVERLAY LOAD                                     1.50
      LOAD FACTOR FOR LIVE LOAD                                        1.75

      MAXIMUM NUMBER OF LANES TO BE LOADED SIMULTANEOUSLY                 3

      LIST OF LOAD COEFFICIENTS CORRESPONDING TO NUMBER OF LANES LOADED
            1              2              3              4              5
          1.200          1.000          0.850
```

PROB 1 (Spans 115'-115', Type TX54 Girder @ 7.33', 7.5" Slab, 2" O'lay)
(CONTINUED)

TABLE 3. LISTS OF STATIONS

	NUM OF LANES	NUM OF STRINGERS	NUM OF SUPPORTS	NUM MOM CONTR PTS	NUM SHEAR CONTR PTS
TOTAL	3	7	2	9	4

LANE LEFT	2	34	65						
LANE RIGHT	34	65	98						
STRINGERS	5.7	20.4	35.1	49.8	64.5	79.2	93.9		
SUPPORTS	18	68							
MOM CONTR	6	18	20	35	50	64	68	79	94
SHEAR CONTR	16	20	66	70					

SHEAR DESIGN CONTROL POINT IS TOO CLOSE TO A
TO A SUPPORT OR STRINGER

SHEAR DESIGN CONTROL POINT IS TOO CLOSE TO A
TO A SUPPORT OR STRINGER

TABLE 4. STIFFNESS AND LOAD DATA

FIXED-OR-MOVABLE			FIXED-POSITION DATA				MOVABLE-POSITION
STA FROM	STA TO	CONTD CAP IF=1	BENDING STIFFNESS (K-FT*FT)	SIDEWALK, SLAB LOADS (K)	STRINGER, CAP LOADS (K)	OVERLAY LOADS (K)	SLAB LOADS (K)
2	100	0	37860000.000	0.000	-1.550	0.000	0.000
6	6	0	0.000	0.000	-98.670	-9.830	0.000
20	20	0	0.000	0.000	-98.670	-9.830	0.000
35	35	0	0.000	0.000	-98.670	-9.830	0.000
50	50	0	0.000	0.000	-98.670	-9.830	0.000
64	64	0	0.000	0.000	-98.670	-9.830	0.000
79	79	0	0.000	0.000	-98.670	-9.830	0.000

94	94	0	0.000	0.000	-98.670	-9.830	0.000
6	6	0	0.000	0.000	-98.670	-9.830	0.000
20	20	0	0.000	0.000	-98.670	-9.830	0.000
35	35	0	0.000	0.000	-98.670	-9.830	0.000
50	50	0	0.000	0.000	-98.670	-9.830	0.000
64	64	0	0.000	0.000	-98.670	-9.830	0.000
79	79	0	0.000	0.000	-98.670	-9.830	0.000
94	94	0	0.000	0.000	-98.670	-9.830	0.000
0	20	0	0.000	0.000	0.000	0.000	-6.000
4	4	0	0.000	0.000	0.000	0.000	-21.300
16	16	0	0.000	0.000	0.000	0.000	-21.300

PROB 1 (Spans 115'-115', Type TX54 Girder @ 7.33', 7.5" Slab, 2" O'lay)
(CONTINUED)

MOMENT (FT-K)

AT STA	DEAD LD EFFECT	LANE ORDER	POSITIVE MAXIMUM	LOAD AT LANE STA	LANE ORDER	NEGATIVE MAXIMUM	LOAD AT LANE STA
94	-13.9						
		0	0.0		0	0.0	
		1	0.0		1	0.0	
		2	0.0		2	0.0	
		3	0.0		3	0.0	
		0*			0*		

PROB 1 (Spans 115'-115', Type TX54 Girder @ 7.33', 7.5" Slab, 2" O'lay)
(CONTINUED)

SHEAR (K)

AT STA	DEAD LD EFFECT	LANE ORDER	POSITIVE MAXIMUM	LOAD AT LANE	STA	LANE ORDER	NEGATIVE MAXIMUM	LOAD AT LANE	STA
16	-238.7								
		0	0.0			0	-93.5	1	2
		1	0.0			1	-93.5	1	2
		2	0.0			2	0.0		
		3	0.0			3	0.0		
		0*				0*			
70	480.5								
		0	162.3	3	78	0	0.0		
		1	162.3	3	78	1	0.0		
		2	0.1	2	45	2	0.0		
		3	0.0			3	0.0		
		0*				0*			

PROB 1 (Spans 115'-115', Type TX54 Girder @ 7.33', 7.5" Slab, 2" O'lay)
(CONTINUED)

REACTION (K)

AT STA	DEAD LD EFFECT	LANE ORDER	POSITIVE MAXIMUM	LOAD AT LANE	STA	LANE ORDER	NEGATIVE MAXIMUM	LOAD AT LANE	STA
18	607.2								
		0	182.1	1	2	0	-65.0	3	78
		1	182.1	1	2	1	-65.0	3	78
		2	78.0	2	34	2	0.0		
		3	0.0			3	0.0		
		2*				0*			
68	1063.7								
		0	227.6	3	78	0	-19.5	1	2
		1	227.6	3	78	1	-19.5	1	2
		2	120.3	2	45	2	0.0		
		3	19.5	1	14	3	0.0		
		2*				0*			

PROB 1 (Spans 115'-115', Type TX54 Girder @ 7.33', 7.5" Slab, 2" O'lay)
(CONTINUED)

TABLE 5. MULTI-LANE LOADING SUMMARY (LOAD FACTOR)
(*--CRITICAL NUMBER OF LANE LOADS)

MOMENT (FT-K)

AT STA	DEAD LD EFFECT	LANE ORDER	POSITIVE MAXIMUM	LOAD AT LANE	STA	LANE ORDER	NEGATIVE MAXIMUM	LOAD AT LANE	STA
6	-7.8								
		0	0.0			0	-24.5	1	2
		1	0.0			1	-24.5	1	2
		2	0.0			2	0.0		
		3	0.0			3	0.0		
		0*				0*			
18	-1781.0								
		0	0.0			0	-1006.1	1	2
		1	0.0			1	-1006.1	1	2
		2	0.0			2	0.0		
		3	0.0			3	0.0		
		0*				1*			
20	-1318.6								
		0	216.3	0	19	0	-851.0	1	2
		1	136.6	2	34	1	-851.0	1	2
		2	101.7	1	14	2	-113.8	3	78
		3	0.0			3	0.0		
		0*				1*			
35	-45.0								
		0	1266.7	0	29	0	-967.5	3	78
		1	1157.6	2	34	1	-967.5	3	78
		2	558.9	1	14	2	-563.5	1	2
		3	0.0			3	0.0		
		2*				2*			
50	-1060.7								
		0	1293.7	2	36	0	-1821.1	3	78
		1	1293.7	2	36	1	-1821.1	3	78
		2	307.3	1	14	2	-307.3	1	2
		3	0.0			3	0.0		
		2*				0*			
64	-4138.5								
		0	394.9	0	46	0	-2617.9	3	78
		1	392.1	2	45	1	-2617.9	3	78
		2	68.3	1	14	2	-68.3	1	2
		3	0.0			3	0.0		
		0*				0*			

```
68    -5605.1
                0        0.0                0    -2846.5      3   78
                1        0.0                1    -2846.5      3   78
                2        0.0                2       -1.0      2   45
                3        0.0                3        0.0
                0*                          0*

79    -2284.8
                0        0.0                0    -1284.6      3   78
                1        0.0                1    -1284.6      3   78
                2        0.0                2        0.0      2   45
                3        0.0                3        0.0
                0*                          0*
```

PROB 1 (Spans 115'-115', Type TX54 Girder @ 7.33', 7.5" Slab, 2" O'lay)
(CONTINUED)

MOMENT (FT-K)

AT STA	DEAD LD EFFECT	LANE ORDER	POSITIVE MAXIMUM	LOAD AT LANE STA	LANE ORDER	NEGATIVE MAXIMUM	LOAD AT LANE STA
94	-17.4						
		0	0.0		0	0.0	
		1	0.0		1	0.0	
		2	0.0		2	0.0	
		3	0.0		3	0.0	
		0*			0*		

PROB 1 (Spans 115'-115', Type TX54 Girder @ 7.33', 7.5" Slab, 2" O'lay)
(CONTINUED)

SHEAR (K)

AT STA	DEAD LD EFFECT	LANE ORDER	POSITIVE MAXIMUM	LOAD AT LANE	STA	LANE ORDER	NEGATIVE MAXIMUM	LOAD AT LANE	STA
16	-303.3								
		0	0.0			0	-163.6	1	2
		1	0.0			1	-163.6	1	2
		2	0.0			2	0.0		
		3	0.0			3	0.0		
		0*				0*			
70	610.5								
		0	284.0	3	78	0	0.0		
		1	284.0	3	78	1	0.0		
		2	0.2	2	45	2	0.0		
		3	0.0			3	0.0		
		0*				0*			

PROB 1 (Spans 115'-115', Type TX54 Girder @ 7.33', 7.5" Slab, 2" O'lay)
(CONTINUED)

REACTION (K)

AT STA	DEAD LD EFFECT	LANE ORDER	POSITIVE MAXIMUM	LOAD AT LANE	STA	LANE ORDER	NEGATIVE MAXIMUM	LOAD AT LANE	STA
18	771.5								
		0	318.7	1	2	0	-113.8	3	78
		1	318.7	1	2	1	-113.8	3	78
		2	136.6	2	34	2	0.0		
		3	0.0			3	0.0		
		2*				0*			
68	1351.5								
		0	398.4	3	78	0	-34.1	1	2
		1	398.4	3	78	1	-34.1	1	2
		2	210.6	2	45	2	0.0		
		3	34.1	1	14	3	0.0		
		2*				0*			

PROB 1 (Spans 115'-115', Type TX54 Girder @ 7.33', 7.5" Slab, 2" O'lay)
(CONTINUED)

TABLE 6. ENVELOPES OF MAXIMUM VALUES (LOAD FACTOR)

STA	DIST X (FT)	MAX + MOM (FT-K)	MAX - MOM (FT-K)	MAX + SHEAR (K)	MAX - SHEAR (K)
-1	-0.50	0.0	0.0	0.0	0.0
0	0.00	0.0	0.0	0.0	0.0
1	0.50	0.0	0.0	0.0	0.0
2	1.00	0.0	0.0	-0.5	-0.5
3	1.50	-0.5	-0.5	-1.9	-1.9
4	2.00	-1.9	-1.9	-3.9	-3.9
5	2.50	-4.4	-4.4	-5.8	-35.3
6	3.00	-7.8	-37.2	-145.8	-273.4
7	3.50	-150.2	-277.8	-285.9	-482.2
8	4.00	-293.6	-519.4	-287.8	-484.1
9	4.50	-438.0	-761.9	-289.7	-486.0
10	5.00	-583.3	-1005.4	-291.7	-488.0
11	5.50	-729.6	-1249.9	-293.6	-489.9
12	6.00	-876.9	-1495.3	-295.5	-491.9
13	6.50	-1025.2	-1741.8	-297.5	-493.8
14	7.00	-1174.4	-1989.1	-299.4	-495.7
15	7.50	-1324.6	-2237.5	-301.4	-497.7
16	8.00	-1475.8	-2486.8	-303.3	-499.6
17	8.50	-1627.9	-2737.1	-305.2	-501.5
18	9.00	-1781.0	-2988.4	251.3	10.3
19	9.50	-1420.7	-2663.6	828.6	325.9
20	10.00	-1059.0	-2339.8	636.5	185.8
21	10.50	-857.6	-2207.1	409.6	45.8
22	11.00	-670.7	-2155.7	372.9	43.9
23	11.50	-484.7	-2105.3	371.0	41.9
24	12.00	-299.7	-2055.9	369.0	40.0
25	12.50	-115.7	-2007.4	367.1	38.1
26	13.00	67.4	-1959.9	365.2	36.1
27	13.50	249.5	-1913.3	363.2	34.2
28	14.00	430.6	-1867.8	361.3	32.3
29	14.50	610.8	-1823.2	359.4	30.3
30	15.00	790.0	-1779.6	357.4	28.4
31	15.50	968.2	-1736.9	355.5	26.4
32	16.00	1145.5	-1695.2	353.5	24.5
33	16.50	1321.8	-1654.5	351.6	22.6
34	17.00	1497.1	-1614.7	349.7	20.6
35	17.50	1671.4	-1576.0	134.8	-119.4
36	18.00	1612.8	-1676.7	-45.8	-259.4
37	18.50	1542.8	-1778.4	-48.4	-261.4
38	19.00	1471.8	-1881.1	-50.3	-263.3
39	19.50	1399.9	-1984.8	-52.2	-265.2
40	20.00	1326.9	-2089.4	-54.2	-267.2
41	20.50	1253.1	-2195.0	-56.1	-269.1
42	21.00	1178.2	-2301.6	-58.1	-271.0

43	21.50	1102.4	-2409.2	-60.0	-273.0
44	22.00	1025.6	-2517.7	-61.9	-274.9
45	22.50	947.8	-2627.2	-63.9	-276.9
46	23.00	869.1	-2737.6	-65.8	-278.8
47	23.50	789.4	-2849.1	-67.7	-280.7
48	24.00	708.7	-2961.4	-69.7	-282.7

PROB 1 (Spans 115'-115', Type TX54 Girder @ 7.33', 7.5" Slab, 2" O'lay)
(CONTINUED)

TABLE 6. ENVELOPES OF MAXIMUM VALUES (LOAD FACTOR)

STA	DIST X (FT)	MAX + MOM (FT-K)	MAX - MOM (FT-K)	MAX + SHEAR (K)	MAX - SHEAR (K)
49	24.50	633.0	-3103.3	-90.9	-284.6
50	25.00	540.4	-3246.0	-247.1	-436.3
51	25.50	239.7	-3527.9	-387.1	-641.7
52	26.00	-61.8	-3810.7	-389.0	-643.6
53	26.50	-364.4	-4094.5	-391.0	-645.5
54	27.00	-667.9	-4379.2	-392.9	-647.5
55	27.50	-972.4	-4664.9	-394.8	-649.4
56	28.00	-1277.8	-4951.6	-396.8	-651.3
57	28.50	-1584.3	-5239.2	-398.7	-653.3
58	29.00	-1891.6	-5527.9	-400.6	-655.2
59	29.50	-2200.0	-5817.5	-402.6	-657.2
60	30.00	-2508.5	-6108.0	-404.5	-659.1
61	30.50	-2805.7	-6399.5	-406.5	-661.0
62	31.00	-3096.5	-6692.0	-408.4	-663.0
63	31.50	-3381.9	-6985.5	-410.3	-664.9
64	32.00	-3664.6	-7279.9	-550.4	-832.7
65	32.50	-4122.0	-7713.6	-690.4	-1028.3
66	33.00	-4617.4	-8148.4	-692.3	-1058.1
67	33.50	-5111.9	-8584.1	-694.2	-1060.0
68	34.00	-5605.1	-9020.9	43.4	-192.6
69	34.50	-5298.4	-8543.8	953.2	612.4
70	35.00	-4992.7	-8067.7	951.2	610.5
71	35.50	-4687.9	-7592.6	949.3	608.5
72	36.00	-4384.1	-7118.4	947.4	606.6
73	36.50	-4081.3	-6645.2	945.4	604.6
74	37.00	-3779.5	-6173.0	943.5	602.7
75	37.50	-3478.6	-5701.7	941.5	600.8
76	38.00	-3178.7	-5231.4	939.6	598.8
77	38.50	-2879.8	-4762.1	937.7	596.9
78	39.00	-2581.8	-4293.8	935.7	595.0
79	39.50	-2284.8	-3826.4	741.4	454.9
80	40.00	-2126.9	-3552.3	533.6	314.9
81	40.50	-1969.9	-3292.8	518.1	313.0
82	41.00	-1813.9	-3034.3	516.1	311.0
83	41.50	-1658.9	-2776.7	514.2	309.1
84	42.00	-1504.8	-2520.1	512.3	307.2
85	42.50	-1351.7	-2264.4	510.3	305.2
86	43.00	-1199.6	-2009.7	508.4	303.3
87	43.50	-1048.4	-1756.0	506.4	301.4
88	44.00	-898.2	-1503.3	504.5	299.4
89	44.50	-749.0	-1251.5	502.6	297.5
90	45.00	-600.8	-1000.7	500.6	295.5
91	45.50	-453.5	-750.9	498.7	293.6
92	46.00	-307.2	-502.0	496.8	291.7

PROB 1 (Spans 115'-115', Type TX54 Girder @ 7.33', 7.5" Slab, 2" O'lay)
(CONTINUED)

TABLE 6. ENVELOPES OF MAXIMUM VALUES (LOAD FACTOR)

STA	DIST X (FT)	MAX + MOM (FT-K)	MAX - MOM (FT-K)	MAX + SHEAR (K)	MAX - SHEAR (K)
93	46.50	-161.8	-254.1	484.6	289.7
94	47.00	-17.4	-17.4	242.0	149.7
95	47.50	-12.1	-12.1	9.7	9.7
96	48.00	-7.8	-7.8	7.8	7.8
97	48.50	-4.4	-4.4	5.8	5.8
98	49.00	-1.9	-1.9	3.9	3.9
99	49.50	-0.5	-0.5	1.9	1.9
100	50.00	0.0	0.0	0.5	0.5
101	50.50	0.0	0.0	0.0	0.0

PROB 1 (Spans 115'-115', Type TX54 Girder @ 7.33', 7.5" Slab, 2" O'lay)
(CONTINUED)

TABLE 7. MAXIMUM SUPPORT REACTIONS (LOAD FACTOR)

STA	DIST X (FT)	MAX + REACT (K)	MAX - REACT (K)
18	9.00	1226.8	635.0
68	34.00	1960.4	1310.5

APPENDIX B. BENT CAP ANALYSIS

B.1 INTRODUCTION

Loading demand and bent cap capacity calculation in this section is performed in accordance with AASHTO (2014) *LRFD Bridge Design Specifications*, 7th Ed., as prescribed by the TxDOT (2015) *Bridge Design Manual—LRFD*.

B.2 BENT CAP GEOMETRY

The bent cap is an in-service structure in Texas originally designed using the sectional method. The superstructure consists of seven AASHO-54 standard girders and a 7.5 in. thick concrete deck. The girders are connected transversely using intermediate and end diaphragms. The bent cap is 48 ft long and 7 ft tall. The stem of the cap is 57.25 in. tall, 30 in. wide, and the ledges protrude 16.5 in. from either side of the stem. The bottom width of the cap at the ledge is therefore 63 in. and the depth of the ledge is 20 in. The columns supporting the cap are 36 in. square. A standard AASHO-54 girder is supported at each of the seven bearing locations. The bent cap has a slight cross slope to accommodate the banked grade of the roadway supported by the bent. The slope is deemed insignificant, and a simplified, orthogonal layout serves as the basis for analysis.

B.3 LOAD DEMAND

B.3.1 Dead Load

■ Interior Girder

Rail weight:

$$Rail = \frac{RailWt \cdot \frac{Span}{2}}{3} = \frac{0.263 \times \frac{115}{2}}{3} = 5.04 \text{ kips/girder}$$

Girder weight:

$$Girder = GdrWt \cdot \frac{Span}{2} = 0.82 \times \frac{115}{2} = 47.15 \text{ kips/girder}$$

Tributary width:

$$TriWth_{\text{int}} = GdrSpa = 88 \text{ in.}$$

Slab weight:

(Increase slab weight by 10% to account for haunch and thickened slab ends)

$$Slab_{\text{int}} = w_c \cdot TriWth_{\text{int}} \cdot SlabThk \cdot \frac{Span}{2} \cdot 1.1$$

$$= 0.15 \times \frac{88}{12} \times \frac{7.5}{12} \times \frac{115}{2} \times 1.1 = 43.47 \text{ kips/girder}$$

Dead load for interior girder:

$$DLRn_{\text{int}} = Rail + Girder + Slab_{\text{int}} = 5.04 + 47.15 + 43.47 = 95.66 \text{ kips/girder}$$

■ Exterior Girder

Tributary width:

$$TriWth_{ext} = \frac{GdrSpa}{2} + C_{end} + SlabOvh = \frac{88}{2} + 22 + 12 = 78 \text{ in.}$$

Slab weight:

(Increase slab weight by 10% to account for haunch and thickened slab ends)

$$Slab_{ext} = w_c \cdot TriWth_{ext} \cdot SlabThk \cdot \frac{Span}{2} \cdot 1.1$$

$$= 0.15 \times \frac{78}{12} \times \frac{7.5}{12} \times \frac{115}{2} \times 1.1 = 38.54 \text{ kips/girder}$$

Dead load for exterior girder:

$$DLRn_{ext} = Rail + Girder + Slab_{ext}$$

$$= 5.04 + 47.15 + 38.54 = 90.73 \text{ kips/girder}$$

■ Bent Cap Weight

$$CapWt = w_c A_g = 0.15 \times \frac{3202.5}{12^2} = 3.34 \text{ kip/ft}$$

B.3.2 Live Load (for Web Shear)

■ Lane Live Load

The standard HL-93 live load model, which is a combination of the design truck and the design lane load is used in the live load calculations. According to the specifications, when the longer span is less than twice the length of the short span, the middle (32 kips) axle is placed over the interior support, the front (8 kips) axle is placed on the short span, and the rear (32 kips) axle is placed on the long span. Combine "Design Truck" and "Design Lane" loadings (AASHTO LRFD 3.6.1.3). Dynamic load allowance, IM, does not apply to "Design Lane" (AASHTO LRFD 3.6.1.2.4).

Span length (same span length):

$Span = 115$ ft

Impact factor:

$IM = 33$ %

Lane load:

$$Lane = 0.64\ klf \cdot \left(\frac{Span}{2} + \frac{Span}{2} \right) = 0.64 \times \left(\frac{115}{2} + \frac{115}{2} \right)$$

$$= 73.6 \text{ kips/lane}$$

Truck load:

$$Truck = 32\ kip + 32\ kip \cdot \left(\frac{Span - 14\ ft.}{Span} \right) + 8\ kip \cdot \left(\frac{Span - 14\ ft.}{Span} \right)$$

$$= 32 + 32 \times \left(\frac{115 - 14}{115} \right) + 8 \times \left(\frac{115 - 14}{115} \right) = 67.13 \text{ kips/lane}$$

Total live load:

$$LLRn = Lane + Truck \cdot (1 + IM) = 73.6 + 67.13 \times (1 + 0.33)$$

$$= 162.88 \text{ kips/lane}$$

■ Lateral Live Load

The live load is applied laterally along the bent cap by two 16 kip wheel loads increased by the dynamic load allowance factor, with the remainder of the live load distributed over a 10 ft design lane width (AASHTO LRFD 3.6.1.2.1). The live load applied to the slab is distributed to the beams, assuming the slab is hinged at each beam except the outside beam (BDM-LRFD, Ch. 4, Sect. 5, Structural Analysis, 2015).

Wheel loads:

$$P = 16\ kip \cdot (1 + IM) = 16 \times (1 + 0.33) = 26.28 \text{ kips}$$

Distributed loads:

$$WLL_{lateral} = \frac{LLRn - 2 \cdot P}{10\ ft.} = \frac{162.88 - 2 \times 26.28}{10} = 12.03 \text{ kip/ft}$$

B.3.3 CAP 18 Output

Multiple presence factors that account for the presence of multiple loaded lanes are provided as an input to the CAP 18 program, in accordance with Table 3.6.1.1.2-1 of AASHTO LRFD (2014). The self-weight of the bent cap and the live loads were applied to the joints of the model since CAP 18 does provide an option to input loads as distributed loads. The analysis of the bent caps considered only the Strength 1 limit state specified in Section 3.4.1 of AASHTO LRFD. CAP 18 was used to calculate the shear and moment demand of the inverted-T bent caps. Maximum shear and moment demand from the CAP 18 output file located in Appendix A are as follows:

■ Maximum Shear (controlled by web shear)

$V_u = 953.2$ kips

■ Maximum Positive Bending Moment

$M_{u\_pos} = 1671.4 \text{ kip} \cdot \text{ft}$

■ Maximum Negative Bending Moment

$M_{u\_neg} = -9020.9 \text{ kip} \cdot \text{ft}$

B.3.4 Girder Reactions

Girder loadings on bent cap ledge (i.e., girder reactions) are composed of dead load and live load, and calculated as follows:

■ Dead Load Reactions

Interior girder:

$DLRe_{int} = 95.66$ kips/girder

Exterior girder:

$DLRe_{ext} = 90.73$ kips/girder

■ Live Load Reactions

Use HL-93 Live Load. For the maximum reaction at interior bents, "Design Truck" will always govern "Design Tandem" for spans greater than 26 ft. For the maximum reaction, place the back axle over the support.

Lane load reaction:

$$LaneRe = 0.64\ klf \cdot \left(\frac{Span}{2}\right) = 0.64 \times \frac{115}{2} = 36.8\ \text{kips/lane}$$

Truck load reaction:

$$TruckRe = 32\ kip + 32\ kip \cdot \left(\frac{Span - 14\ ft.}{Span}\right) + 8\ kip \cdot \left(\frac{Span - 28\ ft.}{Span}\right)$$

$$= 32 + 32 \times \left(\frac{115-14}{115}\right) + 8 \times \left(\frac{115-28}{115}\right) = 66.16\ \text{kips/lane}$$

Live load reaction per lane:

$$LLRe_{Lane} = LaneRe + TruckRe \cdot (1 + IM)$$

$$= 36.8 + 66.16 \times (1 + 0.33) = 124.79\ \text{kips/lane}$$

The girder live load reactions are assumed to be the shear live load distribution factor multiplied by the live load reaction per lane. The shear live load distribution factor was calculated using the LRFD shear live load distribution factors" spreadsheet provided by TxDOT. Note that TxDOT requires the exterior girders to have a live load distribution factor equal to or greater than the interior girder. This is to accommodate a possible future bridge widening since widening the bridge would cause the exterior girders to become interior girders. However, this is a structural analysis of an existing structure rather than the design of a new structure; thus, the distribution factor for the exterior girder was calculated based on its own lane rule regardless of the requirement.

Shear live load distribution factor:

Interior girder:

$$fv_{\text{int}} = 0.767$$

Exterior girder:

$$fv_{ex} = 0.61$$

Total live load reactions:

Interior girder:

$$LLRe_{\text{int}} = LLRe_{lane} \cdot fv_{\text{int}} = 124.79 \times 0.767 = 95.71\ \text{kips/girder}$$

Exterior girder:

$$LLRe_{ext} = LLRe_{lane} \cdot fv_{ext} = 124.79 \times 0.61 = 76.12\ \text{kips/girder}$$

■ Total Girder Reactions

Interior girder:

$$V_{n\_int} = 1.25 \cdot DLRe_{\text{int}} + 1.75 LLRe_{\text{int}}$$

$$= 1.25 \times 95.66 + 1.75 \times 95.71 = 287 \text{ kips/girder}$$

Exterior girder:

$$V_{n\_ext} = 1.25 \cdot DLRe_{ext} + 1.75 LLRe_{ext}$$

$$= 1.25 \times 90.73 + 1.75 \times 76.12 = 246.6 \text{ kips/girder}$$

B.3.5 Torsional Load

As traffic moves across an inverted-T bent cap, the stringers on one side of the web will create a web torque that is opposite to what occurs when the stringers on the opposite side of the web are loaded by traffic. In the presence of significant torsion, flange forces on one side of the web may be significantly larger than forces on the opposite side of the web, and the passage of traffic tends to make such twisting an alternating phenomenon (Furlong and Mirza, 1974). The live load is positioned on the longer span in order to maximize the torsion loads on the bent cap.

Distance from the center line of bearing pad to the face of web:

$a_v = 7.5$ in.

Width of web:

$b_{stem} = 30$ in.

Lever arm:

$$LeverArm = a_v + \frac{b_{stem}}{2} = 7.5 + \frac{30}{2} = 22.5 \text{ in.}$$

Girder reactions for torsional loading model:

Span 1:

$$R_{u\_span1} = 1.25 \cdot DLRe_{\text{int}} = 1.25 \times 96.9 = 121.1 \text{ kips/girder}$$

Span 2:

$$R_{u\_span1} = 1.25 \cdot DLRe_{int} + 1.75 \cdot LLRe_{int}$$

$$= 1.25 \times 96.9 + 1.75 \times 95.71 = 288.6 \text{ kips/girder}$$

Maximum torsional load (occurs at Section B-B shown in Figure 3.18):

$$T_u = 2 \cdot \left| R_{u\_span1} - R_{u\_span2} \right| \cdot LeverArm$$

$$= 2 \times \left| 121.1 - 288.6 \right| \times 22.5 = 628.1 \text{ kip} \cdot \text{ft}$$

B.4 LOAD SUMMARY

B.4.1 Ledge Loadings

- Interior Girder

$V_{u\_int} = 287$ kips/girder

- Exterior Girder

$V_{u\_ext} = 247$ kips/girder

B.4.2 Cap Loadings

These loads are obtained from the CAP 18 output file located in Appendix A.

■ Positive Bending Moment

$M_{u\_pos} = 1671.4 \text{ kip} \cdot \text{ft}$

■ Negative Bending Moment

$M_{u\_neg} = -9020.9 \text{ kip} \cdot \text{ft}$

■ Maximum Torsion and Concurrent Shear and Moment (at Section B-B)

$T_u = 628.1 \text{ kip} \cdot \text{ft}$

$V_u = 953.2 \text{ kips}$ Concurrent shear

$M_u = -8067.7 \text{ kip} \cdot \text{ft}$ Concurrent moment

Note that the maximum torsion and maximum shear is concurrent in this case. If not, it is necessary to check the location of the maximum torsion with its concurrent shear and the location of the maximum shear with its concurrent torsion.

B.5 LOAD-CARRYING CAPACITY OF WEB COMPONENTS

Capacity evaluation of web component includes flexural, combined shear, and torsion strength. The load-carrying capacity of web components is calculated using conventional sectional methods.

B.5.1 Flexural Resistance

■ Minimum Design Moment

Factored flexural resistance, M_r, must not be less than 1.33 times the factored moment or 1.2 times the cracking moment.

Gross moment of inertia:

$I_g = 2.07 \times 10^6 \text{ in}^4$

Distance from bottom of cap to the center of gravity of the cap:

$y_{bar} = 35.7 \text{ in.}$

Distance from center of gravity to tension fiber:

$y_t = h_{cap} - y_{bar} = 84.75 - 35.7 = 49.05 \text{ in.}$

Section modulus for the extreme tension fiber:

$$S_t = \frac{I_g}{y_t} = \frac{2.07 \times 10^6}{35.7} = 4.23 \times 10^4 \text{ in}^3$$

Modulus of rupture (BDM-LRFD, Ch. 4, Sect. 5, Design Criteria):

$$f_r = 0.24 \cdot \sqrt{f'_{c(ksi)}} = 0.24 \times \sqrt{3.6} = 0.46 \text{ ksi}$$

Cracking moment (AASHTO LRFD Eq. 5.7.3.3.2-1):

$$M_{cr} = S_t \cdot f_r = 4.23 \times 10^4 \times 0.46 \times \frac{1}{12} = 1605.1 \text{ kip} \cdot \text{ft}$$

Minimum design moment is lesser of:

$M_f = 1.2 \cdot M_{cr} = 1.2 \times 1605.1 = 1926.1 \text{ kip} \cdot \text{ft}$ (Governs)

$M_f = 1.33 \cdot M_u = 1.33 \times 9020.9 = 11997.8 \text{ kip} \cdot \text{ft}$

■ Flexural Strength

Area of reinforcing bar in tension:

$A_s = 32.22 \text{ in}^2$

Distance from center of tension reinforcing bar to the extreme compression fiber:

$d_{neg} = 74.6 \text{ in.}$

Concrete strength:

$f_c^{'} = 3.6 \text{ ksi}$

Factor β_1:

$\beta_1 = 0.85$ (For concrete strength up to and including 4 ksi)

Depth of section under compression (AASHTO LRFD Eq. 5.7.3.1.2-4):

$$c = \frac{A_s f_y}{0.85 \cdot f_c^{'} \beta_1 b_{flange}} = \frac{32.22 \times 60}{0.85 \times 3.6 \times 0.85 \times 63} = 11.8 \text{ in.}$$

Depth of equivalent stress lock (AASHTO LRFD 5.7.2.2):

$a = c\beta_1 = 11.8 \times 0.85 = 10 \text{ in.}$

Nominal flexural strength (AASHTO LRFD Eq. 5.7.3.2.2-1):

$$M_n = A_s f_y \left(d_{neg} - \frac{a}{2} \right) = 32.22 \times 60 \times \left(74.6 - \frac{10}{2} \right) \times \frac{1}{12} = 11210.3 \text{ kip} \cdot \text{ft}$$

Reduction factor for flexural strength (AASHTO LRFD 5.5.4.2.1):

$\phi = 0.9$

Factored flexural strength:

$\phi M_n = 0.9 \times 11210.3 = 10089.3 \text{ kip} \cdot \text{ft}$

Check minimum design moment:

$\phi M_n = 10089.3 \text{ kip} \cdot \text{ft} > M_f = 1926.1 \text{ kip} \cdot \text{ft}$ O.K.

Check ultimate bending moment:

$\phi M_n = 10089.3 \text{ kip} \cdot \text{ft} > M_{u\_neg} = 9020.9 \text{ kip} \cdot \text{ft}$ O.K.

B.5.2 Combined Shear and Torsion Resistance

■ Web Shear

Effective depth from extreme compression fiber to the centroid of the tensile force in the tensile reinforcement:

$$d_e = \frac{A_{ps} f_{ps} d_p + A_s f_y d_{neg}}{A_{ps} f_{ps} + A_s f_y} = \frac{0 + A_s f_y d_{neg}}{0 + A_s f_y} = d_{neg} = 74.6 \text{ in.}$$

Effective shear depth d_v is the maximum value of:

$$d_v = \frac{M_n}{A_{ps} f_{ps} + A_s f_y} = \frac{11210.3 \times 12}{0 + 32.22 \times 60} = 69.6 \text{ in.}$$ (Governs)

$d_v = 0.9 \cdot d_e = 0.9 \times 74.6 = 67.1 \text{ in.}$

$d_v = 0.72 \cdot h_{cap} = 0.72 \times 84.75 = 61 \text{ in.}$

Recall cap shear and concurrent bending moment:

$V_u = 953.2$ kips

$M_u = -8067.7$ kip·ft

Net longitudinal tensile strain (AASHTO LRFD Eq. 5.8.3.4.2-4):

$$\varepsilon_s = \frac{\frac{|M_u|}{d_v} + 0.5 \cdot N_u + |V_u - V_p| - A_{ps} f_{ps}}{E_p A_{ps} + E_s A_s}$$

$$= \frac{\frac{|-8067.7 \times 12|}{69.6} + 0 + 953.2 - 0}{0 + 29000 \times 32.22} = 0.0025$$

Parameter β:

$$\beta = \frac{4.8}{1 + 750 \cdot \varepsilon_s} = \frac{4.8}{1 + 750 \times 0.0025} = 1.67$$

Angle of inclination of diagonal compressive stresses:

$\theta = 29 + 3500 \cdot \varepsilon_s = 29 + 3500 \times 0.0025 = 37.75$ degree

Concrete shear strength:

$$V_c = 0.0316 \beta \sqrt{f_c^{'}} b_{stem} d_v$$

$$= 0.0316 \times 1.67 \times \sqrt{3.6} \times 30 \times 69.6 = 207 \text{ kips}$$

Area of web shear reinforcement (two #5 double-leg stirrups):

$A_v = 0.31 \times 4 = 1.24$ in^2

Reinforcement steel shear strength:

$$V_s = \frac{A_v f_y d_v (\cot\theta + \cot\alpha) \sin\alpha}{s}$$

$$= \frac{1.24 \times 60 \times 69.6 \times (\cot 37.75 + 0) \times 1}{4.5} = 1486 \text{ kips}$$

Nominal web shear resistance is lesser of:

$V_n = V_c + V_s + V_p = 207 + 1486 + 0 = 1693$ kips (Governs)

$V_n = 0.25 f_c^{'} b_{stem} d_v + V_p = 0.25 \times 3.6 \times 30 \times 69.6 + 0 = 1878.8$ kips

Reduction factor for shear strength (AASHTO LRFD 5.5.4.2.1):

$\phi = 0.9$

Factored web shear strength,

$\phi V_n = 0.9 \times 1693 = 1524$ kips

Check ultimate web shear force,

$\phi V_n = 1524 \text{ kips} > V_u = 953.2 \text{ kips}$ O.K.

■ Torsion

Area of outer stirrup,

$A_t = 0.31$ in^2

Area inside the centerline of the exterior stirrup,

$$A_{oh} = d_{stem}\left(b_{stem} - 2cover\right) + \left(d_{ledge} - 2cover\right)\left(b_{flange} - 2cover\right)$$

$= 2488.75 \text{ in}^2$

Area enclosed by the shear flow path (AASHTO LRFD C5.8.2.1),

$A_o = 0.85A_{oh} = 0.85 \times 2488.75 = 2115.4 \text{ in}^2$

Nominal torsional resistance,

$$T_n = \frac{2A_oA_t f_y \cot\theta}{s} = \frac{2 \times 2115.4 \times 0.31 \times 60 \times \cot 37.75}{4.5} \times \frac{1}{12} = 1882 \text{ kip} \cdot \text{ft}$$

Reduction factor for shear strength (AASHTO LRFD 5.5.4.2.1),

$\phi = 0.9$

Factored torsional strength,

$\phi T_n = 0.9 \times 1882 = 1693.8 \text{ kip} \cdot \text{ft}$

Check ultimate torsion,

$\phi T_n = 1693.8 \text{ kip} \cdot \text{ft} > T_u = 628.1 \text{ kip} \cdot \text{ft}$ O.K.

B.6 LOAD CARRYING CAPACITY OF LEDGE AND HANGER

Load carrying capacity of ledge and hanger are evaluated in accordance with the provisions of Articles 5.13.2.5.2 through 5.13.2.5.5 of AASHTO LRFD (2014).

B.6.1 Ledge

The ledge of the inverted-T must be designed to resist the shear friction and flexure.

B.6.1.1 Shear Friction

■ Interior Girder

Interior ledge load:

$V_{u\_int} = 287 \text{ kips}$

Distribution width is lesser of

$b_{w,int} = W + 4a_v = 22 + 4 \times 7.5 = 51 \text{ in.}$ (Governs)

$b_{w,int} = S = 88 \text{ in.}$

- Required Reinforcement Area for Shear Friction is lesser of:

Shear resistance of concrete:

$V_n = 0.2 f_c' b_w d_e = 0.2 \times 3.6 \times 51 \times 17.5 = 642.6 \text{ kips}$

$V_n = 0.8 b_w d_e = 0.8 \times 51 \times 17.5 = 714 \text{ kips}$

Shear resistance of reinforcing steel:

$V_n = c' A_{cv} + \mu\left(A_{vf} f_y + P_c\right) = \mu A_{vf} f_y = 1.4 \times 7.8 \times 60 = 655.2 \text{ kips}$

where f_c' = specified concrete strength; b_w = distribution width for the shear friction; c = distance from the center of bearing pad to the end of the bent cap; W = width of bearing pad; S = girder spacing; a_v = distance from the center of bearing pad to face of the web of the bent cap; d_e = depth of the center of gravity of negative flexural reinforcements; A_{cv} = area of concrete considered to be engaged in interface shear transfer; A_{vf} = area of interface

shear reinforcement crossing the shear plane within the area A_{cv}; c' = cohesion factor specified in Article 5.8.4.3; μ = friction factor specified in Article 5.8.4.3; and P_c = permanent net compressive force normal to the shear plane.
Thus, interior ledge shear friction capacity is 642.6 kips

■ Exterior Girder
Interior ledge load:
$V_{u\_ext} = 247$ kips
Distribution width is lesser of:
$b_{w,ext} = W + 4a_v = 22 + 4 \times 7.5 = 51$ in.
$b_{w,ext} = c + S/2 = 22 + 88/2 = 66$ in.
$b_{w,ext} = c + (W + 4a_v)/2 = 22 + (21 + 4 \times 7.5)/2 = 47.5$ in. (Governs)
- Required Reinforcement Area for Shear Friction is lesser of:
Shear resistance of concrete:
$V_n = 0.2 f_c' b_w d_e = 0.2 \times 3.6 \times 47.5 \times 17.5 = 598.5$ kips
$V_n = 0.8 b_w d_e = 0.8 \times 47.5 \times 17.5 = 665$ kips
Shear resistance of reinforcing steel:
$V_n = c' A_{cv} + \mu\left(A_{vf} f_y + P_c\right) = \mu A_{vf} f_y = 1.4 \times 7.2 \times 60 = 604.8$ kips
Thus, interior ledge shear friction capacity is 598.5 kip.

B.6.1.2 Flexure

■ Interior girder
Concurrent bending moment:
$$M_{u\_int} = V_{u\_int} a_v + N_{u\_int}\left(h - d_e\right)$$
$$= 287 \times 7.5 + 57.4 \times \left(21.5 - 17.5\right) = 198.5 \text{ kip} \cdot \text{ft}$$
Distribution width is lesser of:
$b_{m,int} = W + 5a_f = 22 + 5 \times 10 = 71$ in. (Governs)
$b_{m,int} = S = 88$ in.
Nominal flexure strength of the ledge:
$$M_n = A_s f_y \left(d_e - \frac{a}{2}\right)$$
where depth of the equivalent stress block with axial tension of N_u:
$$a = \frac{\frac{N_u}{\phi} + A_s f_y}{0.85 f_c' b_{m,int}} = \frac{\frac{57.4}{\phi} + 2.4 \times 60}{0.85 \times 3.6 \times 71} = 0.956 \text{ in.}$$
$$M_n = A_s f_y \left(d_e - \frac{a}{2}\right) = 2.4 \times 60 \times \left(17.5 - \frac{0.956}{2}\right) = 204.3 \text{ kip} \cdot \text{ft}$$

■ Exterior girder
Concurrent bending moment:

$$M_{u\_ext} = V_{u\_ext} a_v + N_{u\_ext}\left(h - d_e\right)$$

$$= 247 \times 7.5 + 54 \times \left(21.5 - 17.5\right) = 170.8 \text{ kip} \cdot \text{ft}$$

Distribution width is lesser of:

$b_{m,ext} = W + 5a_f = 22 + 5 \times 10 = 71$ in.

$b_{m,ext} = c + (W + 5a_f)/2 = 21 + (22 + 5 \times 10)/2 = 57.5$ in. (Governs)

$b_{m,ext} = c + S/2 = 66$ in.

Nominal flexure strength of the ledge:

$$M_n = A_s f_y \left(d_e - \frac{a}{2}\right)$$

where depth of the equivalent stress block with axial tension of N_u:

$$a = \frac{\frac{N_u}{\phi} + A_s f_y}{0.85 f_c^{'} b_{m,ext}} = \frac{\frac{49.4}{\phi} + 2.4 \times 60}{0.85 \times 3.6 \times 57.5} = 1.1 \text{ in.}$$

$$M_n = A_s f_y \left(d_e - \frac{a}{2}\right) = 2.4 \times 60 \times \left(17.5 - \frac{1.1}{2}\right) = 203.2 \text{ kip} \cdot \text{ft}$$

B.6.2 Punching Shear

Length of bearing pad: $L = 8$ in.

Width of bearing pad: $W = 21$ in.

■ Interior girder

With modifications from BDM-LRFD, Ch. 4, Sect. 5, Design Criteria, the nominal punching shear resistance of interior girders is:

$$V_n = 0.125\sqrt{f_c^{'}}\left(W + 2L + 2d_f\right)d_f$$

$$= 0.125 \times \sqrt{3.6} \times \left(21 + 2 \times 8 + 2 \times 17\right) \times 17 = 286.3 \text{ kips}$$

■ Exterior girder

For exterior girders, to consider the limitation of the distribution width to the edge of the cap, TxDOT provides modified equations for the punching shear resistance of exterior girders. The nominal punching shear resistance of exterior girders is the lesser of:

$$V_n = 0.125\sqrt{f_c^{'}}\left(\frac{W}{2} + L + d_f + c\right)d_f$$

(Governs)

$$= 0.125\sqrt{3.6}\left(\frac{21}{2} + 8 + 17 + 22\right)17 = 231.8 \text{ kips}$$

$$V_n = 0.125\sqrt{f_c^{'}}\left(W + 2L + 2d_f\right)d_f$$

$$= 0.125\sqrt{3.6}\left(21 + 2 \times 8 + 2 \times 17\right)17 = 286.3 \text{ kips}$$

B.6.3 Bearing

The ledge of the bent cap should have bearing resistance as described in Article 5.7.5 of AASHTO LRFD (2014). The bearing capacity of the ledge can be obtained by:

$$V_n = 0.85 f'_c A_1 m$$

where A_1 = area under bearing device and m = modification factor, which is the lesser of 2 or:

$$m = \sqrt{\frac{A_2}{A_1}}$$

where $A_2 = (W + 2B)(L + 2B)$.

■ Interior girder

$$B = \min\left((b_{ledge} - a_v) - \frac{L}{2}, (a_v + \frac{b_{stem}}{2}) - \frac{L}{2}, 2d_{ledge}, \frac{S}{2} - \frac{W}{2} \right) = 5 \text{ in.}$$

Thus:

$$A_1 = W \times L = 168 \text{ in}^2$$

$$m = \min\left(2, \sqrt{\frac{A_2}{A_1} = \frac{558}{168}} = 1.8 \right) = 1.8$$

$$V_n = 0.85 f'_c A_1 m = 0.85 \times 3.6 \times 168 \times 1.8 = 936.9 \text{ kips}$$

■ Exterior girder

$$B = \min\left((b_{ledge} - a_v) - \frac{L}{2}, (a_v + \frac{b_{stem}}{2}) - \frac{L}{2}, 2d_{ledge}, \frac{S}{2} - \frac{W}{2}, c - \frac{W}{2} \right) = 5 \text{ in.}$$

Thus:

$$A_1 = W \times L = 168 \text{ in}^2$$

$$m = \min\left(2, \sqrt{\frac{A_2}{A_1} = \frac{558}{168}} = 1.8 \right) = 1.8$$

$$V_n = 0.85 f'_c A_1 m = 0.85 \times 3.6 \times 168 \times 1.8 = 936.9 \text{ kips}$$

B.6.4 Hanger

■ Interior Girder 1

<u>*Service I limit*</u>

Nominal hanger capacity at Service I limit is lesser of:

$$V_n = \frac{A_{hr}\left(\frac{2}{3} f_y\right)}{s}\left(W + 3a_v\right) = 174 \text{ kips} \qquad \text{(Governs)}$$

$$V_n = \frac{A_{hr}\left(\frac{2}{3} f_y\right)}{s} S = 352 \text{ kips}$$

<u>*Strength I limit*</u>

Nominal hanger capacity at Service I limit is lesser of:

$$V_n = \frac{A_{hr} f_y}{s} S = \frac{0.6 \times 60}{6} \times 88 = 528 \text{ kips}$$

$$V_n = 0.063\sqrt{f_c^{'}} b_f d_f + \frac{A_{hr} f_y}{s}(W + 2d_f)$$

(Governs)

$$= 0.063\sqrt{3.6} \times 63 \times 17 + \frac{0.6 \times 60}{6}(22 + 2 \times 17) = 458 \text{ kips}$$

Thus, interior hanger capacity at Service I limit and Strength I limit for single ledge is 174 kips and 229 kips, respectively.

■ Exterior Girder 1

Service I limit

Nominal hanger capacity at Service I limit is lesser of:

$$V_n = \frac{A_{hr}\left(\frac{2}{3} f_y\right)}{s}\left(\frac{(W + 3a_v)}{2} + c\right) = 175 \text{ kips}$$ (Governs)

$$V_n = \frac{A_{hr}\left(\frac{2}{3} f_y\right)}{s}\left(\frac{S}{2} + c\right) = 264 \text{ kips}$$

Strength I limit

Nominal hanger capacity at Service I limit is lesser of:

$$V_n = \frac{A_{hr} f_y}{s}\left(\frac{S}{2} + c\right) = \frac{0.6 \times 60}{6} \times \left(\frac{88}{2} + 21\right) = 396 \text{ kips}$$ (Governs)

$$V_n = 0.063\sqrt{f_c^{'}} b_f d_f + \frac{A_{hr} f_y}{s}\left(\frac{(W + 2d_f)}{2} + c\right)$$

$$= 0.063\sqrt{3.6} \times 63 \times 17 + \frac{0.6 \times 60}{6}\left(\frac{(22 + 2 \times 17)}{2} + 21\right) = 425 \text{ kips}$$

Thus, interior hanger capacity at Service I limit and Strength I limit for single ledge is 175 kips and 198 kips, respectively.

APPENDIX C. RETROFIT SOLUTION

In this appendix, the calculations to design retrofit solutions are presented. The calculations only account for southbound Bent 13, which has the largest deficiency with lane increment. The following sections also include a subsection with cost tables that were used for the evaluation of each solution in Chapter 4.

C.1 SOLUTION 1: PRESTRESSED HIGH-STRENGTH THREADBAR

C.1.1 Introduction

This solution will restrain existing shear cracks across the ledges as well as distribute loads from the girders by providing alternate load paths. The induced prestress resists the flexural and shear force generated by the girders on the ledges. Instead of using embedded anchorage, external anchorages are used to minimize interference with the existing reinforcement layout of the structure, and to avoid bursting stresses.

C.1.2 Threadbar

■ Required Prestressing Force

$M_u = V_u a_v + 0.2V_u(h - d_e) = V_u(a_v + 0.2(h - d_e))$

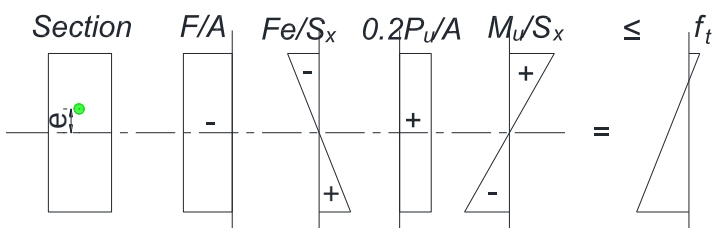

Figure C.1. Stress Block.

$$-\frac{F}{A} - \frac{Fe}{S_x} + \frac{0.2V_u}{A} + \frac{M_u}{S_x} \le f_t$$

$$-\frac{F}{bD} - \frac{6F}{bD^2} + \frac{0.2V_u}{bD} + \frac{6M_u}{bD^2} \le f_t$$

Rearrange above equation as:

$$F + F\frac{6e}{D} - 0.2V_u - \frac{6M_u}{D} \ge -f_t bD$$

where $M_u = V_u(a_v + 0.2(h - d_e))$

$$F\left(1 + \frac{6e}{D}\right) - V_u\left(0.2 + \frac{6\left(a_v + 0.2(h - d_e)\right)}{D}\right) \ge -f_t bD$$

$$F \ge \frac{V_u\left(0.2 + \frac{6\left(a_v + 0.2(h - d_e)\right)}{D}\right) - f_t bD}{\left(1 + \frac{6e}{D}\right)}$$

For no-tension design, set f_t = 0.

Set e at kern point $k_n = D/6 = 3.33\ in.$, then:

$$1 + \frac{6e}{D} = 1 + \frac{6 \times 3}{20} \cong 2$$

$$F \geq \frac{1}{2}V_u\left(0.2 + \frac{6\left(a_v + 0.2(h - d_e)\right)}{D}\right)$$
$$= \frac{1}{2}\left(0.2 + 6 \times \frac{7.5 + 0.2(21 - 17.5)}{20}\right)V_u = 1.33V_u$$
$$= 119.7 \text{ kips}$$

■ Selecting Threadbar

A 150 ksi high-strength threadbar can be used in this retrofit solution. To provide a total minimum required prestress force of 119.7 kip, the number of bars and size are chosen from the bars listed in Table C.1. Using an even number of threadbars is recommended to make the number of threadbars on either side of the girder symmetrical.

Try two 1 in. diameter threadbars:

$F_{req} \leq F = 0.6f_uA_bn_b$

119.7 kips $\leq 76.5 \times 2 = 153$ kips O.K.

Table C.1. Property of 150 KSI All-Thread-Bar (Williams Form Eng. Corp., 2011).

Nominal Bar Diameter & Pitch	Minimum Net Area Thru Threads	Minimum Ultimate Strength	Prestressing Force			Nominal Weight	Approx. Thread Major Dia.	Part Number
			0.80f pu A	0.70f pu A	0.60f pu A			
1" - 4 (26 mm)	0.85 in^2 (549 mm^2)	128 kips (567 kN)	102 kips (454 kN)	89.3 kips (397 kN)	76.5 kips (340 kN)	3.09 lbs./ft. (4.6 Kg/M)	1-1/8" (28.6 mm)	R71-08
1-1/4" - 4 (32 mm)	1.25 in^2 (807 mm^2)	188 kips (834 kN)	150 kips (667 kN)	131 kips (584 kN)	113 kips (500 kN)	4.51 lbs./ft. (6.71 Kg/M)	1-7/16" (36.5 mm)	R71-10
1-3/8" - 4 (36 mm)	1.58 in^2 (1019 mm^2)	237 kips (1054 kN)	190 kips (843 kN)	166 kips (738 kN)	142 kips (633 kN)	5.71 lbs./ft. (8.50 Kg/M)	1-9/16" (39.7 mm)	R71-11
1-3/4" - 3-1/2 (46 mm)	2.60 in^2 (1664 mm^2)	390 kips (1734 kN)	312 kips (1388 kN)	273 kips (1214 kN)	234 kips (1041 kN)	9.06 lbs./ft. (13.5 Kg/M)	2" (50.8 mm)	R71-14
2-1/4"" - 3-1/2 (57 mm) **	4.08 in^2 (2632 mm^2)	613 kips (2727 kN)	490 kips (2181 kN)	429 kips (1909 kN)	368 kips (1636 kN)	14.1 lbs./ft. (20.8 Kg/M)	2-1/2" (63.5 mm)	R71-18
2-1/2" - 3 (65 mm)	5.19 in^2 (3350 mm^2)	778 kips (3457 kN)	622 kips (2766 kN)	545 kips (2422 kN)	467 kips (2074 kN)	18.2 lbs./ft. (27.1 Kg/M)	2-3/4" (69.9 mm)	R71-20
3" - 3 (75 mm)	6.85 in^2 (4419 mm^2)	1027 kips (4568 kN)	822 kips (3656 kN)	719 kips (3198 kN)	616 kips (2740 kN)	24.1 lbs./ft. (35.8 Kg/M)	3-1/8" (79.4 mm)	R71-24

** The 2-1/4" diameter bar is not covered under ASTM A722.

- ACI 355.1R section 3.2.5.1 indicates an ultimate strength in shear has a range of .6 to .7 of the ultimate tensile strength. Designers should provide adequate safety factors for safe shear strengths based on the condition of use.
- Per PTI recommendations for anchoring, anchors should be designed so that:
- The design load is not more than 60% of the specified minimum tensile strength of the prestressing steel.
- The lock-off load should not exceed 70% of the specified minimum tensile strength of the prestressing steel.
- The maximum test load should not exceed 80% of the specified minimum tensile strength of the prestressing steel.

■ Shear Strength of Threadbar

$$V_{req} = \frac{V_u}{n_b} \leq V_d = 0.65T_u$$

$$V_{req} = \frac{V_u}{n_b} = \frac{90\ kips}{2} = 45\ kips \leq V_d = 0.65T_u = 0.65 \times 128 = 83.2\ kips \qquad \text{O.K.}$$

If design strength of the threadbar is less than the required strength, either the diameter or the number of threadbars needs to be increased.

■ Spacing Check

$s_{min} = 6d_b = 6 \times 1 = 6 \text{ in.} \leq 21 \text{ in.}$ O.K.

C.1.3 Steel Angle

■ Required Thickness

$$t_{min,req} = \min\left(\frac{R_n}{\phi 2.0 d_b f_u}, \frac{V_n}{\phi 2.4 b_d f_u}\right) \leq t_s$$

Since the purpose of all threadbars is to strengthen the structure, the yield strength of the steel angle is used instead of the ultimate strength to ensure that there is no effect on the original structure.

$$t_{min,req} = \frac{V_n}{\phi 2.4 d_b f_y} = \frac{76.5}{0.75 \times 2.4 \times 1 \times 36} = 1.18 \text{ in.}$$

1.25 in. thickness steel angle can be used:

$t_{min,req} = 1.18 \text{ in.} \leq 1.25 \text{ in. (provided)}$ O.K.

■ Required Bearing Area

$$A_{b,req} = \frac{F}{n_b}\left(\frac{1}{\phi_c 0.85 f_c'}\right) = \frac{76.5}{0.65 \times 0.85 \times 3.6} = 38.5 \text{ in.}^2$$

The steel angle plate should have a minimum area of 38.5 in.^{2}

A customized 11 ½ × 10 ½ × 1 ¼ steel angle can be used.

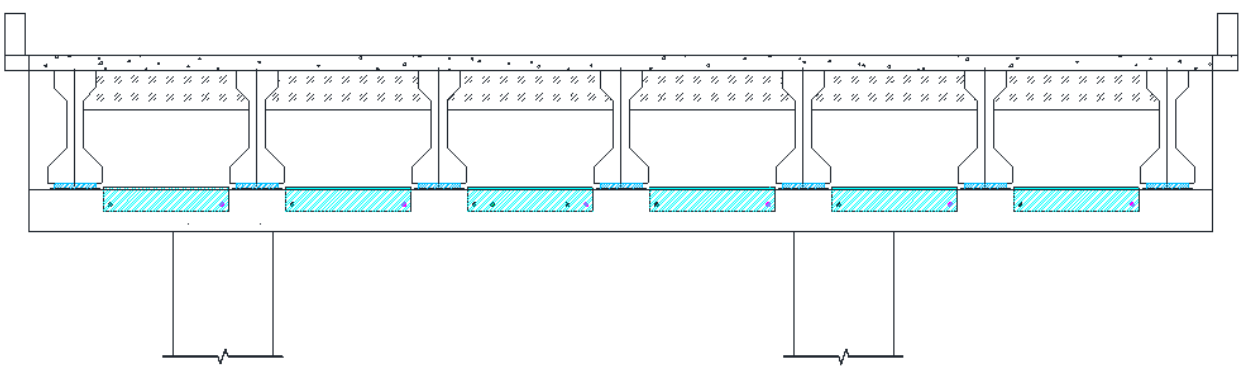

Figure C.2. Schematic View of Solution 1 Applied for Double-Column Bents.

C.1.4
Cost Table

Table C.2. Cost for Solution 1 per Bent.

No.	Description	Unit	Quantity per Item	No. of Items	Total Quantity	Rate/ Unit	Material Cost	Labor Cost	Equipment Cost
1	Boom Lift: 30 ft	HR	84	1	84	$16			$1,344
2	Construction Worker: three people	HR	84	3	252	$35		$8,820	
3	Rebar Locator	HR	0.25	12	3	$3			$9
4	Core Drill Rig	HR	36	1	36	$12			$432
5(a)	Core Driller, Horizontal, Ledge: 1-1/8 in. dia., 63 in. long	HR	2.5	12	30	$60		$1,800	
5(b)	1-1/8"x60" Diamond Core Drill Bit	EA	1	1	1	$365	$365		
6(a)	Telehandler: 30 ft long, 6000 lb capacity	HR	24	1	24	$20			$480
6(b)	Telehandler Operator	HR	24	1	24	$30		$720	
7(a)	Steel Angle: 10"x12"x1.25", 60.5 in. length	LB	473	12	5670	$1	$5,670		
7(b)	Plasma Cutting 1.5" thickness	FT	26	12	312	$7			$2,184
7(c)	Welder	HR	1	12	12	$50		$600	
7(d)	3/32" E7018 Stick Electrode	LB	2	12	24	$3	$72		
7(e)	Welding Wire	LB	1	12	12	$6	$72		
7(f)	Drilling Holes for Steel Angle: 1-1/8 in. dia., 0.75 in. thickness	EA	2	12	24	$3		$72	
8(a)	Threadbar: 1 in. dia.	FT	5	12	60	$5	$300		
8(b)	Washer: 1 in. dia	EA	2	12	24	$1	$24		
8(c)	Nut: 1 in. dia	EA	2	12	24	$5	$120		
8(d)	Torque Wrench and Multiplier	HR	16	1	8	$20			$160
							$6,623	**$12,012**	**$4,609**
		Total Materials, Labor, and Equipment					**$23,244**		
		Mobilization					$5,000		
		Subtotal					**$28,244**		
		Contingencies (~20%)					$5,649		
		Total					**$34,000**		

Major Item

C.2 SOLUTION 2: STEEL HANGER BRACKET

C.2.1 Introduction

Steel brackets with anchoring bolts are placed to provide complementary load paths. The steel bracket is designed to transfer loads, and the anchors are designed to carry shear and tension loads. There are many types of anchoring bolts, and the type of bolts needs to be selected based on their shear and tension capacity in order to minimize the number of bolts.

C.2.2 Anchor

■ Required Tension Force

To obtain the required tension load on a group of anchor bolts, Whitney stress block has been used based on ACI 318R (ACI Committee 318, 2014), and its assumptions are described in Figure 4.4.

The pullout force:

$$T_b = \frac{P_u x}{jd}$$

$$jd = d - a/2$$

$$a = \frac{T_b}{0.85 f_c' b}$$

Assume location of bolts and bracket size based on existing reinforcement layout as shown in Figure 4.3(d). Then:

$$M_{u,N} = V_u x = T_d jd = A_s f_y \left(d - \frac{a}{2}\right) = 0.85 f_c' ab \left(d - \frac{a}{2}\right)$$

$$337.5 = 0.85 \times 3.6 \times a \times 16 \left(21.375 - \frac{a}{2}\right) = 1028.16a - 24.48a^2$$

Solving above equation for *a* gives:

$a = 0.32$ in.

Substitute *a* into:

$$a = \frac{T_d}{0.85 f_c' b} \rightarrow T_d = 0.85 f_c' ab = 0.85 \times 3.6 \times 0.32 \times 16 = 15.91 \text{ kips}$$

Assume, tension force for four bolts is 15.91 kips. Thus, tension strength of each bolt needs to be greater than 3.98 kips.

■ Required Shear Force

Considering the eccentricity of the load on the bracket, the required shear force in the anchor bolt can be calculated using:

$$V_{u,i} = \sqrt{\left(\frac{M_{u,v} d_{iy}}{\sum d^2} + R_x\right)^2 + \left(\frac{M_{u,v} d_{ix}}{\sum d^2} + R_y\right)^2}$$

where

$M_{u,v} = 45 \times 4.5 = 202.5 \text{ kip} \cdot \text{in.}$

$R_x = 0$

$R_y = \frac{45}{4} = 11.25 \text{ kips}$

Therefore, the shear force in each anchor bolt is:

$$V_{u,1} = \sqrt{\left(\frac{202.5\times 5}{164}+0\right)^2 + \left(\frac{202.5\times 4}{164}-11.25\right)^2} = 8.83\,\text{kips}$$

$$V_{u,3} = \sqrt{\left(\frac{202.5\times 5}{164}+0\right)^2 + \left(\frac{202.5\times -4}{164}-11.25\right)^2} = 17.33\,\text{kips}$$

$$V_{u,4} = \sqrt{\left(\frac{202.5\times -5}{164}+0\right)^2 + \left(\frac{202.5\times 4}{164}-11.25\right)^2} = 8.83\,\text{kips}$$

$$V_{u,2} = \sqrt{\left(\frac{202.5\times -5}{164}+0\right)^2 + \left(\frac{202.5\times 4}{164}-11.25\right)^2} = 17.33\,\text{kips}$$

Thus, the maximum required shear strength of an anchor is 17.33 kips.

■ Design Force

The design strength of anchor bolts is generally provided by the manufacturer. In this case, four 1 in. diameter epoxy anchors produced by Hilti with 12 in. embedded depth can be used. The given design strength for the single anchor is:

$\phi V_n = 29.53\,\text{kips}$

$\phi N_n = 38.82\,\text{kips}$

Since four anchors are used, the group effect should be considered by using a spacing factor in tension f_{AN}, spacing factor in shear f_{AV}, and concrete thickness factor in shear f_{HV} given by the manufacturer:

$f_{AN} = 0.61$

$f_{AV} = 0.55$

$f_{HV} = 0.60$

Since there is no edge effect in this case, the reduction factors are:

$f_{AN} = 0.61$

$f_{AV} = f_{AN}$

$f_{HV} = 1.0$

Then, the design strength of an anchor in an anchor group is:

$V_d = \phi V_n f_{AV} f_{HV} = 29.53\times 0.61\times 1.0 = 18.01\,\text{kips}$

$N_d = \phi N_n f_{AN} = 38.82\times 0.61 = 24.07\,\text{kips}$

$V_d = 18.01\,\text{kips} > V_{u,i} = 17.33\,\text{kips}$ O.K.

$N_d = 24.07\,\text{kips} > N_{u,i} = 3.98\,\text{kips}$ O.K.

■ Interaction of Tensile and Shear Forces

$$\left(\frac{N_{u,i}}{N_d}\right)^{\frac{5}{3}} + \left(\frac{V_{u,i}}{V_d}\right)^{\frac{5}{3}} \le 1.0$$

$$\left(\frac{N_{u,i}}{N_d}\right)^{\frac{5}{3}}+\left(\frac{V_{u,i}}{V_d}\right)^{\frac{5}{3}}=\left(\frac{3.98}{24.07}\right)^{\frac{5}{3}}+\left(\frac{17.33}{18.01}\right)^{\frac{5}{3}}=0.96\le 1.0 \qquad \text{O.K.}$$

■ Minimum Spacing between Anchors

$s_{\min}=6d_b=6\times 1=6$ in.

$s=\min(8,10)=8$ in.

$\therefore s_{min}=6$ in. $\le s=8$ in. O.K.

C.2.3 Angle Bracket

■ Minimum Required Thickness and Weld Size

Check bearing:

$$t_{bearing}\ge\frac{V_{u,i}}{\phi 1.8d_b f_u}=\frac{V_{u,i}}{\phi 1.8d_b f_y}=\frac{17.33}{0.75\times 1.8\times 1\times 36}=0.36\text{ in.}$$

Check shear yielding:

$$t_{s,y}\ge\frac{V_u/n_{bracket}}{\phi 0.6h_v f_y}=\frac{90/2}{1\times 0.6\times 30\times 36}=0.07\text{ in.}$$

Check tension yielding:

$$t_{t,y}\ge\frac{V_u/n_{bracket}}{\phi b_v f_y}=\frac{90/2}{0.9\times 16\times 36}=0.09\text{ in.}$$

Check shear rupture:

$$t_{s,r}\ge\frac{V_u/n_{bracket}}{\phi 0.6h_n f_y}=\frac{V_u/n_{bracket}}{\phi 0.6\left[h_v-\Sigma(d_i+1/16)\right]f_y}$$

$$=\frac{90/2}{0.75\times 0.6\times\left[30-\left(1+1/16\right)\times 2\right]\times 36}=0.10\text{ in.}$$

Check tension rupture:

$$t_{t,r}\ge\frac{V_u/n_{bracket}}{\phi b_n f_y}=\frac{V_u/n_{bracket}}{\phi\left[b_v-\Sigma(d_i+1/16)\right]f_y}$$

$$=\frac{90/2}{0.75\times\left[16-\left(1+1/16\right)\times 2\right]\times 36}=0.07\text{ in.}$$

Therefore, the minimum required thickness is:

$t_{min}=\max(t_{bearing},t_{s,y},t_{t,y},t_{s,r},t_{t,r})=0.36$ in.

Let thickness of plates comprising the bracket be $t=0.375$ in.

The thickness t_a also depends on the weld size, and is given as:

$$t_a=\frac{F_{EXX}a}{0.93f_y}\le t$$

Weld size a is decided based on required weld size with E70 electrodes:

$$a_{req}=\frac{f_{wr}}{\phi A_{we}F_{mv}}$$

$$f_{wr} = \sqrt{f_{wv}^2 + f_{wb}^2} = 1.35$$

where $f_{wv} = \dfrac{P_u}{2h_v} = 0.75 \text{ kip/in.}$ *and* $f_{wb} = \dfrac{Me}{2\left[\left(1-h_v^2\right)/12\right]} = 1.125 \text{ kip/in.}$

$$F_{mv} = 0.6F_{EXX}(1.0 + 0.5\sin^{1.5}\theta) = 0.6F_{EXX} = 0.6 \times 70 = 42 \text{ ksi}$$

$$a_{req} = \frac{f_{wr}}{\phi A_{we} F_{mv}} = \frac{1.35}{0.75 \times 0.5\sqrt{2} \times 42} = 0.061 \text{ in.}$$

Use 1/8 in. weld:

$$t_a = \frac{F_{EXX}\, a}{0.93 f_y} = \frac{70 \times 1/8}{0.93 \times 36} = 0.26 \text{ in.} \le t = 0.375 \text{ in.} \qquad \text{O.K.}$$

Check bearing strength for eccentricity and weld size:

$$V_u \le \frac{\phi 1.8 f_y h_l^2}{6e_p - h_l/2} n_{bracket}$$

$$V_u = 90 \text{ kips} \le \frac{0.75 \times 1.8 \times 36 \times 12^2}{6 \times 7.5 - 12/2} 2 = 358.9 \text{ kips} \qquad \text{O.K.}$$

Check strength of triangular plate for an angle bracket:

$$P_u \le f_y t \sin^2\alpha \left(\sqrt{4e^2 + h_l^2} - 2e\right) n_{bracket}$$

$$\alpha = \tan^{-1}\left(\frac{h_v}{h_l}\right) = 1.19$$

$$e = e_s - h_l/2 = 7.5 - 12/2 = 1.5 \text{ in.}$$

$$f_y t \sin^2\alpha \left(\sqrt{4e^2 + h_l^2} - 2e\right) n_{bracket}$$

$$= 36 \times 0.375 \times \sin^2 1.19 \times \left(\sqrt{4 \times 1.5^2 + 12^2} - 2 \times 1.5\right) \times 2 = 218.03 \text{ kips}$$

$$V_u = 90 \text{ kips} \le 218.03 \text{ kips} \qquad \text{O.K.}$$

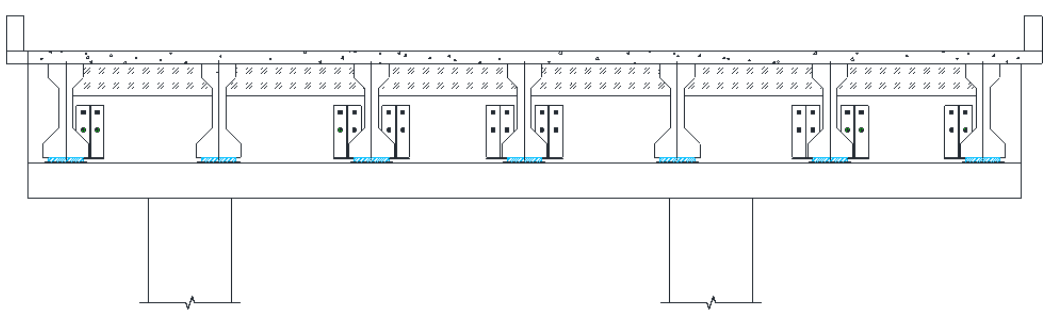

Figure C.3. Schematic View of Solution 2a Applied for Double-Column Bents.

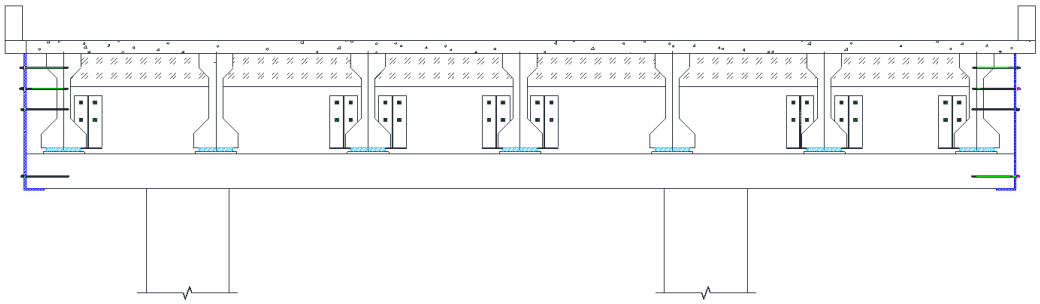

Figure C.4. Schematic View of Solution 2b Applied for Double-Column Bents.

C.2.4 Cost Table

Table C.3. Cost for Solution 2a per Bent.

No.	Description	Unit	Quantity per Item	No. of Items	Total Quantity	Rate/ Unit	Material Cost	Labor Cost	Equipment Cost
1	Boom Lift: 30 ft	HR	36	1	36	$16			$576
2	Construction Worker: three people	HR	36	3	108	$35		$3,780	
3	Rebar Locator	HR	1	8	8	$3			$24
4(a)	Hammer Drill, Horizontal, Web: 1-1/8 in. dia., 12 in. long	HR	0.25	64	16	$12			$192
4(b)	1-1/8"x17" Hammer Drill Bit	EA	1	1	1	$75	$75		
5(a)	Steel Bracket: 30"x16"x0.375": 16 in. wide, one triangular stiffener	LB	105	16	1680	$1	$1,680		
5(b)	Plasma Cutting 0.375" thickness	FT	19	16	304	$3			$912
5(c)	Welder	HR	1	16	16	$50		$800	
5(d)	3/32" E7018 Stick Electrode	LB	2	16	32	$3	$96		
5(e)	Welding Wire	LB	1	16	16	$6	$96		
5(f)	Drilling Holes for Steel Bracket: 1.25 in. dia., 0.375 in. thickness	EA	4	16	64	$3		$192	
6(a)	Anchor Bolt: 1"x14"	EA	4	16	64	$28	$1,792		
6(b)	HIT-RE 500 V3 Epoxy: 11.1 oz	EA	0.2	64	12.8	$57	$730		
6(c)	Manual Epoxy Dispenser	EA	1	1	1	$160	$160		
							$4,629	**$4,772**	**$1,704**
		Total Materials, Labor, and Equipment					**$11,105**		
		Mobilization					$3,000		
		Subtotal					**$14,105**		
		Contingencies (~20%)					$2,821		
		Total					**$17,000**		

Major Item

Table C.4. Cost for Solution 2b per Bent.

No.	Description	Unit	Quantity per Item	No. of Items	Total Quantity	Rate/ Unit	Material Cost	Labor Cost	Equipment Cost
1	Boom Lift: 30 ft	HR	56	1	56	$16			$896
2	Construction Worker: three people	HR	56	3	168	$35		$5,880	
3	Rebar Locator	HR	1	10	10	$3			$30
4(a)	Hammer Drill, Horizontal, Web: 1-1/8 in. dia., 12 in. long	HR	0.25	48	12	$12			$144
4(b)	1-1/8"x17" Hammer Drill Bit	EA	1	1	1	$75	$75		
5(a)	Steel Bracket: 30"x16"x0.375": 16 in. wide, one triangular stiffener	LB	105	12	1260	$1	$1,260		
5(b)	Plasma Cutting 0.375" thickness	FT	19	12	228	$3			$684
5(c)	Welder	HR	1	12	12	$50		$600	
5(d)	3/32" E7018 Stick Electrode	LB	2	12	24	$3	$72		
5(e)	Welding Wire	LB	1	21	21	$6	$126		
5(f)	Drilling Holes for Steel Bracket: 1.25 in. dia., 0.375 in. thickness	EA	4	12	48	$3		$144	
6(a)	Anchor Bolt: 1"x14"	EA	4	12	48	$28	$1,344		
6(b)	HIT-RE 500 V3 Epoxy: 11.1 oz	EA	0.2	48	10	$57	$547		
6(c)	Manual Epoxy Dispenser	EA	1	1	1	$160	$160		
7(a)	Hammer Drill, Horizontal, End Region: 1"x25"	HR	0.5	16	8	$12			$96
7(b)	1-1/4"x25" Hammer Drill Bit	EA	1	1	1	$100		$100	
8(a)	Telehandler: 30 ft long, 6000 lb capacity	HR	8	1	8	$20			$160
8(b)	Telehandler Operator	HR	8	1	8	$30		$240	
9(a)	End Plate: 1 in. thickness	LB	700	2	1400	$1	$1,400		
9(b)	Plasma Cutting 1" thickness	FT	35	2	70	$8			$560
9(c)	Welder	HR	1	2	2	$50		$100	
9(d)	3/32" E7018 Stick Electrode	LB	2	2	4	$3	$12		
9(e)	Welding Wire	LB	1	2	2	$6	$12		
9(f)	Drilling Holes for End Plate: 1.25 in. dia., 1 in. thickness	EA	5	2	10	$3		$30	
10(a)	Threadbar, End Region: 1 in. dia.	FT	3	16	48	$7	$336		
10(b)	Epoxy: 22 oz.	EA	3	1	3	$39	$117		
10(c)	Manual Epoxy Dispenser	EA	1	1	1	$160	$160		
10(d)	Washer: 1 in. dia	EA	1	10	10	$1	$10		
10(e)	Nut: 1 in. dia.	EA	1	10	10	$5	$50		
							$5,681	**$7,094**	**$2,570**
		Total Materials, Labor, and Equipment					**$15,345**		
		Mobilization					$4,000		
		Subtotal					**$19,345**		
		Contingencies (~20%)					$3,870		
		Total					**$24,000**		

Major Item

C.3 SOLUTION 3: END-REGION STIFFENER

C.3.1 Introduction

As shown in Figure 4.7, the end plate should be used as a stiffener to increase the strength of the end regions of the bent cap, where the distress is typically observed. The anchor bolts should be anchored against a stiffener plate at the end of the bent cap structure. Since the weight of the stiffener plate is likely to be significant, its weight should be taken into account while calculating the required forces.

C.3.2 Anchor

To have sufficient embedded depth and shear resistance, adhesive anchors, such as epoxy anchors, are used for this solution. Eight 1 in. diameter epoxy anchors consisting of threadbar and epoxy can be used. The embedment depth of the bar is set as 20 in. to provide sufficient capacity. Figure 4.7(b) presents the arrangement of the threadbar. It is determined based on the minimum spacing, edge distance, and to avoid the steel plate peel off from the end surface. Calculation of the design strength of the threadbar is the minimum of steel strength, concrete breakout strength, concrete pryout strength, and bond strength of the anchor in accordance with ACI 318R (ACI Committee 318, 2014). In this case, the anchors are supposed to resist the shear force, and generally, the steel shear strength governs the design strength of the anchors. The design strength of the anchor is determined by:

$$V_n = 0.6 f_u A_b n_b = 0.6 \times 150 \times 0.85 \times 8 = 612 \text{ kips} > V_{u,total} = V_u \times 2 = 180 \text{ kips}$$

Besides the steel shear strength, to check that the shear capacity of the anchors is greater than the demand, the anchors are separated into two groups. The first group of anchors is installed at the web of the bent cap, and the second group consists of the three threadbars that are installed at the ledge of the bent cap. Each group of anchors must have larger capacity than the demand, V_u.

C.3.3 End Plate

The steel plate is primarily designed for the bearing force. Thus, thickness of the steel plate should be thicker than the required bearing thickness:

$$t_{bearing} \geq \frac{V_{u,total} / n_b}{\phi 1.8 d_b f_y} = \frac{180/8}{0.75 \times 1.8 \times 1 \times 36} = 0.46 \text{ in.}$$

Use a steel plate with a thickness of 0.5 in.

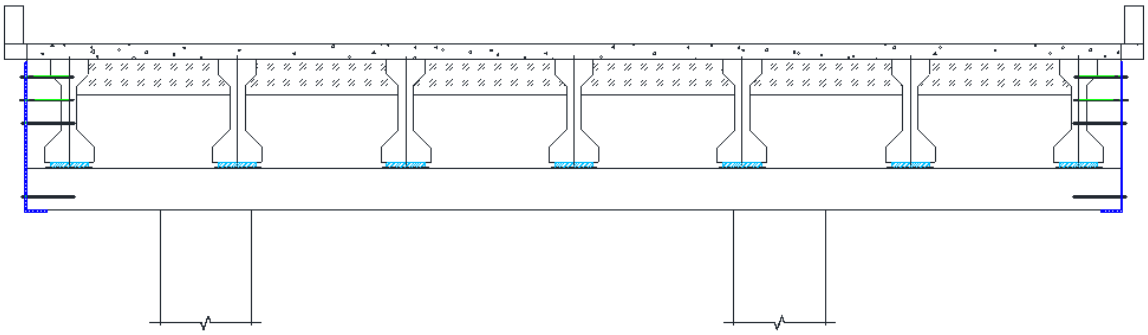

(a) For double-column bent

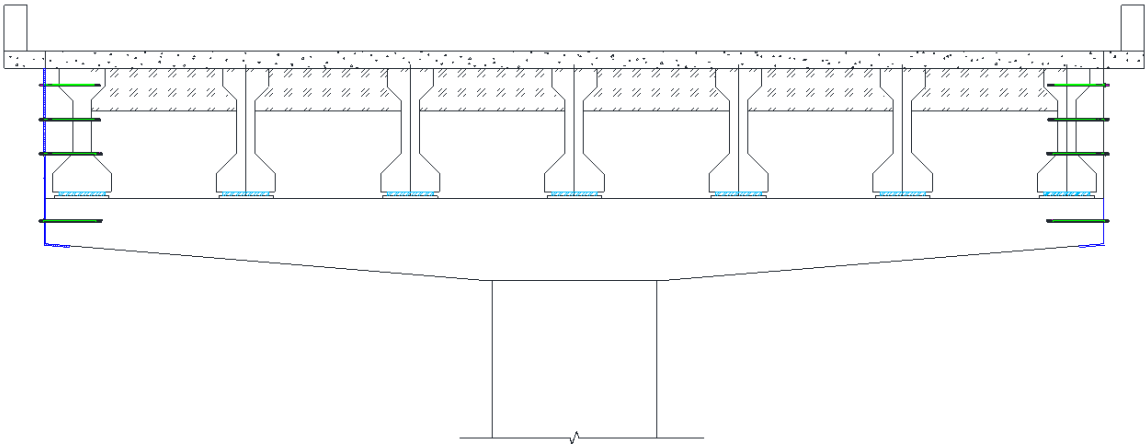

(b) For single-column bent

Figure C.5. Schematic View of Solution 3.

C.3.4 Cost Table

Table C.5. Cost for Solution 3 for a Double-Column Bent.

No.	Description	Unit	Quantity per Item	No. of Items	Total Quantity	Rate/ Unit	Material Cost	Labor Cost	Equipment Cost
1	Boom Lift: 30 ft	HR	20	1	20	$16			$320
2	Construction Worker: three people	HR	20	3	60	$35		$2,100	
3	Rebar Locator	HR	1	2	2	$3			$6
3(a)	Hammer Drill, Horizontal, End Region: 1"x25"	HR	0.5	16	8	$12			$96
3(b)	1-1/4"x25" Hammer Drill Bit	EA	1	1	1	$100		$100	
4(a)	Telehandler: 30 ft long, 6000 lb capacity	HR	8	1	8	$20			$160
4(b)	Telehandler Operator	HR	8	1	8	$30		$240	
5(a)	End Plate: 1 in. thickness	LB	700	2	1400	$1	$1,400		
5(b)	Plasma Cutting 1" thickness	FT	35	2	70	$8			$560
5(c)	Welder	HR	1	2	2	$50		$100	
5(d)	3/32" E7018 Stick Electrode	LB	2	2	4	$3	$12		
5(e)	Welding Wire	LB	1	2	2	$6	$12		
5(f)	Drilling Holes for End Plate: 1.25 in. dia., 1 in. thickness	EA	5	2	10	$3		$30	
6(a)	Threadbar, End Region: 1 in. dia.	FT	3	16	48	$7	$336		
6(b)	Epoxy: 22 oz.	EA	3	1	3	$39	$117		
6(c)	Manual Epoxy Dispenser	EA	1	1	1	$160	$160		
6(d)	Washer: 1 in. dia	EA	1	10	10	$1	$10		
6(e)	Nut: 1 in. dia.	EA	1	10	10	$5	$50		
							$2,097	**$2,570**	**$1,142**
		Total Materials, Labor, and Equipment					**$5,809**		
		Mobilization					$2,000		
		Subtotal					**$7,809**		
		Contingencies (~20%)					$1,562		
		Total					**$10,000**		

Major Item

Table C.6. Cost for Solution 3 for a Single-Column Bent.

No.	Description	Unit	Quantity per Item	No. of Items	Total Quantity	Rate/ Unit	Material Cost	Labor Cost	Equipment Cost
1	Boom Lift: 30 ft	HR	16	1	16	$16			$256
2	Construction Worker: three people	HR	16	3	48	$35		$1,680	
3	Rebar Locator	HR	2	1	2	$3			$6
4(a)	Hammer Drill, Horizontal, End Region: 1.5 in. dia., 20 in. long	HR	0.5	14	7	$12			$84
4(b)	1-1/2"x21" Hammer Drill Bit	EA	1	1	1	$81		$81	
5(a)	Telehandler: 30 ft long, 6000 lb capacity	HR	7	1	7	$20			$140
5(b)	Telehandler Operator	HR	7	1	7	$30		$210	
6(a)	End Plate: 0.5 in. thickness	LB	350	2	700	$1.00	$700		
6(b)	Plasma Cutting 0.5" thickness	FT	35	2	70	$4			$280
6(c)	Welder	HR	1	2	2	$50		$100	
6(d)	3/32" E7018 Stick Electrode	LB	2	2	4	$3	$12		
6(e)	Welding Wire	LB	1	2	2	$6	$12		
6(f)	Drilling Holes for End Plate: 1.25 in. dia., 0.5 in. thickness	EA	7	2	14	$2		$28	
7(a)	Threadbar 1, End Region: 1 in. dia.	FT	3	12	36	$5	$180		
7(c)	Epoxy: 22 oz.	EA	1	3	3	$45	$135		
7(d)	Manual Epoxy Dispenser	EA	1	1	1	$160	$160		
7(e)	Washer: 1 in. dia	EA	6	2	12	$1	$12		
7(f)	Nut: 1 in. dia	EA	6	2	12	$5	$60		
		Total					**$1,271**	**$2,099**	**$766**
							$4,136		
		Mobili					$1,000		
		Subto					**$5,136**		
		Conti					$1,028		
		Total					**$7,000**		

Major Item

C.4 SOLUTION 4: CLAMPED CROSS THREADBAR

C.4.1 Introduction

The threadbars should be anchored using hex nuts, a beveled washer, and a bearing plate at each end. The external anchoring system is used to minimize interference with the existing rebar.

C.4.2 Threadbar

■ Required Strength of Threadbar

$$F_{req} = \frac{V_{u,total}}{n_t \sin\theta}$$

Assume $\theta = 50^\circ$:

$$P_{req} = F_{req} n_t = \frac{V_{u,total}}{\sin\theta} = \frac{90 \times 2}{\sin 50^\circ} = 234.97 \text{ kips}$$

■ Select Thread Rod and the Number of Bars

The design strength of threadbars with an ultimate strength of 150 ksi is defined as 60 percent of the ultimate strength. To minimize the size of the drilled hole, 1 in. diameter threadbars are chosen from Table C.1:

$$n_{t,req} = \frac{P_{req}}{T_d} = \frac{234.97}{76.5} = 3.07 \text{ ea.}$$

In this solution, an even number of threadbars should be used so that the bars will be evenly installed on either side of the girder:

$$\therefore n_{t,req} = 3.07 \text{ ea.} \le n_t = 4 \text{ ea.}$$

$$T_d n_t = 76.5 \times 4 = 306 \text{ kips} \ge P_{req} = 234.97 \text{ kips} \qquad \text{O.K.}$$

The spacing between cross bars is determined based on the layout of the existing reinforcement.

C.4.3 Bearing Plate

■ Required Thickness

$$t_{\min,req} = \frac{R_n}{\phi 2.4 b_b f_y} = \frac{76.5}{0.75 \times 2.4 \times 1 \times 36} = 1.18 \text{ in.} \le t_s$$

Choose a steel plate with 1.25 in. thickness:

$$t_{min} = 1.18 \text{ in.} \le t_s = 1.25 \text{ in.} \qquad \text{O.K.}$$

■ Required Bearing Area

$$A_{b,req} = \frac{P_u}{\phi_c 0.85 f_c'} = \frac{76.5}{0.65 \times 0.85 \times 3.6} = 38.5 \text{ in.}^2$$

For the square plate:

$$l_{s,req} = \sqrt{A_{b,req}} = \sqrt{38.5} = 6.2 \text{ in.}$$

Use a square plate with 7 in. sides:

$$A_{b,req} = 38.5 \text{ in.}^2 \le A_b = 7^2 = 49 \text{ in.}^2 \qquad \text{O.K.}$$

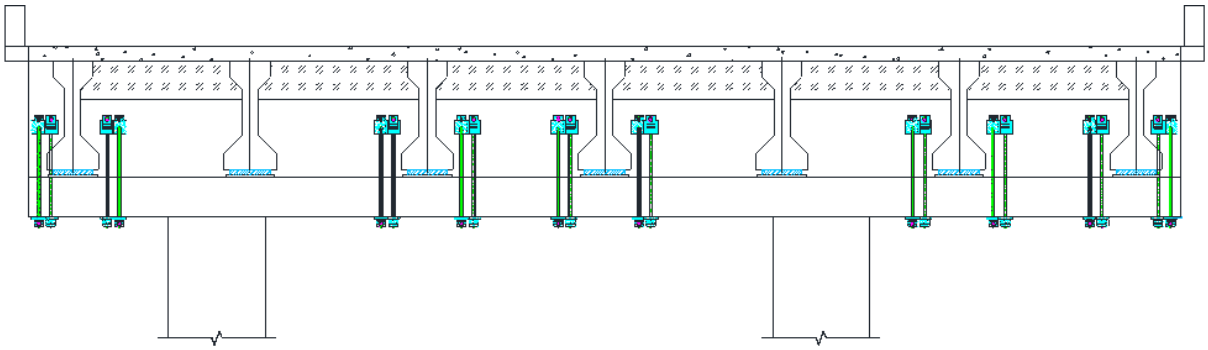

Figure C.6. Schematic View of Solution 4 Applied for Double-Column Bent.

C.4.4 Cost Table

Table C.7. Cost for Solution 4 per Bent.

No.	Description	Unit	Quantity per Item	No. of Items	Total Quantity	Rate/ Unit	Material Cost	Labor Cost	Equipment Cost
1	Boom Lift: 30 ft	HR			128	$16			$2,048
2	Construction Worker: three people	HR	128	3	384	$35		$13,440	
3	Rebar Locator	HR	0.25	20	7	$3			$21
4	Core Drill Rig	HR			96	$12			$1,152
5(a)	Core Driller, Inclined, Web: 1-1/8 in. dia., 6 ft long	HR	4	20	80	$60		$4,800	
5(b)	1-1/8"x60" Diamond Core Drill Bit	EA			1	$365	$365		
5(c)	1-1/8"x12" Core Bit Extension	EA			1	$100	$100		
6(a)	Threadbar: 1 in. dia.	FT	6	20	120	$5	$600		
6(b)	Beveled Washer: 1 in. dia.	EA	6	20	120	$15	$1,800		
6(c)	Nut: 1 in. dia.	EA	2	20	40	$5	$200		
6(d)	Bearing Plate: 7"x7"x1.25"	LB	18	40	720	$1	$720		
6(e)	Drilling Holes for Bearing Plate: 1.25 in. dia., 1.25 in. thickness	EA	1	40	40	$3		$120	
6(f)	Torque Wrench and Multiplier	HR			20	$20			$400
							$3,785	**$18,360**	**$3,621**
		Total Materials, Labor, and Equipment					**$25,766**		
		Mobilization					$6,000		
		Subtotal					**$31,766**		
		Contingencies (~20%)					$6,354		
		Total					**$39,000**		

Major Item

C.5 SOLUTION 5: GROUTED CROSS THREADBAR

C.5.1 Introduction

This retrofit solution can be used when minimal interference with the existing reinforcement may be necessary.

C.5.2 Threadbar

■ Required Strength of Threadbar

$$F_{req} = \frac{V_{u,total}}{n_t \sin\theta}$$

To minimize the use of beveled washer at the anchorage, assume $\theta = 70^\circ$:

$$P_{req} = F_{req} n_t = \frac{V_{u,total}}{\sin\theta} = \frac{90 \times 2}{\sin 70^\circ} = 191.55 \text{ kips}$$

■ Design Strength of Threadbar

Try a 1-1/4 in. diameter thread rod with an ultimate strength of 150 ksi.
The design strength of a grouted threadbar is the lesser of:

-Design tensile strength:

$$T_d = 0.6 A_s f_u = 0.6 \times 1.25 \times 150 = 113 \text{ kips}$$

-Design bond strength with $h_{ef} = 43 \text{ in.}$, $\tau = 1.5$ ksi (US Spec RA Grout):

$$N_{bond} = \tau \pi d h_{ef} = 1.5 \times \pi \times 1.375 \times 43 = 278.58 \text{ kips}$$

Therefore, the design strength of the grouted threadbar is:

$$R_n = \min(T_d, N_{bond}) = 113 \text{ kips}$$

■ The Number of Threadbars

$$P_{req} = F_{req} n_t = 191.55 \text{ kips}$$

$$n_{t,req} = \frac{P_{req}}{R_n} = \frac{191.55}{113} = 1.7 \text{ ea.}$$

$$\therefore n_{t,req} = 1.7 \text{ ea.} \le n_t = 2 \text{ ea.}$$ O.K.

C.5.3 Bearing Plate

■ Required Thickness of Bearing Plate

$$t_{\min,req} = \frac{R_n}{\phi 2.4 b_b f_u} \le t_s$$

$$t_{\min,req} = \frac{R_n}{\phi 2.4 b_b f_u} = \frac{113}{0.75 \times 2.4 \times 1 \times 60} = 1.05 \text{ in.}$$

Use a steel plate with a thickness of 1.125 in.

$$t_{min} = 1.05 \text{ in.} \le t_s = 1.125 \text{ in.}$$ O.K.

■ Required Bearing Area

$$A_{b,req} = \frac{R_n}{\phi_c 0.85 f_c'} = \frac{113}{0.65 \times 0.85 \times 3.6} = 56.9 \text{ in.}^2$$

For a square plate:

$$l_{s,req} = \sqrt{A_{b,req}} = \sqrt{56.9} = 7.54 \text{ in.}$$

Use a square plate with 7.75 in. sides:

$$A_{b,req} = 56.9 \text{ in}^2 \le A_b = 7.75^2 = 60 \text{ in}^2 \qquad \text{O.K.}$$

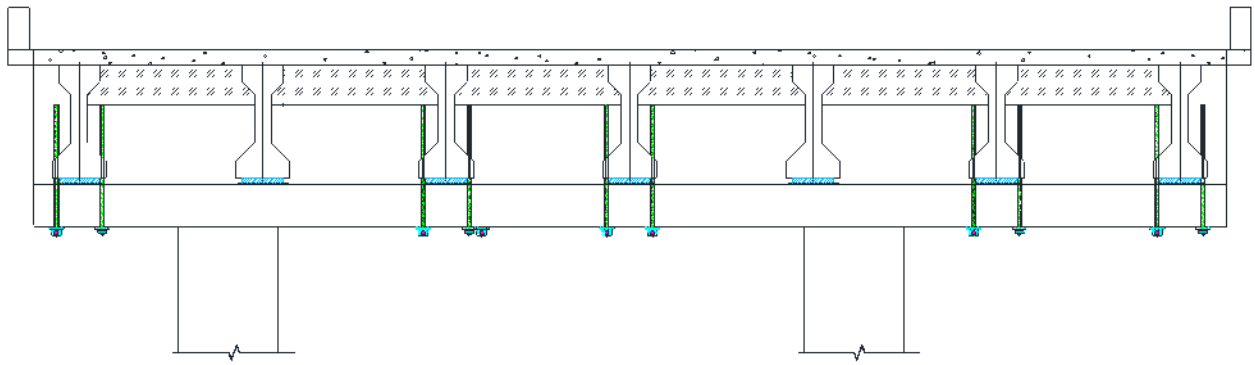

Figure C.7. Schematic View of Solution 5 Applied for Double-Column Bent.

C.5.4 Cost Table

Table C.8. Cost for Solution 5 per Bent.

No.	Description	Unit	Quantity per Item	No. of Items	Total Quantity	Rate/ Unit	Material Cost	Labor Cost	Equipment Cost
1	Boom Lift: 30 ft	HR			127	$16			$2,032
2	Construction Worker: three people	HR	127	3	381	$35		$13,335	
3	Rebar Locator	HR	0.25	10	3	$3			$8
4	Core Drill Rig	HR			48	$12			$576
5(a)	Core Driller, Inclined, Web: 1-1/8 in. dia., 6 ft long	HR	4	10	40	$60		$2,400	
5(b)	1-1/8"x60" Diamond Core Drill Bit	EA			1	$365	$365		
5(c)	1-1/8"x12" Core Bit Extension	EA			1	$100	$100		
6(a)	Hollow Threadbar: 1.5 in. dia.	FT	7	20	140	$5	$700		
6(b)	Beveled Washer: 1 in. dia.	EA	2	20	40	$15	$600		
6(c)	Nut: 1 in. dia.	EA	1	20	20	$5	$100		
6(d)	Bearing Plate: 7"x7"x1"	LB	15	20	300	$1	$300		
6(e)	Drilling Holes for Bearing Plate: 1 in. dia., 1 in. thickness	EA	1	20	20	$3		$60	
7(a)	Grout 0.45 ft^3 bag	EA			1	$10	$10		
7(b)	Grout Mixer	HR			1	$6			$6
7(c)	Grout Pump	HR			5	$6			$30
							$2,175	**$15,795**	**$2,652**
		Total Materials, Labor, and Equipment					**$20,622**		
		Mobilization					$5,000		
		Subtotal					**$25,622**		
		Contingencies (~20%)					$5,125		
		Total					**$31,000**		

Major Item

C.6 SOLUTION 6: UPPER SEAT BRACKETS

C.6.1 Introduction

The seat steel bracket, which consists of lateral, vertical, and triangle steel plates, is designed to support the diaphragms. Anchor bolts are used to anchor the steel brackets to the web of the bent cap.

C.6.2 Anchor

■ Required Tension Force

The required tension load on a group of anchor bolts is obtained in a similar way as the steel hanger bracket solution described in Section C.1. The loads are assumed to be acting at the center of the diaphragm as a point load. Therefore, the eccentricity e of the load is 11.5 in. in this case. The moment demand of the bolt group is:

$$M_{u,N} = \frac{V_u}{2} e = \frac{90}{2} \times 11.5 = 517.5 \text{ kip} \cdot \text{in.}$$

The arrangement of the bolts, shown in Figure 4.10(d), is determined based on the minimum spacing, edge distance, and location of the existing reinforcement.

The tension demands for each row are calculated separately based on strain compatibility, rather than evenly distributing the tension force to every bolt. The tension demands for each bolt from the bottom to the top layer are:

$N_{u1} = 5.56$ kips for bottom row

$N_{u2} = 13.91$ kips for middle row

$N_{u3} = 22.26$ kips for top row

The maximum tension demands for a single bolt can be calculated as:

$$N_u = \frac{N_{u3}}{n_{bolt\_top\ layer}} = \frac{22.26}{2} = 11.13 \text{ kips}$$

■ Required Shear Force

Assume that shear force is evenly resisted by every anchor bolt. The required shear force per anchor bolt can be calculated as:

$$V_{req} = \frac{V_u}{n_{bolt}} = \frac{90}{12} = 7.5 \text{ kips}$$

■ Design Force

The design strength of anchor bolts provided by the manufacturer is used in the design. In this solution, adhesive anchors produced by Hilti, which have relatively larger anchoring forces than mechanical anchors, are chosen. The most effective anchors selected for this solution are HIT-RE 500 adhesive anchor bolts with 0.875 in. diameter and 10.5 in. embedment depth, which provides:

Tensile: $\phi N_n = 31.07$ kips

Shear: $\phi V_n = 22.505$ kips

And reduction factors based on the spacing are given as:

Tensile: $f_{AN} = 0.6$

Shear: $f_{AV} = f_{AN} = 0.6$ (if there is no edge distance)

Final design strength of a single bolt is:

Tensile: $N_d = \phi N_n f_{AN} = 31.07 \times 0.6 = 18.64$ kips

Shear: $V_d = \phi V_n f_{AV} = 22.505 \times 0.6 = 13.503$ kips

Check bolt strength:

Tensile: $N_d = 18.64 \text{ kips} > N_u = 11.18 \text{ kips}$ O.K.

Shear: $V_d = 13.503 \text{ kips} > V_u = 7.5 \text{ kips}$ O.K.

Check tension and shear interaction:

$$\left(\frac{N_u}{N_d}\right)^{\frac{5}{3}} + \left(\frac{V_u}{V_d}\right)^{\frac{5}{3}} = \left(\frac{11.18}{18.64}\right)^{\frac{5}{3}} + \left(\frac{7.5}{13.503}\right)^{\frac{5}{3}} = 0.871 \le 1.0 \quad \text{O.K.}$$

■ Minimum Spacing between Anchors

$s_{\min} = 6d_b = 6 \times 0.875 = 5.25$ in.

$s = \min(6, 7) = 6$ in.

$\therefore s_{min} = 5.25 \text{ in.} \le s = 6 \text{ in.}$ O.K.

C.6.3 Angle Bracket

■ Minimum Required Thickness and Weld Size

Bearing:

$$t_{bearing} \ge \frac{V_{u\_single}}{\phi 1.8 d_b f_y} = \frac{7.5}{0.75 \times 1.8 \times 0.875 \times 36} = 0.18 \text{ in.}$$

Shear yielding:

$$t_{s,y} \ge \frac{V_u / n_{bracket}}{\phi 0.6 h_v f_y} = \frac{90/2}{1 \times 0.6 \times 20 \times 36} = 0.10 \text{ in.}$$

Tension yielding:

$$t_{t,y} \ge \frac{V_u / n_{bracket}}{\phi b_v f_y} = \frac{90/2}{0.9 \times 15 \times 36} = 0.09 \text{ in.}$$

Shear rupture:

$$t_{s,r} \ge \frac{V_u / n_{bracket}}{\phi 0.6 h_n f_y} = \frac{V_u / n_{bracket}}{\phi 0.6 \left[h_v - \Sigma(d_i + 1/16)\right] f_y}$$

$$= \frac{90/2}{0.75 \times 0.6 \times \left[20 - \left(0.875 + 1/16\right) \times 3\right] \times 36} = 0.16 \text{ in.}$$

Tension rupture:

$$t_{t,r} \ge \frac{V_u / n_{bracket}}{\phi b_n f_y} = \frac{V_u / n_{bracket}}{\phi \left[b_v - \Sigma(d_i + 1/16)\right] f_y}$$

$$= \frac{90/2}{0.75 \times \left[15 - \left(0.875 + 1/16\right) \times 2\right] \times 36} = 0.13 \text{ in.}$$

Weld size a is decided based on the required weld size with E70 electrodes:

$$a_{req} = \frac{f_{wr}}{\phi A_{we} F_{mv}}$$

$$f_{wr} = \sqrt{f_{wv}^2 + f_{wb}^2} = \sqrt{1.125^2 + 3.88^2} = 4.04 \text{ kip/in.}$$

$$\text{with } f_{wv} = \frac{V_u}{2h_v} = 1.125 \text{ kip/in. } and \ f_{wb} = \frac{V_u e}{2\left[\left(1 \times h_v^2\right)/12\right]} = 3.88 \text{ kip/in.}$$

Required weld size:

$$a_{req} = \frac{f_{wr}}{\phi 0.707 \cdot 0.6 F_{EXX}} = \frac{3.88}{0.75 \times 0.707 \times 0.6 \times 70} = 0.17 \text{ in.}$$

Use weld size as $a = 0.1875$ in. $= \frac{3}{16}$ in.

Required plate thickness for maximum weld size:

$$t_w \geq \frac{aF_{EXX}}{0.93 f_y} = \frac{0.1875 \times 70}{0.93 \times 36} = 0.39 \text{ in.}$$

Required thickness of triangular plate to avoid buckling failure:

$$t_{buckling} \geq \frac{h_l \sqrt{f_y}}{250\left(h_l / h_v\right)} = \frac{16 \times \sqrt{36}}{250 \times \left(16/20\right)} = 0.48 \text{ in.}$$

Required thickness of bearing strength for eccentricity and weld size:

$$t_{eb} \geq \frac{V_u / n_{bracket}\left(6e_p - h_l / 2\right)}{\phi 1.8 f_y h_l^2} = \frac{90/2 \times \left(6 \times 11.5 - 16/2\right)}{0.75 \times 1.8 \times 36 \times 16^2} = 0.22 \text{ in.}$$

$$t_{min} = \max(t_{bearing}, t_{s,y}, t_{t,y}, t_{s,r}, t_{t,r}, t_{buckling}, t_{eb}) = 0.48 \text{ in.}$$

Use 0.5 in. thick steel plate.

■ Strength of Triangular Plate

$$V_u \leq f_y t \sin^2 \alpha \left(\sqrt{4e^2 + h_l^2} - 2e\right) n_{bracket}$$

$$\alpha = \tan^{-1}\left(\frac{h_v}{h_l}\right) = 0.75$$

$$e = e_s - h_l / 2 = 11.5 - 16/2 = 3.5 \text{ in.}$$

$$f_y t \sin^2 \alpha \left(\sqrt{4e^2 + h_l^2} - 2e\right) n_{bracket}$$

$$= 36 \times 0.5 \times \sin^2 0.75 \times \left(\sqrt{4 \times 3.5^2 + 16^2} - 2 \times 3.5\right) \times 2 = 175.03 \text{ kips}$$

$V_u = 90 \text{ kips} \leq 175.03 \text{ kips}$ O.K.

Greater loads can be supported by increasing the number of anchors.

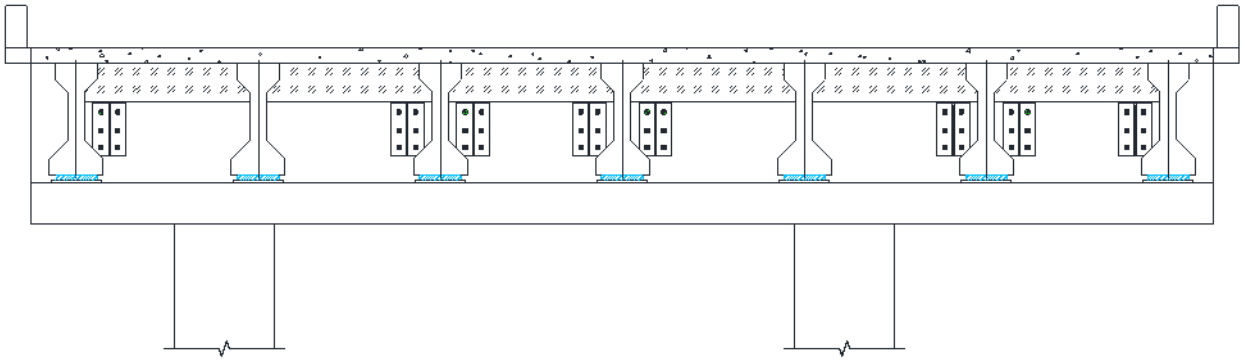

Figure C.8. Schematic View of Solution 6a Applied for Double-Column Bent.

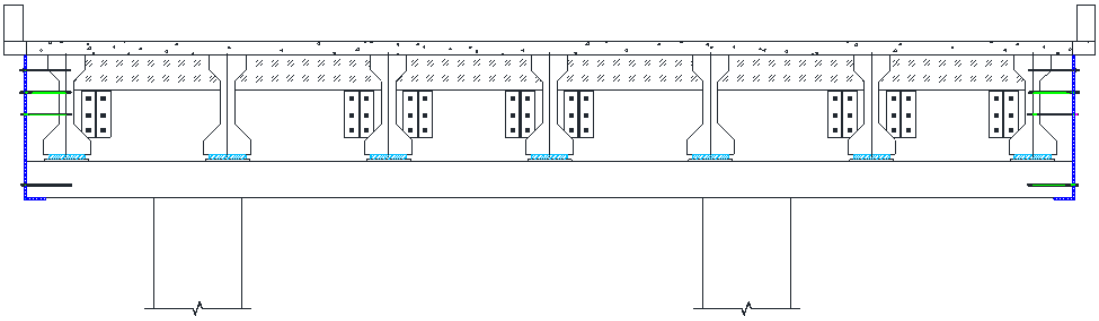

Figure C.9. Schematic View of Solution 6b Applied for Double-Column Bent.

C.6.4 Cost Table

Table C.9. Cost for Solution 6a per Bent.

No.	Description	Unit	Quantity per Item	No. of Items	Total Quantity	Rate/ Unit	Material Cost	Labor Cost	Equipment Cost
1	Boom Lift: 30 ft	HR	52	1	52	$16			$832
2	Construction Worker: three people	HR	52	3	156	$35		$5,460	
3	Rebar Locator	HR	0.25	24	6	$3			$18
4(a)	Hammer Drill, Horizontal, Web: 7/8 in. dia., 10.5 in. long	HR	0.25	96	24	$12			$288
4(b)	1"x14" Hammer Drill Bit	EA	1	1	1	$35	$35		
5(a)	Steel Bracket: 20"x15"x0.5", 16 in. wide, one triangular stiffener	LB	80	24	1920	$1.00	$1,920		
5(b)	Plasma Cutting: 0.5 in. thickness	IN	16	24	384	$5.00			$1,920
5(c)	Welder	HR	1	24	24	$50		$1,200	
5(d)	3/32" E7018 Stick Electrode	LB	2	24	48	$3	$144		
5(e)	Welding Wire	LB	1	24	24	$6	$144		
5(f)	Drilling Holes for Steel Bracket: 1 in. dia., 0.5 in. thickness	EA	6	24	144	$3		$432	
6(a)	Anchor Bolt: 1.25"x11.25"	EA	6	24	144	$24	$3,456		
6(b)	HIT-RE 100 Epoxy: 11.1 oz	EA	0.2	100	20	$15	$300		
6(c)	Manual Epoxy Dispenser	EA	1	1	1	$160	$160		
							$6,159	**$7,092**	**$3,058**
		Total Materials, Labor, and Equipment					**$16,309**		
		Mobilization					$4,000		
		Subtotal					**$20,309**		
		Contingencies (~20%)					$4,062		
		Total					**$25,000**		

Major Item

Table C.10. Cost for Solution 6b per Bent.

No.	Description	Unit	Quantity per Item	No. of Items	Total Quantity	Rate/ Unit	Material Cost	Labor Cost	Equipment Cost
1	Boom Lift: 30 ft	HR	72	1	72	$16			$1,152
2	Construction Worker: three people	HR	72	3	216	$35		$7,560	
3	Rebar Locator	HR	0.25	20	5	$3			$15
4(a)	Hammer Drill, Horizontal, Web: 7/8 in. dia., 10.5 in. long	HR	0.25	96	24	$12			$288
4(b)	1"x14" Hammer Drill Bit	EA	1	1	1	$81	$81		
5(a)	Steel Bracket: 20"x15"x0.5", 16 in. wide, one triangular stiffener	LB	80	20	1600	$1	$1,600		
5(b)	Plasma Cutting: 0.5 in. thickness	IN	16	20	320	$5			$1,600
5(c)	Welder	HR	1	20	20	$50		$1,000	
5(d)	3/32" E7018 Stick Electrode	LB	2	20	40	$3	$120		
5(e)	Welding Wire	LB	1	20	20	$6	$120		
5(f)	Drilling Holes for Steel Bracket: 1 in. dia., 0.5 in. thickness	EA	6	20	120	$3		$360	
6(a)	Anchor Bolt: 1.25"x11.25"	EA	6	20	120	$24	$2,880		
6(b)	HIT-RE 100 Epoxy: 11.1 oz	EA	0.2	96	20	$15	$300		
6(c)	Manual Epoxy Dispenser	EA	1	1	1	$160	$160		
7(a)	Hammer Drill, Horizontal, End Region: 1"x25"	HR	0.5	16	8	$12			$96
7(b)	1-1/4"x25" Hammer Drill Bit	EA			1	$100		$100	
8(a)	Telehandler: 30 ft long, 6000 lb capacity	HR			8	$20			$160
8(b)	Telehandler Operator	HR			8	$30		$240	
9(a)	End Plate: 1 in. thickness	LB	700	2	1400	$1	$1,400		
9(b)	Plasma Cutting 1" thickness	FT	35	2	70	$8			$560
9(c)	Welder	HR	1	2	2	$50		$100	
9(d)	3/32" E7018 Stick Electrode	LB	2	2	4	$3	$12		
9(e)	Welding Wire	LB	1	2	2	$6	$12		
9(f)	Drilling Holes for End Plate: 1.25 in. dia., 1 in. thickness	EA	5	2	10	$3		$30	
10(a)	Threadbar, End Region: 1 in. dia.	FT	3	16	48	$7	$336		
10(b)	Epoxy: 22 oz.	EA			3	$39	$117		
10(c)	Manual Epoxy Dispenser	EA			1	$160	$160		
10(d)	Washer: 1 in. dia	EA	1	10	10	$1	$10		
10(e)	Nut: 1 in. dia.	EA	1	10	10	$5	$50		
							$7,358	**$9,390**	**$3,871**
		Total Materials, Labor, and Equipment					**$20,619**		
		Mobilization					$5,000		
		Subtotal					**$25,619**		
		Contingencies (~20%)					$5,124		
		Total					**$31,000**		

Major Item

C.7 SOLUTION 7: THREADBAR HANGER WITH STEEL BRACKET

C.7.1 Introduction

The threadbars are anchored from the bottom of the ledges to the steel bracket. In addition, washers and nuts are placed at the middle of the threadbars to clamp the ledges as the threadbars penetrate the ledge. The anchoring bolts need to bear shear and tension forces transferred from the girders.

C.7.2 Anchor

Design of anchor bolts for this solution is similar to the previous solution described in Section B.2. The loads acting on the steel bracket are induced from the hanger thread rod and act at the center of the top steel plate as a point load. The eccentricity e of the load is 3 in. in this case, and the moment demand of the bolt group is determined as:

$$M_{u,N} = P_u e = 64.5 \times 3 = 193.5 \text{ kip} \cdot \text{in}$$

The arrangement of the bolts is determined based on the minimum spacing, edge distance, and location of the existing reinforcement. A total of four anchor bolts, in two layers (two bolts per layer), are used per bracket. The tension force demands for each bolt from the bottom to the top layer are:

$$N_{u1} = 6.2 \text{ kips}$$

$$N_{u2} = 18.7 \text{ kips}$$

The maximum tension force demand for a single bolt can be calculated as:

$$N_u = \frac{N_{u2}}{n_{bolt\_top\ layer}} = \frac{18.7}{2} = 9.35 \text{ kips}$$

■ Required Shear Force

Assume that the same product is used for all the bolts, and the shear force is evenly resisted by every anchor bolt. The required shear force per anchor bolt can be calculated as:

$$V_u = \frac{P_u}{n_{bolt}} = \frac{129}{8} = 16.1 \text{ kips}$$

■ Design Force

Adhesive anchors are used to hold the steel bracket.

Try Hilti HAS-E-B7 anchor rods with HIT-RE-100 epoxy (1.25 in. diameter and 11.25 in. embedment depth).

The design strengths of the adhesive anchor bolts provided by the manufacturer are as follows:

Tensile: $N_n = 26.39$ kips

Shear: $V_n = 47.24$ kips

And reduction factors based on the spacing are given as:

Tensile: $f_{AN} = 0.62$

Shear: $f_{AV} = 0.62$

Final design strength of a single bolt is:

Tensile: $N_d = f_{AN} N_n = 0.62 \times 26.39 = 16.36$ kips

Shear: $V_d = f_{AV} V_n = 0.62 \times 47.34 = 29.3$ kips

Check bolt strength:

Tensile: $N_d = 16.36 \text{ kips} > N_u = 9.35 \text{ kips}$ O.K.

Shear: $V_d = 29.3 \text{ kips} > V_u = 16.1 \text{ kips}$ O.K.

Check tension and shear interaction:

$$\left(\frac{N_u}{N_d}\right)^{\frac{5}{3}} + \left(\frac{V_u}{V_d}\right)^{\frac{5}{3}} = \left(\frac{9.35}{16.36}\right)^{\frac{5}{3}} + \left(\frac{16.1}{29.3}\right)^{\frac{5}{3}} = 0.76 \le 1.0 \quad \text{O.K.}$$

■ Minimum Spacing between Anchors

$s_{\min} = 6d_b = 6 \times 1.25 = 7.5$ in.

$s = 8$ in.

$\therefore s_{min} = 7.5\, in. \le s = 8$ in. O.K.

C.7.3 Threadbar

The threadbars manufactured by Williams Form Engineering Corp., which have a maximum tensile strength of 150 ksi, are used. A 1 in. diameter threadbar is selected for this solution, and the design strength is determined as:

$N_n = \phi f_u A_s = 0.75 \times 150 \times 0.85 = 95.63$ kips

Check thread rod strength:

$P_u / n_{rod} = 129/2 = 64.5 \text{ kips} < N_n = 95.63 \text{ kips}$ O.K.

C.7.4 Angle Bracket

■ Minimum Required Thickness and Weld Size

Bearing:

$$t_{bearing} \ge \frac{V_{u\_single}}{\phi 1.8 d_b f_y} = \frac{16.1}{0.75 \times 1.8 \times 1.25 \times 36} = 0.38 \text{ in.}$$

Shear yielding:

$$t_{s,y} \ge \frac{P_u / n_{bracket}}{\phi 0.6 h_v f_y} = \frac{129/2}{1 \times 0.6 \times 14 \times 36} = 0.25 \text{ in.}$$

Tension yielding:

$$t_{t,y} \ge \frac{P_u / n_{bracket}}{\phi b_v f_y} = \frac{129/2}{0.9 \times 16 \times 36} = 0.14 \text{ in.}$$

Shear rupture:

$$t_{s,r} \ge \frac{P_u / n_{bracket}}{\phi 0.6 h_n f_y} = \frac{P_u / n_{bracket}}{\phi 0.6 \left[h_v - \Sigma(d_i + 1/16)\right] f_y}$$

$$= \frac{129/2}{0.75 \times 0.6 \times \left[14 - (1.25 + 1/16) \times 2\right] \times 36} = 0.4 \text{ in.}$$

Tension rupture:

$$t_{t,r} \geq \frac{P_u / n_{bracket}}{\phi b_n f_y} = \frac{P_u / n_{bracket}}{\phi\left[b_v - \Sigma(d_i + 1/16)\right] f_y}$$

$$= \frac{129/2}{0.75 \times \left[16 - \left(1.25 + 1/16\right) \times 2\right] \times 36} = 0.11 \text{ in.}$$

Two triangular stiffeners are used in this solution. Weld size a is decided based on the required weld size with E70 electrodes:

$$a_{req} = \frac{f_{wr}}{\phi A_{we} F_{mv}}$$

$$f_{wr} = \sqrt{f_{wv}^2 + f_{wb}^2}$$

$$f_{wv} = \frac{P_u}{2 \cdot 2h_v} = 1.34 \text{ kip/in. } and \;\; f_{wb} = \frac{Me}{2 \cdot 2\left[\left(1 - h_v^2\right)/12\right]} = 2.02 \text{ kip/in.}$$

$$\therefore\; f_{wr} = \sqrt{1.34^2 + 2.02^2} = 2.42 \text{ kip/in.}$$

Required weld size:

$$a_{req} = \frac{f_{wr}}{\phi 0.707 \cdot 0.6 F_{EXX}} = \frac{2.42}{0.75 \times 0.707 \times 0.6 \times 70} = 0.11 \text{ in.}$$

Use weld size as $a = 0.125$ in. = $\left(\frac{1}{8} \text{ in.}\right)$.

Required plate thickness for maximum weld size:

$$t_w \geq \frac{aF_{EXX}}{0.93 f_y} = \frac{0.125 \times 70}{0.93 \times 36} = 0.26 \text{ in.}$$

Required thickness of triangular plate to avoid buckling failure:

$$t_{buckling} \geq \frac{h_l \sqrt{f_y}}{250} = \frac{16 \times \sqrt{36}}{250} = 0.144 \text{ in.}$$

Required thickness of bearing strength for eccentricity and weld size:

$$t_{eb} \geq \frac{P_u / n_{bracket}\left(6e_p - h_l/2\right)}{2 \cdot \phi 1.8 f_y h_l^2} = \frac{129/2 \times \left(6 \times 3 - 6/2\right)}{2 \times 0.75 \times 1.8 \times 3.6 \times 6^2} = 0.28 \text{ in.}$$

$$t_{min} = \max(t_{bearing}, t_{s,y}, t_{t,y}, t_{s,r}, t_{t,r}, t_{buckling}, t_{eb}) = 0.28 \text{ in.}$$

Use a 0.4375 in. $= \left(\frac{7}{16} \text{ in.}\right)$ thickness steel plate.

■ Strength of Triangular Plate (two triangular plates)

$$P_u \leq 2 f_y t \sin^2 \alpha \left(\sqrt{4e^2 + h_l^2} - 2e\right) n_{bracket}$$

$$\alpha = \tan^{-1}\left(\frac{h_v}{h_l}\right) = 1.17$$

$$e = e_s - h_l/2 = 3 - 6/2 = 0 \text{ in.}$$

$$2 f_y t \sin^2 \alpha \left(\sqrt{4e^2 + h_l^2} - 2e \right) n_{bracket}$$
$$= 2 \times 36 \times 0.4375 \times \sin^2 1.17 \times \left(\sqrt{4 \times 0^2 + 6^2} - 2 \times 0 \right) \times 2 = 302.4 \text{ kips}$$

$P_u = 129 \text{ kips} \leq 302.4 \text{ kips}$ O.K.

Greater loads can be supported by increasing the number of anchors.

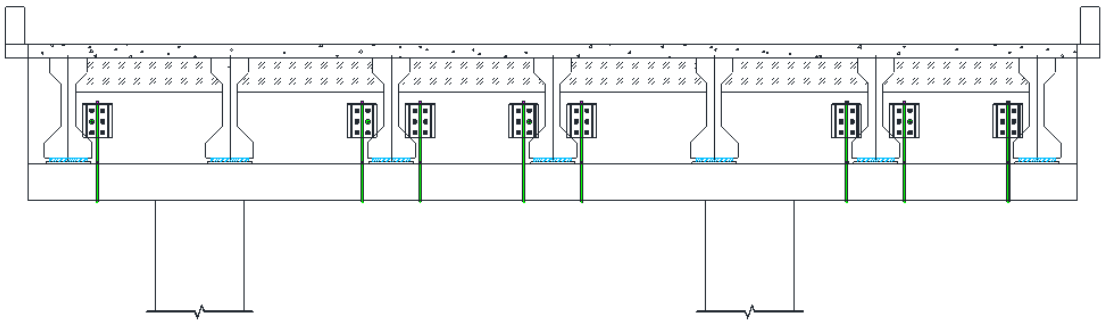

Figure C.10. Schematic View of Solution 7a Applied for Double-Column Bent.

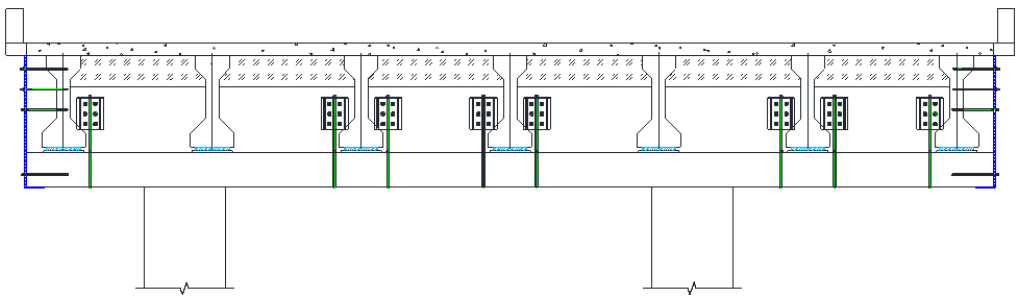

Figure C.11. Schematic View of Solution 7b Applied for Double-Column Bent.

C.7.5
Cost Table

Table C.11. Cost for Solution 7a per Bent.

No.	Description	Unit	Quantity per Item	No. of Items	Total Quantity	Rate/ Unit	Material Cost	Labor Cost	Equipment Cost
1	Boom Lift: 30 ft	HR			56	$16			$896
2	Construction Worker: three people	HR	56	3	168	$35		$5,880	
3	Rebar Locator	HR	0.5	16	8	$3			$24
4(a)	Hammer Drill, Horizontal, Web: 1-1/8 in. dia., 12 in. long	HR	0.25	64	16	$12			$192
4(b)	1-1/8"x17" Hammer Drill Bit	EA			1	$75		$75	
5(a)	Steel Bracket: 14"x7"x0.375", 16 in. wide, two triangular stiffener	LB	55	16	880	$1	$880		
5(b)	Plasma Cutting: 0.375 in. thickness	FT	18	16	288	$4			$1,152
5(c)	Welder	HR	1	16	16	$50		$800	
5(d)	3/32" E7018 Stick Electrode	LB	2	16	32	$3	$96		
5(e)	Welding Wire	LB	1	16	16	$6	$96		
5(f)	Drilling Holes for Steel Bracket: 1.25 in. dia., 0.375 in. thickness	EA	4	16	64	$2		$128	
6(a)	Anchor Bolt: 1"x14"	EA	4	16	64	$15	$960		
6(b)	HIT-RE 500 V3 Epoxy: 11.1 oz	EA	0.2	64	13	$57	$741		
6(c)	Manual Epoxy Dispenser	EA			1	$160	$160		
7(a)	Hammer Drill, Vertical, Ledge: 1-1/8 in. dia., 20 in. long	HR	0.5	16	8	$12			$96
7(b)	1-1/8"x21" Hammer Drill Bit	EA			1	$80		$80	
8(a)	Threadbar: 1 in. dia.	FT	5	16	80	$5	$400		
8(b)	Washer: 1 in. dia	EA	3	16	48	$1	$48		
8(c)	Nut: 1 in. dia	EA	3	16	48	$5	$240		
8(d)	Bearing Plate: 8"x45"x0.375"	LB	40	8	320	$1	$320		
8(e)	Plasma Cutting: 0.375 in. thickness	FT	9	8	72	$4			$288
8(f)	Drilling Holes for Bearing Plate: 1-1/4 in. dia., 0.375 in. thickness	EA	2	8	16	$2		$32	
8(g)	Torque Wrench and Multiplier	HR			8	$20			$160
							$3,941	**$6,995**	**$2,808**
		Total Materials, Labor, and Equipment					**$13,744**		
		Mobilization					$3,000		
		Subtotal					**$16,744**		
		Contingencies (~20%)					$3,349		
		Total					**$21,000**		

Major Item

Table C.12. Cost for Solution 7b per Bent.

No.	Description	Unit	Quantity per Item	No. of Items	Total Quantity	Rate/ Unit	Material Cost	Labor Cost	Equipment Cost
1	Boom Lift: 30 ft	HR			80	$16			$1,280
2	Construction Worker: three people	HR	80	3	240	$35		$8,400	
3	Rebar Locator	HR			10	$3			$30
4(a)	Hammer Drill, Horizontal, Web: 1-1/8 in. dia., 12 in. long	HR	0.25	48	12	$12			$144
4(b)	1-1/8"x17" Hammer Drill Bit	EA			1	$75		$75	
5(a)	Steel Bracket: 14"x7"x0.375", 16 in. wide, two triangular stiffener	LB	55	12	660	$1	$660		
5(b)	Plasma Cutting: 0.375 in. thickness	FT	18	12	216	$5			$1,080
5(c)	Welder	HR	1	12	12	$50		$600	
5(d)	3/32" E7018 Stick Electrode	LB	2	12	24	$3	$72		
5(e)	Welding Wire	LB	1	12	12	$6	$72		
5(f)	Drilling Holes for Steel Bracket: 1.25 in. dia., 0.375 in. thickness	EA	4	12	48	$2		$96	
6(a)	Anchor Bolt: 1"x14"	EA	4	12	48	$15	$720		
6(b)	HIT-RE 500 V3 Epoxy: 11.1 oz	EA	0.2	48	13	$57	$741		
6(c)	Manual Epoxy Dispenser	EA			1	$160	$160		
7(a)	Hammer Drill, Vertical, Ledge: 1-1/8 in. dia., 20 in. long	HR	0.5	12	6	$12			$72
7(b)	1-1/8"x21" Hammer Drill Bit	EA			1	$80		$80	
8(a)	Threadbar: 1 in. dia.	FT	5	12	60	$5	$300		
8(b)	Washer: 1 in. dia	EA	3	12	36	$1	$36		
8(c)	Nut: 1 in. dia	EA	3	12	36	$5	$180		
8(d)	Bearing Plate: 8"x45"x0.375"	LB	40	6	240	$1	$240		
8(e)	Plasma Cutting: 0.375 in. thickness	FT	9	6	54	$4			$216
8(f)	Drilling Holes for Bearing Plate: 1-1/4 in. dia., 0.375 in. thickness	EA	2	6	12	$2		$24	
8(g)	Torque Wrench and Multiplier	HR			8	$20			$160
9(a)	Hammer Drill, Horizontal, End Region: 1"x25"	HR	0.5	16	8	$12			$96
9(b)	1-1/4"x25" Hammer Drill Bit	EA	1	1	1	$100		$100	
10(a)	Telehandler: 30 ft long, 6000 lb capacity	HR	8	1	8	$20			$160
10(b)	Telehandler Operator	HR	8	1	8	$30		$240	
11(a)	End Plate: 1 in. thickness	LB	700	2	1400	$1	$1,400		
11(b)	Plasma Cutting 1" thickness	FT	35	2	70	$8			$560
11(c)	Welder	HR	1	2	2	$50		$100	
11(d)	3/32" E7018 Stick Electrode	LB	2	2	4	$3	$12		
11(e)	Welding Wire	LB	1	2	2	$6	$12		
11(f)	Drilling Holes for End Plate: 1.25 in. dia., 1 in. thickness	EA	5	2	10	$3		$30	
12(a)	Threadbar, End Region: 1 in. dia.	FT	3	16	48	$7	$336		
12(b)	Epoxy: 22 oz.	EA	3	1	3	$39	$117		
12(c)	Manual Epoxy Dispenser	EA	1	1	1	$160	$160		
12(d)	Washer: 1 in. dia	EA	1	10	10	$1	$10		
12(e)	Nut: 1 in. dia.	EA	1	10	10	$5	$50		
							$5,278	**$9,745**	**$3,798**
		Total Materials, Labor, and Equipment					**$18,821**		
		Mobilization					$4,000		
		Subtotal					**$22,821**		
		Contingencies (~20%)					$4,565		
		Total					**$28,000**		

Major Item

C.8 SOLUTION 8: CLAMPED THREADBAR WITH CHANNEL

C.8.1 Introduction

This solution uses threadbars to clamp the ledges of the inverted-T bent caps by anchoring them into the web with a steel channel.

C.8.2 Threadbar

■ Required Strength of Threadbar

$$F_{req} = \frac{V_u}{n_t \sin\theta} \text{ with } \theta = 90^\circ,$$

$$P_{req} = F_{req} n_t = \frac{V_u}{\sin\theta} = \frac{90 \times 2}{\sin 90^\circ} = 180 \text{ kips}$$

■ Design Strength of Threadbar

Among the bars listed in Table C.1, try a 1 in. diameter threadbar.
As a design strength of threadbars, the yield strength is used as:

$$T = A_s f_y = 0.85 \times 120 = 102 \text{ kips}$$

■ The Number of Threadbars

$$P_{req} = F_{req} n_t = 180 \text{ kips}$$

$$n_{t,req} = \frac{P_{req}}{R_n} = \frac{P_{req}}{T} = \frac{180}{102} = 1.76 \text{ ea.}$$

$$\therefore n_{t,req} = 1.76 \text{ ea.} \le n_t = 2 \text{ ea.}$$ O.K.

C.8.3 Bearing Plate

■ Required Thickness

$$t_{\min,req} = \frac{T_{pre} / n_t}{\phi 2.4 b_b f_u} \le t_s, \text{ where } T_{pre} = 0.6 A_s f_u = 0.6 \times 0.85 \times 150 = 76.5 \text{ kips}$$

$$t_{\min,req} = \frac{T_{pre}}{\phi 2.4 b_b f_u} = \frac{76.5}{0.75 \times 2.4 \times 1 \times 60} = 0.71 \text{ in.}$$

Use a 0.75 in. thickness plate.

■ Required Area

$$A_{b,req} = \frac{T_{pre}}{\phi_c 0.85 f_c'} = \frac{76.5}{0.65 \times 0.85 \times 3.6} = 38.46 \text{ in.}^2$$

Use either an 8 in. by 5 in. rectangular plate or a circular plate with 7 in. diameter.

C.8.4 Steel Channel

To have the required bearing strength, the thickness and the area of the steel channel should meet required thickness and area as described above.

Table C.13. Misc. Steel Channels (A36, W44).

Imperial Size	Depth *d* (in.)	Flange Width *b* (in.)	Flange Thickness *t* (in.)	Web Thickness *w* (in.)
MC10x41	10	4.32	0.575	0.796
MC12x45	12	4.01	0.7	0.71
MC12x50	12	4.14	0.7	0.835
MC13x50	13	4.41	0.61	0.787
MC18x58	18	4.2	0.625	0.7

Try MC 10×41, which has a web thickness of 0.796 in.

■ Check Compactness

$$\frac{b}{t} = \frac{4.313}{0.563} = 7.66$$

$$0.84\sqrt{\frac{E}{f_y}} = 0.38\sqrt{\frac{29000}{36}} = 10.79$$

$$\therefore \frac{b}{t} = 7.66 \le 0.38\sqrt{\frac{E}{f_y}} = 10.79$$ Compact Section

■ Check Flexural Force

$$M_u \le \min(F_y Z_y, 1.6 F_y S_y)$$

where $M_u = 163.8\ \text{kip}\cdot\text{in.}$, $F_y = 36$ ksi, $S_y = 5.64\ \text{in}^3$, and $Z_y = 9.49\ \text{in}^3$

$$\min(F_y Z_y, 1.6 F_y S_y) = \min(341.64, 279.36) = 279.36\ \text{kip}\cdot\text{in.}$$

$$\therefore M_u = 163.8\ \text{kip}\cdot\text{in} \le 379.36\ \text{kip}\cdot\text{in.}$$ O.K.

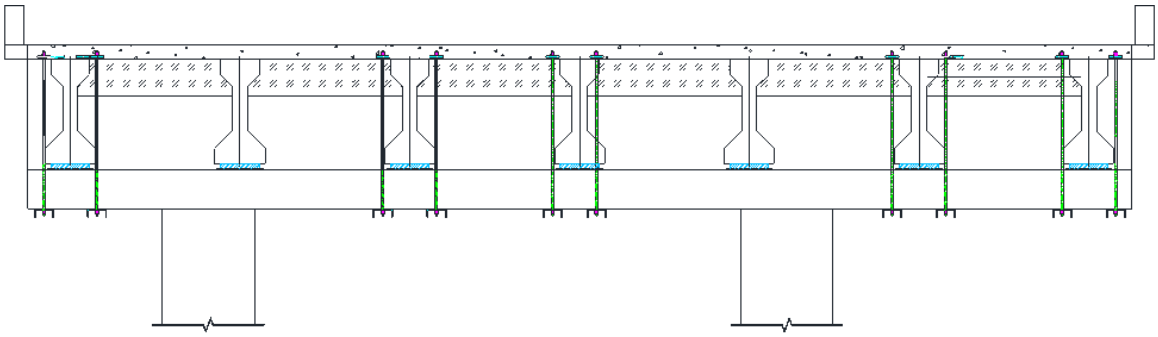

(a) For double-column bent

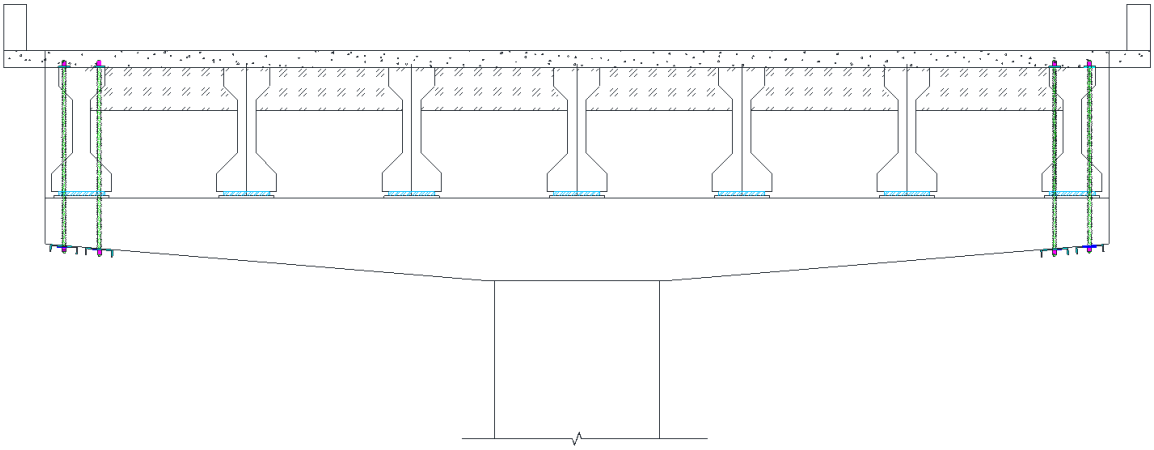

(b) For single-column bent

Figure C.12. Schematic View of Solution 8.

C.8.5
Cost Table

Table C.14. Cost for Solution 8 for a Double-Column Bent.

No.	Description	Unit	Quantity per Item	No. of Items	Total Quantity	Rate/ Unit	Material Cost	Labor Cost	Equipment Cost
1	Construction Worker: three people	HR	64	3	192	$35		$6,720	
2(a)	Slab Removal Equipment	SF	5	1	5	$55			$275
2(b)	Slab Removal Debris	SF	5	1	5	$22			$110
2(c)	Slab Removal Labor	HR	0.25	10	3	$60		$180	
3	Rebar Locator	HR	0.5	10	5	$3			$15
4	Core Drill Rig	HR	25	1	25	$12			$300
5(c)	Core Driller, Vertical, Web: 1-1/8 in. dia., 7 ft long	HR	2.5	10	25	$60		$1,500	
5(d)	1-1/8"x60" Diamond Core Drill Bit	EA	1	1	1	$365	$365		
5(e)	1-1/8"x24" Core Bit Extension	EA	1	1	1	$116	$116		
6	Boom Lift: 30 ft	HR	24	1	24	$16			$384
7(a)	Steel Channel-MC 10x41: 63 in. length	FT	6	10	60	$10	$600		
7(b)	Plasma Cutting 0.8" thickness	FT	2	10	20	$5			$100
7(c)	Drilling Holes for Steel Channel: 1.5 in. dia., 0.8 in. thickness	EA	4	20	80	$6		$480	
8(a)	Threadbar, Web: 1 in. dia.	FT	7	20	140	$5	$700		
8(b)	Washer: 1 in. dia.	EA	2	20	40	$1	$40		
8(c)	Nut: 1 in. dia.	EA	2	20	40	$5	$200		
8(d)	Bearing Plate: 7"x5"x0.75"	LB	8	20	160	$1	$160		
8(e)	Drilling Holes for Bearing Plate: 1 in. dia., 0.75 in. thickness	EA	1	20	20	$3		$60	
8(f)	Torque Wrench and Multiplier	HR	1	20	20	$20	-	-	$400
							$2,181	**$8,940**	**$1,584**
		Total Materials, Labor, and Equipment					**$12,705**		
		Mobilization					$3,000		
		Subtotal					**$15,705**		
		Contingencies (~20%)					$3,141		
		Total					**$19,000**		

Major Item

Table C.15. Cost for Solution 8 for a Single-Column Bent.

No.	Description	Unit	Quantity per Item	No. of Items	Total Quantity	Rate/ Unit	Material Cost	Labor Cost	Equipment Cost
1	Construction Worker: three people	HR	24	3	72	$35		$2,520	
2(a)	Slab Removal Equipment	SF	1	1	1	$55			$55
2(b)	Slab Removal Debris	SF	1	1	1	$22			
2(c)	Slab Removal Labor	HR	0.25	4	1	$60		$60	
3	Rebar Locator	HR	0.5	4	2	$3			$6
4	Core Drill Rig	HR	2.5	4	10	$12			$120
5(c)	Core Driller, Vertical, Web: 1 in. dia., 7 ft long	HR	2.5	4	10	$60		$600	
5(d)	1-1/8"x60" Diamond Core Drill Bit	EA	1	1	1	$365	$365		
5(e)	1-1/8"x24" Core Bit Extension	EA	1	1	1	$116	$116		
6	Boom Lift: 30 ft	HR	8	1	8	$16			$128
10(a)	Threadbar, Web: 5/8 in. dia.	FT	7	4	28	$5	$140		
10(b)	Washer: 5/8 in. dia.	EA	1	4	4	$10	$40		
10(c)	Nut: 5/8 in. dia.	EA	1	4	4	$15	$60		
10d)	Bearing Plate: 4"x4"x0.375"	LB	2	4	8	$1	$8		
10(e)	Drilling Holes for Bearing Plate: 3/4 in. dia., 0.375 in. thickness	EA	1	4	4	$3		$12	
10(f)	Torque Wrench and Multiplier	HR	1	4	4	$20	-	-	$80
							$729	**$3,192**	**$389**
		Total Materials, Labor, and Equipment					**$4,310**		
		Mobilization					$1,000		
		Subtotal					**$5,310**		
		Contingencies (~20%)					$1,062		
		Total					**$7,000**		

Major Item

C.9 SOLUTION 9: GROUTED THREADBARS ANCHORED WITH CHANNEL

C.9.1 Introduction

This solution uses grout to anchor the threadbar from the bottom of the ledge into the web anchored with a steel channel. The bonded threadbars should be used as internally anchored bars at the web when there is not enough gap to access the top of the web.

C.9.2 Threadbar

■ Required Strength of Threadbar

$$F_{req} = \frac{P_u}{n_t \sin\theta} \text{ with } \theta = 90^\circ,$$

$$P_{req} = F_{req} n_t = \frac{P_u}{\sin\theta} = \frac{129 \times 2}{\sin 90^\circ} = 258 \text{ kips}$$

■ Design Strength of Thread Rod

Use 1 in. diameter thread rod with ultimate strength of 150 ksi.

Bond strength with $h_{ef} = 40$ in. and $\tau = 1.5$ ksi :

$$N_{bond} = \tau \pi d_h h_{ef} = 1.5 \times \pi \times (1 + 1/16) \times 40 = 200.18 \text{ kips}$$

Yield strength:

$$T_d = A_s f_u = 127.5 \text{ kips}$$

$$R_n = \min(N_{bond}, T_d) = 127.5 \text{ kips}$$

■ The Number of Threadbars

$$P_{req} = F_{req} n_t = 180 \text{ kips}$$

$$n_{t,req} = \frac{P_{req}}{R_n} = \frac{180}{127.5} = 1.4 \text{ ea.}$$

$$\therefore n_{t,req} = 1.4 \text{ ea.} \le n_t = 2 \text{ ea.} \qquad \text{O.K.}$$

$$R_n n_t = 127.5 \times 2 = 255 \text{ kips} \ge P_{req} = 180 \text{ kips} \qquad \text{O.K.}$$

C.9.3 Steel Channel

■ Required Web Thickness

$$t_{\min,req} = \frac{V_u / n_t}{\phi 2.4 b_b f_u} \le t_s$$

$$t_{\min,req} = \frac{P_{req} / n_t}{\phi 2.4 b_b f_u} = \frac{180/2}{0.75 \times 2.4 \times 1 \times 60} = 0.83 \text{ in.}$$

■ Required Web Height

$$A_{b,req} = \frac{P_{req} / n_t}{\phi_c 0.85 f_c'} = \frac{180/2}{0.65 \times 0.85 \times 3.6} = 45.25 \text{ in.}^2$$

Use MC 12×50:

$$t_{min,req} = 0.83 \text{ in.} \le w = 0.835 \text{ in.} \qquad \text{O.K.}$$

$$A_b = d \times width\ of\ \ stem = 12 \times 30 = 360\ \text{in.}^2 \geq A_{b,req} = 42.25\ \text{in}^2 \quad \text{O.K.}$$

■ Check Compactness

$$\frac{b}{t} = \frac{4.14}{0.7} = 5.91$$

$$0.38\sqrt{\frac{E}{f_y}} = 0.38\sqrt{\frac{29000}{36}} = 10.79$$

$$\therefore \frac{b}{t} = 5.91 \leq 0.38\sqrt{\frac{E}{f_y}} = 10.79 \qquad \text{Compact Section}$$

■ Check Flexural Force

$$M_u \leq \min(F_y Z_y, 1.6 F_y S_y)$$

$$F_y = 36\ \text{ksi}$$

$$S_y = 5.64\ \text{in.}$$

$$\text{Z}_y = 10.9\ \text{in.}$$

$$\min(F_y Z_y, 1.6 F_y S_y) = \min(392.4, 324.86) = 324.86\ \text{kip} \cdot \text{in.}$$

$$M_u = 163.8\ \text{kip} \cdot \text{in}$$

$$\therefore M_u = 163.8\ \text{kip} \cdot \text{in.} \leq 324.86\ \text{kip} \cdot \text{in.} \qquad \text{O.K.}$$

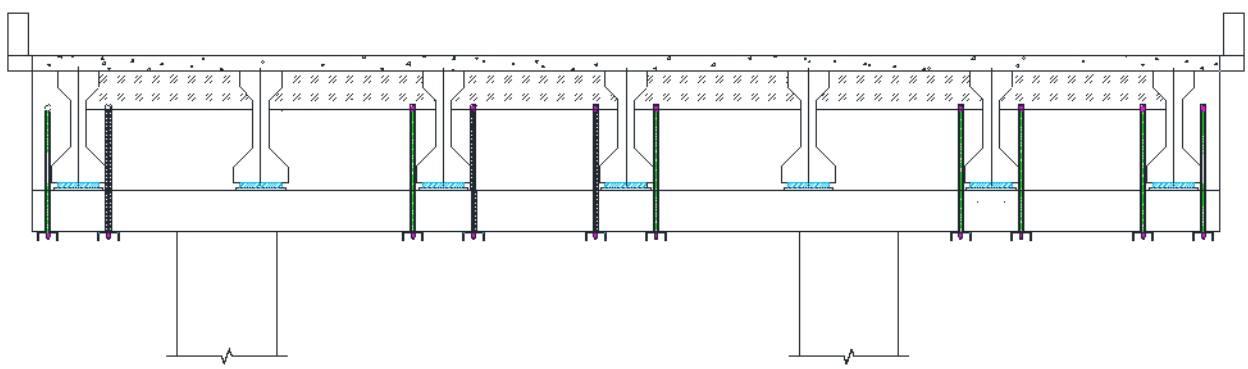

Figure C.13. Schematic View of Solution 9 Applied for Double-Column Bent.

C.9.4
Cost Table

Table C.16. Cost for Solution 9 per Bent.

No.	Description	Unit	Quantity per Item	No. of Items	Total Quantity	Rate/ Unit	Material Cost	Labor Cost	Equipment Cost
1	Boom Lift: 30 ft	HR	80	1	80	$16			$1,280
2	Construction Worker: three people	HR	80	3	240	$35		$8,400	
3	Rebar Locator	HR	0.5	10	5	$3			$15
4	Core Drill Rig	HR	48	1	48	$12			$576
5(a)	Core Driller, Vertical, Web: 1.5 in. dia., 6 ft long	HR	4	10	40	$60		$2,400	
5(b)	1-1/2"x60" Diamond Core Drill Bit	EA	1	1	1	$365	$365		
5(c)	1-1/2"x12" Core Bit Extension	EA	1	1	1	$100	$100		
6	Boom Lift: 30 ft	HR	40	1	40	$16			$640
7(a)	Steel Channel-MC 10x41: 63 in. length	FT	5	10	50	$10	$500		
7(b)	Plasma Cutting 0.8" thickness	FT	1.5	10	15	$5			$75
7(c)	Drilling Holes for Steel Channel: 1.5 in. dia., 0.8 in. thickness	EA	4	10	40	$6		$240	
8(a)	Hollow Threadbar, Web: 1.5 in. dia.	FT	6	10	60	$5	$300		
8(b)	Washer: 1 in. dia.	EA	1	10	10	$1	$10		
8(c)	Nut: 1 in. dia.	EA	1	10	10	$5	$50		
9(a)	Grout 0.45 ft^3 bag	EA	1	1	1	$10	$10		
9(b)	Grout Mixer	HR	1	1	1	$6			$6
9(c)	Grout Pump	HR	5	1	5	$6			$30
							$1,335	**$11,040**	**$2,622**
		Total Materials, Labor, and Equipment					**$14,997**		
		Mobilization					$3,000		
		Subtotal					**$17,997**		
		Contingencies (~20%)					$3,600		
		Total					**$22,000**		

Major Item

C.10 SOLUTION 10: ANCHORED FRP WRAP FOR DOUBLE-COLUMN BENTS

C.10.1 Introduction

FRP strips are attached to the web and ledge in critical regions on either side of the girder for strengthening the inverted-T bent cap. Steel angles are mechanically anchored at the reentrant corner at the web-ledge interface by anchor bolts to solve the debonding issue at the corner. FRP anchors are provided near the mid-depth of the web to provide additional anchorage to FRP strips.

C.10.2 FRP Strip

The FRP strips are attached all around to the inverted-T bent cap except at the top of the web due to limited accessibility. The wrapping scheme of the FRP strip is similar to the three-side bonded "U-wrap" shape as defined in ACI 440.2R (ACI Committee 440, 2008). A CF fabric Tyfo SCH-41-2X, which has a tensile strength of 121 ksi, is used for the retrofit. FRP properties specified by the manufacturer are as follows:

Tensile modulus:

$E_f = 11900$ ksi

Thickness:

$t_f = 0.08$ in.

Rupture strain:

$\varepsilon_u = 0.085$

Number of FRP layers:

$n = 1$

Since the FRP strips are anchored at the end region and reentrant corner, the effective strain of the FRP strip is taken as 0.004 in accordance with ACI 440.2R:

$\varepsilon_{fe} = 0.004$

Effective stress on FRP strip:

$f_{fe} = \varepsilon_{fe} E_f = 0.004 \times 11900 = 47.60$ ksi

Width of a single FRP strip:

$w_f = 16$ in.

Effective sectional area of FRP strip per girder:

$A_{vf} = 2nt_f w_f = 2 \times 1 \times 0.08 \times 16 = 2.56$ in.^{2}

Inclination angle of FRP strip:

$\alpha = 90°$

Nominal strength of FRP strip:

$$V_f = A_{fv} f_{fe} (\sin\alpha + \cos\alpha)$$

$$= 2.56 \times 47.60 \times (1 + 0) = 121.86 \text{ kips}$$

Reduction factor for FRP shear reinforcement based on wrapping scheme (ACI 440.2R):

$\psi_f = 0.85$

Reduced strength of FRP strip:

$\psi_f V_f = 0.85 \times 121.86 = 103.51$ kips

Shear deficiency of the bent cap (i.e., required strength of FRP strip):

$V_u = 90$ kips

Check FRP strength:

$\psi_f V_f = 103.51 \text{ kips} > V_u = 90 \text{ kips}$ O.K.

C.10.3 Anchor and Steel Angle

Steel angles are anchored using mechanical anchor bolts on either reentrant corner of the bent cap to avoid the FRP strips peeling off from the corner. As shown in Figure C.14, anchor bolts are designed to simultaneously resist tension and shear forces. The inclined load acting from the reentrant corner is assumed to have the same magnitude as the shear load demand. Load demand per side is:

$$P_u = \frac{90}{2} = 45 \text{ kips}$$

Load demand for the anchor bolt group on each side is determined as:

Tensile force: $N_u = \sin\alpha P_u = \sin 45° \times 45 = 31.8$ kips

Shear force: $V_u = \sin\alpha P_u = \sin 45° \times 45 = 31.8$ kips

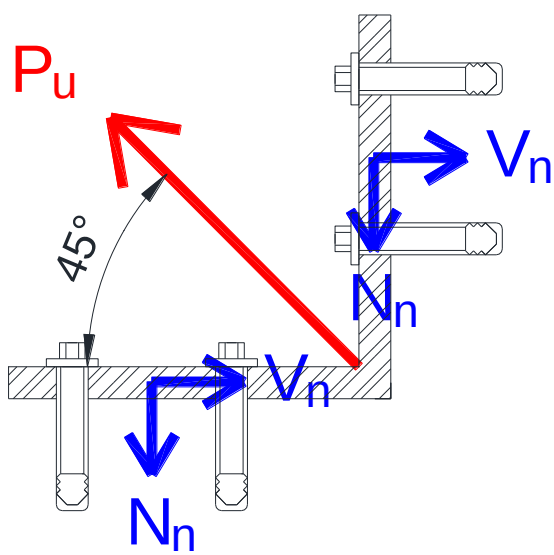

Figure C.14. Load Acting on Steel Angle and Anchor Bolt Group.

C.10.3.1 Anchor Bolt

A mechanical anchor bolt, Power bolt+ with a diameter of 0.75 in., manufactured by Power Fasteners, is used for anchoring the steel angle to prevent detachment of the FRP at the edges. A steel angle plate with dimensions of 12 in. × 12 in. × 1 in. is used. Four bolts are installed on each side of the steel angle with 8 in. spacing, 5 in. edge distance, and 4.75 in. embedment depth.

Design bolt strength of Power bolt+ (Powers Product Manual, 2015):
Tensile: $N_n = 14.5$ kips
Shear: $V_n = 14.8$ kips
Reduction factors based on the spacing:
Tensile: $\phi_t = 0.77$
Shear: $\phi_s = 0.84$
Strength of the bolt group:
Tensile: $N_d = 6 \cdot \phi_t N_t = 6 \times 0.77 \times 14.5 = 67$ kips
Shear: $V_d = 6 \cdot \phi_s V_n = 6 \times 0.84 \times 14.8 = 74.6$ kips
Check strength of the bolt group:
Tensile: $N_d = 67 \text{ kips} > N_u = 31.8 \text{ kips}$ O.K.
Shear: $V_d = 74.6 \text{ kips} > V_u = 31.8 \text{ kips}$ O.K.
Check tension and shear interaction:

$$\left(\frac{N_u}{N_d}\right)^{\frac{5}{3}} + \left(\frac{V_u}{V_d}\right)^{\frac{5}{3}} = \left(\frac{31.8}{67}\right)^{\frac{5}{3}} + \left(\frac{31.8}{74.6}\right)^{\frac{5}{3}} = 0.53 \le 1.0 \quad \text{O.K.}$$

C.10.3.2 Steel Angle

Required thickness for bearing strength:

$$t_{bearing} \ge \frac{V_u / n_{bolt}}{\phi 2.4 d_b f_y} = \frac{31.8/4}{0.75 \times 2.4 \times 0.75 \times 36} = 0.16 \text{ in.}$$

Height of the leg:
$h_v = 12$ in.
Required thickness for shear yielding:

$$t_{s,y} \ge \frac{V_u}{\phi 0.6 h_v f_y} = \frac{31.8}{1 \times 0.6 \times 12 \times 36} = 0.12 \text{ in.}$$

Nominal height of the leg:

$$h_n = h_v - \sum\left(d_{b,i} + \frac{1}{16}\right) = 12 - 2 \times \left(\frac{3}{4} + \frac{1}{16}\right) = 10.4 \text{ in.}$$

Required thickness for shear rupture:

$$t_{s,r} \ge \frac{V_u}{\phi 0.6 h_n f_y} = \frac{31.8}{0.75 \times 0.6 \times 10.4 \times 36} = 0.19 \text{ in.}$$

Width of the leg:
$b_v = 16$ in.
Required thickness for tension yielding:

$$t_{t,y} \ge \frac{N_u}{\phi b_v f_y} = \frac{31.8}{0.9 \times 16 \times 36} = 0.06 \text{ in.}$$

Nominal width of the leg:

$$b_n = b_v - \sum\left(d_{b,i} + \frac{1}{16}\right) = 16 - 2 \times \left(\frac{3}{4} + \frac{1}{16}\right) = 14.4 \text{ in.}$$

Required thickness for tension rupture:

$$t_{t,r} \geq \frac{N_u}{\phi b_n f_y} = \frac{44.4}{0.75 \times 14.4 \times 36} = 0.08 \text{ in.}$$

The critical section of the steel angle is taken at 3/8 in. from the face of the angle. Try a thickness of 0.5 in.

Eccentricity of the load (i.e., moment arm):

$$e = t_{angle} + \frac{3}{8} = 0.5 + \frac{3}{8} = 0.875 \text{ in.}$$

Required thickness for bending moment at critical section:

$$t_m \geq \sqrt{\frac{4V_u e}{\phi_f L f_y}} = \sqrt{\frac{4 \times 31.8 \times 0.875}{0.9 \times 16 \times 36}} = 0.46 \text{ in.}$$

Check angle thickness:

$$t_{angle} = 0.5 \text{ in.} > t_m = 0.46 \text{ in.} \qquad \text{O.K.}$$

Use a 0.5 in. thick steel angle.

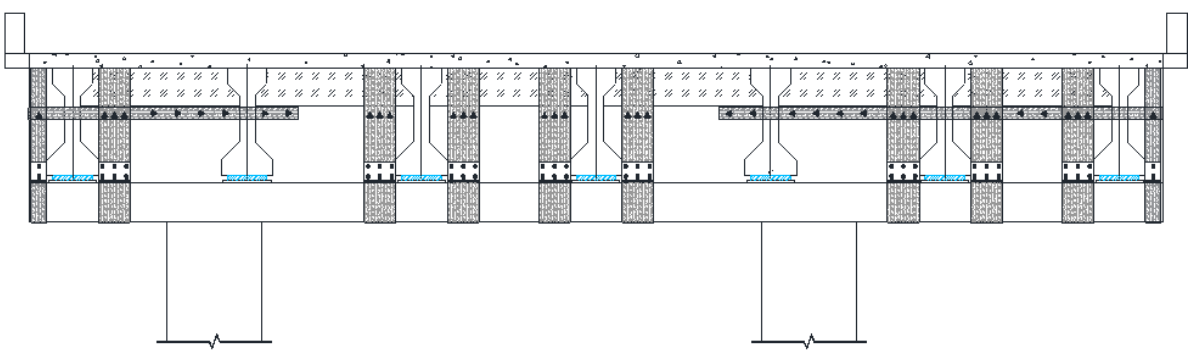

(a) For double-column bent

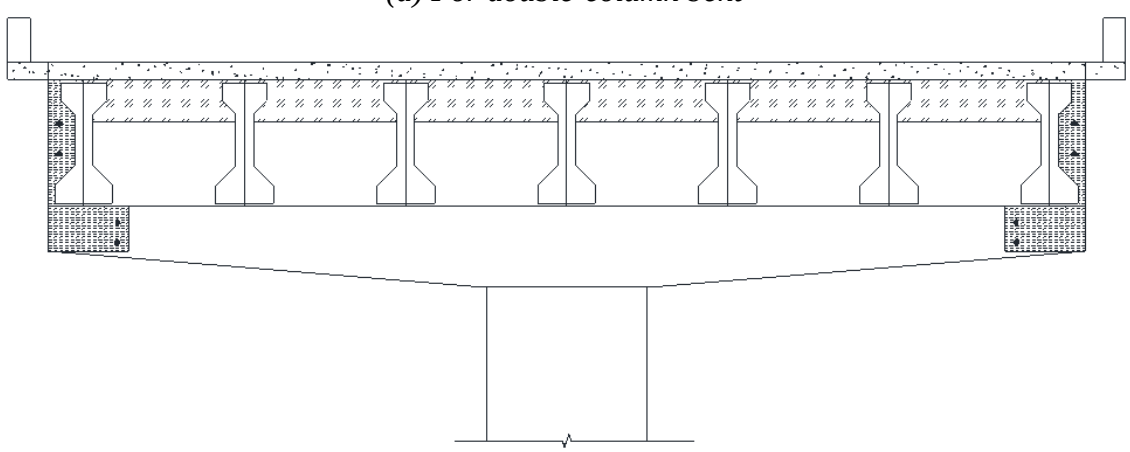

(b) For single-column bent

Figure C.15. Schematic View of Solution 10 Applied for Double-Column Bent.

C.10.4 Cost Table

Table C.17. Cost for Solution 10 for a Double-Column Bent.

No.	Description	Unit	Quantity per Item	No. of Items	Total Quantity	Rate/ Unit	Material Cost	Labor Cost	Equipment Cost
1	Boom Lift: 30 ft	HR	8	12	96	$16			$1,536
2	Construction Worker: three people	HR	96	3	288	$30		$8,640	
3	Grinder	HR	2	12	24	$7			$168
4	Rebar Detector	HR	2	10	20	$3			$60
5(a)	Hammer Drill	HR	1	12	12	$10			$120
5(b)	Hammer Drill Bit for FRP Anchor : 1/2 in. dia. 12 in.	EA	-	-	2	$33	$66		
5(c)	Hammer Drill Bit for Anchor Bolts: 3/4 in dia. 8 in	EA	-	-	2	$35	$70		
6(a)	0.08 in. thick CFRP sheet : int. ver. 250 in x16 in	YD	7	8	56	$87	$4,853		
6(b)	0.08 in. thick CFRP sheet: ext. ver. strip 250in x 8in	YD	7	2	14	$43	$607		
6(c)	0.08 in. thick CFRP sheet: left lateral strip, 270 in x 6 in	YD	8	1	8	$33	$260		
6(d)	0.08 in. thick CFRP sheet: right Lateral Strip, 510 in. x 6 in.	YD	15	2	30	$31	$915		
6(e)	Epoxy Resin + Hardener: 1.25gal kit	EA			8	$70	$560		
6(f)	FRP Anchor: 0.5 in.dia	EA			64	$30	$1,920		
7(a)	Steel Angle: 12"x12"x0.625"	LB	65	16	1040	$2	$2,080		
7(b)	Plasma Steel Cutting 0.625" thick	FT	2	20	40	$5	$200		
7(c)	Drilling Holes for Steel Angle: 7/8 in. dia., 0.625 in. thickness	EA	12	20	240	$3		$720	
8	Anchor Bolt: Power Bolt+ 4.5 in. x 0.75 in.	EA			160	$4	$640		
							$12,171	**$9,360**	**$1,884**
		Total Materials, Labor, and Equipment					**$23,415**		
		Mobilization					$5,000		
		Subtotal					**$28,415**		
		Contingencies (~20%)					$5,683		
		Total					**$35,000**		

Major Item

Table C.18. Cost for Solution 10 for a Single-Column Bent.

No.	Description	Unit	Quantity per Item	No. of Items	Total Quantity	Rate/ Unit	Material Cost	Labor Cost	Equipment Cost
1	Boom Lift: 30 ft	HR			36	$16			$576
2	Construction Worker: three people	HR	36	3	108	$30		$3,240	
3	Grinder	HR	4	2	8	$7			$56
4	Rebar Detector	HR	2	2	4	$3			$12
5(a)	Hammer Drill	HR	4	2	8	$10			$80
5(b)	Hammer Drill Bit for FRP Anchor : 0.5 in. dia. 12 in.	EA	-	-	1	$33	$33		
6(a)	0.08 in. thick CFRP sheet : external vertical strip	SQFT	65	2	130	$22	$2,860		
6(b)	0.08 in. thick CFRP sheet: external lateral strip	SQFT	19	2	38	$22	$836		
6(d)	Epoxy Resin + Hardener: 1.25gal kit	EA			5	$70	$350		
6(e)	FRP Anchor: 0.5 in.dia	EA	14	2	28	$30	$840		
							$4,919	**$3,240**	**$724**
		Total Materials, Labor, and Equipment					**$8,883**		
		Mobilization					$2,000		
		Subtotal					**$10,883**		
		Contingencies (~20%)					$2,177		
		Total					**$14,000**		

Major Item

C.11 SOLUTION 11: CONCRETE INFILL WITH PRESTRESSING THREADBARS

C.11.1 Introduction

This retrofit solution is proposed to provide additional load paths by transforming the inverted-T bent cap into an I-shaped bent cap. The gap between the web of the inverted-T bent cap and the diaphragms is filled with concrete to form a flange-hung double-T shape to bypass the loads to the column. Prestressed threadbars are installed through the diaphragms to induce prestress force through the newly formed flange to the main body of the inverted-T bent cap.

C.11.2 Prestressing Threadbar

Design of the prestressed threadbars is similar to that of the prestressed high-strength threadbar retrofit solution. The prestressed threadbars are designed to resist shear force induced from the deck live load and the weight of the newly formed flange. It is assumed that each bar equally resists the shear force. The width of the gap between the diaphragm and web of the bent cap is 7.5 in. Concrete is infilled through the entire length of the bent; therefore, the tributary width of one girder is equal to the girder spacing (88 in.). The weight of the newly formed flange is determined by the area of the shaded part shown in Figure C.16 multiplied by the width of the gap:

$$A_f = 88 \times 18.75 - 282 = 1368 \text{ in.}^2$$

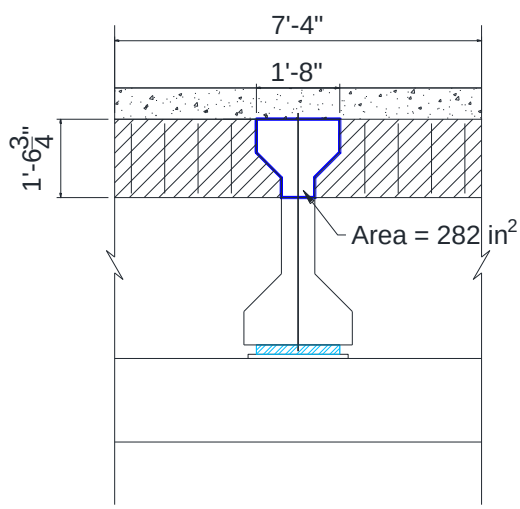

Figure C.16. Elevation View of Newly Formed Flange.

Assume that normal weight concrete with a unit weight of 0.15 kcf is used for the infill. Then, the factored weight of the newly formed flange can be obtained as:

$$W_f = 1.25 \times \frac{0.15 \times (1368 \times 7.5)}{12^3} = 1.11 \text{ kips/girder}$$

The load demand per one girder is:

$$P_{girder} = 129 + 1.11 = 130.11 \text{ kips}$$

This solution uses infilled concrete and threadbars to transform the whole bent cap section into an I-shaped girder. Therefore, the threadbar should resist the load induced from both sides of the bent cap. The whole load demand for the thread rod is:

$$P_u = n_{girder} P_{girder} = 2 \times 130.11 = 260.22 \text{ kips}$$

Threadbars that have a maximum tensile strength of 150 ksi are used. Both the design prestressing force and shear strength of the threadbar is 60 percent of the ultimate stress provided by the manufacturer. Based on the prestress and shear capacity of the threadbars, four threadbars with 1 in. diameter and 0.85 in^2 net area are used. The total shear strength of the threadbar is:

$$V_n = 0.6 \cdot n_{bar} f_u A_n = 0.6 \times 4 \times 150 \times 0.85 = 306 \text{ kips} > P_u = 260.22 \text{ kips} \quad \text{O.K.}$$

The first threadbar is placed 20 in. away from the centerline of the girder, and the rest of the rods are spaced equally with a spacing of 24 in., based on the consideration of minimum spacing:

$$s_{\min} = 6d_b = 6 \times 1 = 6 \text{ in.}$$

Note that the prestressed threadbar is placed 6 in. from the bottom face of the diaphragm to ensure an available load path from the deck to the threadbars. The negative moment caused by the eccentric prestress is ignored since the concrete deck is expected to have sufficient stiffness to resist the negative moment.

C.11.3 Steel Bearing Plate

■ Required Thickness of Bearing Steel Plate

$$t_{\min,req} = \frac{R_n}{\phi 2.4 b_b f_u} \le t_s$$

Since the purpose of the bars is to strengthen the structure, the yield strength of the plate is used instead of the ultimate strength to ensure that there is no effect on the original structure:

$$t_{\min,req} = \frac{R_n}{\phi 2.4 d_b f_u} = \frac{P_u / n_{bar}}{\phi 2.4 d_b f_y} = \frac{260.22/4}{0.75 \times 2.4 \times 1 \times 36} = 1 \text{ in.}$$

A 1 in. thick steel plate should be used for the bearing steel plate.

■ Required Bearing Area

$$A_{b,req} = \frac{P_u / n_{bar}}{\phi_c 0.85 f_c^{'}} = \frac{260.22/4}{0.65 \times 0.85 \times 3.6} = 32.7 \text{ in.}^2$$

A square steel plate with 6 in. sides is used.

C.11.4 Stirrup

To prevent shear failure of the newly formed flange, stirrups are placed in the gap between the diaphragm and the web of the bent cap. Assume the clear cover of the newly formed concrete section is 2.25 in. The shear strength of the concrete part is determined using:

$$V_c = 2\lambda \sqrt{f_c^{'}} b_w d = 2 \times 1 \times \sqrt{3600} \times 15.5 \times 16.5 = 30.7 \text{ kips}$$

Required stirrup strength:

$$V_s = V_u/\phi - V_c = \left(P_{girder}/2\right)/\phi - V_c$$

$$= (130.11/2)/0.75 - 30.7 = 56 \text{ kips}$$

Use No. 5 double-legged stirrups with a yield strength of $f_{yt} = 60$ ksi :

$$A_v = 2 \times 0.31 = 0.62 \text{ in.}^2$$

Required stirrup spacing to resist shear force:

$$s \le \frac{A_v f_{yt} d}{V_u/\phi - V_c} = \frac{A_v f_{yt} d}{V_s} = \frac{0.62 \times 60 \times 16.5}{56} = 11 \text{ in.}$$

Maximum spacing of the stirrups is lesser of:

$$s \le \frac{d}{2} = \frac{16.5}{2} = 8.25 \text{ in.} \qquad \text{Governs}$$

$$s \le \frac{A_v f_y}{0.75\sqrt{f_c'}\, b_w} = \frac{0.62 \times 60000}{0.75 \times \sqrt{3600} \times 15.5} = 53.3 \text{ in.}$$

$$s \le \frac{A_v f_y}{50 b_w} = \frac{0.62 \times 60000}{50 \times 15.5} = 48 \text{ in.}$$

Place the first stirrup 6 in. from the surface of the girder and then distribute stirrups with an even spacing of 8 in. on center.

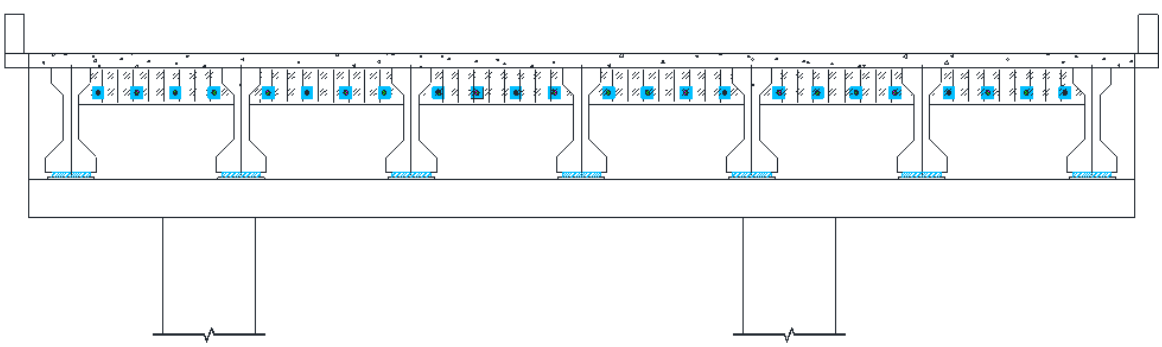

Figure C.17. Schematic View of Solution 11a Applied for Double-Column Bent.

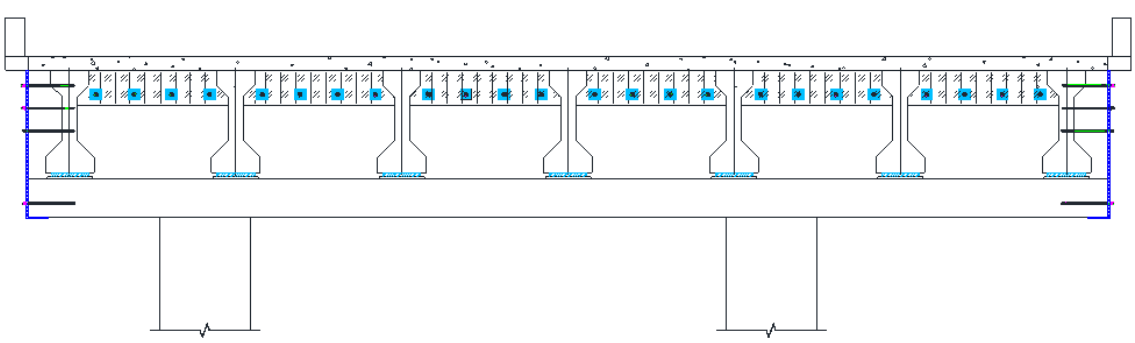

Figure C.18. Schematic View of Solution 11b Applied for Double-Column Bent.

C.11.5
Cost Table

Table C.19. Cost for Solution 11a per Bent.

No.	Description	Unit	Quantity per Item	No. of Items	Total Quantity	Rate/ Unit	Material Cost	Labor Cost	Equipment Cost
1	Boom Lift: 30 ft	HR			90	$10			$900
2(a)	Telehandler: 30 ft long, 6000 lb capacity	HR			90	$20			$1,800
2(b)	Telehandler Operator	HR			90	$30		$2,700	
3	Construction Worker: three people	HR	90	3	270	$30		$8,100	
4	Rebar Detector	HR	2	10	20	$3			$60
4(a)	Core Driller, Horizontal, Web+Diaphragm: 1.5 in. dia., 63 in. long	HR	2.5	18	45	$60		$2,700	
4(b)	1-1/2"x60" Diamond Core Drill Bit	EA			1	$365	$365		
5	Threadbar: 1 in. dia.	FT	6	18	108	$5	$540		
6(a)	Bearing Plate	LB	10.1	36	363.6	$1	$364		
6(b)	Plasma Cutting 1" thickness	FT	0.6	18	10.8	$6			$65
6(c)	Drilling Holes for Bearing Plate: 1.25 in. dia. 1in. Thick	EA	1	18	18	$4	$63		
6(d)	Washer: 1 in. dia	EA	1	54	54	$1	$54		
6(e)	Nut: 1 in. dia	EA	1	54	54	$5	$270		
6(f)	Torque Wrench and Multiplier	HR			9	$20			$180
7(a)	Concrete	CY			2.5	$125	$313		
7(b)	Rebar #5	LB			293.4	$0.63	$185		
7(c)	Formwork: plywood 12' 2"x4"	SF	1.5	49	73.5	$0.75	$55		
7(d)	Formwork: plywood 4'x8'	SF	32	3	96	$2	$144		
7(e)	Stirrups #5 Double Leg	LB	3.04	48	145.92	$0.63	$92		
							$2,444	**$13,500**	**$3,005**
		Total Materials, Labor, and Equipment					**$18,949**		
		Mobilization					$4,000		
		Subtotal					**$22,949**		
		Contingencies (~20%)					$4,590		
		Total					**$28,000**		

Major Item

Table C.20. Cost for Solution 11b per Bent.

No.	Description	Unit	Quantity per Item	No. of Items	Total Quantity	Rate/ Unit	Material Cost	Labor Cost	Equipment Cost
1	Boom Lift: 30 ft	HR			110	$10			$1,100
2(a)	Telehandler: 30 ft long, 6000 lb capacity	HR			110	$20			$2,200
2(b)	Telehandler Operator	HR			110	$30		$3,300	
3	Construction Worker: three people	HR	110	3	330	$30		$9,900	
4	Rebar Detector	HR	2	11	22	$3			$66
4(a)	Core Driller, Horizontal, Web+Diaphragm: 1.5 in. dia., 63 in. long	HR	2.5	18	45	$60		$2,700	
4(b)	1-1/2"x60" Diamond Core Drill Bit	EA			1	$365	$365		
5	Threadbar: 1 in. dia.	FT	6	18	108	$5	$540		
6(a)	Bearing Plate	LB	10.1	36	363.6	$1	$364		
6(b)	Plasma Cutting 1" thickness	FT	0.6	18	10.8	$6			$65
6(c)	Drilling Holes for Bearing Plate: 1.25 in. dia. 1in. Thick	EA	1	18	18	$4	$63		
6(d)	Washer: 1 in. dia	EA	1	54	54	$1	$54		
6(e)	Nut: 1 in. dia	EA	1	54	54	$5	$270		
6(f)	Torque Wrench and Multiplier	HR			9	$20			$180
7(a)	Concrete	CY			2.5	$125	$313		
7(b)	Rebar #5	LB			293.4	$0.63	$185		
7(c)	Formwork: plywood 12' 2"x4"	SF	1.5	49	73.5	$0.75	$55		
7(d)	Formwork: plywood 4'x8'	SF	32	3	96	$2	$144		
7(e)	Stirrups #5 Double Leg	LB	3.04	48	145.92	$0.63	$92		
8(a)	Hammer Drill, Horizontal, End Region: 1"x25"	HR	0.5	16	8	$12			$96
8(b)	1-1/4"x25" Hammer Drill Bit	EA	1	1	1	$100		$100	
9(a)	Telehandler: 30 ft long, 6000 lb capacity	HR	8	1	8	$20			$160
9(b)	Telehandler Operator	HR	8	1	8	$30		$240	
10(a)	End Plate: 1 in. thickness	LB	700	2	1400	$1	$1,400		
10(b)	Plasma Cutting 1" thickness	FT	35	2	70	$8			$560
10(c)	Welder	HR	1	2	2	$50		$100	
10(d)	3/32" E7018 Stick Electrode	LB	2	2	4	$3	$12		
10(e)	Welding Wire	LB	1	2	2	$6	$12		
10(f)	Drilling Holes for End Plate: 1.25 in. dia., 1 in. thickness	EA	5	2	10	$3		$30	
11(a)	Threadbar, End Region: 1 in. dia.	FT	3	16	48	$7	$336		
11(b)	Epoxy: 22 oz.	EA	3	1	3	$39	$117		
11(c)	Manual Epoxy Dispenser	EA	1	1	1	$160	$160		
11(d)	Washer: 1 in. dia	EA	1	10	10	$1	$10		
11(e)	Nut: 1 in. dia.	EA	1	10	10	$5	$50		
							$4,541	**$16,370**	**$4,427**
		Total Materials, Labor, and Equipment					**$25,338**		
		Mobilization					$6,000		
		Subtotal					**$31,338**		
		Contingencies (~20%)					$6,268		
		Total					**$38,000**		

Major Item

C.12 SOLUTION 12: CONCRETE INFILL WITH HANGER THREADBARS

C.12.1 Introduction

The web of the inverted-T bent cap is made thicker by a concrete infill so that the bent cap behaves as an I-beam. The hanger threadbars are vertically cast inside the concrete infill to transfer the ledge load to the top of the web and distribute it through reactions of the bearing steel plate. A lateral prestressed threadbar is also installed through the diaphragms. The lateral rod is designed to suspend the load transferred by the hanger threadbars, and to transfer the load to the web. It also induces prestress through diaphragms to connect the diaphragms, infilled concrete, and main body of the bent cap to form an integral system.

C.12.2 Hanger Thread Bar

■ Required Strength of Hanger Threadbar

The weight of infilled concrete is computed similar to the solution using concrete infill with prestressing threadbar:

$$W_c = 1.25 \times \frac{0.15 \times (1833 \times 7.5)}{12^3} = 6.37 \text{ kips/girder}$$

$$P_{req} = V_u + W_c = 129 + 6.37 = 135.4 \text{ kips}$$

■ Design Strength of Threadbar

Steel tensile strength of thread rod with 1 in. diameter:

$$T_d = 0.6 A_s f_u = 0.6 \times 0.85 \times 150 = 76.5 \text{ kips}$$

Pullout strength:

$$N_{pn} = \psi_{c,P} N_p$$

$$N_p = 8 A_{brg} f_c^{'}$$

For bearing area A_{brg}, assume bearing thickness $t = 1$ in. Then:

$$A_{brg} = 2\pi r t = 2 \times \pi \times 1 \times 1 = 6.3 \text{ in.}^2$$

$$N_p = 8 A_{brg} f_c^{'} = 8 \times 6.3 \times 3.6 = 181.44 \text{ kips}$$

Since there is no eccentricity, $\psi_{c,P} = 1.0$. Therefore:

$$N_{c,P} = 1.0 \times 181.44 = 181.44 \text{ kips}$$

Side blowout strength:

$$N_{sbg} = \left(1 + \frac{s}{6c_{a1}}\right) 160 c_{a1} \sqrt{A_{brg}} \lambda_a \sqrt{f_c^{'}}$$

Threadbar spacing is taken as: $s = 29$ in.

Critical edge distance: $c_{a1} = 3$ in.

Modification factor for concrete: $\lambda = 1.0$ (normal weight concrete)

Concrete strength: $f_c^{'} = 3600$ psi

$$N_{sbg} = \left(1 + \frac{29}{6 \times 3}\right) \times 160 \times 29 \times \sqrt{4.71} \times 1.0 \times \sqrt{3600} = 188{,}751 \text{ lb} = 188.8 \text{ kips}$$

$$R_n = \min(T_d, N_{c,P}, N_{sbg}) = 76.5 \text{ kips}$$

■ Number of Threadbars

$P_{req} = 135.4$ kips

$$n_{t,req} = \frac{P_{req}}{R_n} = \frac{135.4}{76.5} = 1.77 \text{ ea./girder}$$

Use two 1 in. diameter threadbars per girder:

$R_n n_t = 76.5 \times 2 = 153 \text{ kips} \geq P_{req} = 135.4 \text{ kips}$ O.K.

■ Required Thickness of Bearing Steel Plate

$$t_{\min,req} = \frac{R_n}{\phi 2.4 d_b f_u} = \frac{P_{req}/n_t}{\phi 2.4 d_b f_y} = \frac{135.4/2}{0.75 \times 2.4 \times 1 \times 36} = 1 \text{ in.}$$

A 1 in. thick steel plate is used for the bearing plate.

■ Required Bearing Area

$$A_{b,req} = \frac{P_{req}/n_t}{\phi_c 0.85 f_c'} = \frac{135.4/2}{0.65 \times 0.85 \times 3.6} = 34 \text{ in.}^2$$

A rectangular steel plate with dimensions 5.5 in. × 7 in. is used due to the limited spacing in the deck.

C.12.3 Lateral Thread Rod

The lateral threadbar is designed to suspend the load transferred by the hanger threadbars, and induces prestress through diaphragms to connect the diaphragms, infilled concrete, and main body of the bent cap to form an integral system. Threadbars with 1 in. diameter and 150 ksi maximum tensile strength are used. Two lateral threadbars are used on either side of the girder. The prestress force induced by the lateral threadbar is:

$P_e = 0.6 f_u A_b n_b = 0.6 \times 150 \times 0.85 \times 2 = 153$ kips

Additionally, the lateral threadbar is design to sustain a concurrent axial force that may be produced by the vertical load rather than to resist the whole shear loading. The concurrent axial tension force is taken as:

$N_u = 2 \cdot 0.2 P_{req} = 2 \times 0.2 \times 135.4 = 54.2$ kips < $P_e = 153$ kips O.K.

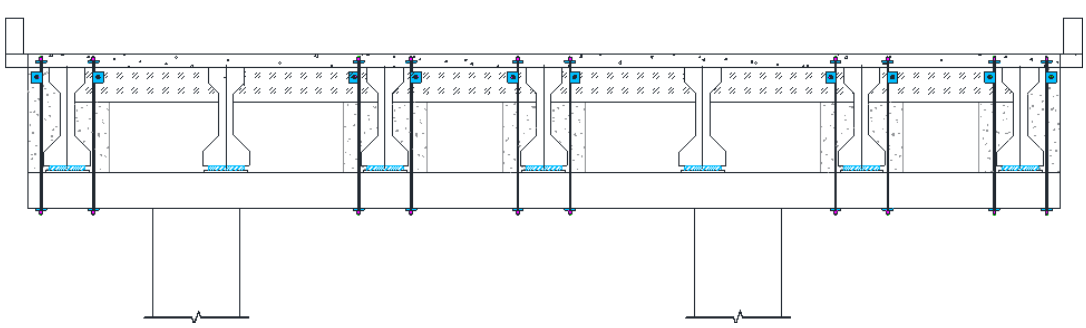

Figure C.19. Schematic View of Solution 12 Applied for Double-Column Bent.

C.12.4 Cost Table

Table C.21. Cost for Solution 12 per Bent.

No.	Description	Unit	Quantity per Item	No. of Items	Total Quantity	Rate/ Unit	Material Cost	Labor Cost	Equipment Cost
1	Boom Lift: 30 ft	HR			180	$16			$2,880
2(a)	Telehandler: 30 ft long, 6000 lb capacity	HR			180	$20			$3,600
2(b)	Telehandler Operator	HR			180	$30		$5,400	
3	Construction Worker: three people	HR	183	3	549	$30		$16,470	
4	Rebar Detector	HR	2	10	20	$3			$60
4(a)	Concrete Slab Removal Debris Disposal: 8 in. dia. 7.5in. Thick	SF	0.4	20	8	$3		$24	
4(b)	Concrete Slab Removal Equipment Allowance	SF	0.4	20	8	$7			$56
5(a)	Hammer drill, Vertical, ledge: 1.5 in. dia., 20 in. long	HR	0.2	20	4	$8			$32
5(b)	1-1/2"x21" Hammer Drill Bit	EA			1	$81	$81		
6(a)	Core Driller: 1-1/16 in. dia. hor., web+diaphragm	HR	2.5	24	60	$60		$3,600	
6(b)	1-1/2"x60" Diamond Core Drill Bit	EA			1	$365	$365		
7(a)	Threadbar: 1 in. dia. Hor	FT	6	10	60	$30	$1,800		
7(b)	Bearing Plate: 6x6x1	LB	10.1	20	202	$0.60	$121		
7(c)	Plasma Cutting 1" thickness	FT	0.5	20	10	$6			$60
7(d)	Drilling Holes for Bearing Plate: 1.25 in. dia. 1in. Thick	EA	1	20	20	$3.50	$70		
7(e)	Washer: 1 in. dia	EA	2	10	20	$8	$160		
7(f)	Nut: 1 in. dia	EA	2	10	20	$2	$40		
7(g)	Torque Wrench and Multiplier	HR			10	$20			$200
8(a)	Threadbar: 1 in. dia. Ver	FT	7.5	20	150	$30	$4,500		
8(b)	Bearing Plate: 6x46x1	LB	77.3	10	773	$0.60	$464		
8(c)	Bearing Plate: 7x 5.5 x1	LB	10.8	10	108	$0.60	$65		
8(d)	Plasma Cutting 1" thickness	FT	0.5	30	15	$6			$90
8(e)	Drilling Holes for Bearing Plate: 1.25 in. dia.	EA	2	20	40	$3.50	$140		
8(f)	Washer: 1 in. dia	EA	2	20	40	$10	$400		
8(g)	Nut: 1 in. dia	EA	2	20	40	$15	$600		
8(h)	Torque Wrench and Multiplier	HR			20	$20			$400
9(a)	Concrete	CY			4.5	$125	$563		
9(b)	Rebar #5	LB			520	$1	$328		
9(c)	Formwork: plywood 12' 2"x4"	SF	1.5	92	138	$1	$104		
9(d)	Formwork: plywood 4'x8'	SF	32	5	160	$2	$240		
							$10,039	**$25,494**	**$7,378**
		Total Materials, Labor, and Equipment					**$42,911**		
		Mobilization					$9,000		
		Subtotal					**$51,911**		
		Contingencies (~20%)					$10,383		
		Total					**$63,000**		

Major Item

C.13 SOLUTION 13: CONCRETE MASONRY PIERS

C.13.1 Introduction

It is essential to establish a foundation to support the CMU columns. The foundation is constructed as a beam connecting the drilled shaft for the existing columns. It is assumed that only axial compression forces acting on the column apply to the design of the concrete masonry column. Design of masonry columns should meet the requirements of *Building Code Requirements and Specifications for Masonry Structures* (MSJC, 2011).

C.13.2 Column

■ Required Number of Masonry Concrete Unit

Use 8 in. units:

$A_n = 71.5 \text{ in.}^2$, $I = 36691.1 \text{ in.}^2$, and $r = 22.7$ in.

$f_m^{'} = 1.35$ ksi (Specification and Commentary Table 2)

$P_u = 129$ kips

$$A_{req} = \frac{P_u}{\phi f_m^{'}} = \frac{129}{0.9 \times 1.35} = 106.2 \text{ in.}^2$$

$$n_{m,req} = \frac{A_{req}}{A_n} = 1.5 \text{ ea.}$$

To support the ledge of the bent cap, the masonry column needs to be as wide as the existing column. Therefore, let $n_m = 6$ ea.

■ Nominal Axial Strength of Masonry Column

Check $\frac{h}{r}$:

$h_{main} = 22 \text{ ft} = 264 \text{ in and } h_{bound} = 25 \text{ ft} = 300 \text{ in.}$

$$\therefore \frac{h_{main}}{r} = \frac{264}{22.7} = 11.7 \; or \; \frac{h_{bound}}{r} = \frac{300}{22.7} = 13.2 \le 99$$

Design axial strength of an 8 in. concrete masonry unit:

$$\phi P_n = \phi 0.80 \left[0.80 f_m^{'} A_n \left[1 - \left(\frac{h}{140r} \right)^2 \right] \right] \text{ for unreinforced masonry concrete}$$

$$\phi P_n = \phi 0.80 \left[0.80 f_m^{'} A_n \left[1 - \left(\frac{h}{140r} \right)^2 \right] \right]$$

$$= 0.9 \times 0.80 \left[0.80 \times 1.35 \times 71.5 \left[1 - \left(\frac{264}{140 \times 22.7} \right)^2 \right] \right] = 55.2 \text{ kips}$$

Therefore:

$\phi P_n n_m = 55.2 \times 5 = 276 \text{ kips} \ge P_u = 129$ kips O.K.

Vertical reinforcement is required in masonry columns to prevent brittle failure, and at least four bars are required so that ties can be used to provide a confined core for the masonry.

■ Vertical Reinforcement

The amount of vertical reinforcement is determined based on the nominal strength of unreinforced masonry columns as well as its requirements. In addition, vertical reinforcement in the columns should not be larger than a No. 9 bar, and at least four vertical reinforcements are required to be tied. Since unreinforced masonry concrete itself has enough strength, the minimum amount of reinforcement should be used.

Use Grade 60, four #3 rebar:

$A_{st} = n_s A_s = 4 \times 0.11 = 0.44 \text{ in.}^2$

The limit of reinforcing area is:

$0.0025A_n \le A_{st} \le 0.04A_n$

$0.0025A_n = 0.0025 \times 71.5 = 0.18 \text{ in.}^2$

$0.04A_n = 0.04 \times 71.5 = 2.86 \text{ in.}^2$

$\therefore 0.0025A_n = 0.18 \text{ in.}^2 \le A_{st} = 0.44 \text{ in.}^2 \le 0.04A_n = 2.86 \text{ in.}^2$ O.K.

Lap length:

$l_l = \max(12, l_d)$

where $l_d = \dfrac{0.13 d_b^2 f_y \gamma}{K\sqrt{f_m^{'}}}$

with $f_y = 60{,}000$ psi, $f_m^{'} = 1350$ psi, $\gamma = 1.0$ and $K = 1.0$

$$l_d = \frac{0.13 d_b^2 f_y \gamma}{K\sqrt{f_m^{'}}} = \frac{0.13 \times 0.375^2 \times 60000 \times 1.0}{1.0 \times \sqrt{1350}} = 29.85 \text{ in.}$$

$\therefore l_l = \max(12, l_d) = 29.85 \text{ in.}$

Standard hooks should consist of a 90-degree bend plus minimum $12d_b$ extension at the free end.

Vertical reinforcement should be enclosed by lateral ties at least ¼ in. in diameter.

■ Lateral Tie

Use #2 ties:

$A_{sl} = 0.05 \text{ in.}^2$ with spacing of 16 in.

Maximum spacing:

$48A_{sl} = 48 \times 0.05 = 18 \text{ in.}$

$s = 16 \text{ in.} \le 48A_{sl} = 18 \text{ in.}$ O.K.

■ Design Strength of the Column

Design strength of the reinforced masonry concrete column:

$$\phi P_n = \phi 0.80\left[0.80 f_m^{'}(A_n - A_{st}) + f_y A_{st}\right]\left[1 - \left(\frac{h}{140r}\right)^2\right]$$

$$= 0.9 \times 0.80\left[0.80 \times 1.35 \times (71.5 \times 5 - 0.44) + 60 \times 0.44\right]\left[1 - \left(\frac{264}{140 \times 22.7}\right)\right]$$

$$= 369.1 \text{ kips}$$

$$\therefore P_d = 369.1 \text{ kips} \geq P_u = 129 \text{ kips}$$ O.K.

C.13.3 Foundation

■ Assumptions

- The foundation beam is assumed to be a fixed-fixed beam.
- There is nothing under the beam to support the beam.
- It is completely connected to the existing drilled shaft.
- The entire loads from the girders located between the columns act as point load on the foundation beam (129 kip/girder):
  - $M_{u+} = 2287 \text{ kip} \cdot \text{ft}$
  - $M_{u-} = 2678 \text{ kip} \cdot \text{ft}$
  - $V_{\max} = 585.02 \text{ kips}$

■ Dimension of Foundation Beam

$$\rho_{target} = 0.5 \times \rho_b = 0.5 \times \frac{0.85\beta_1 f_c^{'}}{f_y} \times \frac{3}{5} = 0.255\frac{\beta_1 f_c^{'}}{f_y}$$

In this case:

$f_c^{'} = 3.6$ ksi, $f_y = 60$ ksi, and $\beta_1 = 0.85$

$$\therefore \rho_{target} = 0.255\frac{\beta_1 f_c^{'}}{f_y} = 0.255 \times \frac{0.85 \times 3.6}{60} = 0.013$$

The reinforcement index:

$$\omega = \rho\frac{f_y}{f_c^{'}} = 0.013 \times \frac{60}{3.6} = 0.22$$

The flexural resistance factor:

$$R = \omega f_c^{'}(1 - 0.59\omega) = 0.22 \times 3.6(1 - 0.59 \times 0.22) = 0.68 \text{ ksi}$$

$$bd^2 \geq \frac{M_u}{\phi R} = \frac{2678 \times 12}{0.9 \times 0.68} = 52509.8 \text{ in}^3$$

$$d^2 \geq \frac{M_u}{\phi Rb} = \frac{52509.8}{72} = 729.3 \text{ in}^2 \rightarrow d \geq \sqrt{\frac{M_u}{\phi Rb}} = \sqrt{729.3} = 27 \text{ in.}$$

Use $d = 39$ in.

$h \approx d + 2.5$ (thickness of cover concrete) $= 41.5$ *in.*

Let $h = 42$ in.

■ Lateral Reinforcements

The nominal flexural strength:

$$M_n = A_s f_y\left(d - \frac{a}{2}\right)$$

The depth of the compression stress block:

$$a = \frac{A_s f_y}{0.85 f_c^{'} b} \times \frac{d}{d} = \frac{A_s}{bd} \times \frac{f_y}{f_c^{'}} \times \frac{d}{0.85} = \rho \frac{f_y}{f_c^{'}} \times \frac{d}{0.85} = \frac{\omega d}{0.85} = \frac{0.22 \times 39}{0.85} = 10.1 \text{ in.}$$

$$M_u = 2678 \times 12 \text{ kip} \cdot \text{in} \le \phi M_n = \phi A_s f_y \left(d - \frac{a}{2} \right)$$

$$= 0.9 \times A_{s,req} \times 60 \left(39 - \frac{10.1}{2} \right) = 1833.3 A_{s,req}$$

$$\rightarrow A_{s,req} = \frac{2678 \times 12}{1833.3} = 18.8 \text{ in}^2$$

Use Grade 60 #11 bars

$$n_{s,req} = \frac{A_{s,req}}{A_s} = \frac{18.8}{1.56} = 11.23 \text{ ea.} \le n_s = 12 \text{ ea.}$$ O.K.

■ Shear Reinforcement

$$V_u \le \phi V_n \rightarrow V_n = V_u / \phi = 585.02 / 0.75 = 780.03 \text{ kips}$$

$$V_c = 2\lambda \sqrt{f_c^{'}} b_w d = 2 \times 1 \sqrt{3600} \times 72 \times 39 = 259200 \text{ lb} = 336.96 \text{ kips}$$

$$V_u / \phi = 780.03 \text{ kips} \ge V_c / 2 = 336.96 / 2 = 168.48 \text{ kips (stirrups are required)}$$

Check section:

$$V_{s,max} = 8 \sqrt{f_c^{'}} bd$$

$$(V_u / \phi)_{max} = V_c + V_{s,max} = 10 \sqrt{f_c^{'}} bd = 5 V_c = 842.4 \text{ kips}$$

$$V_u / \phi = 780.03 \text{ kips} \le (V_u / \phi)_{max} = 842.4 \text{ kips}$$ O.K.

Try No. 6 six-leg stirrups, $f_{yt} = 60$ ksi

$$A_v = 6 \times 0.44 = 2.64 \text{ in}^2$$

Take $s = 12$ in.

$$s \le \frac{A_v f_{yt} d}{V_u / \phi - V_c} = \frac{2.64 \times 60 \times 39}{780.03 - 336.96} = 13.94 \text{ in.}$$

Lesser of $A_{v,\min} = 0.75 \sqrt{f_c^{'}} \dfrac{bs}{f_{yt}}$ or $A_{v,\min} = 50 \dfrac{bs}{f_{yt}}$

$$0.75 \sqrt{f_c^{'}} = 45 \le 50$$

$$\therefore A_{v,\min} = 50 \frac{bs}{f_{yt}} = 50 \frac{72 \times 12}{60000} = 0.72 \text{ in}^2$$ O.K.

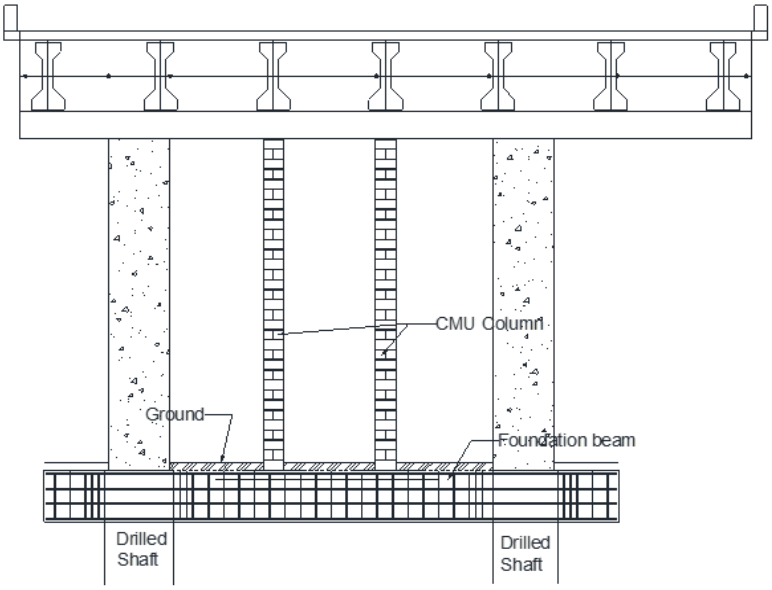

Figure C.20. Schematic View of Solution 13 Applied for Double-Column Bent.

C.13.4 Cost Table

Table C.22. Cost for Solution 13 per Bent.

No.	Description	Unit	Quantity per Item	No. of Items	Total Quantity	Rate/ Unit	Material Cost	Labor Cost	Equipment Cost
1(a)	Concrete Masonry Unit: 8 in.	EA	165	5	825	$1.65	$1,361		
1(b)	Rebar #6 :	LB	132	5	660	$0.56	$370		
1(c)	#4 Tie	LB	61	16	976	$0.47	$459		
1(d)	Grout 0.45 ft^3 bag	EA	94	5	470	$10	$4,700		
1(e)	Grout Mixer	HR	1	5	5	$6			$30
1(f)	Grout Pump	HR	2	5	10	$6			$60
2(a)	Boom Lift: 30 ft	HR			180	$16			$2,880
2(b)	Construction Worker: three people	HR	30	3	90	$30		$2,700	
3(a)	Slab Removal Debris	SF	324	1	324	$22			
3(b)	Slab Removal Equipment	SF	324.0	1	324	$55			$17,820
3(c)	Slab Removal Labor	HR	33	1	33	$61		$2,013	
4(a)	Land Excavation Debris Disposal	CY	42.0	1	42	$35	$1,470		
4(b)	Land Excavation Equipment	CY	42.0	1	42	$200			$8,400
4(c)	Land Excavation Labor	HR	2		60	$80		$4,800	
5(a)	Concrete	CY	42.0	1	42	$125	$5,250		
5(b)	Rebar #11	LB	5111	1	5111	$0.40	$2,044		
5(c)	Formwork: plywood 12' 2"x4"	SF	1.5	600	900	$0.75	$675		
5(d)	Formwork: plywood 4'x8'	SF	32	28.8	921.6	$2	$1,382		
							$17,711	**$9,513**	**$29,190**
		Total Materials, Labor, and Equipment					**$56,414**		
		Mobilization					$12,000		
		Subtotal					**$68,414**		
		Contingencies (~20%)					$13,683		
		Total					**$83,000**		

Major Item

C.14 SOLUTION 14: LOAD-BALANCING PT

C.14.1 Introduction

A reinforced concrete saddle is newly formed over the column. PT strands are installed over the bent cap and anchored at the end of the bent cap with the end-region stiffener. As shown in Figure 4.20(b), a different approach is implemented for the double-column bent cap due to the relatively long mid-span of the double-column bent.

The strand configurations for both bents are shown in Figure 4.20(a) and (b). Concrete saddles reinforced with No. 5 rebar are placed around the column to ensure the effective inclination angle of the post-tension bars. The required strength of the strand can be obtained from the geometry.

C.14.2 Single-Column Bent

■ Required Number of Strands

The deficiency of the single-column bent is:

$D_{e1} = D_{e2} = 36$ kips

The inclination angle of the strand for both parts is:

$\alpha = 16°$

The required strength of the stand can be obtained by:

$$F_{req,pt} = \frac{De}{\sin(\alpha)} = \frac{36}{\sin(16°)} = 137.9 \text{ kips}$$

Greased and sheathed strands with 0.6 in. diameter and 150 ksi ultimate strength should be used for this solution. According to AASHTO (2014), initial stress loss of post tension is 25 percent of the jacking force. The total time dependent losses can conservatively be considered as 20 percent for this case. Therefore, the final PT force of a single strand can be obtained by:

$P_{pt} = 0.75 \cdot 0.8 \cdot A_n f_{pu} = 0.75 \times 0.8 \times 0.217 \times 270 = 35.2$ kips

The required number of the strand is determined as:

$$n_s = \frac{F_{req,pt}}{P_{pt}} = \frac{137.9}{35.2} = 3.91 \text{ ea.}$$

Use four 0.6 in. diameter strands for the single-column bent (Bent 22).

■ End Stiffener

The resultant force induced by the PT strands is:

$P_n = n_s \times P_{pt} = 4 \times 35.2 = 140.8$ kips

Assume the diameter of the strand bundle to be 2 in.

Required plate thickness for axial bearing:

$$t_a \geq \frac{P_n \cos(\alpha)}{\phi 2 d_b f_y} = \frac{140.8 \times \cos(16°)}{0.75 \times 2 \times 2 \times 36} = 1.25 \text{ in.} \qquad \text{Governs}$$

Required plate thickness for shear bearing:

$$t_s \geq \frac{P_n \sin(\alpha)}{\phi 2 d_b f_y} = \frac{140.8 \times \cos(16°)}{0.75 \times 2 \times 2 \times 36} = 0.36 \text{ in.}$$

Use a 1.25 in. thick steel plate.

C.14.3 Double-Column Bent

■ Required Number of Strands

The deficiencies of the double-column bent are:

$D_{e1} = D_{e4} = 67$ kips

$D_{e2} = D_{e3} = 90$ kips

The inclination angles of the post-tension bars for D_{e1} to D_{e4} are:

$\alpha_1 = 35°$; $\alpha_2 = 29°$; $\alpha_3 = 28°$; $\alpha_4 = 20°$, respectively.

The required strength of the stand for each part should be obtained by:

$$F_{req,pt1} = \frac{D_{e1}}{\sin(\alpha_1)} = \frac{76}{\sin(35°)} = 132.5 \text{ kips}$$

$$F_{req,pt2} = \frac{D_{e2}}{\sin(\alpha_2)} = \frac{90}{\sin(29°)} = 185.64 \text{ kips}$$

$$F_{req,pt3} = \frac{D_{e3}}{\sin(\alpha_3)} = \frac{90}{\sin(28°)} = 191.7 \text{ kips}$$

$$F_{req,pt4} = \frac{D_{e4}}{\sin(\alpha_4)} = \frac{67}{\sin(20°)} = 195.9 \text{ kips} \qquad \text{Governs}$$

Greased and sheathed strands with 0.6 in. diameter and 150 ksi ultimate strength should be used for this solution. The final PT force in a single strand is:

$$P_{pt} = 0.75 \cdot 0.8 \cdot A_n f_{pu} = 0.75 \times 0.8 \times 0.217 \times 270 = 35.2 \text{ kips}$$

The required number of strands is determined as:

$$n_s = \frac{F_{req,pt4}}{P_{pt}} = \frac{195.9}{35.2} = 5.5 \text{ ea.}$$

Use six 0.6 in. diameter strands for the double-column bent (Bent 13).

■ End Stiffener

The resultant force induced by the PT strands is:

$P_n = n_s \times P_{pt} = 6 \times 35.2 = 211.2$ kips

Assume the diameter of the strand bundle to be 2 in.

Required plate thickness for axial bearing:

$$t_a \geq \frac{P_n \cos(\alpha)}{\phi 2 d_b f_y} = \frac{211.2 \times \cos(35°)}{0.75 \times 2 \times 2 \times 36} = 1.575 \text{ in.} \qquad \text{Governs}$$

Required plate thickness for shear bearing:

$$t_s \geq \frac{P_n \sin(\alpha)}{\phi 2 d_b f_y} = \frac{211.2 \times \cos(35°)}{0.75 \times 2 \times 2 \times 36} = 1.125 \text{ in.}$$

Use a 1.75 in. thick steel plate for the left overhang of the double bent.

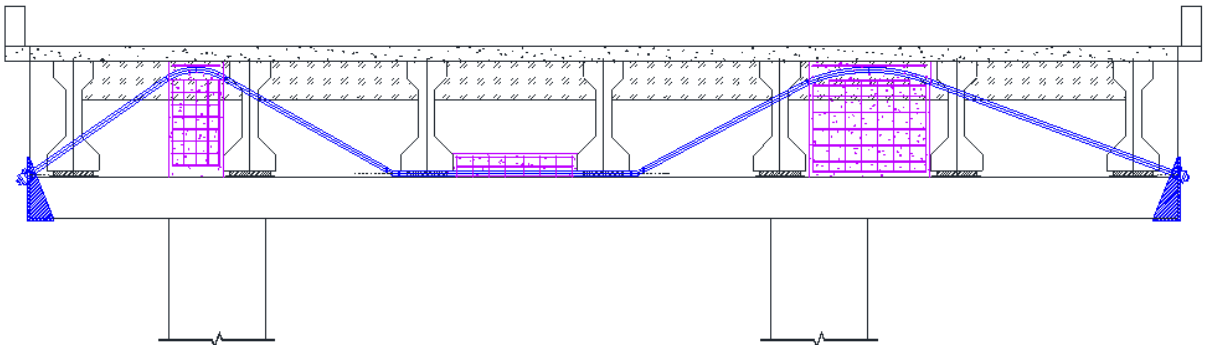

(a) For double-column bent

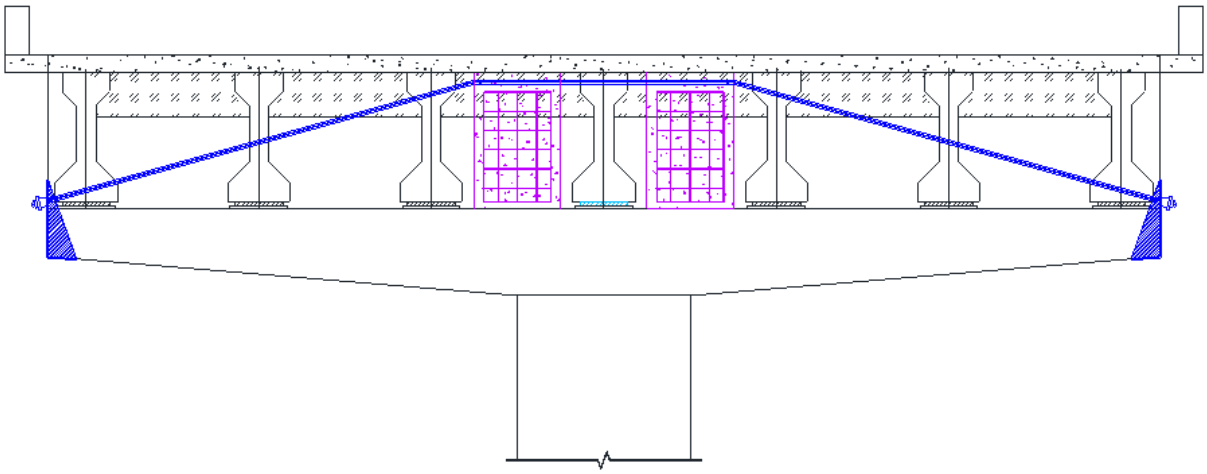

(b) For single-column bent

Figure C.21. Schematic View of Solution 14.

C.14.4 Cost Table

Table C.23. Cost for Solution 14 for a Double-Column Bent.

No.	Description	Unit	Quantity per Item	No. of Items	Total Quantity	Rate/ Unit	Material Cost	Labor Cost	Equipment Cost
1(a)	Boom Lift: 30 ft	HR	32	1	32	$16			$512
1(b)	Construction worker	HR	32	3	96	$30			$2,880
2(a)	Telehandler: 30 ft long, 6000 lb capacity	HR	32	1	32	$20			$640
2(b)	Telehandler Operator	HR	32	1	32	$30		$960	
3(a)	Greased and Sheathed Strand: 0.6 in.	LB	400	2	800	$2.13	$1,700		
3(b)	Anchor + wedge for 0.6" strand	EA	2	2	4	$150	$600		
3(c)	Post-Tensioning Jack	HR	4	2	8	$17			$136
3(d)	PT Specialist	HR	4	2	8	$70		$560	
4(a)	End Plate: 1.25 in.	LB	1000	2	2000	$1.00	$2,000		
4(b)	Drilling Holes for End Plate: 2.75 in. dia.	EA	2	2	4	$20	$80		
4(c)	Welder	HR	2	2	4	$50		$200	
4(d)	3/32" E7018 Stick Electrode	LB	2	12	24	$3	$72		
4(e)	Welding Wire	LB	1	12	12	$6	$72		
4(f)	Plasma Steel Cutting 1.25" thick	IN	30	11	330	$10	$3,300		
5(a)	Concrete	CY	4	2	8	$125	$1,000		
5(b)	Rebar #9	LB	876	1	876	$0.45	$394		
5(c)	Formwork: plywood 12' 2"x4"	SF	1.5	200	300	$0.75	$225		
5(d)	Formwork: plywood 4'x8'	SF	32	10	320	$2	$480		
							$9,923	**$1,720**	**$4,168**
		Total Materials, Labor, and Equipment					**$15,811**		
		Mobilization					$4,000		
		Subtotal					**$19,811**		
		Contingencies (~20%)					$3,963		
		Total					**$24,000**		

Major Item

Table C.24. Cost for Solution 14 for a Single-Column Bent.

No.	Description	Unit	Quantity per Item	No. of Items	Total Quantity	Rate/ Unit	Material Cost	Labor Cost	Equipment Cost
1(a)	Boom Lift: 30 ft	HR	24	1	24	$16			$384
1(b)	Construction worker	HR	24	3	72	$30			$2,160
2(a)	Telehandler: 30 ft long, 6000 lb capacity	HR	32	1	32	$20			$640
2(b)	Telehandler Operator	HR	32	1	32	$30		$960	
3(a)	Greased and Sheathed Strand: 0.6 in.	LB	200	2	400	$2.13	$850		
3(b)	Anchor + wedge for 0.6" strand	EA	2	2	4	$150	$600		
3(c)	Post-Tensioning Jack	HR	4	2	8	$17			$136
3(d)	PT Specialist	HR	4	2	8	$70		$560	
4(a)	End Plate: 1.25 in.	LB	1000	2	2000	$1.00	$2,000		
4(b)	Drilling Holes for End Plate: 2.75 in. dia.	EA	2	2	4	$20	$80		
4(c)	Welder	HR	2	2	4	$50		$200	
4(d)	3/32" E7018 Stick Electrode	LB	2	12	24	$3	$72		
4(e)	Welding Wire	LB	1	12	12	$6	$72		
4(f)	Plasma Steel Cutting 1.25" thick	IN	30	11	330	$10	$3,300		
5(a)	Concrete	CY	1.8	2	4	$125	$500		
5(b)	Rebar #9	LB	120	4	480	$0.45	$216		
5(c)	Formwork: plywood 12' 2"x4"	SF	1.5	200	300	$0.75	$225		
5(d)	Formwork: plywood 4'x8'	SF	32	10	320	$2	$480		
							$8,395	**$1,720**	**$3,320**
		Total Materials, Labor, and Equipment					**$13,435**		
		Mobilization					$3,000		
		Subtotal					**$16,435**		
		Contingencies (~20%)					$3,287		
		Total					**$20,000**		

Major Item

C.15 SOLUTION 15: CONCRETE INFILL WITH FRP ANCHORED BY FRP ANCHORS

C.15.1 Introduction

Partial-depth infill concrete is placed between the girders to transform the inverted-T cross-section to a rectangular cross-section. Embedded threadbars are provided in two layers to connect the infill concrete and web. Since the infill concrete is not loaded significantly, minimum reinforcement is provided. FRP strips are attached to the transformed section for strengthening the inverted-T bent cap. FRP strips are anchored at the termination region by FRP anchors.

C.15.2 FRP Strip

The FRP strips are attached around the side of the ledge and with infill concrete with a three-side bonded "U-warp" wrapping scheme. A carbon fiber fabric Mbrace CF160 is used for the retrofit. FRP properties specified by the manufacturer are as follows:

Tensile modulus:

$E_f = 33000$ ksi

Thickness:

$t_f = 0.013$ in.

Rupture strain:

$\varepsilon_u = 0.0167$

Number of FRP layers:

$n = 1$

Since the FRP strips are anchored at the termination region, the effective strain of the FRP strip is taken as 0.004 in accordance with ACI 440.2R (ACI Committee 440, 2008):

$\varepsilon_{fe} = 0.004$

Effective stress on FRP strip:

$f_{fe} = \varepsilon_{fe} E_f = 0.004 \times 33000 = 132$ ksi

Assume half the width of the infill concrete on each side of the girder is effectively engaged in transferring the girder load.

Width of the FRP strip per girder:

$w_f = 62$ in.

Effective sectional area of FRP strip per girder:

$A_{vf} = n t_f w_f = 1 \times 0.013 \times 61 = 0.793$ in.^{2}

Inclination angle of FRP strip:

$\alpha = 90°$

Nominal strength of FRP strip:

$$V_f = A_{fv} f_{fe} (\sin\alpha + \cos\alpha)$$
$$= 0.793 \times 132 \times (1 + 0) = 104.68 \text{ kips}$$

Reduction factor for FRP shear reinforcement based on wrapping scheme (ACI 440.2R):

$\psi_f = 0.85$

Reduced strength of FRP strip:

$\psi_f V_f = 0.85 \times 104.68 = 94.2$ kips

Shear deficiency of the bent cap (i.e., required strength of FRP strip):

$V_u = 90$ kips

Check FRP strength:

$\psi_f V_f = 94.2 \text{ kips} > V_u = 90 \text{ kips}$ O.K.

C.15.3 FRP Anchor

FRP anchors made of the same material (Mbrace CF160) with a 0.5 in. diameter are used to provide end anchorage to the FRP strips.

Sectional area of FRP anchor:

$A_{fa} = 0.19 \text{ in}^2$

Assume same effective stress as used for FRP strip:

$f_{fe} = \varepsilon_{fe} E_f = 0.004 \times 33000 = 132$ ksi

Strength contribution of single FRP anchors:

$V_{fa} = \mathrm{A}_{fa} f_{fe} = 0.19 \times 132 = 25$ kips

Required number of FRP anchors per girder:

$n_{fa} = V_u / V_{fa} = 90/25 = 3.6$

Considering the geometry of the infill concrete and the reinforcement configuration, six FRP anchors are provided with 10 in. spacing.

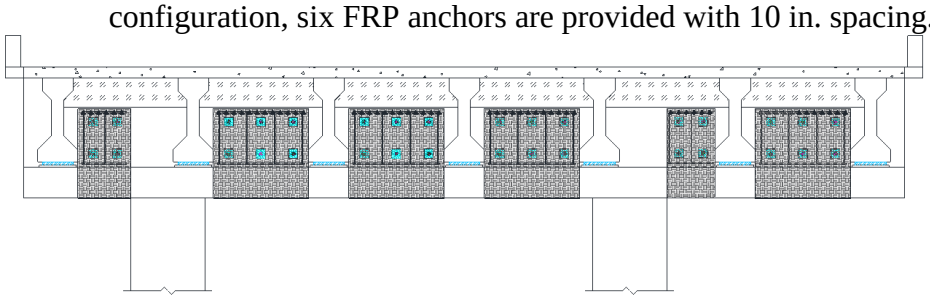

(a) For double-column bent

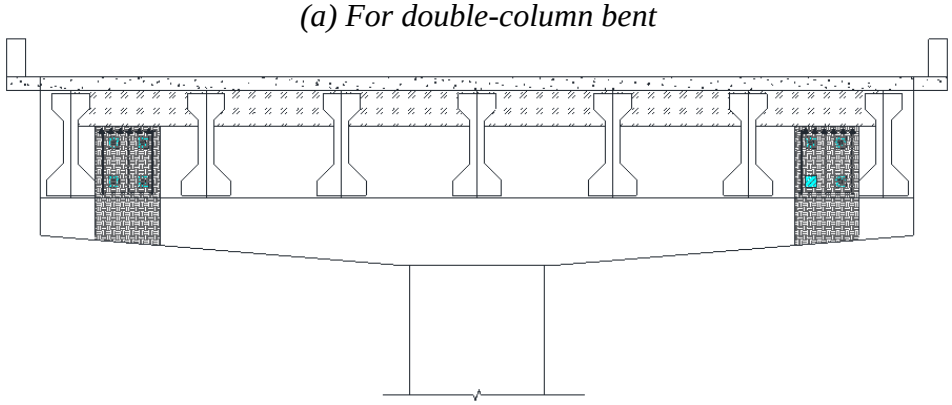

(b) For single-column bent

Figure C.22. Schematic View of Solution 15.

C.15.4 Cost Table

Table C.25. Cost for Solution 15 for a Double-Column Bent.

No.	Description	Unit	Quantity per Item	No. of Items	Total Quantity	Rate/ Unit	Material Cost	Labor Cost	Equipment Cost
1	Boom Lift: 30 ft	HR	8	6	48	$16			$768
2(a)	Telehandler: 30 ft long, 6000 lb capacity	HR			180	$20			$3,600
2(b)	Telehandler Operator	HR			180	$30		$5,400	
3	Construction Worker: three people	HR	48	3	144	$30		$4,320	
4	Rebar Detector	HR	2	10	20	$3			$60
5(a)	Hammer drill: 1 in. dia., 30 in. long	HR	0.3	28	8.4	$8			$67
5(b)	1"x36" Hammer Drill Bit	EA			1	$91	$91		
6(a)	Threadbar: 1 in. dia. Hor	FT	4	28	112	$30	$3,360		
6(b)	Bearing Plate: 6x6x0.75	LB	7.56	28	211.68	$0.60	$127		
6(c)	Plasma Cutting 0.75" thickness	FT	0.5	28	14	$6			$84
6(d)	Drilling Holes for Bearing Plate: 1.25 in. dia. 0.75in. Thick	EA	1	28	28	$3.00	$84		
6(e)	Washer: 1 in. dia	EA	2	28	56	$8	$448		
6(f)	Nut: 1 in. dia	EA	4	28	112	$2	$224		
7(a)	Concrete Slab Removal Debris Disposal: 7.5 in. dia. 7.5in. Thick	SF	0.4	6	2.4	$3		$7	
7(b)	Concrete Slab Removal Equipment Allowance	SF	0.4	6	8	$7			$56
8(a)	Concrete	CY			7	$125	$913		
8(b)	Rebar #8	LB			889	$1	$560		
8(c)	Formwork: plywood 12' 2"x4"	SF	1.5	237	355.5	$0.75	$267		
8(d)	Formwork: plywood 4'x8'	SF	32	12	384	$2	$576		
8(e)	Stirrups #4 Double Leg	LB	4.06	16	65.01867	$0.63	$41		
9	Grinder	HR	3	12	36	$7			$252
10(a)	0.08 in. thick CFRP sheet : int. ver. 184 in x 62 in	YD	5	4	20	$678	$13,557		
10(b)	0.08 in. thick CFRP sheet: ext. strip 90 in x 50in	YD	2.5	2	5	$273	$1,367		
10(e)	Epoxy Resin + Hardener: 1.25gal kit	EA			24	$70	$1,680		
11(a)	Hammer Drill: 0.5" in. dia. 12 in.	HR	1	108	108	$10			$1,080
11(b)	Hammer Drill Bit for FRP Anchor : 0.5 in. dia. 12 in.	EA	-	-	3	$33	$99		
11(c)	FRP Anchor: 0.5 in.dia	EA			108	$30	$3,240		
							$26,634	**$9,727**	**$5,967**
		Total Materials, Labor, and Equipment					**$42,328**		
		Mobilization					$9,000		
		Subtotal					**$51,328**		
		Contingencies (~20%)					$10,266		
		Total					**$62,000**		

Major Item

Table C.26. Cost for Solution 15 for a Single-Column Bent.

No.	Description	Unit	Quantity per Item	No. of Items	Total Quantity	Rate/ Unit	Material Cost	Labor Cost	Equipment Cost
1	Boom Lift: 30 ft	HR	8	6	48	$16			$768
2(a)	Telehandler: 30 ft long, 6000 lb capacity	HR			180	$20			$3,600
2(b)	Telehandler Operator	HR			180	$30		$5,400	
3	Construction Worker: three people	HR	48	3	144	$30		$4,320	
4	Rebar Detector	HR	2	10	20	$3			$60
5(a)	Hammer drill: 1 in. dia., 30 in. long	HR	0.3	40	12	$8			$96
5(b)	1"x36" Hammer Drill Bit	EA			1	$91	$91		
6(a)	Threadbar: 1 in. dia. Hor	FT	4	20	80	$30	$2,400		
6(b)	Bearing Plate: 6x6x0.75	LB	7.56	20	151.2	$0.60	$91		
6(c)	Plasma Cutting 0.75" thickness	FT	0.5	20	10	$6			$60
6(d)	Drilling Holes for Bearing Plate: 1.25 in. dia. 0.75in. Thick	EA	1	20	20	$3.00	$60		
6(e)	Washer: 1 in. dia	EA	2	20	40	$8	$320		
6(f)	Nut: 1 in. dia	EA	4	20	80	$2	$160		
7(a)	Concrete Slab Removal Debris Disposal: 7.5 in. dia. 7.5in. Thick	SF	0.4	6	2.4	$3		$7	
7(b)	Concrete Slab Removal Equipment Allowance	SF	0.4	6	8	$7			$56
8(a)	Concrete	CY			5	$125	$571		
8(b)	Rebar #8	LB			556	$1	$350		
8(c)	Formwork: plywood 12' 2"x4"	SF	1.5	127	190.5	$0.75	$143		
8(d)	Formwork: plywood 4'x8'	SF	32	6	192	$2	$288		
8(e)	Stirrups #4 Double Leg	LB	4.06	12	48.8	$0.63	$31		
9	Grinder	HR	3	12	36	$7			$252
10(a)	0.08 in. thick CFRP sheet : int. ver. 205 in x 62 in	YD	6	4	24	$339	$8,134		
10(b)	0.08 in. thick CFRP sheet: ext. strip 70 in x 70 in	YD	2	2	4	$383	$1,531		
10(e)	Epoxy Resin + Hardener: 1.25gal kit	EA			20	$70	$1,400		
11(a)	Hammer Drill: 0.5" in. dia. 12 in.	HR	1	84	84	$10			$840
11(b)	Hammer Drill Bit for FRP Anchor : 0.5 in. dia. 12 in.	EA	-	-	2	$33	$66		
11(c)	FRP Anchor: 0.5 in.dia	EA			84	$30	$2,520		
							$18,155	**$9,727**	**$5,732**
		Total Materials, Labor, and Equipment					**$33,615**		
		Mobilization					$7,000		
		Subtotal					**$40,615**		
		Contingencies (~20%)					$8,123		
		Total					**$49,000**		

Major Item

C.16 SOLUTION 16: CONCRETE INFILL WITH PARTIAL-DEPTH FRP ANCHORED BY STEEL WALING

C.16.1 Introduction

A shallower infill concrete is placed between the girders to transform the inverted-T cross-section to a rectangular cross-section. Though threadbars are provided to connect the infill concrete and web, also provide a location for attachment of the waling. Minimum reinforcement is provided for the infill concrete. FRP strips anchored by steel waling at the termination region are attached to the transformed section for strengthening the inverted-T bent cap.

C.16.2 FRP Strip

The FRP strips are attached around the side of the ledge and with infill concrete with a three-side bonded "U-warp" wrapping scheme. A carbon fiber fabric Mbrace CF160 is used for the retrofit. FRP properties specified by the manufacturer are as follows:

Tensile modulus:

$E_f = 33000 \text{ ksi}$

Thickness:

$t_f = 0.013 \text{ in.}$

Rupture strain:

$\varepsilon_u = 0.0167$

Number of FRP layers:

$n = 1$

Since the FRP strips are anchored at the termination region, the effective strain of the FRP strip is taken as 0.004 in accordance with ACI 440.2R (ACI Committee 440, 2008):

$\varepsilon_{fe} = 0.004$

Effective stress on FRP strip:

$f_{fe} = \varepsilon_{fe} E_f = 0.004 \times 33000 = 132 \text{ ksi}$

Assume half the width of the infill concrete on each side of the girder is effectively engaged in transferring the girder load.

Width of the FRP strip per girder:

$w_f = 62 \text{ in.}$

Effective sectional area of FRP strip per girder:

$A_{vf} = n t_f w_f = 1 \times 0.013 \times 61 = 0.793 \text{ in.}^2$

Inclination angle of FRP strip:

$\alpha = 90°$

Nominal strength of FRP strip:

$$V_f = A_{fv} f_{fe} (\sin\alpha + \cos\alpha)$$

$$= 0.793 \times 132 \times (1 + 0) = 104.68 \text{ kips}$$

Reduction factor for FRP shear reinforcement based on wrapping scheme (ACI 440.2R):

$\psi_f = 0.85$

Reduced strength of FRP strip:

$\psi_f V_f = 0.85 \times 104.68 = 94.2$ kips

Shear deficiency of the bent cap (i.e., required strength of FRP strip):

$V_u = 90$ kips

Check FRP strength:

$\psi_f V_f = 94.2 \text{ kips} > V_u = 90 \text{ kips}$ O.K.

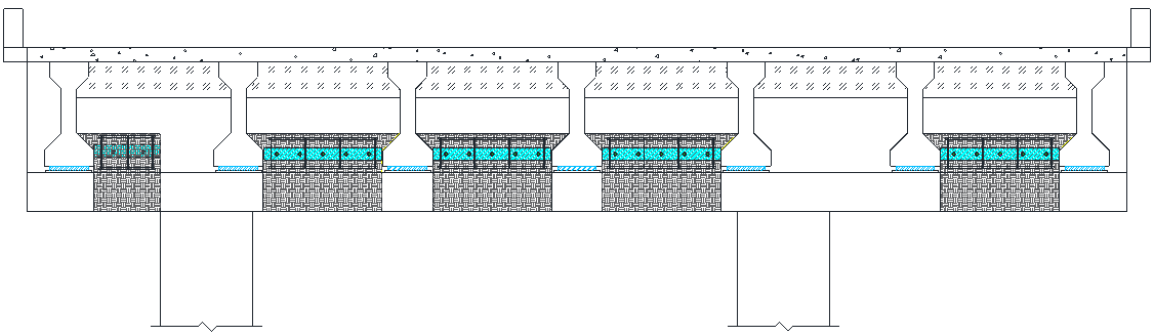

(a) For double-column bent

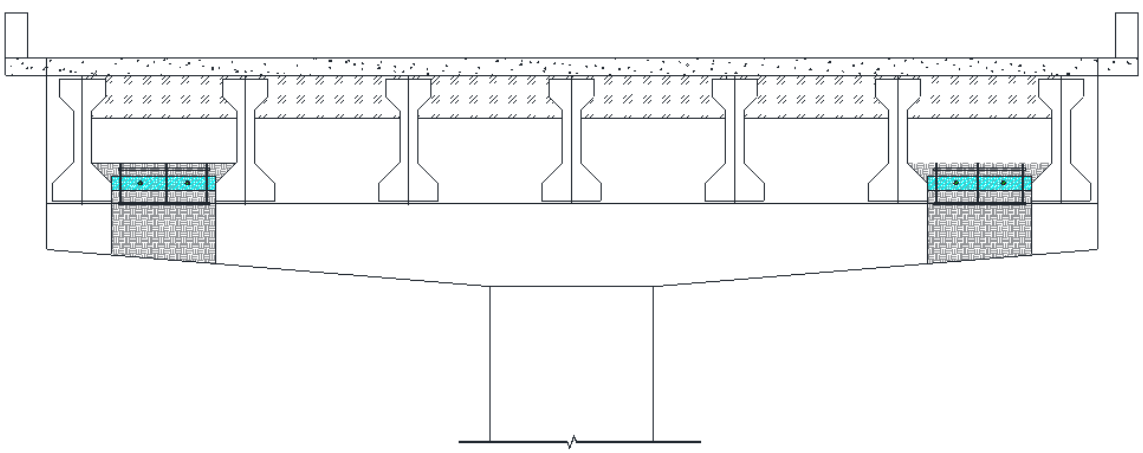

(b) For single-column bent

Figure C.23. Schematic View of Solution 16.

C.16.3
Cost Table

Table C.27. Cost for Solution 16 for a Double-Column Bent.

No.	Description	Unit	Quantity per Item	No. of Items	Total Quantity	Rate/ Unit	Material Cost	Labor Cost	Equipment Cost
1	Boom Lift: 30 ft	HR	8	6	48	$16			$768
2(a)	Telehandler: 30 ft long, 6000 lb capacity	HR			180	$20			$3,600
2(b)	Telehandler Operator	HR			180	$30		$5,400	
3	Construction Worker: three people	HR	48	3	144	$30		$4,320	
4	Rebar Detector	HR	2	10	20	$3			$60
5(a)	Hammer drill: 1 in. dia., 30 in. long	HR	0.15	22	3.3	$8			$26
5(b)	1"x36" Hammer Drill Bit	EA			1	$57	$57		
6(a)	Threadbar: 1 in. dia. Hor	EA	5	22	114	$30	$3,420		
6(b)	Waling Steel: 6.5x62x0.75	LB	85	8	680	$0.60	$408		
6(c)	Plasma Cutting 0.75" thickness	FT	5	8	40	$6			$240
6(d)	Drilling Holes for Waling Steel: 1.25 in. dia. 0.75in. Thick	EA	5	24	120	$3.00	$360		
6(e)	Washer: 1 in. dia	EA	2	22	44	$8	$352		
6(f)	Nut: 1 in. dia	EA	2	22	44	$2	$88		
7(a)	Concrete	CY			4	$125	$533		
7(b)	Rebar #8	LB			519	$1	$327		
7(c)	Formwork: plywood 12' 2"x4"	SF	1.5	31	46.5	$0.75	$35		
7(d)	Formwork: plywood 4'x8'	SF	32	2	64	$2	$96		
7(e)	Stirrups #4 Double Leg	LB	3.34	16	53.44	$0.63	$34		
8	Grinder	HR	3	12	36	$7			$252
9(a)	0.023 in. thick CFRP sheet : int. ver. 143 in x 62 in	YD	4	4	16	$97	$1,559		
9(b)	0.023 in. thick CFRP sheet: ext. strip 90 in x 40 in	YD	2.5	2	5	$27	$137		
9(e)	Epoxy Resin + Hardener: 1.25gal kit	EA			19	$70	$1,330		
							$8,736	**$9,720**	**$4,946**
		Total Materials, Labor, and Equipment					**$23,402**		
		Mobilization					$5,000		
		Subtotal					**$28,402**		
		Contingencies (~20%)					$5,681		
		Total					**$35,000**		

Major Item

Table C.28. Cost for Solution 16 for a Single-Column Bent.

No.	Description	Unit	Quantity per Item	No. of Items	Total Quantity	Rate/ Unit	Material Cost	Labor Cost	Equipment Cost
1	Boom Lift: 30 ft	HR	8	6	48	$16			$768
2(a)	Telehandler: 30 ft long, 6000 lb capacity	HR			180	$20			$3,600
2(b)	Telehandler Operator	HR			180	$30		$5,400	
3	Construction Worker: three people	HR	48	3	144	$30		$4,320	
4	Rebar Detector	HR	2	10	20	$3			$60
5(a)	Hammer drill: 1 in. dia., 30 in. long	HR	0.15	18	2.7	$8			$22
5(b)	1"x36" Hammer Drill Bit	EA			1	$57	$57		
6(a)	Threadbar: 1 in. dia. Hor	EA	5	18	94	$30	$2,820		
6(b)	Waling Steel: 6.5x62x0.75	LB	85	8	680	$0.60	$408		
6(c)	Plasma Cutting 0.75" thickness	FT	5	8	40	$6			$240
6(d)	Drilling Holes for Waling Steel: 1.25 in. dia. 0.75in. Thick	EA	5	18	90	$3.00	$270		
6(e)	Washer: 1 in. dia	EA	2	18	36	$8	$288		
6(f)	Nut: 1 in. dia	EA	2	18	36	$2	$72		
7(a)	Concrete	CY			3	$125	$333		
7(b)	Rebar #8	LB			325	$1	$204		
7(c)	Formwork: plywood 12' 2"x4"	SF	1.5	31	46.5	$0.75	$35		
7(d)	Formwork: plywood 4'x8'	SF	32	2	64	$2	$96		
7(e)	Stirrups #4 Double Leg	LB	3.34	12	40.08	$0.63	$25		
8	Grinder	HR	3	8	24	$7			$168
9(a)	0.023 in. thick CFRP sheet : int. ver. 205 in x 46 in	YD	6	4	24	$72	$1,735		
9(b)	0.023 in. thick CFRP sheet: ext. strip 70 in x 40 in	YD	2	2	4	$16	$64		
9(e)	Epoxy Resin + Hardener: 1.25gal kit	EA			19	$70	$1,330		
							$7,738	**$9,720**	**$4,858**
		Total Materials, Labor, and Equipment					**$22,316**		
		Mobilization					$5,000		
		Subtotal					**$27,316**		
		Contingencies (~20%)					$5,464		
		Total					**$33,000**		

Major Item

C.17 SOLUTION 17: CONCRETE INFILL WITH FULL-DEPTH FRP ANCHORED BY STEEL WALING

C.17.1 Introduction

Full-depth infill concrete is placed between the girders to transform the inverted-T cross-section to a rectangular cross-section. Threadbars are provided in two layers, with the top layer passing through the full width of the infill. Minimum reinforcement is provided for the infill concrete. FRP strips anchored by steel waling at the termination region are attached to the transformed section for strengthening the inverted-T bent cap.

C.17.2 FRP Strip

The FRP strips are attached around the side of the ledge and with infill concrete with a three-side bonded "U-warp" wrapping scheme. A carbon fiber fabric Mbrace CF160 is used for the retrofit. FRP properties specified by the manufacturer are as follows:

Tensile modulus:

$E_f = 33000 \text{ ksi}$

Thickness:

$t_f = 0.013 \text{ in.}$

Rupture strain:

$\varepsilon_u = 0.0167$

Number of FRP layers:

$n = 1$

Since the FRP strips are anchored at the termination region, the effective strain of the FRP strip is taken as 0.004 in accordance with ACI 440.2R (ACI Committee 440, 2008):

$\varepsilon_{fe} = 0.004$

Effective stress on FRP strip:

$f_{fe} = \varepsilon_{fe} E_f = 0.004 \times 33000 = 132 \text{ ksi}$

Assume half the width of the infill concrete on each side of the girder is effectively engaged in transferring girder load.

Width of FRP strip per girder:

$w_f = 62 \text{ in.}$

Effective sectional area of FRP strip per girder:

$A_{vf} = n t_f w_f = 1 \times 0.013 \times 61 = 0.793 \text{ in.}^2$

Inclination angle of FRP strip:

$\alpha = 90°$

Nominal strength of FRP strip:

$$V_f = A_{fv} f_{fe} (\sin\alpha + \cos\alpha)$$

$$= 0.793 \times 132 \times (1 + 0) = 104.68 \text{ kips}$$

Reduction factor for FRP shear reinforcement based on wrapping scheme (ACI 440.2R):

$\psi_f = 0.85$

Reduced strength of FRP strip:

$\psi_f V_f = 0.85 \times 104.68 = 94.2$ kips

Shear deficiency of the bent cap (i.e., required strength of FRP strip):

$V_u = 90$ kips

Check FRP strength:

$\psi_f V_f = 94.2 \text{ kips} > V_u = 90 \text{ kips}$ O.K.

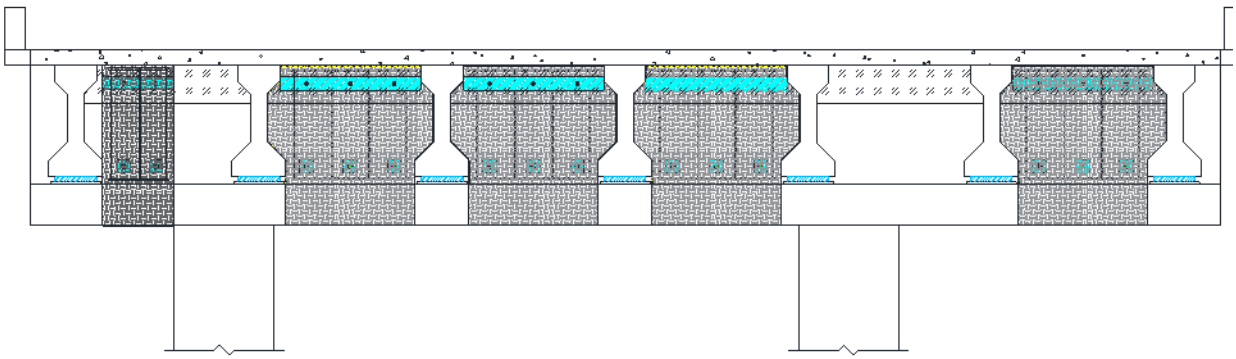

(a) For double-column bent

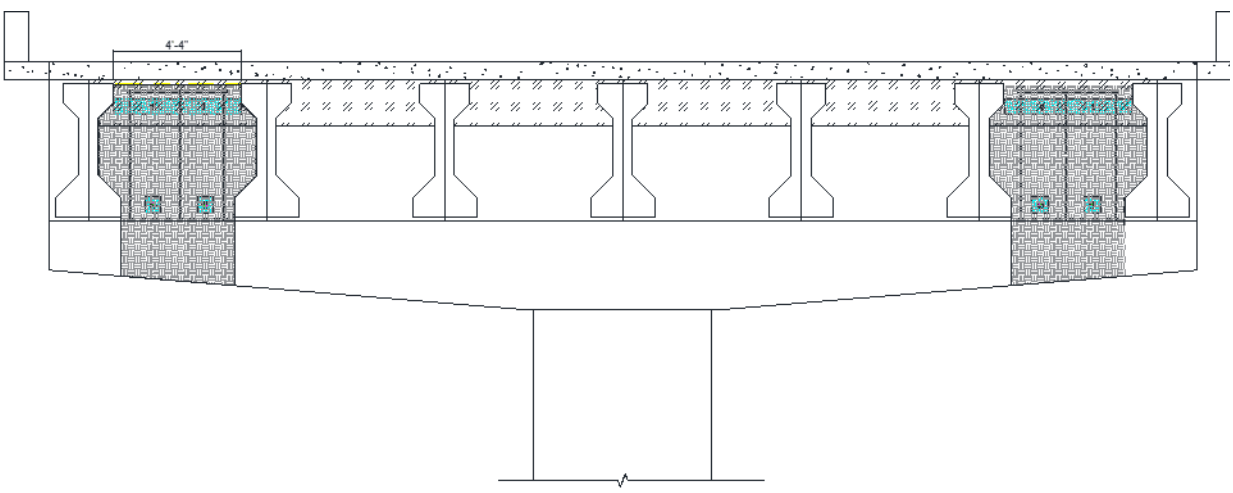

(b) For single-column bent

Figure C.24. Schematic View of Solution 17.

C.17.3 Cost Table

Table C.29. Cost for Solution 17 for a Double-Column Bent.

No.	Description	Unit	Quantity per Item	No. of Items	Total Quantity	Rate/ Unit	Material Cost	Labor Cost	Equipment Cost
1	Boom Lift: 30 ft	HR	8	6	48	$16			$768
2(a)	Telehandler: 30 ft long, 6000 lb capacity	HR			180	$20			$3,600
2(b)	Telehandler Operator	HR			180	$30		$5,400	
3	Construction Worker: three people	HR	48	3	144	$30		$4,320	
4	Rebar Detector	HR	2	10	20	$3			$60
5(a)	Hammer drill: 1 in. dia., 30 in. long	HR	0.3	28	8.4	$8			$67
5(b)	1"x36" Hammer Drill Bit	EA			1	$91	$91		
6(a)	Threadbar: 1 in. dia. Hor	FT	4	14	56	$30	$1,680		
6(b)	Bearing Plate: 6x6x0.75	LB	7.56	24	181.44	$0.60	$109		
6(c)	Plasma Cutting 0.75" thickness	FT	0.5	24	12	$6			$72
6(d)	Drilling Holes for Bearing Plate: 1.25 in. dia. 0.75in. Thick	EA	1	24	24	$3.00	$72		
6(e)	Washer: 1 in. dia	EA	2	14	28	$8	$224		
6(f)	Nut: 1 in. dia	EA	4	14	56	$2	$112		
6(a)	Threadbar: 1 in. dia. Hor	FT	5	14	74	$30	$2,220		
6(b)	Waling Steel: 6.5x62x0.75	LB	90	8	720	$0.60	$432		
6(c)	Plasma Cutting 0.75" thickness	FT	5	8	40	$6			$240
6(d)	Drilling Holes for Waling Steel: 1.25 in. dia. 0.75in. Thick	EA	3	8	24	$3.00	$72		
6(e)	Washer: 1 in. dia	EA	2	14	28	$8	$224		
6(f)	Nut: 1 in. dia	EA	2	14	28	$2	$56		
7(a)	Concrete Slab Removal Debris Disposal: 7.5 in. dia. 7.5in. Thick	SF	0.4	6	2.4	$3		$7	
7(b)	Concrete Slab Removal Equipment Allowance	SF	0.4	6	8	$7			$56
8(a)	Concrete	CY			8	$125	$1,000		
8(b)	Rebar #8	LB			974	$1	$613		
8(c)	Formwork: plywood 12' 2"x4"	SF	1.5	24	36	$0.75	$27		
8(d)	Formwork: plywood 4'x8'	SF	32	2	64	$2	$96		
8(e)	Stirrups #4 Double Leg	LB	5	16	80	$0.63	$50		
9	Grinder	HR	3	12	36	$7			$252
10(a)	0.023 in. thick CFRP sheet : int. ver. 184 in x 62 in	YD	5	4	20	$97	$1,949		
10(b)	0.023 in. thick CFRP sheet: ext. strip 90 in x 78 in	YD	2.5	2	5	$53	$267		
10(e)	Epoxy Resin + Hardener: 1.25gal kit	EA			24	$70	$1,680		
							$10,974	**$9,727**	**$5,115**
		Total Materials, Labor, and Equipment					**$25,816**		
		Mobilization					$6,000		
		Subtotal					**$31,816**		
		Contingencies (~20%)					$6,364		
		Total					**$39,000**		

Major Item

Table C.30. Cost for Solution 17 for a Single-Column Bent.

No.	Description	Unit	Quantity per Item	No. of Items	Total Quantity	Rate/ Unit	Material Cost	Labor Cost	Equipment Cost
1	Boom Lift: 30 ft	HR	8	6	48	$16			$768
2(a)	Telehandler: 30 ft long, 6000 lb capacity	HR			180	$20			$3,600
2(b)	Telehandler Operator	HR			180	$30		$5,400	
3	Construction Worker: three people	HR	48	3	144	$30		$4,320	
4	Rebar Detector	HR	2	10	20	$3			$60
5(a)	Hammer drill: 1 in. dia., 30 in. long	HR	0.3	20	6	$8			$48
5(b)	1"x36" Hammer Drill Bit	EA			1	$91	$91		
6(a)	Threadbar: 1 in. dia. Hor	FT	4	10	40	$30	$1,200		
6(b)	Bearing Plate: 6x6x0.75	LB	7.56	20	151.2	$0.60	$91		
6(c)	Plasma Cutting 0.75" thickness	FT	0.5	20	10	$6			$60
6(d)	Drilling Holes for Bearing Plate: 1.25 in. dia. 0.75in. Thick	EA	1	20	20	$3.00	$60		
6(e)	Washer: 1 in. dia	EA	2	10	20	$8	$160		
6(f)	Nut: 1 in. dia	EA	4	10	40	$2	$80		
6(a)	Threadbar: 1 in. dia. Hor	FT	5	10	54	$30	$1,620		
6(b)	Waling Steel: 6.5x62x0.75	LB	90	8	720	$0.60	$432		
6(c)	Plasma Cutting 0.75" thickness	FT	5	8	40	$6			$240
6(d)	Drilling Holes for Waling Steel: 1.25 in. dia. 0.75in. Thick	EA	3	8	24	$3.00	$72		
6(e)	Washer: 1 in. dia	EA	2	10	20	$8	$160		
6(f)	Nut: 1 in. dia	EA	2	10	20	$2	$40		
7(a)	Concrete Slab Removal Debris Disposal: 7.5 in. dia. 7.5in. Thick	SF	0.4	6	2.4	$3		$7	
7(b)	Concrete Slab Removal Equipment Allowance	SF	0.4	6	8	$7			$56
8(a)	Concrete	CY			5	$125	$600		
8(b)	Rebar #8	LB			584	$1	$368		
8(c)	Formwork: plywood 12' 2"x4"	SF	1.5	18	27	$0.75	$20		
8(d)	Formwork: plywood 4'x8'	SF	32	1	32	$2	$48		
8(e)	Stirrups #4 Double Leg	LB	5	12	60	$0.63	$38		
9	Grinder	HR	3	12	36	$7			$252
10(a)	0.023 in. thick CFRP sheet : int. ver. 205in x 46 in	YD	5.5	4	22	$72	$1,591		
10(b)	0.023 in. thick CFRP sheet: ext. strip 70 in x 78 in	YD	2	2	4	$53	$213		
10(e)	Epoxy Resin + Hardener: 1.25gal kit	EA			24	$70	$1,680		
							$8,563	**$9,727**	**$5,084**
		Total Materials, Labor, and Equipment					**$23,375**		
		Mobilization					$5,000		
		Subtotal					**$28,375**		
		Contingencies (~20%)					$5,675		
		Total					**$35,000**		

Major Item

C.18 SOLUTION 18: LARGE BEARING PAD

C.18.1 Introduction

The original bearing pad is replaced by a larger bearing pad, which can enhance the punching shear capacity of the inverted-T bent cap.

C.18.2 Bearing Pad

The bearing pad solution is designed for the exterior since it is found to be critical. The required increment of bearing pad size can be calculated as:

$$\Delta\left(\frac{W}{2}+L\right)=\frac{V_u}{0.125\sqrt{f'_c}d_f}=22.3 \text{ in.}$$

The required increment cannot be achieved due to the geometry of the girder and ledge. Considering the geometry restriction, the maximum viable bearing pad that can be achieved is 25 in. x 14 in., which can enhance the punching shear capacity to:

$$V_{n,increment}=0.125\sqrt{f'_c}\Delta(\frac{W}{2}+L)d_f=0.125\times\sqrt{3.6}\times 8\times 17=32.3 \text{ kips}$$

Shear deficiency of the bent cap:

$V_u=90$ kips

Check strength increment:

$V_{n,increment}=32.2 \text{ kips}<V_u=90 \text{ kips}$ N.G.

The maximum strength increment that can be achieved from the bearing pad solution is 32.3 kip out of the 90 kip deficiency.

C.18.3 Cost Table

Table C.31. Cost for Solution 18 for a Double-Column Bent.

No.	Description	Unit	Quantity per Item	No. of Items	Total Quantity	Rate/ Unit	Material Cost	Labor Cost	Equipment Cost
1	Boom Lift: 30 ft	HR			12	$16			$192
2	Construction Worker: three people	HR	12	3	36	$35		$1,260	
3 (a)	Hydraulic Jack: 60 ton	HR	12	1	12	$7			$84
3 (b)	Flat Jack Hydraulic Cylinders: 25 ton x 2	HR	12	2	24	$4			$96
4	Bearing Pad: 24"x14"	EA	1	6	6	$300			$1,800
							$0	**$1,260**	**$2,172**
		Total Materials, Labor, and Equipment					**$3,432**		
		Mobilization					$1,000		
		Subtotal					**$4,432**		
		Contingencies (~20%)					$887		
		Total					**$6,000**		

Major Item

Table C.32. Cost for Solution 18 for a Single-Column Bent.

No.	Description	Unit	Quantity per Item	No. of Items	Total Quantity	Rate/ Unit	Material Cost	Labor Cost	Equipment Cost
1	Boom Lift: 30 ft	HR			8	$16			$128
2	Construction Worker: three people	HR	8	3	24	$35		$840	
3 (a)	Hydraulic Jack: 60 ton	HR	8	1	8	$7			$56
3 (b)	Flat Jack Hydraulic Cylinders: 25 ton x 2	HR	8	2	16	$4			$64
4	Bearing Pad: 24"x14"	EA	1	4	4	$300			$1,200
							$0	**$840**	**$1,448**
		Total Materials, Labor, and Equipment					**$2,288**		
		Mobilization					$1,000		
		Subtotal					**$3,288**		
		Contingencies (~20%)					$658		
		Total					**$4,000**		

Major Item

REFERENCES

AASHO. (1965). *Standard Specifications for Highway Bridges*, Ninth Edition. American Association of State Highway Officials, Washington DC.

AASHTO. (2014). *LRFD Bridge Design Specifications*, Seventh Edition. American Association of State Highway and Transportation Officials, Washington DC.

ACI Committee 318. (2014). *Building Code Requirements for Structural Concrete (ACI 318-14) and Commentary*. American Concrete Institute, Farmington Hills, MI.

ACI Committee 364.2T. (2008). *Increasing Shear Capacity within Existing Reinforced Concrete Structures*. American Concrete Institute, Farmington Hills, MI.

ACI Committee 440. (2008). *Guide for the Design and Construction of Externally Bonded FRP Systems for Strengthening Concrete Structures*. American Concrete Institute, Farmington Hills, MI.

AISC. (2010a). *Specification for Structural Steel Buildings*. American Institute of Steel Construction, Chicago, IL.

AISC. (2010b). *Steel Construction Manual*. American Institute of Steel Construction, Chicago, IL.

Basler, M., White, D., and Desroches, M. (2003). *Shear Strengthening with Bonded CFRP L Shaped Plates*. ACI International SP-215-23, pp. 373–384.

Bentz, E.C. (2000). Response-2000: Reinforced Concrete Sectional Analysis Using Modified Compression Field Theory (Version 1.0.5) [Computer software]. University of Toronto.

Breveglieri, M., Aprile, A., Barros, J.A.O. (2015). "Embedded Through-Section Shear Strengthening Technique using Steel and CFRP Bars in RC Beams of Different Percentage of Existing Strrups," *Composite Structures*, Vol. 126 pp. 101-113.

Chaallal, O., Mofidi, A., Benmokrane, B., and Neale, K. (2011). "Embedded Through-Section FRP Rod Method for Shear Strengthening of RC Beams: Performance and Comparison with Existing Techniques," *Journal of Composites for Construction*, Vol. 15, No. 3, pp. 374–383.

Deifalla, A., Awad, A., and Elgarhy, M. (2013). "Effectiveness of Externally Bonded CFRP Strips for Strengthening Flanged Beams Under Torsion: An Experimental Study," *Engineering Structures*, Vol. 56, pp. 2065–2075.

Deifalla, A., and Ghobarah, A. (2010a). "Full Torsional Behavior of RC Beams Wrapped with FRP: Analytical Model," *Journal of Composite Construction*, Vol. 14, No. 3, pp. 289–300.

Deifalla, A., and Ghobarah, A. (2010b). "Strengthening RC T-beams Subjected to Combined Torsion and Shear Using FRP Fabrics: Experimental Study," *Journal of Composite Construction*, Vol. 14, No. 3, pp. 301–311.

Deifalla, A., and Ghobarah, A. (2014). "Behavior and Analysis of Inverted T-shaped RC Beams under Shear and Torsion," *Engineering Structures*, Vol. 68, pp. 57–70.

DeLorenzis, L., and Nanni, A. (2001). “Shear Strength of Reinforced Concrete Beams with Near-Surface Mounted Fiber-Reinforced Polymer Rods,” *ACI Structural Journal*, Vol. 98, No. 1, pp. 60–68.

Dias, S.J.E., Baincco, V., Barros, J.O.A., and Monti, G. (2007). “Low Strength T-Cross Section RC Beams Shear-Strengthened By NSM Technique,” *Materiali ed Approcci Innovativi per il Progetto in Zona Sismica e la Mitigazione della Vulnerabilità delle Strutture*, ISBN 978-88-7699-065-6.

Dias, S.J.E., and Barros, J.O.A. (2008). “Shear Strengthening of T Cross Section Reinforced Concrete Beams by Near-Surface Mounted Technique,” *Journal of Composites for Construction*, Vol. 12, No. 3, pp. 300–311.

Dias, S.J.E., and Barros, J.O.A. (2010). “Performance Of Reinforced Concrete T Beams Strengthened In Shear With NSM CFRP Laminates,” *Engineering Structures*, Vol. 32, No. 2, pp. 373–384.

Furlong, R.W., Ferguson, P.M., and Ma, J.S. (1971). *Shear and Anchorage Study of Reinforcement in Inverted T-beam Bent-Cap Girders*. TxDOT Report #113-4, Center for Highway Research, The University of Texas at Austin, Austin, TX.

Furlong, R.W., and Mirza, S.A. (1974). *Strength and Serviceability of Inverted T-beam Bent-Caps Subject to Combined Flexure, Shear, and Torsion*. TxDOT Report #153-1F, Center for Highway Research, University of Texas at Austin, Austin, TX.

Galal, K., and Mofidi, A. (2010). “Shear Strengthening of RC T-beams Using Mechanically Anchored Unbonded Dry Carbon Fiber Sheets,” *Journal of Performance and Constructed Facilities*, Vol. 24, No. 1, pp. 31–39.

Galal, K., and Sekar, M. (2008). “Rehabilitation of RC Inverted T Girders Using Anchored CFRP Sheets,” *Composites: Part B*, Vol. 39, No. 4, pp. 604–617.

Goebel, J.H., Johnson, B.A., and Higgins, C. (2012). *Strength and Durability of Near-Surface Mounted CFRP Bars for Shear Strengthening Reinforced Concrete Bridge Girders*. SPR 712, Oregon Department of Transportation & FHWA, Oregon State University.

Hassan, T., Lucier, G., Rizkalla, S., and Zia, P. (2007). “Modeling of L-Shaped, Precast, Prestressed Concrete Spandrels,” *PCI Journal*, pp. 78–92.

Higgins, C., Howell, D.A., Smith, M.T., and Senturk A.E. (2009). *Shear Repair Methods for Conventionally Reinforced Concrete Girders and Bent Caps*. SPR 636, Oregon Department of Transportation & FHWA, Oregon State University.

Howell, D.A. (2009). “Shear Repair Methods for Conventionally Reinforced Concrete Girders and Deep Beams,” *Doctor’s Thesis*, Oregon State University.

Hurlebaus, S., Mander, J.B., Birely, A.C., Terzioglu, T., Cui, J., and Park, S.H. (2018a). *Strengthening of Existing Inverted-T Bent Caps-Volume 2: Experimental Test Program*. Rep. No. FHWA/TX-18/0-6893-R1-Vol2, Texas A&M Transportation Institute, The Texas A&M University System.

Hurlebaus, S., Mander, J.B., Birely, A.C., Terzioglu, T., Cui, J., and Park, S.H. (2018b). *Strengthening of Existing Inverted-T Bent Caps: Design Recommendations and Examples*. Rep. No. FHWA/TX-18/0-6893-P1, Texas A&M Transportation Institute, The Texas A&M University System.

Hueste, M.B.D., Adil, M.S.U., Adman, M., and Keating, P.B. (2006). *Impact of LRFD Specifications on Design of Texas Bridges Volume 1: Parametric Study*. Rep. No. FHWA/TX-07/0-4751-1 Vol. 1, Texas A&M Transportation Institute, The Texas A&M University System.

Hwang, S.J., and Lee, H.J. (1999). "Analytical Model for Predicting Shear Strengths of Exterior Reinforced Concrete Beam-Column Joints for Seismic Resistance," *ACI Structural Journal*, Vol. 96, No. 5, pp. 846–858.

Karayannis, C.G. (1995). "Torsional Analysis Of Flanged Concrete Elements With Tension Softening," *J Comput Struct*, Vol. 54, No. 1, pp. 97–110.

Kim, J.H., and Mander, J.B. (1999). *Truss Modeling of Reinforced Concrete Shear-Flexure Behavior*. Technical Report MCEER-99–0005, University at Buffalo, New York.

Kim, J.H., and Mander, J.B. (2000a). *Cyclic Inelastic Strut-Tie Modeling of Shear-Critical Reinforced Concrete Members*. American Concrete Institute, SP 193, pp. 707–728.

Kim, J.H., and Mander, J.B. (2000b). "Seismic Detailing of Reinforced Concrete Beam-Column Connections," *Structural Engineering and Mechanics*, Vol. 10, No. 6, pp. 589–601.

Kim, J.H., and Mander, J.B. (2007). "Influence of Transverse Reinforcement on Elastic Shear Stiffness of Cracked Concrete Elements," *Engineering Structures*, Vol. 29, No. 8, pp. 1798–1807.

Larson, N., Gómez, E.F., Garber, D., Bayrak, O., and Ghannoum, W. (2013). *Strength And Serviceability Design Of Reinforced Concrete Inverted T Beams*. TxDOT Report #0-6416-1, Center for Highway Research, University of Texas at Austin, Austin, TX.

Mander, J.B., Bracci, J.M., Hurlebaus, S., Grasley, Z., Karthik, M.M., Liu, S.-H., and Scott, R.M. (2012). *Structural Assessment of "D" Region Affected by Premature Concrete Deterioration: Technical Report*. Report No. FHWA/TX-12/0-5997-1, Texas Transportation Institute, Texas A&M University, College Station, TX.

Mander, J.B., Karthik, M.M., and Hurlebaus, S. (2015). *Guidelines for Analyzing the Capacity of D-Regions with Premature Concrete Deterioration of ASR/DEF*. Product No: 0-5997-P2, Texas A&M Transportation Institute.

MSJC. (2011). *Building Code Requirements and Specifications for Masonry Structures*. Masonry Standards Joint Committee, Boulder, CO.

Nanni, A., Di Ludovico, M., and Parretti, R. (2004). "Shear Strengthening of a PC Bridge Girder with NSM CFRP Rectangular Bars," *Advances in Structural Engineering*, Vol. 7, No. 4, pp. 97–109.

Pan., Z., and Li, B. (2013). "Truss-Arch Model for Shear Strength of Shear-Critical Reinforced Concrete Columns," *Journal of Structural Engineering*, Vol. 39, No. 4, pp. 548–560.

Powers Fasteners, Inc. (2014). Power Bolt+ Heavy Duty Sleeve Anchor General Information. http://www.powers.com/pdfs/mechanical/6930SD.pdf. Accessed June 2016.

Rahal, K.N., and Collins, M.P. (1995). "Analysis of Sections Subjected to Combined Shear and Torsion—A Theoretical Model," *ACI Structural Journal*, Vol. 92, No. 4, pp. 459–469.

Scott, R.M., Mander, J.B., and Bracci, J.M. (2012a). "Compatibility Strut-and-Tie Modeling: Part I—Formulation," *ACI Structural Journal*, Vol. 109, No. 5, pp. 635–644.

Scott, R.M., Mander, J.B., and Bracci, J.M. (2012b). "Compatibility Strut-and-Tie Modeling: Part II—Implementation," *ACI Structural Journal*, Vol. 109, No. 5, pp. 645–653.

Shahawy, M., and Beitelman, T.E. (1999). "Static and Fatigue Performance of RC Beams Strengthened with CFRP Laminates," *Journal of Structural Engineering*, Vol. 125, No. 6, pp. 613–621.

Thiemamn, Z. (2009). "Pretest 3-D Finite Element Analysis of the Girder-to-Cap-Beam Connection of an Inverted-Tee Cap Beam Designed for Seismic Loadings," *Master's Thesis*, Iowa State University.

Thomsen, H., Spacone, E., Limkatanyu, S., and Camata, G. (2004). "Failure Mode Analysis of RC Beams Str in Flexural with Externally Bonded FRP by Henrik Thomsen," *Journal of Composites for Construction*, Vol. 8, No. 2, pp. 123–131.

To, N.H.T., Ingham, J.M., and Sritharan, S. (2001). "Monotonic Nonlinear Strut-and-Tie Computer Models," *Bulletin of the New Zealand Society for Earthquake Engineering*, Vol. 34, No. 3, pp. 169–190.

To, N.H.T., Sritharan, S., and Ingham, J.M. (2009). "Strut-and-Tie Nonlinear Cyclic Analysis of Concrete Frames," *Journal of Structural Engineering*, Vol. 135, No. 10, pp. 1259–1268.

TxDOT (2010). "Inverted-T Bent Cap Design Example," *Bridge Division, Texas Department of Transportation*, Austin, Texas.

TxDOT. (2015). *Bridge Design Manual—LRFD*. Texas Department of Transportation, Center for Highway Research, University of Texas at Austin, Austin, TX.

Williams Form Engineering Corporation. (2011). 150 KSI All-Thread-Bar. http://www.williamsform.com/Threaded_Bars/150_KSI_All-Thread_Bar/150_ksi_all-thread_bar.html. Accessed June 2016.

Willis, L.K. (1975). *Bent Cap Program User Manual*. Bridge Division, Texas Highways and Public Department, Austin, revised September 1978.

Zhu, R.H., Dhonde, H., and Hsu, T.T.C. (2003). *Crack Control of Ledges in Inverted T Bent-Caps*. TxDOT Report #0-1854-5, Department of Civil and Environmental Engineering, University of Houston, Houston, TX.

Zhu, R.H., and Hsu, T.T.C. (2003). *Crack Width Prediction for Exterior Portion of Inverted T Bent-Caps*. TxDOT Report #0-1854-4, Department of Civil and Environmental Engineering, University of Houston, Houston, TX.

Zhu, R.H., Wanichakorn, W., and Hsu, T.T.C. (2001). *Crack Width Prediction for Interior Portion of Inverted T Bent-Caps*. TxDOT Report #0-1854-3, Department of Civil and Environmental Engineering, University of Houston, Houston, TX.